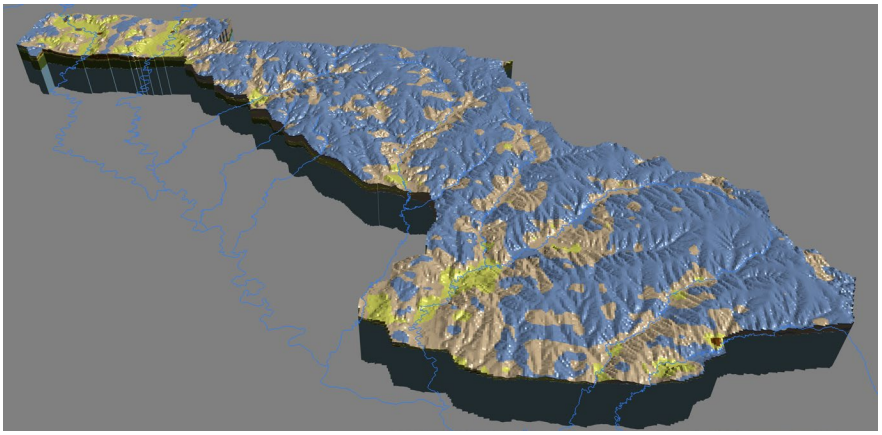
2025 Airborne Electromagnetic Mapping and Hydrogeologic Framework of a Selected Area within the Lower Big Blue Natural Resources District



March 31, 2026

Prepared for the:
Lower Big Blue Natural Resources District
805 Dorsey Street, PO Box 826
Beatrice, NE 68310

Submitted by:
Aqua Geo Frameworks, LLC
10848 Ridge Road
Fort Laramie, WY 82212

Jared D. Abraham, P.G. #422
jabraham@aquageoframeworks.com

Theodore H. Asch, P.G. #430
tasch@aquageoframeworks.com

Tammi L. Renninger, ElephantFish, LLC
tammi@elephantfishco.com



Disclaimer: AGF conducted this project using the current standards of the geophysical industry and used in-house quality control standards to produce this geophysical survey and products. The geophysical methods and procedures described in this report are applicable to the particular project objectives, and these methods have been successfully applied by AGF to investigations and projects of similar size and nature. However, field or subsurface conditions may differ from those anticipated, and the resultant data may not achieve the project objectives. AGF's services were performed consistent with the professional skill and care ordinarily provided by professional geophysicists under the same or similar circumstances. No other warranty or representation, either expressed or implied, is made by AGF in connection with its services unless in writing and signed by an authorized representative of AGF.

Executive Summary

Aqua Geo Frameworks, LLC. (AGF) is pleased to submit this report titled "2025 Airborne Electromagnetic Mapping and Hydrogeologic Framework of a Selected Area within the Lower Big Blue Natural Resources District". An understanding of the hydrogeological framework in the survey area is desired to assist in resource management. AGF entered into an agreement with the Lower Big Blue Natural Resources District (LBBNRD) to collect, process, and interpret airborne electromagnetic (AEM) data, and to use it in conjunction with other available background information to develop a 3D hydrogeologic framework.

The scope of work for this project was as follows:

1. SCOPE OF WORK

1.1 An AEM survey utilizing the SkyTEM304M system was flown over a portion of the northeast part of LBBNRD. The area was north of US Highway 136 and north of NE Highway 41, Nebraska, encompassing the area northeast of Beatrice and southeast of Pleasant Hill and between the towns of Pickrell, Clatonia, Hallam, Cortland, Filley, and Rockford. These flights have been provided as preliminary AEM inversions and the final AEM data and inversions are included as products attached to this data report.

1.2 AGF began project planning upon signing of the contract between AGF and the LBBNRD. This work included flight plans, database development, and review of hydrogeologic and geologic work for the area. The LBBNRD assisted in providing information such as water table measurements and water quality. The LBBNRD also assisted in obtaining powerline maps used in the flight planning process.

Upon conclusion of the design process, the 2025 LBBNRD flight lines had a maximum length of approximately 22.3 miles (35.8 km) in the east-west direction and about 17.4 miles (28.0 km) at their longest in the north-south direction. The flight lines were separated by approximately 0.97 mile (1.56 km) in both north-south and east-west directions.

1.4 AGF acquired AEM data over the LBBNRD, commencing 05 July 2025 and finishing on 06 July 2025, to support development of the hydrogeological framework. During this time frame, data collected over approximately 494 line-miles (794 line-kilometers) were acquired over the LBBNRD 2025 AEM survey area. Status reports of the flying were provided to the Contract Representative of LBBNRD daily, including the areas flown, production rates, and flight plan for the following day.

1.5 AGF processed and conducted quality assurance and quality control (QA/QC) procedures on all data collected from the acquisition system. AGF delivered preliminary data and inversions on July 7, 2025.

1.6 AGF inverted the AEM data. After final processing, approximately 393.9-line-miles (633.8-line kilometers) were retained for inversion amounting to a retention rate of 79.8%. This high rate is the result of careful flight line planning and design given the infrastructure that was encountered during the acquisition. These final inverted georeferenced data are delivered to the LBBNRD with this report. AGF-derived 2D sections, 3D electrical models, and interpreted geologic and hydrogeologic surfaces of the surveyed area are also delivered with this report.

1.7 AGF is providing a hydrogeologic framework report that includes maps of aquifer materials and

their relationships to current test holes and production groundwater wells, estimated transmissivity maps, areas of potential water quality concerns, and maps of estimated potential recharge areas under the AEM flight lines. This report, as mentioned above, also includes all data (acquired, processed, and developed) files. The report is delivered in PDF digital format and the data in native formats, ASCII, and ESRI map products.

2. KEY FINDINGS

2.1 Boreholes - Information from boreholes was used to analyze the Airborne Electromagnetic (AEM) inversion results. These included Nebraska Conservation Survey Division (CSD) information on 53 test holes containing lithology and stratigraphic information, and three (3) test holes containing geophysical information. Nebraska-Department of Water, Energy, and Environment (NE-DWEE) wells totaled 1,213 registered well records containing usable lithology information. These boreholes were essential in the interpretation of the AEM.

2.2 Digitizing Interpreted Geological Contacts - Characterization and interpretation of the subsurface was performed in cross-section and in derived surface grid formats. Contacts between the geologic units were digitized in 2D including the Quaternary (***Q***), Cretaceous Greenhorn and Graneros (***Kgg***), Cretaceous Dakota Group (***Kd***), and the undifferentiated Permian (***P***) composed of the Permian Chase (***Pc***) and Permian Council Grove Groups (***Pcg***), and Permian Admire (***Pa***). The interpretive process benefited from the use of CSD and NE-DWEE borehole logs. Geological outcrop maps previously published were also used on the far western side of the survey area, but all outcrops were outside the survey area. Surface grids of the interpreted geologic formations were then produced. Each flight line profile with interpretation including the Quaternary/Cretaceous Dakota Group aquifer material mapping is included in the appendices as well as interpretative surface grids.

2.3 Resistivity/Lithology Relationship - Assessment of the sediment character in both the Quaternary (***Q***), Cretaceous Greenhorn and Graneros (***Kgg***), Cretaceous Dakota Group (***Kd***) aquifer system, and the undifferentiated Permian/Pennsylvanian bedrock was conducted to determine the overall composition of the major categories used to define the aquifer and aquitards in the survey area. A numerical assessment of the resistivity thresholds within the ***Q*** was used to characterize non-aquifer (<12 ohm-m), marginal (12-25 ohm-m), aquifer (25-50 ohm-m), and coarse sand-rich intervals (>50 ohm-m) material. The ***Kgg*** was only present on the far western edge of the survey area and composed of the Graneros Shale with low resistivities in the range of 12 ohm-m. The ***Kgg*** is a confining layer and is not considered an aquifer. The ***Kd*** within the LBBNRD AEM survey area was split into four parts based on empirical comparisons to lithology logs. The four parts were classified as follows: 1) 0-3 ohm-m as Shale/Clay Dominant materials; 2) 3-18 ohm-m as Siltstone/Silt Dominant materials; 3) 18-35 ohm-m as Sand/Silt Dominant; and 4) 35 ohm-m and greater as Sandstone/Sand Dominant materials. This is the same distribution used in the pervious report from the AEM in the LBBNRD in 2023 and 2024 (AGF, 2024a; AGF, 2025). The undifferentiated Permian/Pennsylvanian bedrock varied greatly but generally had moderate resistivities in the range of 15-30 ohm-m except for the areas that contain saline waters; these areas had resistivities <7 ohm-m. The shallowest area that contains saline waters is 142 feet.

2.4 Hydrogeological Framework of the LBBNRD 2025 AEM Survey Area -The AEM reveals considerable variability in the Quaternary (***Q***) and Cretaceous Dakota Group (***Kd***) deposits across the AEM survey area. The groundwater within the LBBNRD 2025 AEM survey area is within the limited alluvial sediments of the present streams, glacial sediments, and the paleovalley sediments of the ***Q***. There is also groundwater in the fluvial and deltaic sediments of the ***Kd***. The actual groundwater

availability is dependent upon the material type of both the ***Q*** and ***Kd***. In the western third of the survey area, the ***Q*** overlies the ***Kd*** and is in hydrogeological connection with the ***Kd***. In general, the ***Q*** groundwater is available within paleovalley sediments and glacial outwash sediments, and the ***Kd*** groundwater is available in the sandstone and sand deposits of the fluvial/delta deposits. Some NE-DWEE wells are completed in both the ***Q*** and the ***Kd***.

An estimated Transmissivity (**T**) map was developed for the ***Q*** aquifers. This is related to the thickness of the saturated aquifer material and the estimated hydraulic conductivities. Most of the higher Specific Capacity (**SC**) values calculated from the NE-DWEE well database are within the higher estimated **T** values of the paleovalley and thick glacial outwash.

The AEM successfully mapped the limited sand rich deposits of the ***Kd***. Some of the ***Kd*** completed wells are in this sand dominant region that has electrical resistivity > 35 ohm-m; these would be the sand dominant materials of the fluvial deposits. While most of the ***Kd*** is saturated, the low yielding shales, siltstone, silts, and clays reduce the actual Specific Yield of the ***Kd*** wells. There is also an area within the ***Kd*** that displays a very low resistivity range that is related to saline waters.

An estimated **T** map was developed for the ***Kd*** in the 2025 LBBNRD AEM survey area using the thickness of the sand dominant materials and hydraulic conductivities from published references (e.g., O'Connor (1987) and Gannon and Vogelgesang (2015)) in the area of eastern Nebraska and western Iowa. The values compare well with the neighboring Lancaster County (Divine, 2014). This map can be helpful, but needs to be used with caution due to the lack of local hydrogeological information on the ***Kd***.

2.5 Estimation of Aquifer Volume and Water in Storage in the LBBNRD AEM Survey Area - The values for the saturated Quaternary (***Q***) aquifer (based on the LBBNRD spring 2025 water table) and Cretaceous Dakota Group (***Kd***) aquifer volumes were calculated. Three-dimensional digital representation (3-D Voxel model) of the subsurface resulting from the AEM interpretation allowed the total saturated aquifer volume and the amount of extractable water to be estimated more accurately. An area of approximately 254.51 square miles (approximately 162,884.51 acres) of AEM data were collected in the LBBNRD 2025 AEM survey, and using estimates of porosity and specific yield from the published literature as well as the 3-D Voxel models, the total volume of groundwater in storage and the total volume of extractable groundwater within the saturated ***Q***, ***Kd***, and ***Q*** and ***Kd*** combined were calculated and are as follows:

- ***Q***
    - Total volume of saturated ***Q*** materials: **14,460,190** acre-ft (or approximately 46.61% of total ***Q*** material volume)
    - Estimated groundwater in storage: **4,507,005** acre-ft
    - Estimated extractable volume of groundwater: **1,397,951** acre-ft
- ***Kd***
    - Total volume of saturated ***Kd***: **7,213,844** acre-ft (or approximately 100 % of total ***Kd*** volume)
    - Estimated groundwater in storage: **2,749,752** acre-ft
    - Estimated extractable volume of groundwater: **400,208** acre-ft
- ***Q*** and ***Kd*** combined
    - Total volume of saturated ***Q*** and ***Kd*** combined: **21,674,033** acre-ft (or approximately 56.67% of total ***Q*** and ***Kd*** combined volume)
    - Estimated groundwater in storage: **7,256,757** acre-ft

- Estimated extractable volume of groundwater: **1,798,159** acre-ft

2.6 Groundwater Quality in the LBBNRD 2025 AEM Survey Area - The AEM provided information on the near-surface (unsaturated) materials in the 2025 LBBNRD AEM survey area. Near-surface occurrences of sandy soils and sand deposits (aquifer materials) may provide conduits for contaminants to migrate into the groundwater. Using the 3D interpretation of the AEM, a near-surface occurrence of the aquifer materials 2D grid was generated. A map depicting water quality (nitrate) data collected by the LBBNRD (*Personal Communication, Tyler Weishahn, January 2026*) overlying the near-surface occurrence of aquifer materials grid was made to visually determine if there is a correlation between the near-surface material type and water quality. While there is a low correlation of the water quality to the near-surface materials, other mechanisms and groundwater flow may be contributing to the nitrate distribution.

The AEM survey detected an area of low resistivity of < 7 ohm-m and is interpreted as a regional saline water interface. The interface is shallow in the northwestern corner of the survey area near the Big Blue River and Turkey Creek. The shallowest area is 142 feet. This area would need to be confirmed with water quality sampling but there is a high probability that these areas contain saline waters. Clay layers can impact this estimation due to the similar resistivity values. It is also possible that the saline water is at the level of a clay layer and that the clay layer is impeding the upward migration of the deeper saline waters. Care would need to be exercised in drilling to not penetrate any confining clay layers.

2.7 Potential Recharge Zones within the LBBNRD 2025 AEM Survey Area - Using the AEM near-surface (unsaturated) 2D grid of the coarse and aquifer materials, a map was developed to assist in identifying and investigating areas where these materials could be used for recharge. Many of these areas are along the streams where the till and loess have been eroded away exposing the deeper coarse aquifer and aquifer material and may be considered windows into these deeper aquifer materials.

Utilizing the recharge target map to locate recharge areas can be done. However, it is imperative that accurate test holes, which may include sonic cores, are used to assess the geological materials. Any possible thin clay layers that were not detected with the AEM or may have been missed in the test hole drilling may be detected by calibrated borehole geophysical induction logs and natural gamma. Infiltration tests also need to be conducted to fully evaluate recharge rates. Additionally, determining the areas that are impacted by nitrates due to the configuration of the near-surface materials is critical because these same areas can also be targets for recharge due to the nature of the material type. The maps produced in this study can guide both management of nitrate control areas as well as allow implementation of recharge projects.

2.8 Using AEM Results to Implement Groundwater Management - All management plans can be improved as new information is gathered and considered for modifying the management practices. Much of this study was focused on the determination of the groundwater availability within the LBBNRD AEM survey area. Previous mapping was based on surficial exposures and limited test hole drilling coupled with monitoring well networks. While this provided some understanding of the hydrogeology, the AEM provides a much higher resolution of the aquifer configuration. The important findings that can have an impact on the management of the area are related to the estimated shape and configuration of the aquifers. Examples of these estimates are the transmissivity (**T**) maps that were made of both the ***Q*** and the ***Kd*** aquifers as part of this study. The hydraulic conductivity values used to estimate the ***Q*** transmissivity were based on the known material type (established with interpretation of the AEM) present within the survey area. The estimated transmissivity produced a **T** map that is in general

agreement with the map produced by Summerside and Myers (2005). The AEM-produced **T** map provides a much higher resolution view of the area as compared with the previous mapping, but that is expected and is the goal of this study. The hydraulic conductivity value used to estimate the transmissivity of the ***Kd*** aquifer was based on an average of two published values. The uncertainties in the hydrogeological parameters used in the ***Kd*** transmissivity estimates need to be acknowledged, but the map can serve as a starting point to the understanding of the area.

3. RECOMMENDATIONS

Recommendations provided to the LBBNRD in this section are based on the interpretation and understanding gained from the addition of the AEM data to existing information and from discussions with the LBBNRD about their management challenges.

3.1 Additional AEM Mapping - The aquifer maps provided in this report represent the detailed hydrogeologic framework developed for the LBBNRD 2025 AEM survey area. The AEM interpretations used to create the aquifer maps match well with the CSD and NE-DWEE borehole lithologic, stratigraphic, and/or geophysical logs. It is recommended that additional areas be flown in the LBBNRD so that these aquifer maps may be broadened to cover a larger geographic extent. Additional survey flight lines can be of a reconnaissance nature to begin with but, later, closely spaced lines or "block flights" should be collected over project areas such as well fields, well head protection areas, and/or areas of detailed recharge projects to develop more detailed frameworks. The line spacing for the block flights should be on the order of 0.25 mile (1,320 ft). It is important to note that AEM data is not meant to replace existing data, such as borehole lithology or aquifer tests, but to provide a framework in which to place the existing hydrogeological data. Therefore, AEM mapping can assist with targeting areas where more expensive technologies including borehole drilling can be implemented, especially when a block flight is flown over an area.

Future AEM mapping projects could potentially be done in cooperation with the neighboring NRDs to get details on the continuous aquifer system that is shared in the area. The Little Blue NRD is a great example of an NRD the LBBNRD can partner with to share an AEM mapping project. A benefit for partnering with other NRDs is to have a combined comprehensive estimate of groundwater storage capacity, which may be calculated by understanding the aquifer characteristics through AEM interpretation.

3.2 Siting new test holes and production wells - The AEM framework maps and profiles provided in this report give insight into the 3D relationship between current test holes and production groundwater wells and the material in which they are drilled into. At the time of this report, the current available lithology data for the LBBNRD area was used to help build the framework maps and profiles. It is recommended that the results from this report be used to site new test holes, monitoring wells, and/or water supply wells. Based on more data, the AEM framework maps and profiles provide detail in areas where the previously existing data may have been more regional in nature; this enables better decision-making when siting new wells.

The location of any future water supply wells can also use the results in this report to guide development of new water supply wells. Planners should locate wells in areas of greatest saturated thickness with the least potential for non-point source pollution.

3.3 Aquifer testing and borehole logging – Aquifer tests are recommended to improve estimates of aquifer characteristics. A robust aquifer characterization program is highly recommended at the state, regional (NRD's), and smaller municipal levels. Aquifer tests can be designed based on the results of AEM surveys and existing production wells.

Additional test holes with detailed, functional, and well calibrated geophysical logging for aquifer characteristics is highly recommended. The few test holes with calibrated geophysical logs in the LBBNRD survey area were inadequate. The borehole geophysical logs provided for this investigation demonstrate that additional calibrated and verified geophysical logs are required in the LBBNRD.

Examples of additional logging would be borehole flow meter logs and geophysical logs including gamma, neutron, electrical, and induction logs. Detailed aquifer characteristics can be accomplished with nuclear magnetic resonance logging (NMR). This is a quick and effective way to characterize porosity and water content, estimates of permeability, mobile/bound water fraction, and pore-size distributions with depth. This is very cost effective when compared to traditional aquifer tests.

3.4 Groundwater Management: Control Areas, Recharge Areas - The hydrogeologic framework in this report provides the location and extent of high transmissive and saturated aquifers. Conversely, it also shows areas where high-capacity wells may be limited due to the aquifer characteristics. It is recommended that these areas be used to define the control areas based on empirical data of the AEM coupled with water quality and groundwater levels. The geospatial data products delivered with this report can be directly opened in ESRI's ArcGIS Pro and can be used to provide guidance in the establishment on control areas. These data can also be invaluable to the producers/developers within the area in replacing wells and drilling new wells. These data can be used by the LBBNRD in assessing the well permits of the area and assisting the interested parties to drill successful wells. This study mapped areas that are windows to the deeper aquifers. These areas may be considered for special recharge projects. These areas also may require additional protections to be added to avoid groundwater quality issues due to the direct conduit of the surface to the deeper aquifer systems. Any management decisions that would propose recharge would need to be weighed against current land use and recharge water availability. The low resistivity < 7 ohm-m depth map that is interpreted as a regional saline water interface can be used to provide guidance in well permitting to avoid any potential wells from penetrating a confining clay or to allowing infiltration of saline waters into the Quaternary aquifer system. Utilizing the 3D products including the profiles and maps can allow the staff and board of the LBBNRD to make informed decisions on the management of the water resources within the District.

4. DELIVERABLES

The following are included as deliverables:

- Raw Data Files - SkyTEM files *.gex, *.skb, *.lin
- Raw EM Mag data as ASCII *.xyz
- SCI inversion as ASCII *.xyz in array column format
- Interpretations as ASCII *.xyz
- ESRI GIS files – raster grids (*.tif) and shapefiles in an ESRI ArcGIS Pro map package (.mpkx).
- 2D profiles, Surfaces, and 3D fence diagrams of the AEM survey inversion results
- Files compatible with GeoScene3D and the Nebraska GeoCloud
- LBBNRD 2025 AEM 3D voxel files (LeapFrog compatible)
- KMZs for LBBNRD AEM flight lines

Table of Contents

1 Introduction 1
1.1 Purpose of Current Project 1
2 Summary of the Geology and Hydrogeology of the Lower Big Blue Natural Resources District 7
2.1 Bedrock Geology 7
2.2 Hydrogeology in the LBBNRD 9
3 Additional Background Information 20
3.1 Boreholes 20
4 Geophysical Methodology, Acquisition and Processing 22
4.1 Geophysical Methodology 22
4.2 Flight Planning/Utility Mapping 23
4.3 AEM Survey Instrumentation 24
4.4 Data Acquisition 26
4.4.1 Primary Field Compensation 32
4.4.2 Automatic Processing 32
4.4.3 Manual Processing and Laterally-Constrained Inversions 32
4.4.4 Power Line Noise Intensity (PLNI) 35
4.4.5 Magnetic Field Data 38
4.5 Spatially-Constrained Inversion 39
5 AEM Results and Interpretation 43
5.1 Interpretative Process 43
5.1.1 Merging AEM Flight Lines 43
5.1.2 Construction of the Project Digital Elevation Model 45
5.1.3 Borehole-Only Surface of the Bedrock 47
5.1.4 Interpretative 2D Profiles 48
5.1.5 Interpretative Surface Grids 56
5.1.6 Water Table 69
5.1.7 Transmissivity Maps 75
5.1.8 Specific Capacity Maps 80
5.1.9 Geologic Map Updates 80
5.1.10 3D Interpretative Voxel Grids 81
5.2 Comparison of AEM Inversion Resistivity to Borehole Geophysical Resistivity Logs 88

5.2.1 Resistivity Relationship in the Quaternary Aquifer System 93
5.2.2 Resistivity Relationship in the Cretaceous Dakota Group Aquifer System 94
5.3 Hydrogeological Framework of the LBBNRD 2025 AEM Survey Area 95
5.3.1 The Hydrogeology of the Quaternary 100
5.3.2 Hydrogeology of the Cretaceous Dakota Group 113
5.3.3 The Permian/Pennsylvanian Bedrock Hydrology 124
5.3.4 Groundwater in LBBNRD 2025 AEM Survey Area 124
5.3.5 Estimation of Aquifer Volume/Water Storage for the 2025 LBBNRD AEM Survey Area .. 134
5.3.6 Groundwater Quality in the LBBNRD 2025 AEM Survey Area 139
5.3.7 Recharge in the LBBNRD 2025 AEM Survey Area 143
5.4 New Understanding of AEM Framework Applied to Water Management Efforts in in the LBBNRD 2025 AEM Survey Area 148
5.5 Key AEM Findings 149
5.5.1 Boreholes 149
5.5.2 Digitizing Interpreted Geological Contacts 149
5.5.3 Resistivity/Lithology Relationship 149
5.5.4 Hydrogeological Framework of the LBBNRD 2025 AEM Survey Area 150
5.5.5 Estimation of Aquifer Volume and Water in Storage in the LBBNRD AEM Survey Area .. 150
5.5.6 Groundwater Quality in the LBBNRD 2025 AEM Survey Area 151
5.5.7 Potential Recharge Zones within the LBBNRD 2025 AEM Survey Area 152
5.5.8 Using AEM Results to Implement Groundwater Management 152
5.6 Recommendations 153
5.6.1 Additional AEM Mapping 153
5.6.2 Siting new test holes and production wells 153
5.6.3 Aquifer testing and borehole logging 154
5.6.4 Groundwater Management: Control Areas, Recharge areas 154
6 Description of Data Delivered 155
6.1 Tables Describing Included Data Files 155
6.2 Description of Included Google Earth KMZ Data and Profiles 167
6.2.1 Included README for the LBBNRD 2025 Interpretation KMZ 167
7 References 172
Appendix 1. LBBNRD AEM Flight Line 2D Profiles A1-1

Appendix 2. LBBNRD 3D Images A2-1

Appendix 3. Data Deliverables

List of Figures

Figure 1-1. Natural resources district map showing the location of the Lower Big Blue Natural Resources District (LBBNRD) in southeastern Nebraska 4

Figure 1-2. Google Earth image of the LBBNRD 2025 AEM survey area including major roads 5

Figure 1-3. Map of 2025 LBBNRD AEM flight lines with line number labels 6

Figure 2-1. Nebraska bedrock geology map (Burchett and Pabian, 1992) 11

Figure 2-2. Upper-most bedrock geology units map of eastern Nebraska (from Divine and Sibray, 2017, originally Burchett, 1986) 12

Figure 2-3. Locations of wells in secondary aquifers relative to the High Plains aquifer 13

Figure 2-4. Areas of Nebraska underlain by paleovalley aquifers (modified from Korus et al. (2013)) 14

Figure 2-5. Areas of Nebraska underlain by glacial deposits (modified from Korus et al. (2013)) 15

Figure 2-6. Areas of Nebraska underlain by alluvial aquifers (modified from Korus et al. (2013)) 16

Figure 2-7. Average annual net recharge to groundwater based on data from 2000 to 2009 (modified from Szilagyi and Jozsa, 2012) 17

Figure 2-8. Elevation of the potentiometric surface in the paleovalley aquifers of eastern Nebraska (modified from Korus et al. (2013)) 18

Figure 2-9. Transmissivity of the primary aquifers of Nebraska, including the High Plains aquifer, alluvial aquifers, glacial aquifers, and paleovalley aquifers 19

Figure 3-1. NE-CSD and NE-DNR borehole logs used for quality control and interpretative purposes 21

Figure 4-1. Schematic of an airborne electromagnetic survey 22

Figure 4-2. A) Example of a dB/dt sounding curve. B) Corresponding inverted model values. C) Corresponding resistivity earth model. 23

Figure 4-3. SkyTEM304M frame, including instrumentation locations and X and Y axes. Distances are in meters. Instrumentation locations listed in Table 4-1. 25

Figure 4-4. Photo of the SkyTEM304M system in suspension beneath the helicopter 25

Figure 4-5. LBBNRD 2025 AEM flight lines grouped by acquisition date 27

Figure 4-6. LBBNRD 2025 AEM flight lines ground speed 28

Figure 4-7. LBBNRD 2025 AEM flight lines flight height above the ground surface 29

Figure 4-8. LBBNRD 2025 AEM flight lines pitch angle in the +/-X direction of travel 30

Figure 4-9. LBBNRD 2025 AEM flight lines Y roll angle perpendicular to the direction of travel 31

Figure 4-10. Example locations of electromagnetic coupling with pipelines or power lines. 33

Figure 4-11. A) Example of AEM data affected by electromagnetic coupling in the Aarhus Workbench editor. The top group of lines is the unedited data with the Low Moment on top and the High Moment on the bottom. The bottom group shows the same data after editing..... 34

Figure 4-12. A) Example of Laterally-Constrained inversion results where AEM data affected by coupling with pipelines and power lines were not removed. B) Inversion results where AEM data affected by coupling were removed. 35

Figure 4-13. Power Line Noise Intensity (PLNI) map of the LBBNRD 2025 project area. 36

Figure 4-14. Locations of inverted data (blue lines) along the AEM flight lines (red lines) on the LBBNRD 2025 AEM survey area. 37

Figure 4-15. Residual magnetic Total Field intensity data for the LBBNRD 2025 AEM survey area corrected for diurnal drift, with the International Geomagnetic Reference Field (IGRF) removed..... 38

Figure 4-16. An example of an AEM profile illustrating increasing model layer thicknesses with depth. . 39

Figure 4-17. Data/model residual histogram for the LBBNRD 2025 SCI inversion results 41

Figure 4-18. Map of data inversion model residuals for the LBBNRD 2025 SCI inversion results..... 42

Figure 5-1. The flight lines and the connected merged lines for the 2025 LBBNRD AEM survey..... 44

Figure 5-2. Map of the ground surface Digital Elevation Model for the 2025 LBBNRD AEM survey 46

Figure 5-3. Map of the project boundary showing the data points used to interpolate the bedrock surface elevation..... 51

Figure 5-4. 8.5-mile-long southwest-northeast line L100011 52

Figure 5-5. 8.5-mile-long east-west line L100070..... 53

Figure 5-6. 17.5-mile-long north-south line L190191 54

Figure 5-7. 9.5-mile-long north-south line L190271 55

Figure 5-8. Map displaying the elevation of the top of the Cretaceous Greenhorn/Graneros (***Kgg***) Group 58

Figure 5-9. Map displaying the elevation of the top of the Cretaceous Dakota (***Kd***) Group..... 59

Figure 5-10. Map displaying the elevation of the top of undifferentiated Permian units 60

Figure 5-11. Map displaying the elevation of the top of bedrock 61

Figure 5-12. Map displaying the depth to the top of Cretaceous Greenhorn/Graneros (***Kgg***) Group..... 62

Figure 5-13. Map displaying the depth to the top of Cretaceous Dakota (***Kd***) Group 63

Figure 5-14. Map displaying the depth to the top of undifferentiated Permian units..... 64

Figure 5-15. Map displaying the depth to the top of bedrock 65

Figure 5-16. Map of displaying the total thickness of the Quaternary (***Q***) material 66

Figure 5-17. Map of displaying the total thickness of the Cretaceous Greenhorn/Graneros (***Kgg***) material 67

Figure 5-18. Map displaying the total thickness of Cretaceous Dakota (***Kd***) Group 68

Figure 5-19. Map of water table elevation surface and the control points used to interpolate the surface 70

Figure 5-20. Map showing the (a) elevation and (b) depth of and to the water table (ft bgs) 71

Figure 5-21. Map displaying the saturated thickness of the Quaternary (***Q***) materials 72

Figure 5-22. Map displaying the saturated thickness of the Cretaceous Greenhorn and Graneros (***Kgg***) Group 73

Figure 5-23. Map displaying the saturated thickness of the Cretaceous Dakota (***Kd***) Group 74

Figure 5-24. Map of the calculated transmissivities within the marginal, aquifer, and coarse aquifer materials of the ***Q*** deposits in the LBBNRD 2025 AEM survey area with an overlay of digitized contours from Summerside and Myers (2005) 77

Figure 5-25. Map of the calculated transmissivity within the marginal, aquifer, and coarse aquifer material of the ***Q*** deposits in the LBBNRD 2025 AEM survey area without the Summerside and Myers (2005) transmissivity contours 78

Figure 5-26. Map of the calculated transmissivity within Cretaceous Dakota Group (*Kd*) deposits over > 18 ohm-m “Sand Dominant Materials” in the LBBNRD 2025 AEM survey area 79

Figure 5-27. Map of the calculated transmissivities within the saturated Coarse, Aquifer, and Marginal materials within the ***Q*** deposits along with the specific capacity of the NE-DWEE wells designated as being completed within the ***Q*** deposits based on screen interval 82

Figure 5-28. Map of saturated ***Kd*** (over 18 ohm-m) along with the specific capacity of the NE-DWEE wells screened within the ***Kd*** 83

Figure 5-29. Map of saturated ***Kd*** (over 35 ohm-m) along with the specific capacity of the DNR wells screened within the ***Kd*** 84

Figure 5-30. Map of geologic units by Burchett (1986) and Burchett and Pabian (1992) with the refined extent of ***Kd*** shown in bright green and ***Kgg*** shown in yellow 85

Figure 5-31. Exploded 3D Voxel model of the stratigraphy of the LBBNRD 2025 AEM area showing unsaturated and saturated Quaternary (***Q***) and Cretaceous Dakota Group (***Kd***) material and undifferentiated Permian Chase and Council Grove Groups (***P***) 86

Figure 5-32. Interpreted depth to the top of the saline water interface 87

Figure 5-33. Graph of the three 16-inch normal resistivity log values (blue line) and the inverted airborne electromagnetic average resistivity values and errors bars of one standard deviation (red line) within 1,500 feet of 01-CS-2019 and 03-CS-2019 and 2,700 feet for 01-LBB-2023 89

Figure 5-34. A segment of survey line L100041 90

Figure 5-35. A segment of survey line L100011 91

Figure 5-36. A segment of survey line L100031 92

Figure 5-37. Plot displaying the resistivities by major Quaternary (***Q***) aquifer material color categories used in the LBBNRD 2025 AEM survey: blue- non-aquifer materials, tan- marginal aquifer materials, yellow- aquifer materials, brown- coarse aquifer materials 93

Figure 5-38. Plot displaying the Cretaceous Dakota Group (***Kd***) resistivities by dominant material and the color categories used in the LBBNRD 2025 AEM survey 94

Figure 5-39. Bedrock map of the survey area modified from Burchett and Pabian (1992) using the LBBNRD 2025 AEM survey results 96

Figure 5-40. 3D Fence Diagram looking to the north of the interpreted distributions of aquifer material within the LBBNRD 2025 AEM survey area 97

Figure 5-41. 3D Fence Diagram looking to the north of the interpreted distributions of aquifer material within the LBBNRD 2025 AEM survey area 98

Figure 5-42. 3D exploded voxel model looking north of the LBBNRD 2025 AEM survey area showing Quaternary (***Q***) unsaturated and saturated, Cretaceous Greenhorn and Graneros (***Kgg***), and Cretaceous Dakota Group (***Kd***) saturated, and the undifferentiated Permian/Pennsylvanian Groups (***P***) 99

Figure 5-43. Map of the Quaternary (***Q***) total thickness within the LBBNRD 2025 AEM survey area 102

Figure 5-44. 3D Voxel diagram looking to the north of the interpreted distributions of total aquifer and coarse aquifer material of the Quaternary (***Q***) within the LBBNRD 2025 AEM survey area 103

Figure 5-45. 3D Voxel diagram looking to the north of the interpreted distributions of the total non- and marginal-aquifer materials of the Quaternary (*Q*) within the LBBNRD 2025 AEM survey area 104

Figure 5-46. East-West AEM flight line L100041 105

Figure 5-47. North-south AEM flight line L190191 106

Figure 5-48. North-south AEM flight line L190253 107

Figure 5-49. Map of the total saturated Quaternary (***Q***) thickness within the LBBNRD 2025 AEM survey area calculated using the Spring 2025 LBBNRD water levels 108

Figure 5-50. Map of the Quaternary (***Q***) aquifer and coarse aquifer material saturated thickness within the LBBNRD 2025 AEM survey area calculated using the Spring 2025 LBBNRD water levels 109

Figure 5-51. Map of the saturated Quaternary (***Q***) marginal aquifer materials (a), and saturated non-aquifer material thickness (b) within the LBBNRD 2025 AEM survey area calculated using the Spring 2025 LBBNRD water levels 110

Figure 5-52. Map of the estimated transmissivity (gpd/feet) of the Quaternary (***Q***) marginal aquifer materials, aquifer materials, and coarse aquifer materials within the LBBNRD 2025 AEM survey area . 111

Figure 5-53. Map of the estimated transmissivity (gpd/feet) of the Quaternary (**Q**) marginal aquifer materials, aquifer materials, and coarse aquifer material transmissivity within the LBBNRD 2025 AEM survey area 112

Figure 5-54. Map of the depth to the top of Cretaceous Dakota Group (***Kd***) 114

Figure 5-55. Map of the total thickness (a) and the of the saturated thickness (b) of the Cretaceous Dakota Group (***Kd***) 115

Figure 5-56. 3D Voxel diagram looking to the north of the interpreted Cretaceous Dakota Group (***Kd***) distributions of cemented sand and sand dominant as well as sand and silt dominant material > 18 ohm-m within the LBBNRD 2025 AEM survey area 116

Figure 5-57. 3D Voxel diagram looking to the north of the interpreted Cretaceous Dakota Group (***Kd***) distributions of cemented sand and sand dominant material > 35 ohm-m within the LBBNRD 2025 AEM survey area 117

Figure 5-58. 3D Voxel diagram looking to the north of the interpreted Cretaceous Dakota Group (***Kd***) distributions of silt and sand dominant material > 18 ohm-m and the red-yellow area of < 7 ohm-m indicating the estimated saline water within the LBBNRD 2025 AEM survey area 118

Figure 5-59. East-west AEM flight line L100041 119

Figure 5-60. Map of the Cretaceous Dakota Group (***Kd***) total saturated thickness of the sandstone and sand-dominant materials within the LBBNRD 2025 AEM survey are with resistivities >18 ohm-m 120

Figure 5-61. East-west AEM flight line L100061 121

Figure 5-62. North-south AEM flight line L190201 122

Figure 5-63. Map of the estimated transmissivity (gpd/feet) of the Cretaceous Dakota Group (***Kd***) saturated thickness of the sandstone and sand dominant materials with resistivities > 18 ohm-m within the LBBNRD 2025 AEM survey area 123

Figure 5-64. Map of the extent of the bedrock units (Cretaceous Greenhorn/Graneros (***Kgg***), Cretaceous Dakota Group (***Kd***), Undifferentiated Permian/Pennsylvanian (***P***) and the NE-DWEE wells that are dually completed in the Quaternary (***Q***) and the bedrock units 126

Figure 5-65. Map of the estimated Transmissivity (T) (gpd/ft) of the Quaternary (***Q***) coarse, aquifer, and marginal aquifer materials with the Specific Capacity (SC) of the NE-DWEE registered wells completed within the ***Q*** 127

Figure 5-66. Map of the saturated Transmissivity (T) (gpd/ft) Cretaceous Dakota Group (***Kd***) with resistivities >18 ohm-m cemented sand and sand dominant with the Specific Capacity (SC) of the NE-DWEE registered wells completed within the ***Q*** and ***Kd*** 128

Figure 5-67. 3D voxel model of the saturated Quaternary (***Q***) coarse and aquifer materials plus the saturated Cretaceous Dakota Group (***Kd***) with resistivities > 18 ohm-m cemented sand and sand

dominant material with the Specific Capacity (SC) of the all NE-DWEE registered wells completed within the area 129

Figure 5-68. North-south AEM flight line L190291 130

Figure 5-69. 3D Fence Diagram looking to the west of the interpreted distributions of aquifer material within the NNRD (AGF, 2024b), LBBNRD 2024 (AGF, 2025) and LBBNRD 2025 AEM survey area 131

Figure 5-70. Map of the elevation of the bedrock in the area of the LBBNRD 2025 survey including the adjacent bedrock from the 2024 LBBNRD (AGF, 2025), NNRD (AGF, 2024b) and the Lower Platte South Natural Resources District 132

Figure 5-71. 3D Fence Diagram looking to the north of the interpreted distributions of aquifer material within the NNRD (AGF, 2024b), LBBNRD 2024 (AGF, 2025) and LBBNRD 2025 AEM survey area 133

Figure 5-72. Map of the Non- and Marginal-Aquifer materials within the unsaturated portion of the Quaternary (***Q***) potentially creating a confined aquifer beneath 138

Figure 5-73. Map of the thickness of the unsaturated non- and marginal-aquifer material and the LBBNRD nitrate samples 140

Figure 5-74. Map of the thickness of the unsaturated coarse- and aquifer-material and the LBBNRD nitrate samples 141

Figure 5-75. Map of the depth to the estimated saline water based on the < 7 ohm-m cutoff 142

Figure 5-76. Map of the thickness of the unsaturated coarse and aquifer material that is in the near surface that may provide recharge pathway to lower aquifers 144

Figure 5-77. 3D voxel plot of the near-surface aquifer materials looking to the north 145

Figure 5-78. Northeast-southwest AEM flight line L100011 146

Figure 5-79. Map of the potential recharge locations based on the presence of Coarse and Aquifer materials in the near surface with connections to the deeper aquifers 147

Figure 6-1. Google Earth KMZ of the LBBNRD 2025 AEM survey area showing the AEM Interpretation locations 169

Figure 6-2. Example of clicking on a location in the LBBNRD 2025 AEM survey area 170

Figure 6-3. Example of clicking on link to Profile image for line L190241 in the LBBNRD 2025 interpretation KMZ 171

List of Tables

Table 2-1. Percent coverage of the uppermost bedrock geological units in the Nebraska counties where the Lower Big Blue NRD is located 8

Table 2-2. Ranges of porosity and hydraulic conductivity for different materials (from Divine et al., 2009; adapted from Dominico and Schwartz, 1998) 10

Table 2-3. Ranges of intrinsic permeabilities and hydraulic conductivities for unconsolidated sediments (from Table 4-6, Fetter, 1988) 10

Table 4-1. Positions of instruments on the SkyTEM304M frame, using the center of the frame as the origin, in feet 26

Table 4-2. Positions of corners of the SkyTEM304M transmitter coil, using the center of the frame as the origin in feet 26

Table 4-3. Thickness and depth to bottom for each layer in the Spatially Constrained inversion (SCI) AEM earth models. The thickness of the model layers increase with depth as the resolution of the AEM technique decreases 40

Table 5-1. LBBNRD 2025 AEM lines merged 43

Table 5-2. Number of data points used to interpolate the elevation of the top of ***Kgg***, ***Kd,*** and ***P*** surfaces 56

Table 5-3. Summary of the input into ESRI's raster calculator and the resultant output 57

Table 5-4. Summary of Hydraulic Conductivities, **K**, used to calculate transmissivities 75

Table 5-5. Volumes for Saturated Quaternary (***Q***) aquifer materials underlying the LBBNRD 2025 AEM survey area 137

Table 5-6. Volumes for Saturated Cretaceous Dakota Group (***Kd***) aquifer materials underlying the LBBNRD 2025 AEM survey area 137

Table 6-1. Raw SkyTEM data files 156

Table 6-2. Channel name, description, and units for LBBNRD2025_EM_MAG_AUX.xyz with DEM, magnetic, DGPS, Inclinometer, altitude, and associated data 156

Table 6-3. Channel name, description, and units for LBBNRD2025_AEM_SCI01_INV_v1.xyz with EM inversion results 157

Table 6-4. Channel name description and units for the interpretation results file LBBNRD2025_AEMInterp.xyz 158

Table 6-5. Files containing LBBNRD 2025 raster datasets (.tif format) 159

Table 6-6. Relevant features and extents as LBBNRD 2025 ESRI Shapefiles included in the ESRI map package, LBBNRD2025_AEMSurvey.mpkx 164

Table 6-7. Nebraska Geocloud-import file: LBBNRD2025_SCI01_GeoScene.xyz 165

Table 6-8. Columns in LBBNRD 2025 AEM 3D Voxel files LBBNRD2025_Voxel_AllRho.xyz and LBBNRD2025_Voxel_Quaternary 166

List of Abbreviations

2D	Two-dimensional
3D	Three-dimensional
A*m^2	Ampere meter squared
AEM	Airborne Electromagnetic
AGF	Aqua Geo Frameworks, LLC
AM	Aquifer Material
ASR	Aquifer Storage and Recovery
b	Saturated thickness
dB/dt	Change in amplitude of magnetic field with time
CA	Coarse Aquifer Material
CSD	Nebraska Conservation and Survey Division
DEM	Digital Elevation Model
DOI	Depth of Investigation
DGPS	Differential global positioning system
em, EM	Electromagnetic
ESWL	Estimated Saline Water Level
FEM	Frequency-Domain Electromagnetic
FT	Fourier Transform
FT, ft	Feet
ft^3	cubic feet
Fm	Formation
GIS	Geographic Information System
gpm	Gallons per minute
GWQMA	Groundwater Quantity Management Area
Hr, hr	hours
Hz	Hertz (cycles per second)
IGRF	International Geomagnetic Reference Field
K	Hydraulic Conductivity
Kd	Cretaceous Dakota Group
Kgg	Cretaceous Greenhorn Limestone and Graneros Shale
Km, km	Kilometers
KMZ, kmz	Keyhole Markup language Zipped file
LCI	Laterally-constrained Inversions
LBBNRD	Lower Big Blue Natural Resources District
LPSNRD	Lower Platte South Natural Resources District
M, m	Meters
MAG	Magnetic (data); Magnetometer (instrument)
MCG	Minimum curvature gridding
mg/L	milligram per liter or parts per million (ppm)
mi^2	Miles squared
NAD83	North American Datum of 1983
MAR	Managed Aquifer Recharge
NAVD88	North American Vertical Datum of 1988
NE	Nebraska
NED	National Elevation Dataset
NE-DWEE	Nebraska Department of Water, Energy, and Environment

NMR	Nuclear Magnetic Resonance
NNRD	Nemaha Natural Resources District
NRD	Natural Resources Districts
OM	Geosoft Oasis montaj
P	Undifferentiated Permian/Pennsylvanian Units
Pc	Permian Chase Formation
Pcg	Permian Council Grove Formation
PFC	Primary Field Compensation
PLNI	Power Line Noise Intensity
PPM	Parts per Million also milligrams per Liter (mg/L)
IP	Pennsylvanian
Pa	Permian Admire Group
IPw	Pennsylvanian Wabaunsee Group
Q	Quaternary
Rx	Receiver
recon	Reconnaissance
sec	second
SC	Specific Capacity
SCI	Spatially-Constrained Inversion
SPCS	State Plane Coordinate System
STD	Standard Deviation
SWL	Saline Water Level
T	Transmissivity
TEM	Transient, Time-Domain Electromagnetic
TDEM	Time-Domain Electromagnetic
Tx	Transmitter
UBC	University of British Columbia
UNL	University of Nebraska Lincoln
USGS	United States Geological Survey
UTM	Universal Transverse Mercator
VE	Vertical Exaggeration
V/m^2	Volts per meter squared
WSF	Nebraska Water Sustainability Fund
X, x	The x-direction in a cartesian coordinate system
Y, y	The y-direction in a cartesian coordinate system
Z, z	The z-direction (positive is up) in a cartesian coordinate system

1 Introduction

1.1 Purpose of Current Project

Sound management of groundwater and surface water in eastern Nebraska has become increasingly important in recent years. There are expanding pressures placed on the resources by the ever growing and dynamic demands of: agricultural production, population growth and urbanization, potential contamination from natural and anthropogenic sources, industrial and commercial needs; along with the persistent threat of drought. The discussion below is largely taken from the 2024 LBBNRD Water Sustainability Fund (WSF) application that funded the 2025 AEM survey.

The Lower Big Blue NRD (LBBNRD) Airborne Electromagnetic Hydrogeologic Mapping project (Project) offers the District the ability to understand the geometry and vulnerability of its aquifer formations for use in assessing groundwater quantity and quality. This understanding is particularly vital in areas like the LBBNRD, where aquifer formations are highly variable both in horizontal and vertical space and in terms of water quality. For example, there are two main types of aquifers in the LBBNRD: aquifers in the unconsolidated units that overlie the bedrock, and bedrock aquifers. Within the first group are three main subtypes, including paleovalley aquifers (buried ancient stream valleys), alluvial aquifers, and isolated small-scale aquifers. Within the Project area, the University of Nebraska Conservation Survey Division (CSD) indicates the presence of all the described aquifer types. The CSD principal aquifer dataset represents a useful resource in identifying the presence of aquifer materials. However, it is coarse in resolution as it is based on discrete points where test holes have been drilled. The collection of AEM data provides an understanding of the spatial variability of the aquifer along flight lines where hydrogeologic conditions can change over short distances. The LBBNRD is particularly interested in gaining more information on the aquifer resource in areas of groundwater depletion and/or contamination, increased development, and in areas where well interference between landowners is becoming more commonplace. Historical groundwater quantity and quality monitoring in the LBBNRD has aided the District in exploring the relationships between subsurface composition, recharge, and contamination (i.e., coarse sediments/thin unsaturated zones = higher recharge/more contamination vulnerability, fine-grained sediments/thick unsaturated zones = lower recharge/less contamination vulnerability) in discrete locations, but the spatial extent of these potential impacts is not well understood. It is the LBBNRD's objective to ultimately conduct AEM studies throughout the District, thereby providing a completely robust framework. Funding and feasibility dictate a progressive and phased approach, which began with the award of WSF money in 2022 (WSF #10036) and 2023 (WSF#10061). This specific Project continued this phased approach and applied a more scientifically based method to delineating complex aquifer formations in an area of the LBBNRD that has experienced significant water quantity and quality concerns.

Within the 210-square mile area proposed for this effort, the primary groundwater concerns revolve around quantity and quality. The area contains 16 dedicated monitoring wells used in the NRD's monitoring network for measuring water levels and water quality. Of the 16 dedicated quantity monitoring wells, 5 have water level measurements from 1981 and 4 have water level measurements

from 2011. Seven additional dedicated monitoring wells were constructed in 2016, and have groundwater level measurement data since then, and nitrate concentration data since 2017. While relatively less water quality data has been collected in the area when compared to water quantity, nitrate contamination is a major concern for the area. The LBBNRD has enforced a Water Quality Phase II area just outside of the project area. Within the Phase II area are the wellhead protection areas for drinking water supplied to the City of Beatrice and Village of DeWitt. Within the Project area, are the wellhead protection areas for the Village of Cortland, Village of Clatonia and Village of Pickrell.

Data from the Nebraska Department of Water Energy and Environment (NE-WDEE) Clearinghouse website indicates that at least one well sampled in the project area has a nitrate concentration above 14 mg/L, which is over the drinking water maximum contaminant limit of 10 mg/L. The AEM data collected through the proposed Project would aid the LBBNRD in identifying the connection between areas of high nitrate contamination and the underlying aquifer materials. With this information, the LBBNRD can take a very targeted approach to best management implementation and incentivization.

Regarding water quantity, LBBNRD Groundwater Rules and Regulations dictate that any monitoring network well with a static water level decrease of five feet or more below the baseline level or five percent or more below the upper elevation of the saturated thickness for any well with saturated thickness less than 100 feet for a period of three consecutive years initiates the delineation of a Phase II Groundwater Quantity Management Area (GWQMA). The LBBNRD is currently working to clarify this process with the goal of delineating GWQMAs across the entirety of the District, regardless of an area hitting the water level trigger or not. Information gleaned from this project will facilitate the delineation of these areas. AEM data collected through previous efforts has been effectively used to refine management area boundaries in places where data is scarce or low resolution. Providing graphics and information generated from the AEM data helps aid public understanding of how boundaries are determined and will be vital in promoting acceptance of the areas during public engagement.

One well in the Project area has been at the Phase II designation level for three consecutive years. Several other observation wells have hit the Phase II trigger level at some point over the last five years, and water quantity is a growing concern for the area. The proposed Project would aid the LBBNRD in more clearly assessing groundwater declines and their impacts, as well as refining the boundaries of GWQMAs. While LBBNRD rules dictate increased monitoring of established individually drilled boreholes to assess subsurface materials in a Phase II GWQMA, the remote sensing technique of AEM has the capability of collecting thousands of virtual boreholes at a fraction of the cost of traditional drilling and monitoring. Combining AEM with existing studies and monitoring will result in a robust hydrogeologic framework from which to operate and will provide the best information available to the LBBNRD.

Mapping results produced from the AEM data for this project provide three-dimensional subsurface views of the aquifer materials and estimates of the extents and volumes of the groundwater resources available (See Section 5 and *Appendix 2 – 3D Images*).

This Project mapped a flight block across Saline and Gage counties, covering approximately 493 miles of AEM survey to develop a three-dimensional view of the subsurface. The project consisted of flight line planning within the block area, collection of AEM data along the flight lines, processing of the raw AEM data, interpretation of the processed data (tied to local geologic interpretations from traditional subsurface mapping), and reporting of the overall results. The AEM survey results have been incorporated into a Geographic Information System (GIS) (ESRI's ArcGIS Pro) for use by LBBNRD. The interpretations and GIS will be provided to Nebraska GeoCloud for public use, the CSD, and the NE-DWEE at the time of this final report delivery.

District geologists will have the opportunity to evaluate the AEM survey results with cross-section and ancillary data to make interpretations of the regional geologic setting types encountered and evaluate how well the AEM results match up relative to the cross-sectional data. The resulting map publication and results will provide those interested in the hydrogeology of southeast Nebraska a comprehensive and improved understanding of the varying hydrogeological settings. That interpretation will likely follow the approach used for previous Eastern Nebraska Water Resources Assessment (ENWRA) areas. The LBBNRD will have groundwater aquifer delineations and associated maps to address groundwater quality problems occurring in this block and to help mitigate potential quantity concerns in the area.

A location map showing the LBBNRD is presented in Figure 1-1, a flight line map is presented in Figure 1-2 (also in *Appendix 3 – Deliverables**KMZ**FlightLines*) and a labeled flight line map is presented in Figure 1-3.

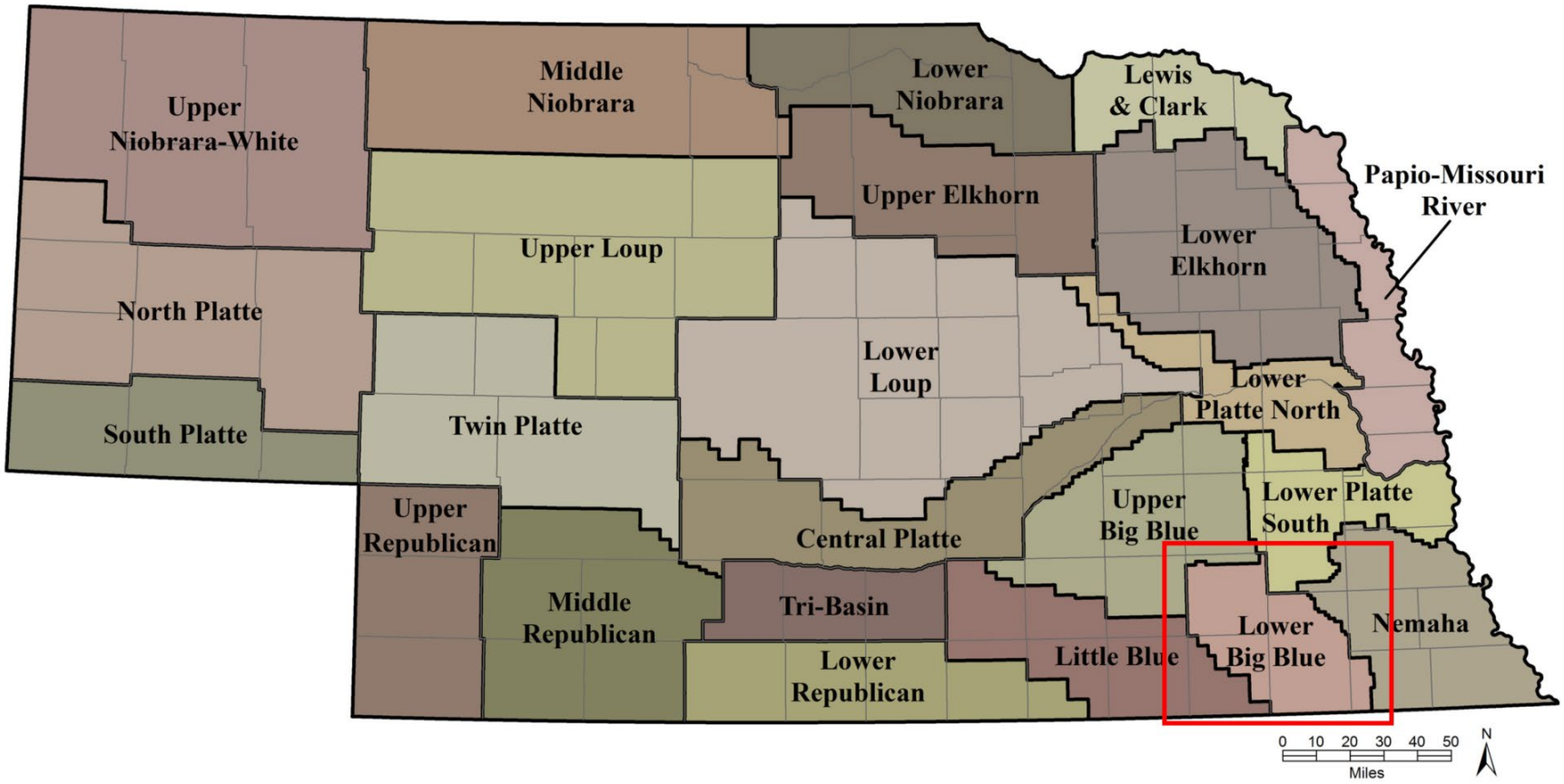


Figure 1-1. Natural resources district map showing the location of the Lower Big Blue Natural Resources District (LBBNRD) in southeastern Nebraska (https://www.lbbnrd.net/) in the red box.

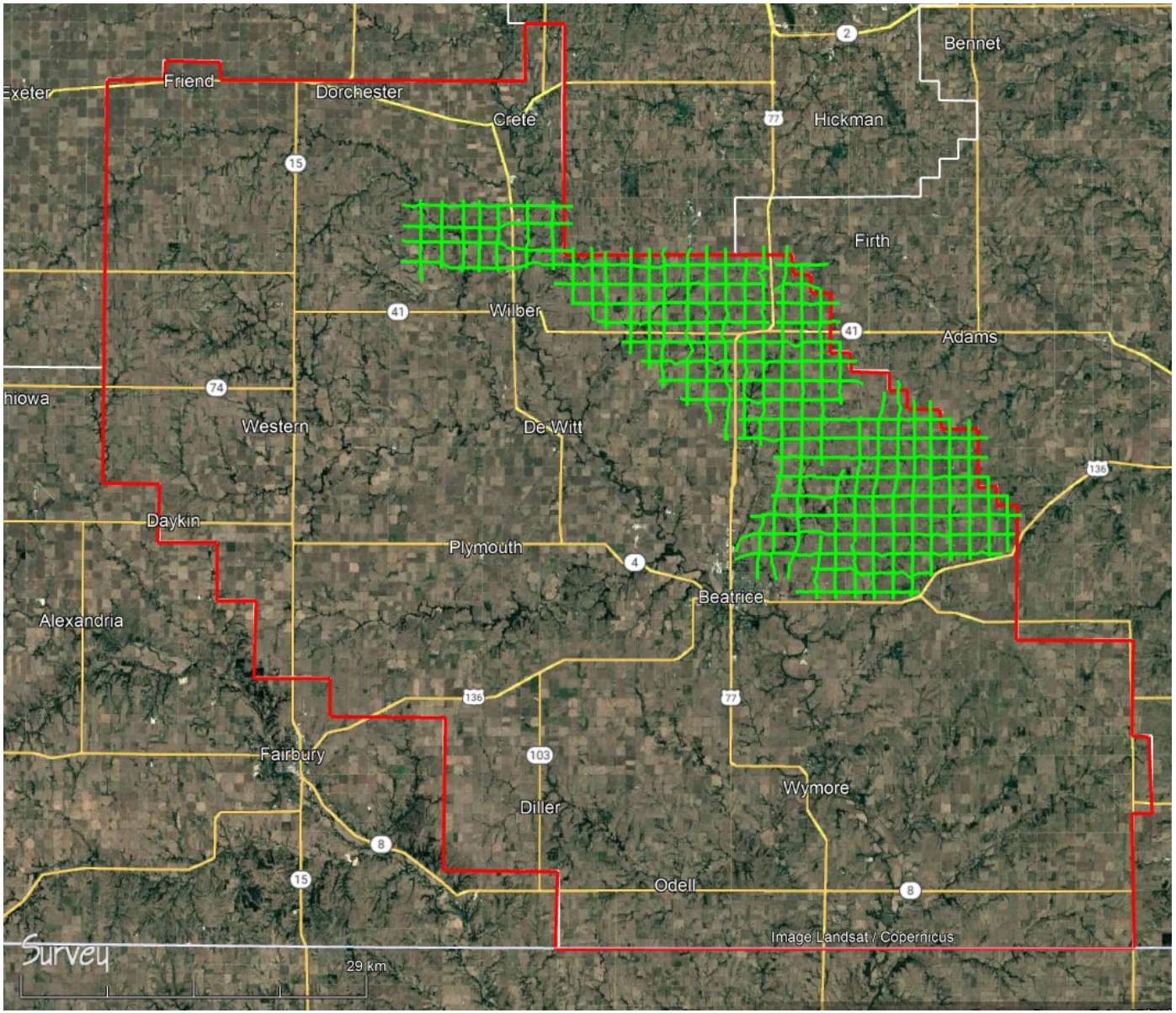


Figure 1-2. Google Earth image of the LBBNRD 2025 AEM survey area with As-Flown flight lines (green), including major roads.

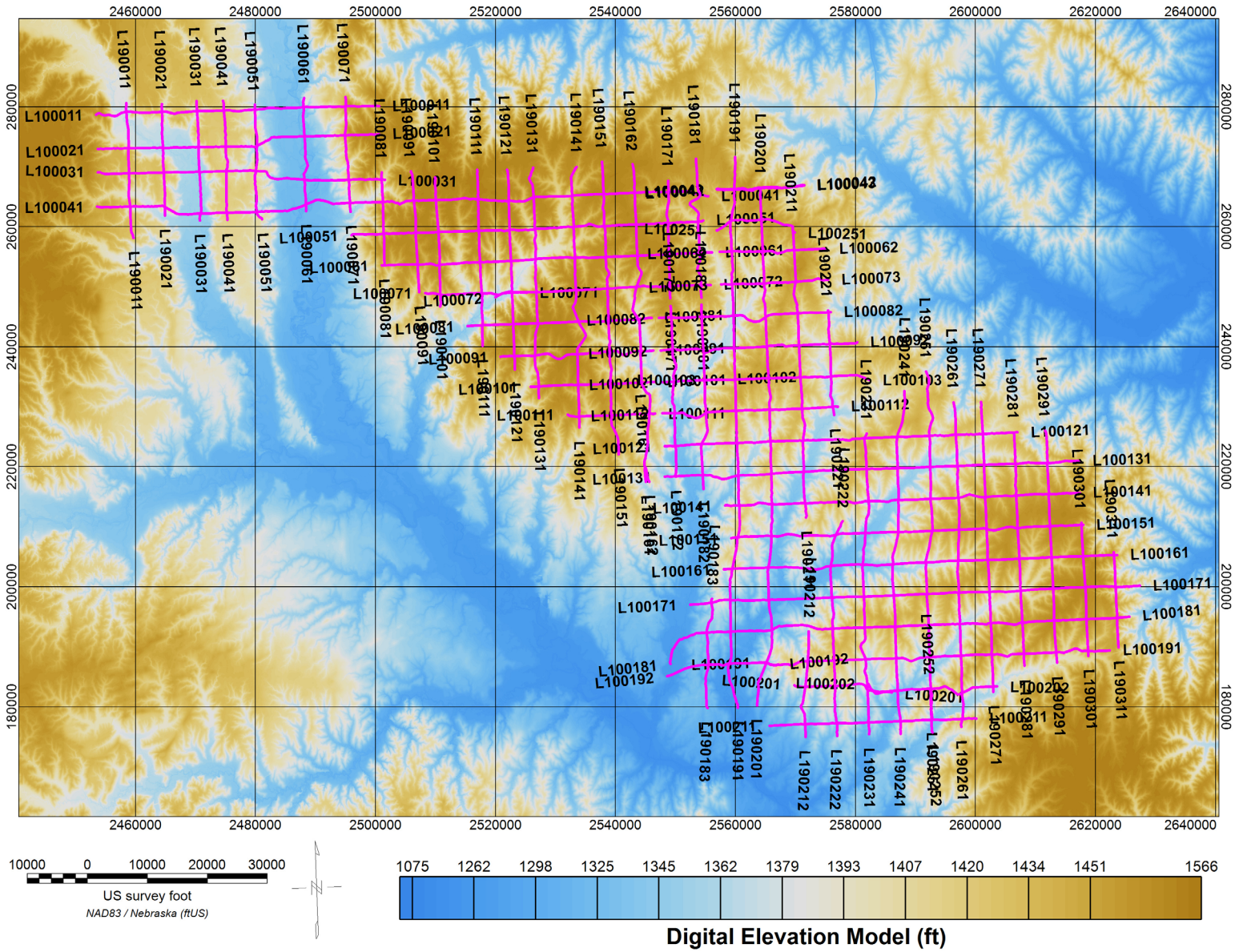


Figure 1-3. Map of 2025 LBBNRD AEM flight lines with line number labels. Map projection is NAD83, Nebraska State Plane, feet.

2 Summary of the Geology and Hydrogeology of the Lower Big Blue Natural Resources District

2.1 Bedrock Geology

The bedrock geology of southeastern Nebraska consists of several, well known, Late-Pennsylvanian to Late-Cretaceous units that have been discussed in many USGS, Nebraska Conservation and Survey Division, and Nebraska Department of Natural Resources reports including Reed (1959), Burchett and Reed (1967), Burchett (1986), Burchett and Pabian (1992), Stoeser et al. (2005), Divine et al. (2009), Korus et al. (2013), Divine and Sibray (2017), Joeckel et al. (2018), and Joeckel et al. (2019).

The geological formation descriptions below are from the USGS "MrData" website (USGS MrData, 2023). The bedrock geologic units in the counties in which the Lower Big Blue Natural Resources District is located, including Saline, Jefferson, Gage, and Pawnee counties, are:

Carlile Shale (Late Cretaceous) - Shale, limestone, and sandstone. At top, locally 5 feet of gray to pale-yellowish brown siltstone or very fine-grained sandstone. Upper 200 feet of shale is dark gray to medium gray; locally contains ironstone concretions, and interbedded with thin siltstone. Lower 80 feet of shale is medium gray, calcareous, and contains many very thin bedded, fossiliferous, shaly limestone and calcareous shale layers. Approximate maximum thickness of 300 ft.

Greenhorn Limestone and Graneros Shale (Late Cretaceous) - Greenhorn Limestone- medium- to light-gray limestone interbedded with argillaceous limestone, marl, and calcareous shale; contains Inoceramus fossils. Upper and lower contacts gradational. Approximate maximum thickness of 30 ft. Graneros Shale- medium- to dark-gray, partly calcareous shale. Interbeds of siltstone, sandstone, and carbonaceous shale, and thin bentonite layers in upper part. Approximate maximum thickness of 60 ft.

Dakota Group (Early Cretaceous) - Upper part is white, light-gray, brownish-gray, yellow, reddish-brown, and red sandstone and shale. Sandstone is very fine to coarse grained, friable, micaceous, cross-bedded, and lenticular; locally contains gravel near base. contains numerous zones of ironstone and siltstone concretions of variable thickness. Middle part is light-gray, yellow, red brown and dark-gray, sandy carbonaceous shale; commonly contains a zone of concretions near top. Lower part is sandstone similar to that in the upper part except there are zones of siderite concretions and, locally, a basal zone of chert pebbles. Approximate maximum thickness of 600 ft.

Chase Group (Permian) - Limestone and shale. Limestone is light gray to dark gray, yellowish gray to pale yellowish brown. Two limestones in the upper part are thin bedded to medium bedded, argillaceous, cherty and fossiliferous. Two limestones in the lower part of the Chase Group are medium to massive bedded, very cherty, and fossiliferous. Shale is gray, green, red, reddish brown, calcareous, arenaceous, fossiliferous, and, locally, fissile. Approximate maximum thickness of 300 ft.

Council Grove Group (Permian) - Shale and interbedded limestone. Shale is gray, green, red, reddish brown, or maroon, sandy, calcareous, fossiliferous, locally fissile; several fissile black shale beds are in the lower 75 feet. Interbedded dark- to light-gray, medium- to thick-bedded, argillaceous, cherty

limestone beds are very fossiliferous and locally contain shale partings. Approximate maximum thickness of 300 ft.

Admire Group (Permian) - Shale and interbedded limestone. Shale is dark gray to light gray, brown, red, or green, sandy, calcareous, and fossiliferous. The Admire Group is interbedded dark- to light-gray, very thin to medium bedded, argillaceous, very fossiliferous limestone beds. Near top of the Admire Group is a fine-grained, micaceous sandstone bed that underlies a stromatolite limestone bed which has distinctive lobate bedding. Approximate maximum thickness of 150 ft.

Wabaunsee Group (Late Pennsylvanian - Virgilian) - Shale, sandstone, and interbedded limestone. Shale is light gray to dark gray, greenish gray, red, or blacks that contains very thin layers of siltstone and is, locally, very fossiliferous and carbonaceous. The sandstone is brownish gray to yellowish gray, or gray, argillaceous, and micaceous. The limestone is dark gray to medium gray, yellowish gray, thin bedded to thick bedded; very fossiliferous. The Wabaunsee Group contains coal beds less than 1 ft. thick. The Wabaunsee Group has an approximate maximum thickness of 300 ft.

Shawnee Group (Late Pennsylvanian - Virgilian) - Limestone, shale, and siltstone. Limestone is dark gray to very light gray, yellowish gray, very thin bedded to massive bedded, and fossiliferous. Locally, thin beds are argillaceous and other beds are oolitic and a few contain chert. The shale is medium gray, greenish gray, pale red, dark reddish brown, black, sandy fossiliferous and calcareous. Black shale is, in part, fissile. Siltstone is light gray to greenish yellow, massive, calcareous, and, locally, sandy. The Shawnee Group has an approximate maximum thickness of 200 ft.

A bedrock geology map of all of Nebraska from Burchett and Pabian (1992) is presented in Figure 2-1. The bedrock geology of just eastern Nebraska is presented in Figure 2-2. Table 2-1 presents the percentage of surface area for the different geologic units in the counties in which the LBBNRD is located.

Table 2-1. Percent coverage of the uppermost bedrock geological units in the Nebraska counties where the Lower Big Blue NRD is located (modified from USGS MrData, 2024).

Unit name	Age	Saline (% at surface)	Jefferson (% at surface)	Gage (% at surface)	Pawnee (% at surface)
Carlile Shale	Late Cretaceous	7.6	0.5	-	-
Greenhorn Limestone and Graneros Shale	Late Cretaceous	28.5	10.6	-	-
Dakota Group	Early Cretaceous	63.8	88.2	21.0	-
Chase Group	Permian	-	0.3	48.7	10.0
Council Grove Group	Permian	< 0.1	0.6	26.6	36.4
Admire Group	Permian	-	-	3.7	10.7
Wabaunsee Group	Late Pennsylvanian - Virgilian	-	-	-	42.1
Shawnee Group	Late Pennsylvanian - Virgilian	-	-	-	0.8

2.2 Hydrogeology in the LBBNRD

This section presents images of hydrogeological features in Nebraska that have relevance to the hydrogeological framework in the LBBNRD. Figure 2-3 presents the spatial distribution of the High Plains Aquifer and shows that the northwest half of the LBBNRD includes access to the High Plains Aquifer (modified from Divine and Sibray, 2017). Figure 2-4 presents areas of Nebraska, particularly in southeastern Nebraska, that are underlain by paleovalley aquifers and shows that the LBBNRD has several areas with paleovalley aquifers, including the area over which the 2025 AEM survey was conducted (Korus et al., 2013). Figure 2-5 shows areas of eastern Nebraska that are underlain by glacial deposits and Figure 2-6 shows areas of Nebraska that are underlain by alluvial aquifers including the LBBNRD (Korus et al., 2013).

A map of the average annual net recharge to groundwater in Nebraska (Korus et al., 2013), based on data from 2000 to 2009 (modified from Szilagyi and Jozsa, 2012), is presented in Figure 2-7. The map in Figure 2-7 shows that the LBBNRD has a positive net recharge from 2000 to 2009.

A map of the elevation of the potentiometric surface in the paleovalley aquifers of eastern Nebraska is presented in Figure 2-8 (Korus et al., 2013). In the LBBNRD, the potentiometric surface has an elevation of about 1300 ft to 1400 ft.

A map of the transmissivity of the primary aquifers of Nebraska including the High Plains aquifer, alluvial aquifers, glacial aquifers, and paleovalley aquifers is presented in Figure 2-9 (Korus et al., 2013). The map in Figure 2-9 shows that the paleovalley aquifers in the LBBNRD have moderate to good transmissivity.

Table 2-2 lists different materials and their measured porosity and hydraulic conductivity (**K**) per Dominico and Schwartz (1998). Note that Transmissivity (**T**) (L^2/T) = Hydraulic Conductivity (L/T) x Aquifer Thickness (L) (i.e., **T = K*b**).

Table 2-3 presents another set of permeabilities and hydraulic conductivities from Fetter (1988) that were utilized to develop the transmissivities used in the 2025 LBBNRD AEM interpretation.

Table 2-2. Ranges of porosity and hydraulic conductivity for different materials (from Divine et al., 2009; adapted from Dominico and Schwartz, 1998)

	Material porosity (%)	Hydraulic conductivity (ft/day)	Hydraulic conductivity (m/s)
Gravel	25 to 40	85 to 8,500	$3x10^{-4}$ to 0.03
Coarse sand	30 to 45	0.2 to 1,700	$9x10^{-7}$ to $6x10^{-3}$
Fine sand	25 to 50	0.06 to 60	$2x10^{-7}$ to $2x10^{-4}$
Sandstone	5 to 30	$9x10^{-5}$ to 1.7	$3x10^{-10}$ to $6x10^{-6}$
Silt, loess	35 to 60	$3x10^{-4}$ to 6	$1x10^{-9}$ to $2x10^{-5}$
Till	25 to 40	$3x10^{-7}$ to 0.6	$1x10^{-12}$ to $2x10^{-6}$
Clay	35 to 60	$3x10^{-6}$ to $1x10^{-3}$	$1x10^{-11}$ to $5x10^{-9}$
Shale	0 to 10	$3x10^{-8}$ to $6x10^{-4}$	$1x10^{-13}$ to $2x10^{-9}$

Table 2-3. Ranges of intrinsic permeabilities and hydraulic conductivities for unconsolidated sediments (from Table 4-6, Fetter, 1988).

Material	Intrinsic Permeability (darcys)	Hydraulic Conductivity (cm/s)
Clay	10^{-6} - 10^{-3}	10^{-9} - 10^{-6}
Silt,sandy silts, clayey sands, till	10^{-3} - 10^{-1}	10^{-6} - 10^{-4}
Silty sands, fine sands	10^{-3} - 1	10^{-5} - 10^{-3}
Well-sorted sands, glacial outwash	1 - 10^{2}	10^{-3} - 10^{-1}
Well-sorted gravel	10 - 10^{3}	10^{-3} - 10^{0}

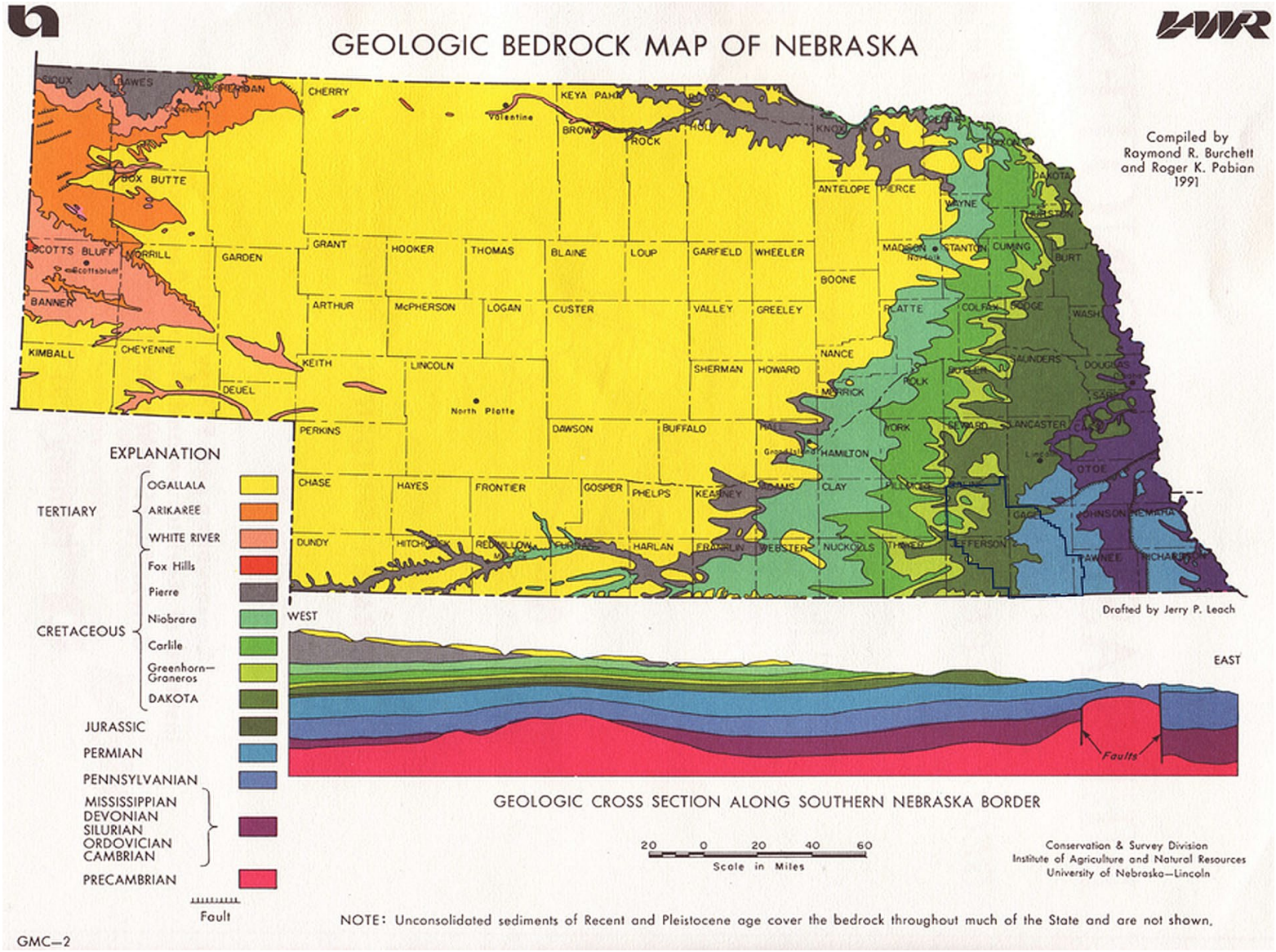


Figure 2-1. Nebraska bedrock geology map (Burchett and Pabian, 1992). Black polygon in southeast corner is the approximate location of the Lower Big Blue Natural Resources District.

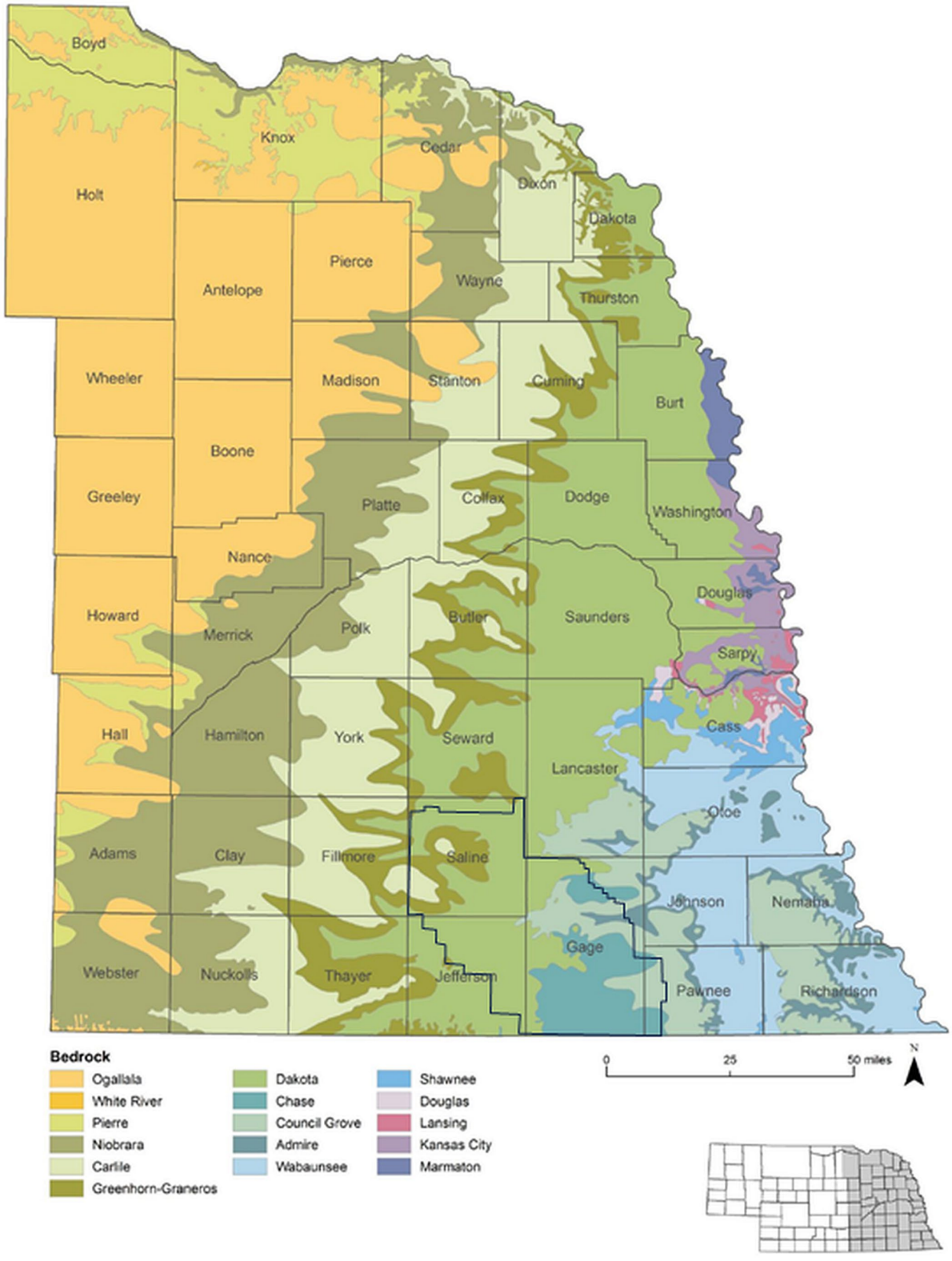


Figure 2-2. Upper-most bedrock geology units map of eastern Nebraska (from Divine and Sibray, 2017, originally Burchett, 1986). Black polygon in southeast corner is the approximate location of the Lower Big Blue Natural Resources District.

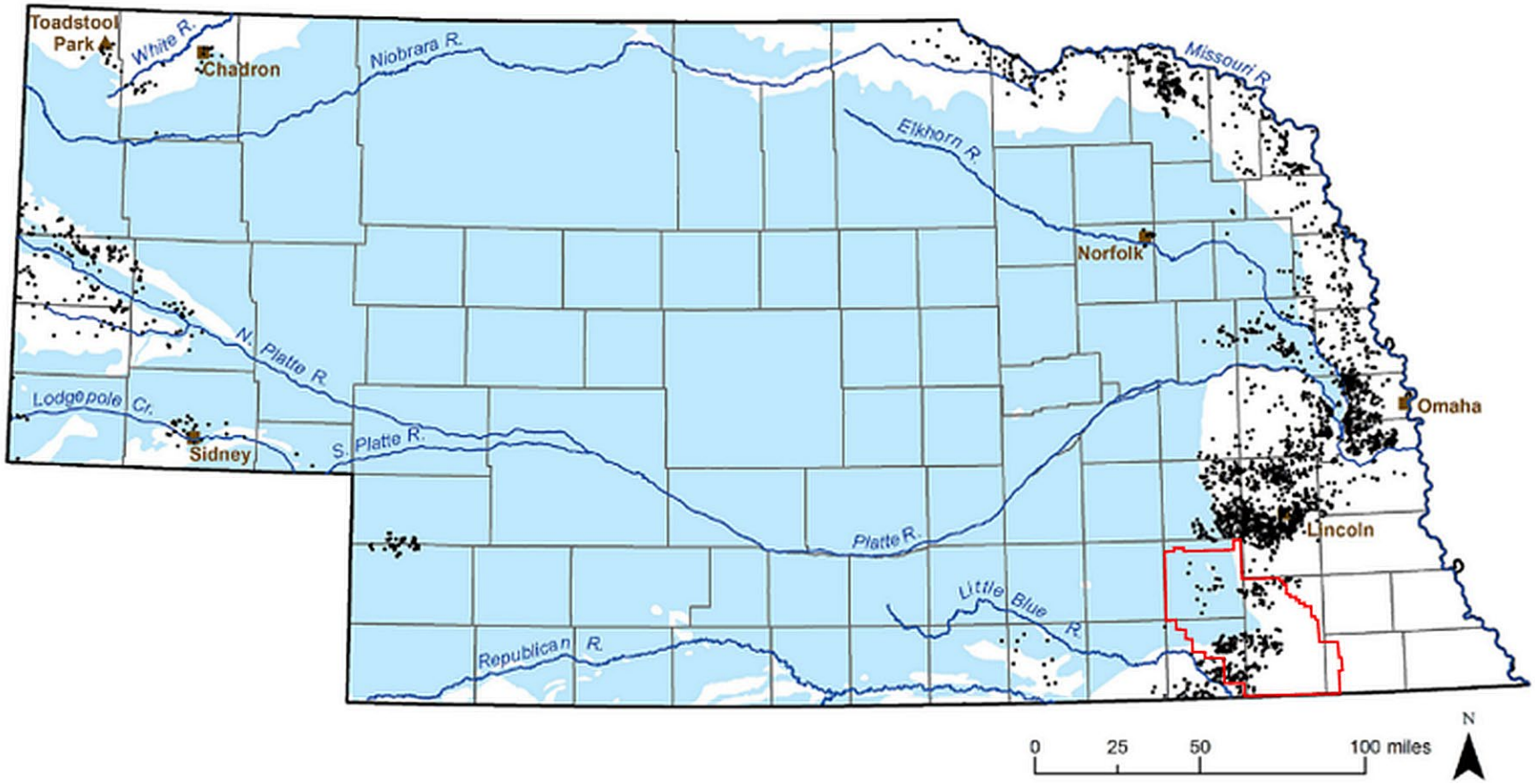


Figure 2-3. Locations of wells in secondary aquifers (black dots) relative to the High Plains aquifer (shown in blue). The approximate position of the Lower Big Blue Natural Resources District is indicated with the red polygon. Modified from Divine and Sibray (2017). The red polygon is the approximate location of the Lower Big Blue Natural Resources District.

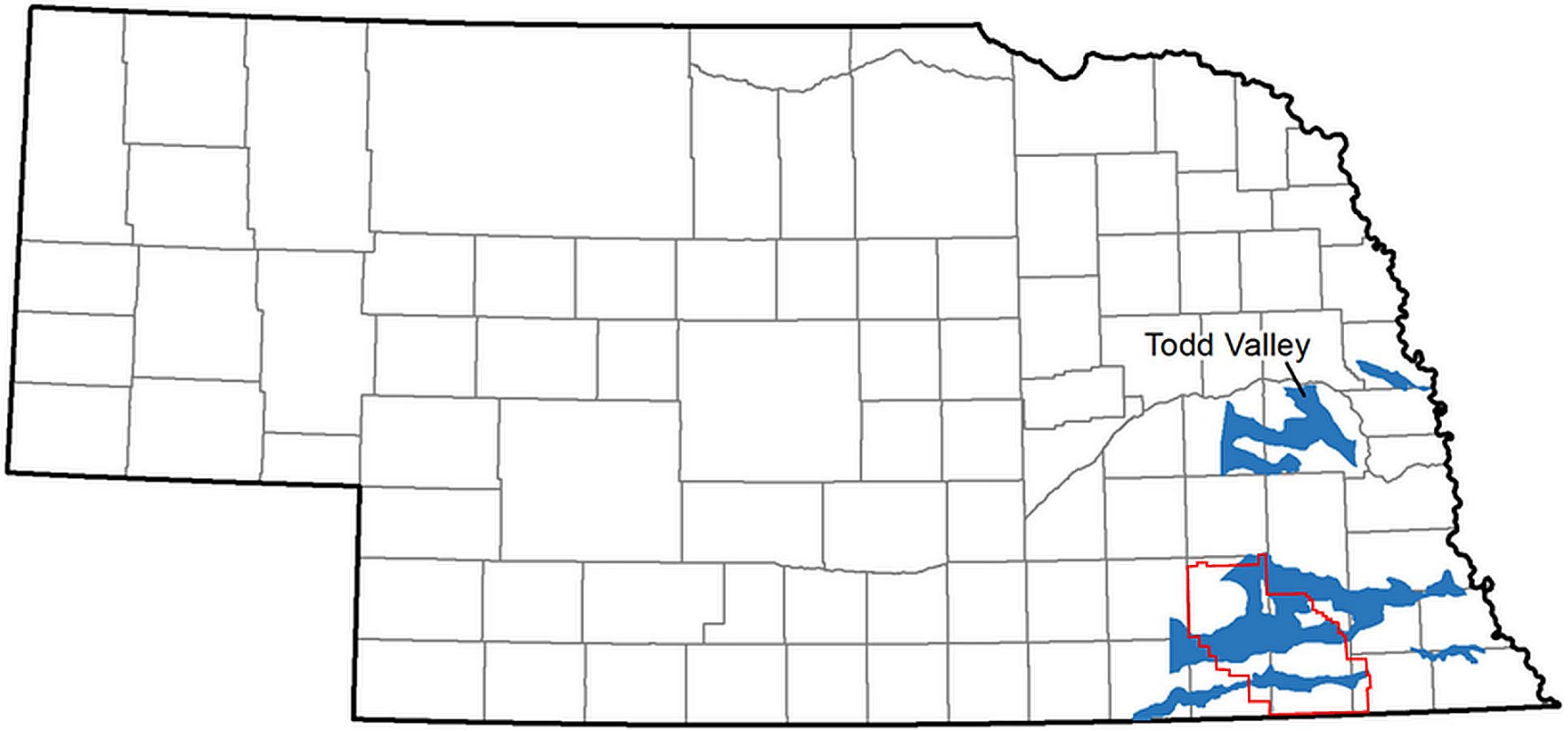


Figure 2-4. Areas of Nebraska underlain by paleovalley aquifers (modified from Korus et al. (2013)). The red polygon is the approximate location of the Lower Big Blue Natural Resources District.

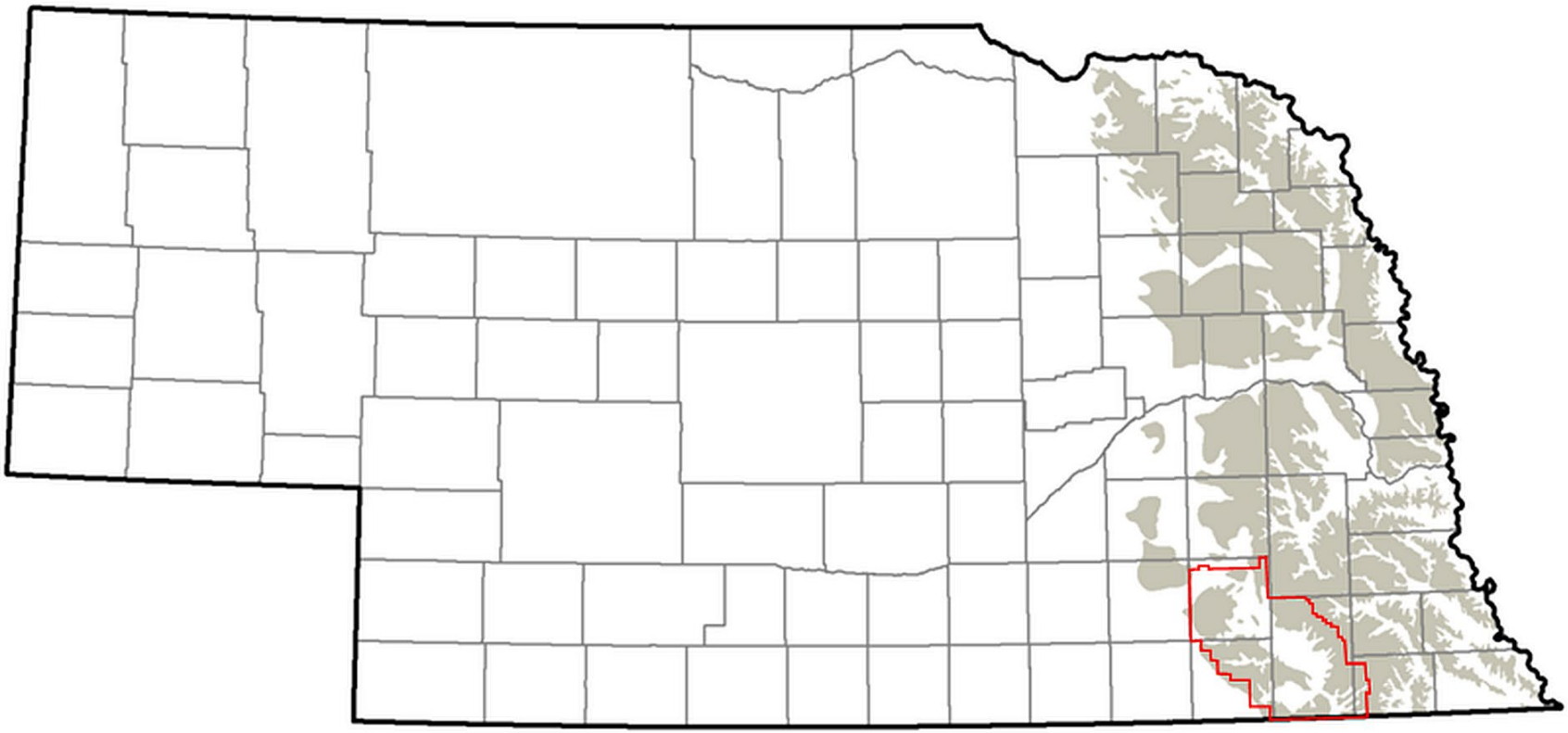


Figure 2-5. Areas of Nebraska underlain by glacial deposits (modified from Korus et al. (2013)). The red polygon is the approximate location of the Lower Big Blue Natural Resources District. Localized aquifers are contained within these deposits.

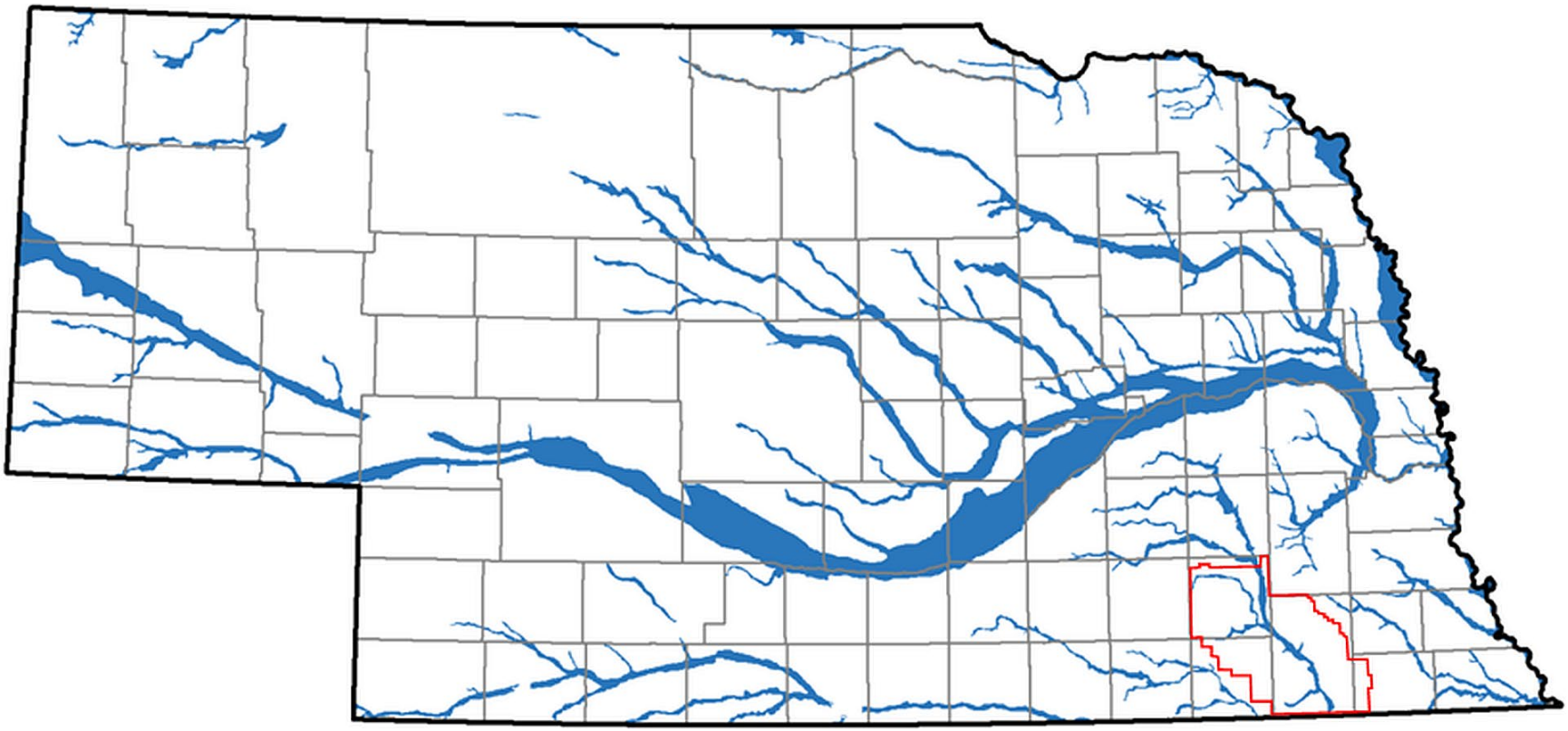


Figure 2-6. Areas of Nebraska underlain by alluvial aquifers (modified from Korus et al. (2013)). The red polygon is the approximate location of the Lower Big Blue Natural Resources District.

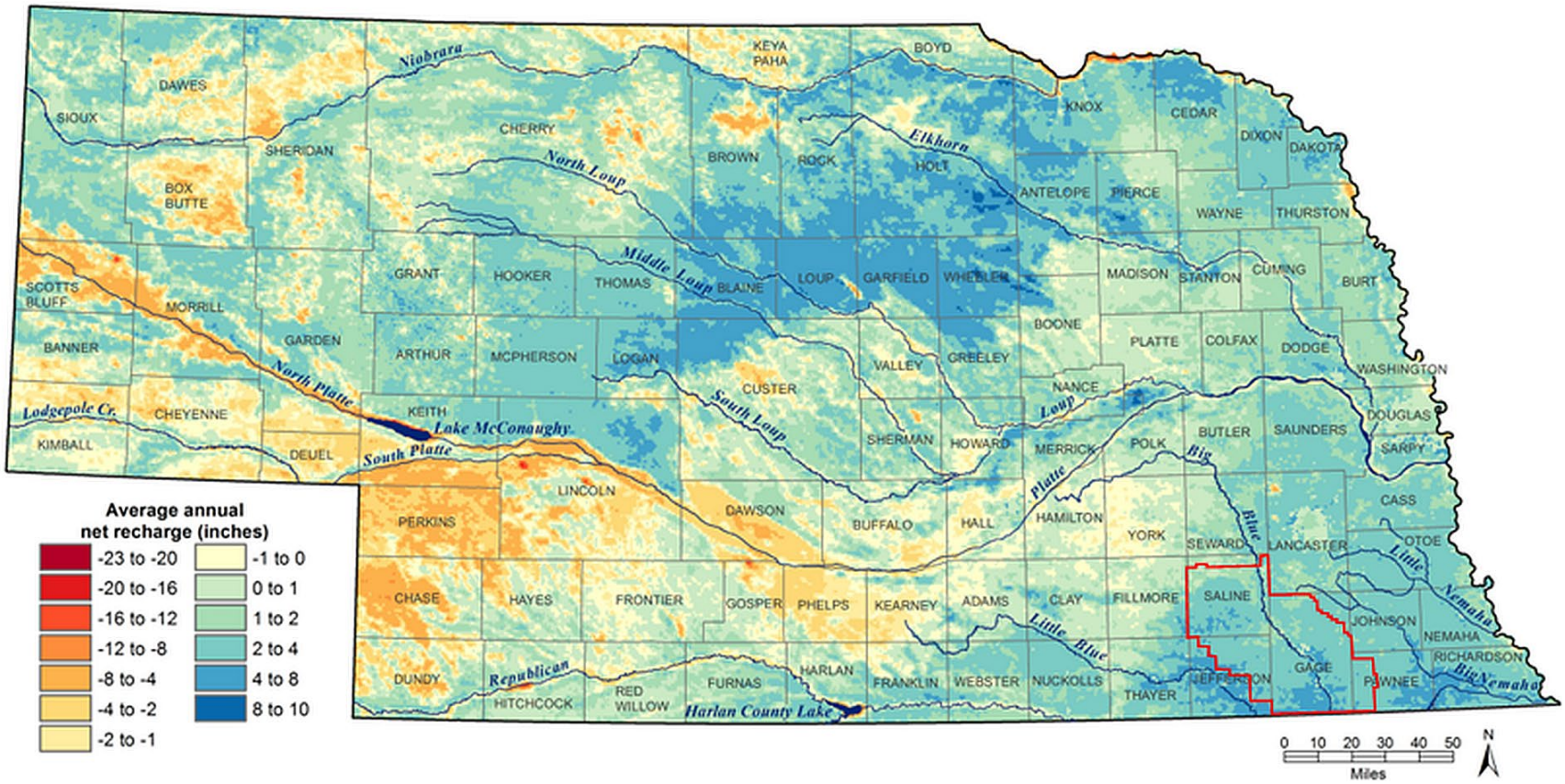


Figure 2-7. Average annual net recharge to groundwater based on data from 2000 to 2009 (modified from Szilagyi and Jozsa, 2012). Negative values indicate that evapotranspiration is greater than precipitation (modified from Korus et al. (2013)). The red polygon is the approximate location of the Lower Big Blue Natural Resources District.

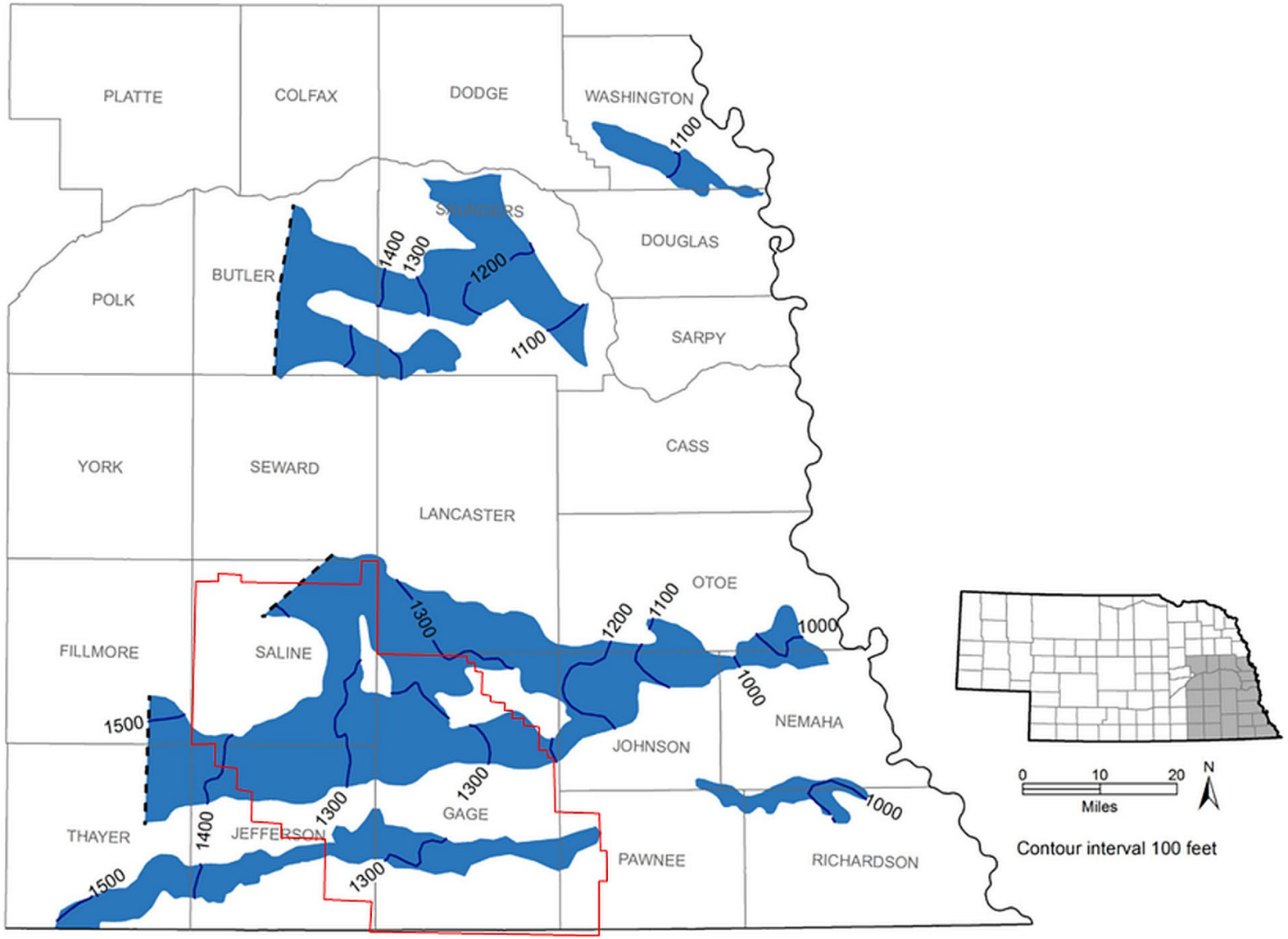


Figure 2-8. Elevation of the potentiometric surface in the paleovalley aquifers of eastern Nebraska (modified from Korus et al. (2013)). The red polygon is the approximate location of the Lower Big Blue Natural Resources District.

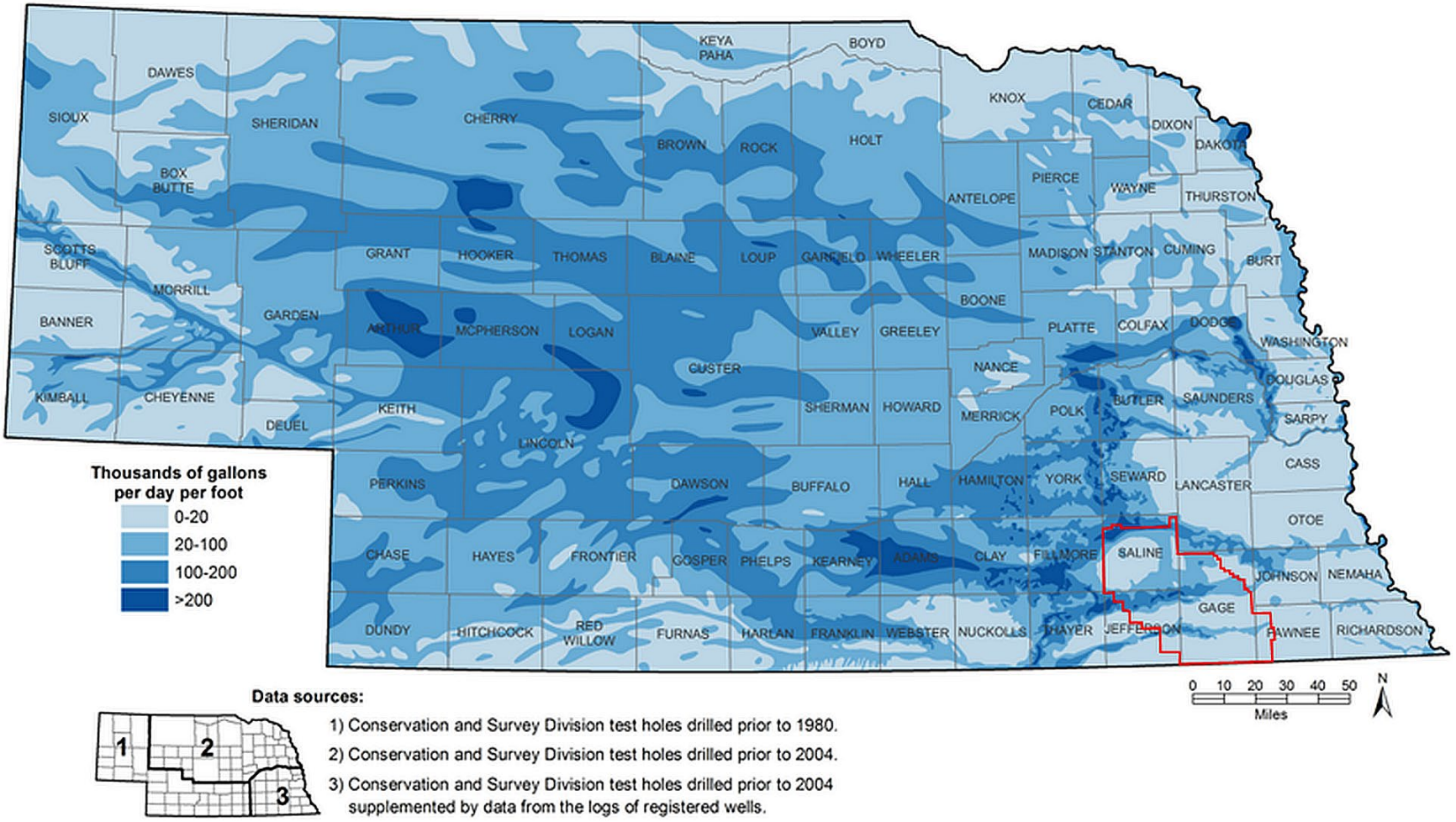


Figure 2-9. Transmissivity of the primary aquifers of Nebraska, including the High Plains aquifer, alluvial aquifers, glacial aquifers, and paleovalley aquifers. Sources of data vary by area, shown in inset map: 1) modified from an unpublished CSD map, 2) modified from Summerside et al. (2005), and 3) modified from Summerside et al. (2005), in which test hole data were supplemented by data from the logs of registered wells (modified from Korus et al. (2013)). The red polygon is the approximate location of the Lower Big Blue Natural Resources District.

3 Additional Background Information

3.1 Boreholes

Borehole data for this project consisted of a combination of lithologic, stratigraphic, and downhole geophysical logs (Figure 3-1). The borehole information was gathered from two sources: 1) CSD Nebraska Statewide Test Hole Database (UNL, 2026), including 53 wells within and adjacent to the project boundary with information from boreholes (lithology and stratigraphy) drilled between 1944 and 2023 by the CSD and other cooperating agencies; and 2) NE-DWEE registered wells database, including 1,213 wells within and adjacent to the project boundary (Nebraska DWEE-GW, 2026). Three (3) of the CSD wells in the LBBNRD 2025 AEM survey area had geophysical logs.

The boreholes used in this study can be found as ESRI shapefiles in the *Appendix 3 – Deliverables\ESRI Products*.

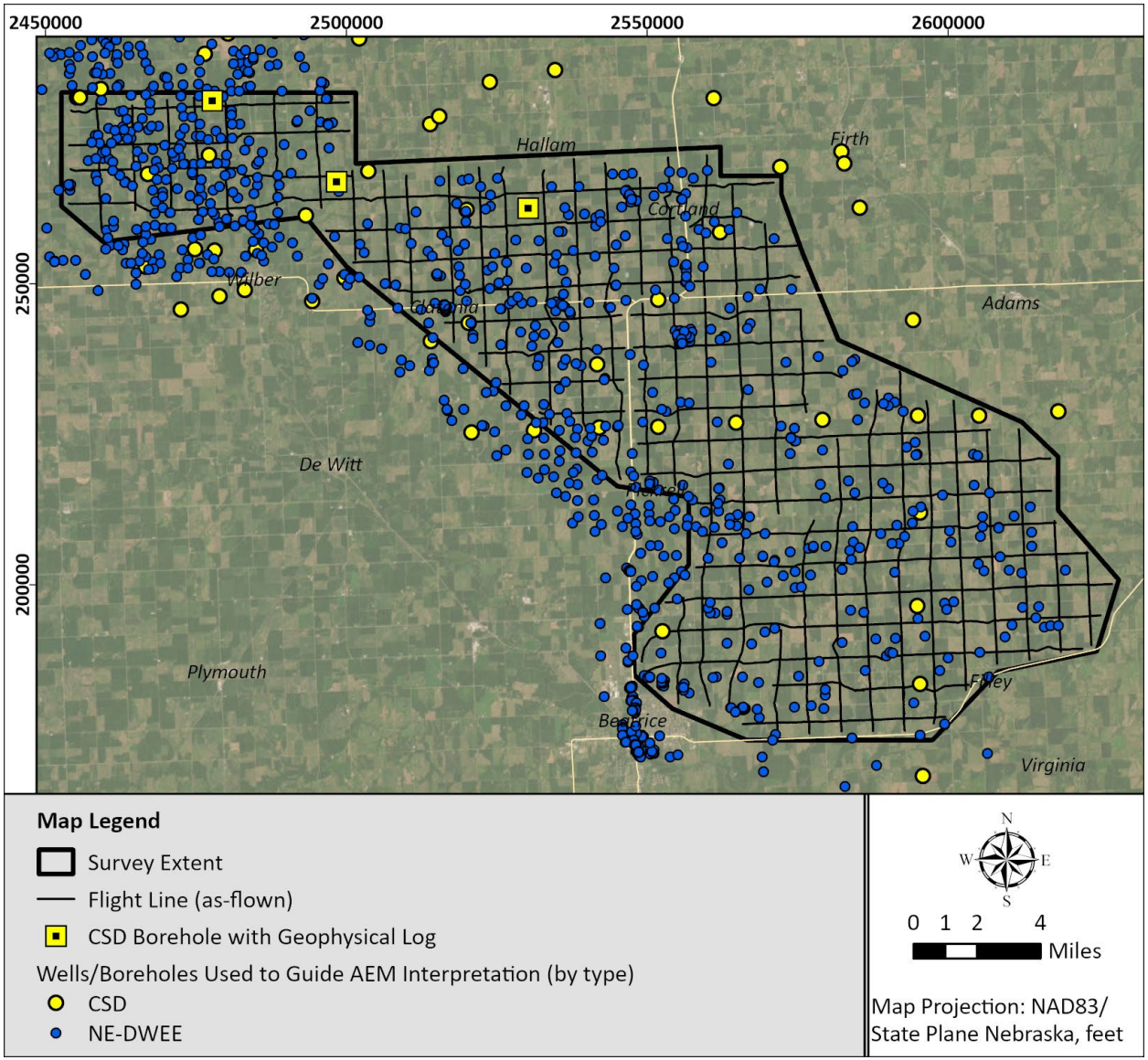


Figure 3-1. Map of the Nebraska CSD and DWEE boreholes used to guide the LBBNRD 2025 AEM interpretation.

4 Geophysical Methodology, Acquisition and Processing

4.1 Geophysical Methodology

Airborne Transient Electromagnetic (TEM) or airborne Time-Domain Electromagnetic (TDEM), or generally AEM, investigations provide characterization of electrical properties of earth materials from the land surface downward using electromagnetic induction. Figure 4-1 gives a conceptual illustration of the airborne TEM method.

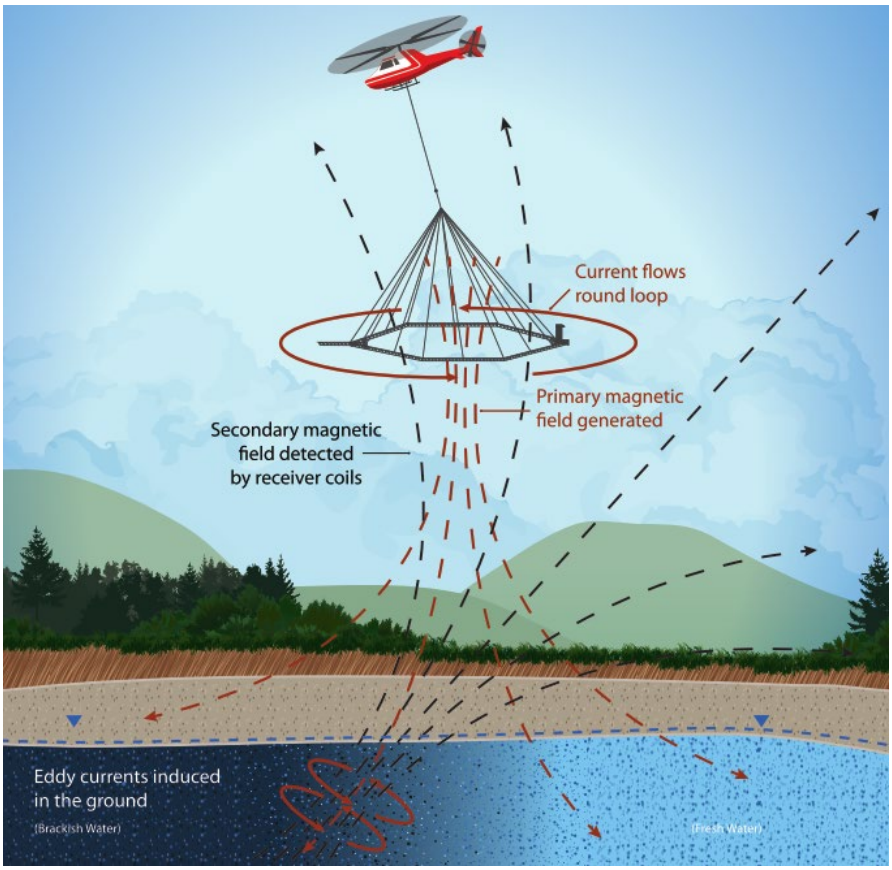


Figure 4-1: Schematic of an airborne electromagnetic survey, modified from Carney et al. (2015).

To collect TEM data, an electrical current is sent through a large loop of wire consisting of multiple turns which generates an electromagnetic (EM) field. This is called the transmitter (Tx) coil. After the EM field produced by the Tx coil is stable, it is switched off as abruptly as possible. The EM field dissipates and decays with time, traveling deeper and spreading wider into the subsurface. The rate of dissipation is dependent on the electrical properties of the subsurface (controlled by the material composition of the geology including the amount of mineralogical clay, the water content, the presence of dissolved solids, the metallic mineralization, and the percentage of void space). At the moment of turnoff, a secondary EM field, which also begins to decay, is generated within the subsurface. The decaying secondary EM field generates a current in a receiver (Rx) coil, per Ampere's Law. This current in the Rx coil is measured at several different moments in time (each moment being within a time band called a "gate"). From the

induced current, the time rate of decay of the magnetic field, B, is determined (dB/dt). When compiled in time, these measurements constitute a “sounding” at that location. Each TEM measurement produces an EM sounding at one point on the surface.

The sounding curves are numerically inverted to produce a model of subsurface resistivity as a function of depth. Inversion relates the measured geophysical data to probable physical earth properties. Figure 4-2 shows an example of a dual-moment TEM dB/dt sounding curve and the result of the inversion, the corresponding electrical resistivity model.

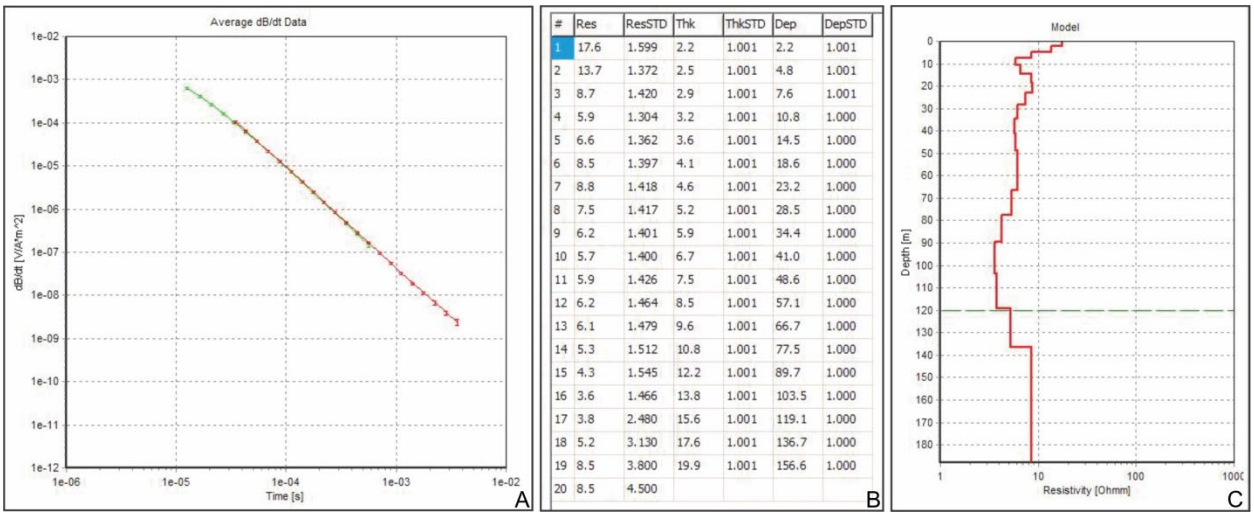


Figure 4-2: A) Example of a dB/dt sounding curve. B) Corresponding inverted model values. C) Corresponding resistivity earth model.

4.2 Flight Planning/Utility Mapping

The primary source of noise in geophysical electromagnetic surveys are other electromagnetic devices that are part of typical municipal utility infrastructure. These include, but are not limited to, power lines, railroads, pipelines, and water pumps. Prior to AEM data acquisition in the LBBNRD, three types of utilities (pipelines, railroads, and power lines) were located by inspection from Google Earth imagery.

The locations of the flight lines were modified from a regularly spaced grid to one with flight lines optimized to avoid electromagnetic coupling with identified utilities. This was done by moving along each flight line in ESRI ArcGIS Pro to inspect the path for visible power lines, radio towers, railroads, highways and roads, confined feeding operations and buildings, and any other obstructions that needed to be avoided during flight.

Upon conclusion of the design process, the 2025 LBBNRD flight lines had a maximum length of approximately 22.3 miles (35.8 km) in the east-west direction and about 17.4 miles (28.0 km) at their longest in the north-south direction. The flight lines were separated by approximately 0.97 mile (1.56 km) in both north-south and east-west directions.

4.3 AEM Survey Instrumentation

AEM data were acquired using the SkyTEM304M (304) airborne electromagnetic system (SkyTem Airborne Surveys Worldwide, 2025). The 304 is a rigid frame, dual-magnetic moment (Low and High) TEM system. The area of the 304 Tx coil is 342 m^2 and the coil contains four (4) turns of wire. A peak current of nine (9) amps is passed through one turn of wire in the Tx for Low Moment measurements and a peak current of about 110 amps is passed through the four turns of wire for High Moment measurements. This results in peak Tx Low and High magnetic moments of ~3,000 Ampere-meter-squared ($A*m^2$) and ~150,000 $A*m^2$, respectively.

The SkyTEM304M system utilizes an offset Rx positioned slightly behind the Tx resulting in a 'null' position which is a location where the intensity of the primary field from the system transmitter is minimized. This is desirable as to minimize the amplitude of the primary field at the Rx to maximize the sensitivity of the Rx to the secondary fields. The SkyTEM304M multi-turn Rx coil has an effective area of 105 m^2. In addition to the Tx and Rx that constitute the TEM instrument, the SkyTEM304M is also equipped with a Total Field magnetometer (MAG) and data acquisition systems for both instruments. The SkyTEM304M also includes two each of laser altimeters, inclinometers/tilt meters, and differential global positioning system (DGPS) receivers. Positional data from the frame mounted DGPS receivers are recorded by the AEM data acquisition system. The magnetometer includes a third DGPS receiver whose positional data is recorded by the magnetometer data acquisition system. Figure 4-3 gives a simple illustration of the SkyTEM304M frame and instrument locations. The image is viewed along the +z axis looking at the horizontal x-y plane. The axes for the image are labeled with distance in meters. The magnetometer is located on a boom off the front of the frame (right side of image). The Tx coil is located around the octagonal frame and the Rx Coil is located at the back of the frame (left side of image).

The coordinate system used by the 304 defines the +x direction as the direction of flight, the +y direction is defined 90 degrees to the right, and the +z direction is downward. The center of the transmitter loop, mounted to the octagonal SkyTEM frame is used as the origin in reference to instrumentation positions. Table 4-1 lists the positions of the instruments (in feet) and Table 4-2 lists the corners of the transmitter loop in feet (whereas units of meters are presented in Figure 4-3). Figure 4-4 displays a couple of images of the 304 in operation.

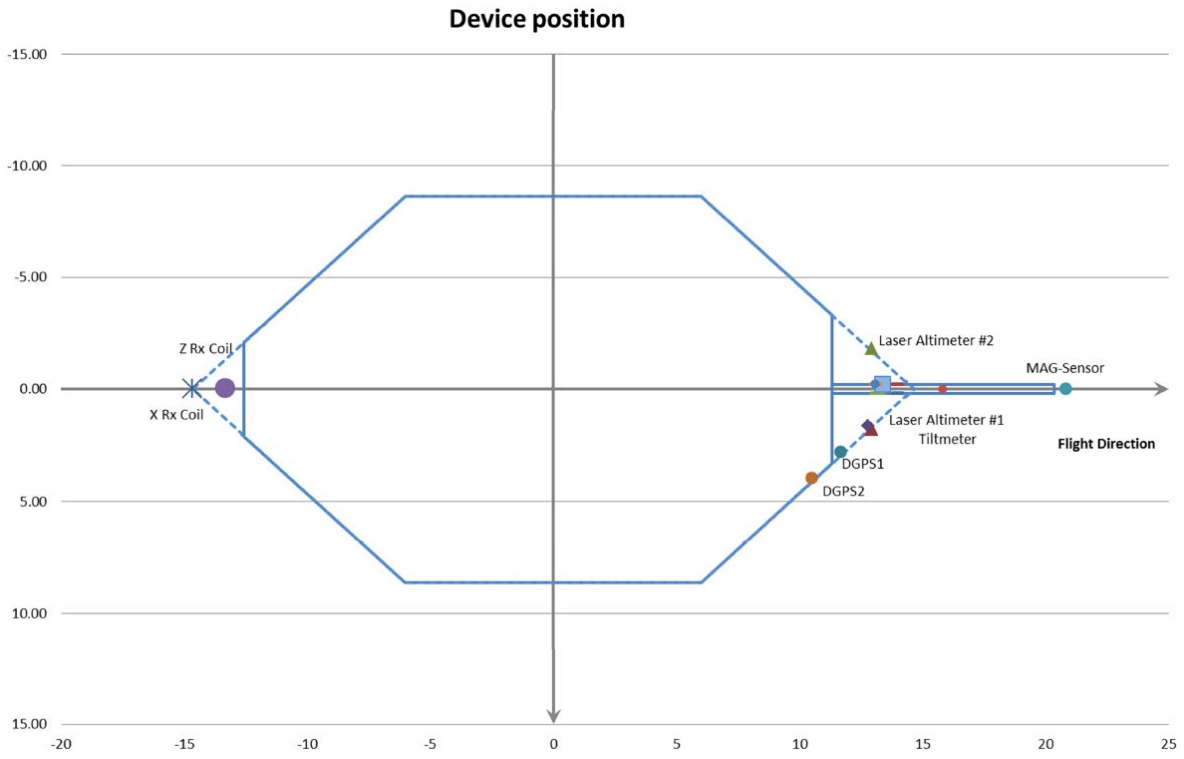


Figure 4-3: SkyTEM 304M frame, including instrumentation locations and X and Y axes. Distances are in meters. Instrumentation locations listed in Table 4-1.



Figure 4-4: Photos of the SkyTEM 304M system in suspension beneath the helicopter.

Table 4-1: Positions of instruments on the SkyTEM 304M frame, using the center of the frame as the origin, in feet.

	DGPS 1	DGPS 2	Inclinometer 1	Inclinometer 2	Altimeter 1	Altimeter 2	Magnetic Sensor	Rx Coil
X	34.48	30.64	41.96	41.96	42.45	42.45	67.24	-43.04
Y	12.96	16.80	5.38	5.38	5.87	-5.87	0	0
Z	-0.52	-0.52	-0.39	-0.39	-0.39	-0.39	-1.71	-6.56

Table 4-2: Positions of corners of the SkyTEM 304M transmitter coil, using the center of the frame as the origin in feet.

Tx Corners	1	2	3	4	5	6	7	8
X	-41.17	-19.78	19.78	37.20	37.20	19.78	-19.78	-41.17
Y	-6.89	-28.31	-28.31	-10.86	10.86	28.31	28.31	6.89

4.4 Data Acquisition

All SkyTEM systems are calibrated to a ground test site in Lyngby, Denmark prior to being used for production work (HydroGeophysics Group Aarhus University, 2010; HydroGeophysics Group Aarhus University, 2011; Foged et al., 2013). The calibration process involves acquiring data with the system hovering at different altitudes, from 16 ft to 164 ft, over the Lyngby site. Acquired data are processed and a scale factor (time and amplitude) is applied so that the inversion process produces the model that approximates the known geology at Lyngby. Installation of the navigational instruments in the helicopter and assembly of the SkyTEM304 system commenced at the end of May in Scott City, Kansas at the beginning of the 2025 AGF AEM project campaign and the system was ferried from Kansas to the Beatrice Municipal Airport on July 4, 2025. Calibration test flights were flown to ensure that the equipment was operating within technical specifications. Survey set-up procedures included measurement of the transmitter waveforms, verification that the receiver was properly located in a null position, and verification that all positioning instruments were functioning properly. A high-altitude test, used to verify system performance, was flown prior to the beginning of the survey's production flights. In the field, quality control of the operational parameters for the EM and magnetic field sensors including current levels, positioning sensor dropouts, acquisition speed, and system orientation were conducted with proprietary SkyTEM software following each flight. Approximately 494 line-miles (794 line-kilometers) were acquired over the LBBNRD AEM survey area between 05 July 2025 and finishing on 06 July 2025. A data acquisition map for the flight lines is presented in Figure 4-5, grouped by acquisition date. For this LBBNRD project, the 304 was flown at an average speed of 49.4 mi/hr (79.4 kilometers/hr) and at an average flight height of 116.5 ft (35.5 m) above land surface, using the sling-load cargo system of a Eurocopter AS350 B2 helicopter. The average pitch (tilt angle in the +/- X direction of travel) was 0.37 degrees and the average roll (tilt angle perpendicular to the direction of travel) was 0.99 degrees. Images of the 2025 LBBNRD AEM survey ground speeds are presented in Figure 4-6. Flight heights are presented in Figure 4-7. Images of the pitch (X) angle and yaw (Y) angle are presented in Figure 4-8 and Figure 4-9, respectively.

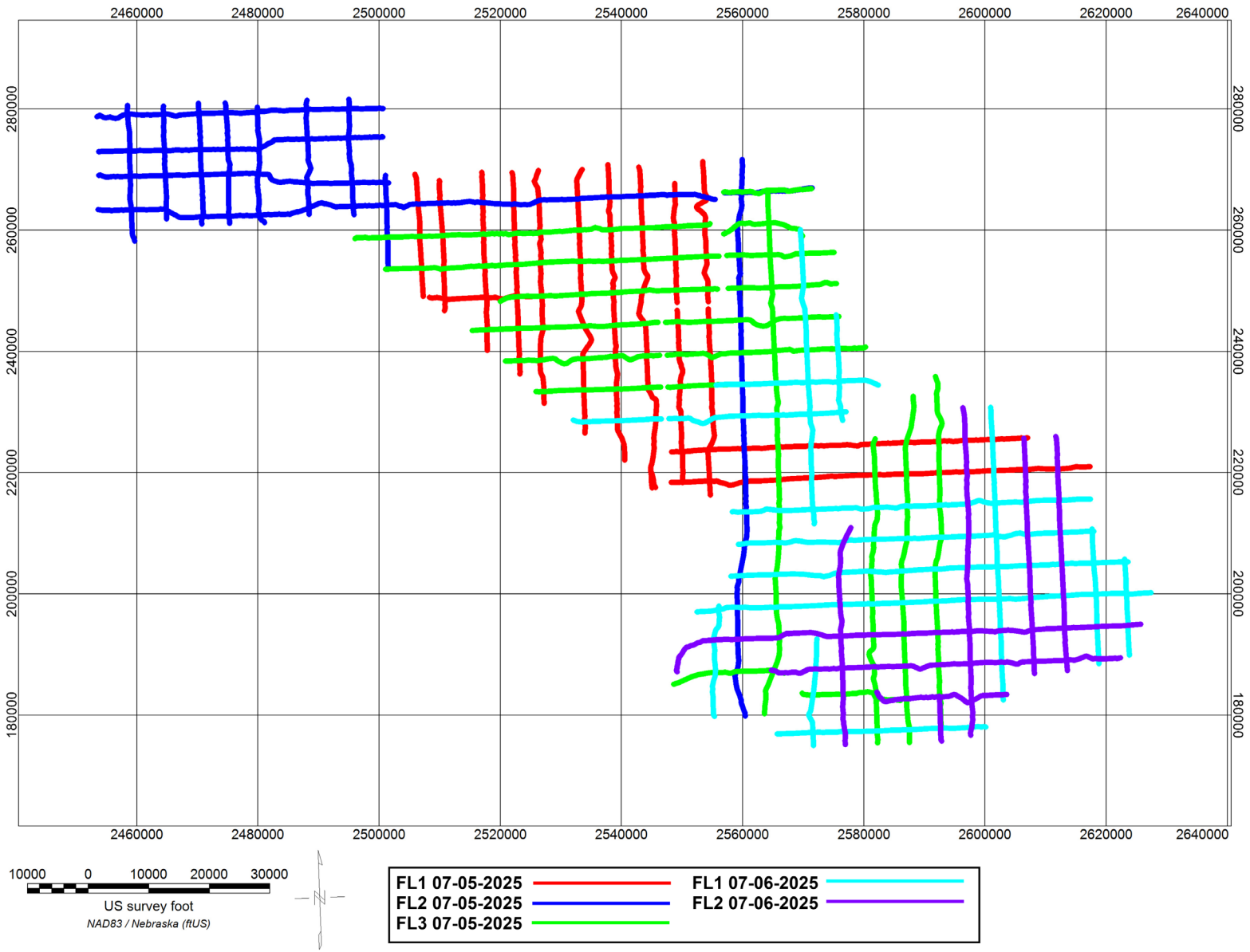


Figure 4-5. LBBNRD 2025 AEM flight lines grouped by acquisition date. Projection is Nebraska State Plane NAD83, feet.

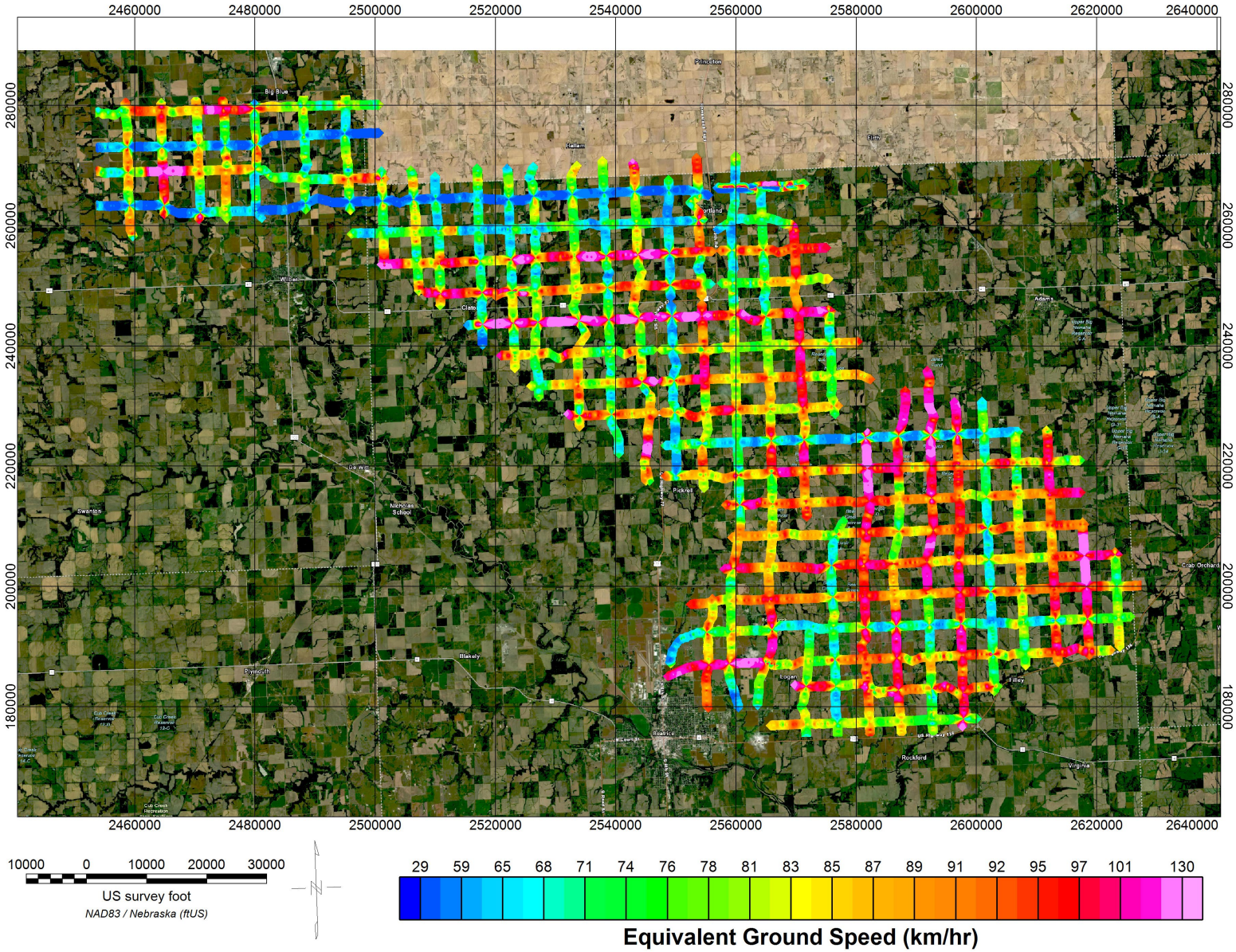


Figure 4-6. LBBNRD 2025 AEM survey ground speed. Projection is Nebraska State Plane NAD83, feet.

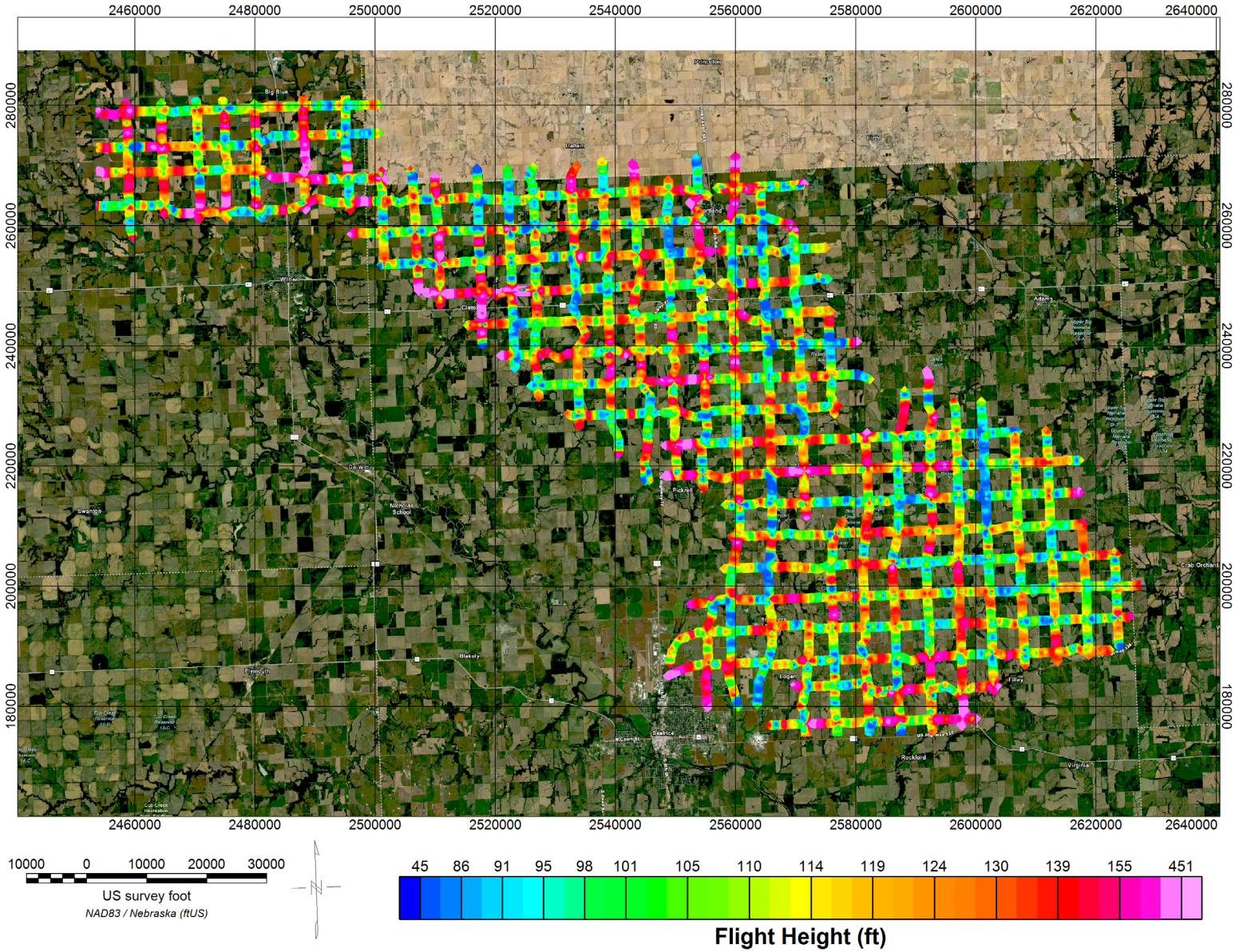


Figure 4-7. LBBNRD 2025 AEM flight lines flight height above the ground surface. Projection is Nebraska State Plane NAD83, feet.

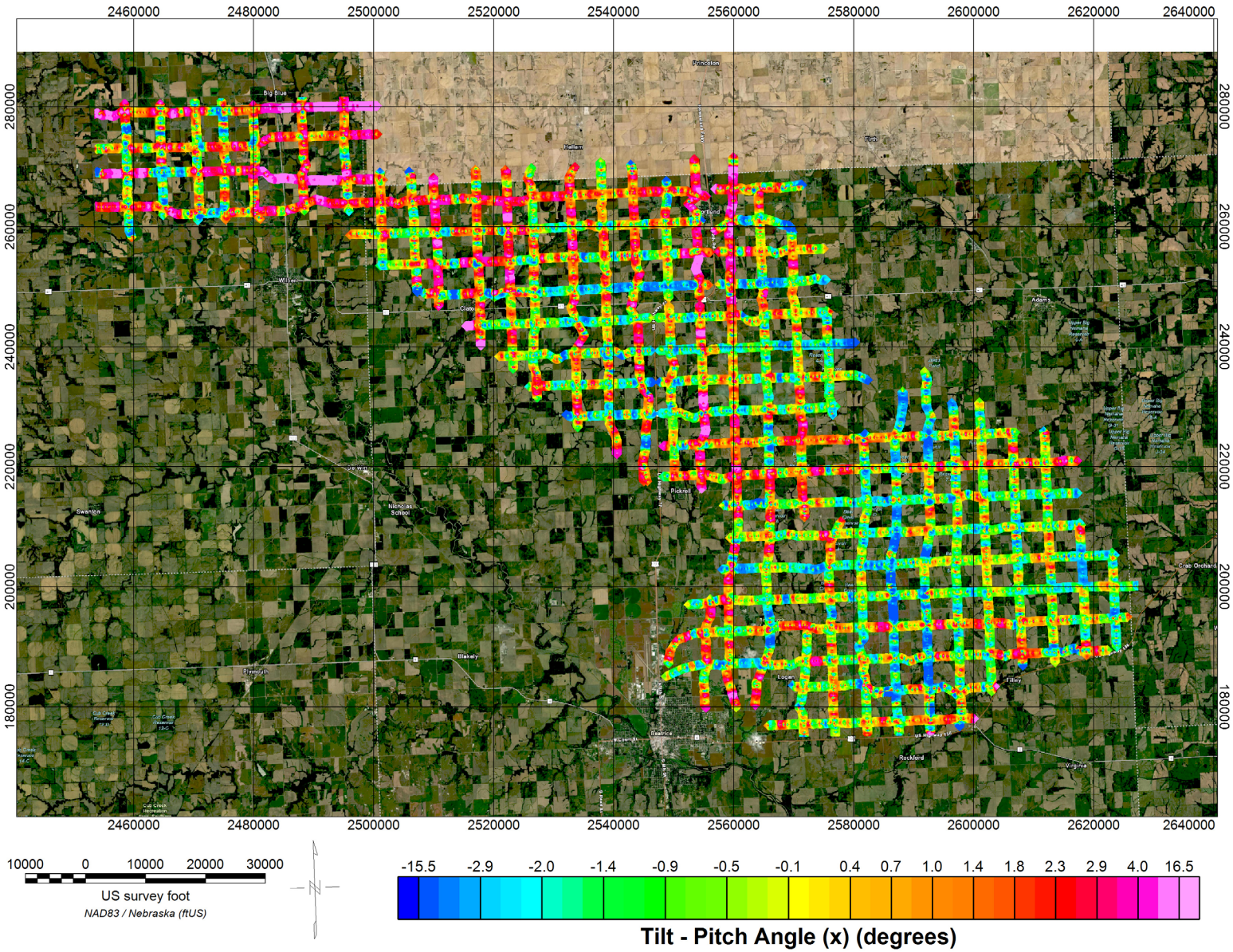


Figure 4-8. LBBNRD 2025 AEM flight lines pitch angle in the +/-X direction of travel. Projection is Nebraska State Plane NAD83, feet.

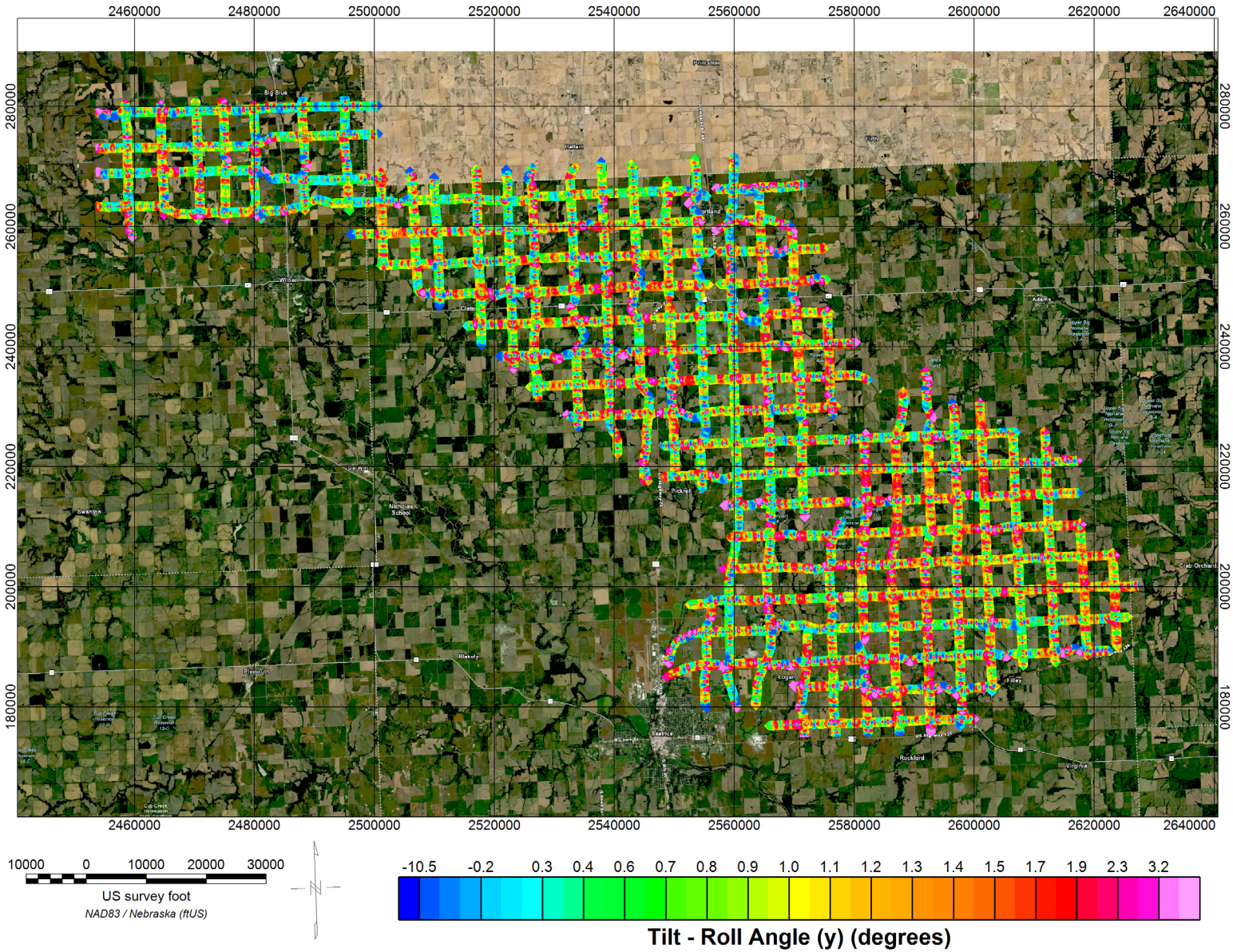


Figure 4-9. LBBNRD 2025 AEM flight lines Y roll angle perpendicular to the direction of travel. Projection is Nebraska State Plane NAD83, feet.

4.4.1 Primary Field Compensation

A standard SkyTEM data acquisition procedure involves review of acquired raw data by SkyTEM in Denmark for Primary Field Compensation (PFC) prior to continued data processing by AGF (Schamper et al., 2014). The primary field of the transmitter affects the recorded early time gates, which in the case of the Low Moment, are helpful in resolving the near surface resistivity structure of the ground. The Low Moment uses a saw tooth waveform which is calculated and then used in the PFC correction to correct the early time gates.

4.4.2 Automatic Processing

The AEM data collected by the 304 were processed using Aarhus Workbench version 2025.1.0 (Aarhus Geosoftware (https://www.aarhusgeosoftware.dk/aarhus-workbench) described in HydroGeophysics Group, Aarhus University (2011).

Automatic processing algorithms provided within the Workbench program are initially applied to the AEM data. DGPS locations were filtered using a stepwise, second-order polynomial filter of ten seconds with a beat time of 0.5 seconds, based on flight acquisition parameters. The AEM data are corrected for tilt deviations from level and so filters were also applied to both tilt meter readings with a median filter of three seconds and an average filter of two seconds. The altitude data were corrected using a series of two polynomial filters. The lengths of both eighth-order polynomial filters were set to 15 seconds with shift lengths of twelve (12) seconds. The lower and upper thresholds were 1 and 100 meters, respectively.

Trapezoidal spatial averaging filters were next applied to the AEM data. The times used to define the trapezoidal filters for the Low Moment were $1.0x10^{-5}$ sec, $1.0x10^{-4}$ sec, and $1.0x10^{-3}$ sec with widths of 3, 6, and 18 seconds. The times used to define the trapezoid for the High Moment were $1.0x10^{-4}$ sec, $1.0x10^{-3}$ sec, and $1.0x10^{-2}$ sec with widths of 3, 6, and 18 seconds. The trapezoid sounding distance was set to 1.0 seconds and the left/right setting, which requires the trapezoid to be complete on both sides, was turned on. The spike factor and minimum number of gates were both set to 20 percent for both moments. Lastly, the locations of the averaged soundings were synchronized between the two moments.

4.4.3 Manual Processing and Laterally-Constrained Inversions

After the implementation of the automatic filtering, the AEM data were manually examined using a sliding two-minute time window. The data were examined for possible electromagnetic coupling with surface and buried utilities and metal, as well as for late time-gate noise. Data affected by these were removed. An example of flight light passing over possible sources of EM coupling is shown in Figure 4-10 Figure 4-11 displays what an EM coupling looks like in Aarhus Workbench both before and after removal. Example inversion results with coupling and that coupling removed are shown in Figure 4-12. Data were also removed where the system height was greater than 230 feet (70 m) which causes a decrease in the signal level. This occurred at several locations due to object avoidance.

The AEM data were then inverted using a Laterally-Constrained Inversion (LCI) algorithm (HydroGeophysics Group Aarhus University, 2011). The profile and depth slices were examined, and any remaining electromagnetic couplings were masked out of the data set. Once acceptable LCI results were obtained, the data were then inverted using the Spatially Constrained Inversion (SCI) discussed below.

After final processing, 393.9 line-miles (633.8 line-kilometers) were retained for inversion amounting to a retention rate of 79.8%. This high rate is the result of careful flight line planning and design to avoid the infrastructure present in the survey area.

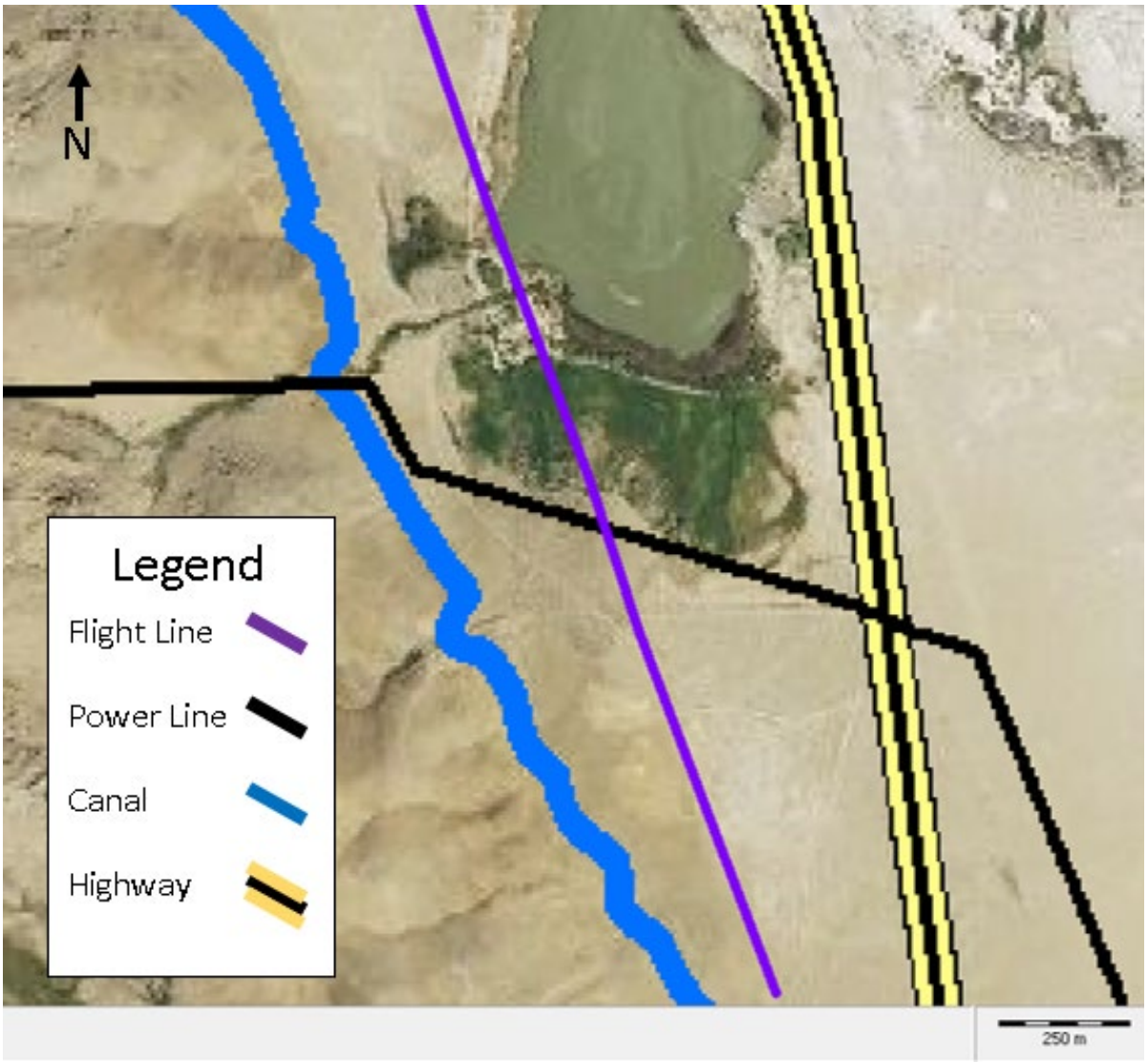


Figure 4-10: Example locations of electromagnetic coupling with pipelines or power lines.

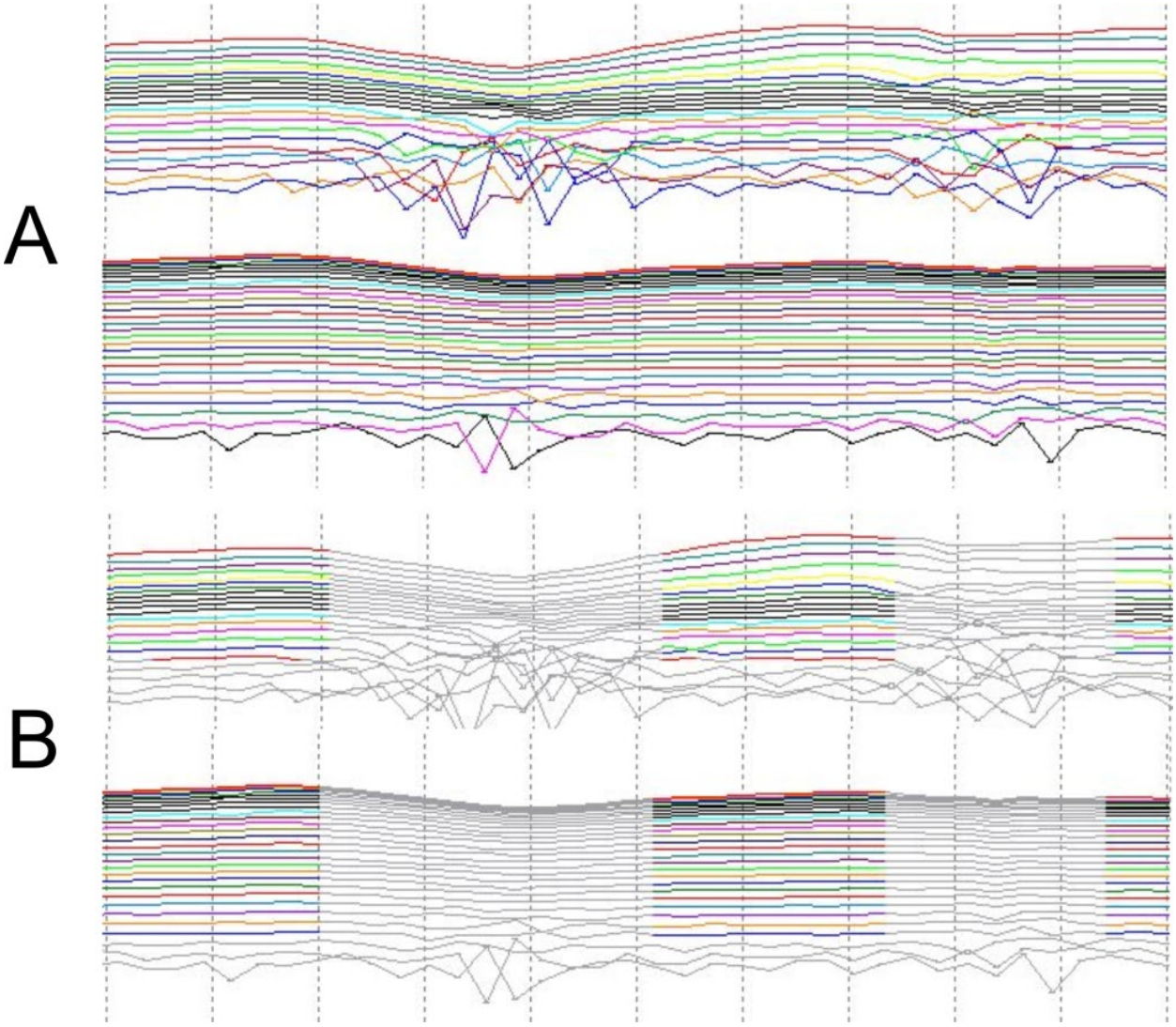


Figure 4-11: A) Example of AEM data affected by electromagnetic coupling as presented in the Aarhus Workbench editor. The top group of lines is the unedited data with the Low Moment on top and the High Moment on the bottom. The bottom group shows the same data after editing.

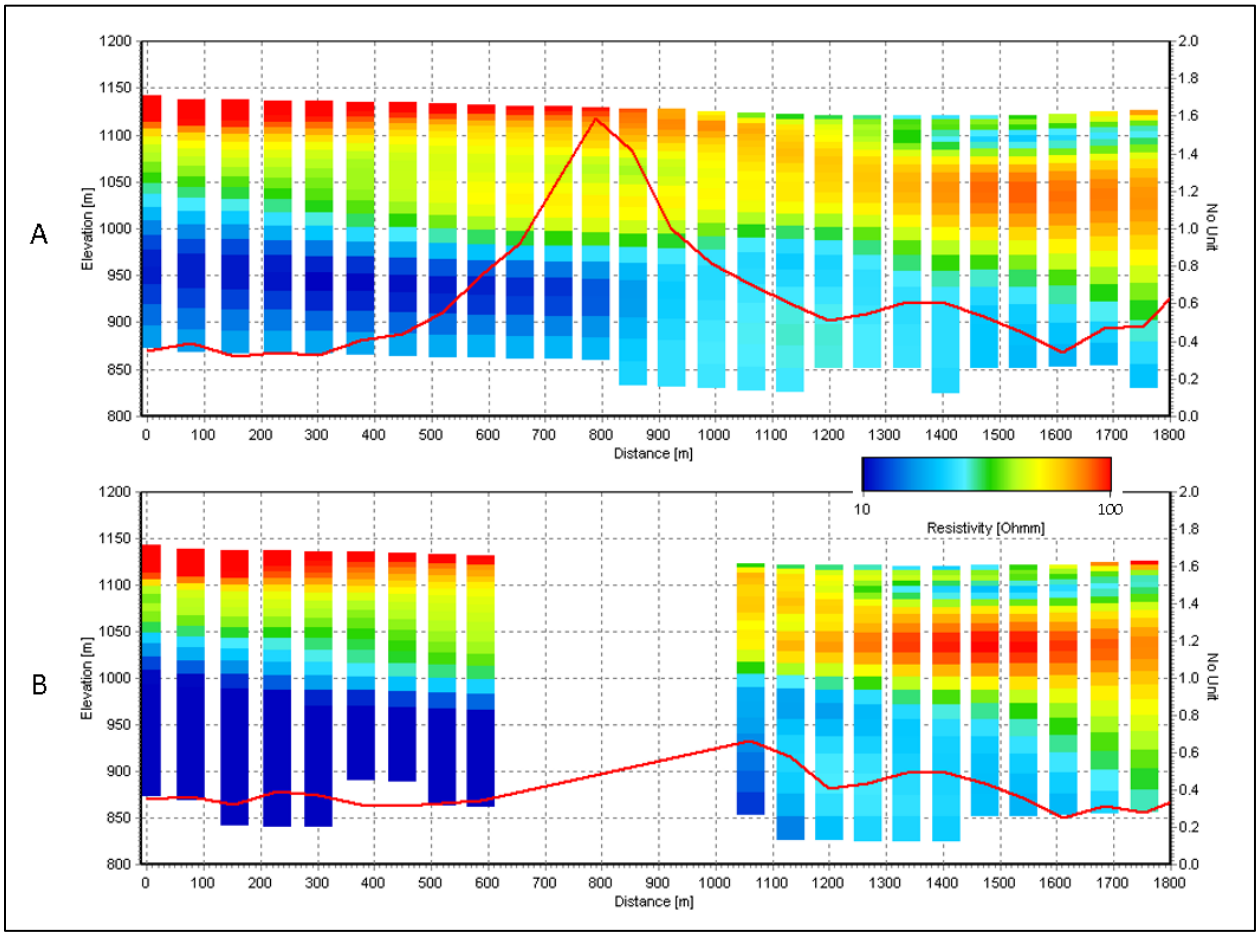


Figure 4-12: A) Example of Laterally-Constrained inversion results where AEM data affected by coupling with pipelines and power lines were not removed resulting in high residual values (red line). B) Inversion results where AEM data affected by coupling were removed. Models with high residual values can yield erroneous results.

4.4.4 Power Line Noise Intensity (PLNI)

The Power Line Noise Intensity (PLNI) channel assists in identifying possible sources of noise from power lines. Pipelines, unless they are cathodically-protected, are not mapped by the PLNI. The PLNI is produced by performing a spectral frequency content analysis on the raw received Z-component SkyTEM data. For every Low Moment data block, a Fourier Transform (FT) is performed on the latest usable time gate data. The FT is evaluated at the local power line transmission frequency (60 Hz) yielding the amplitude spectral density of the local power line noise. The PLNI data for the LBBNRD 2025 AEM survey are presented as a grid in Figure 4-13. The LBBNRD 2025 survey As-Flown data and the data retained for inversion are presented in Figure 4-14. The blue lines represent the 79.8% of data retained for inversion and red lines representing data removed due to infrastructure and noise.

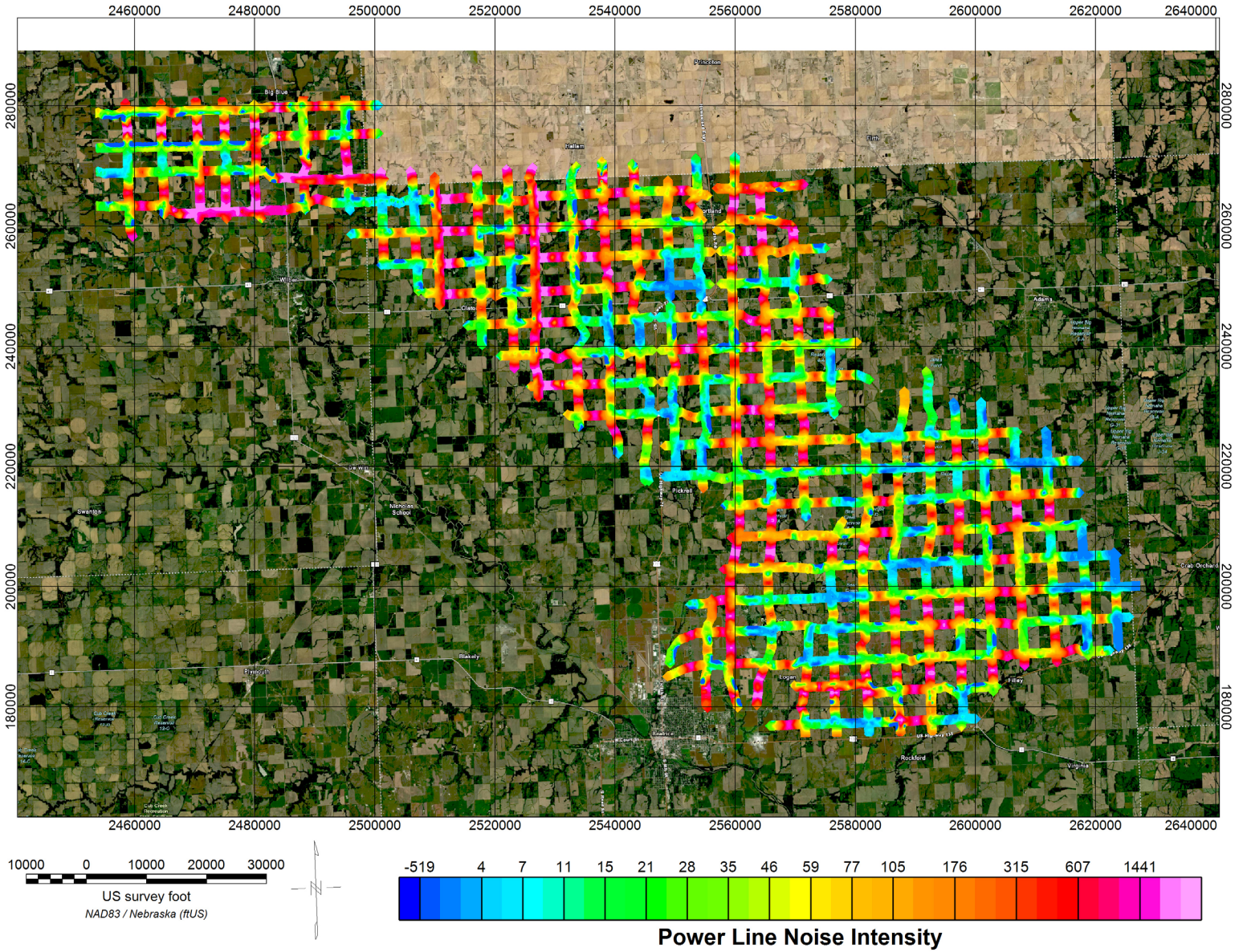


Figure 4-13: Power Line Noise Intensity (PLNI) map of the LBBNRD 2025 project area. Projection is Nebraska State Plane NAD83, feet.

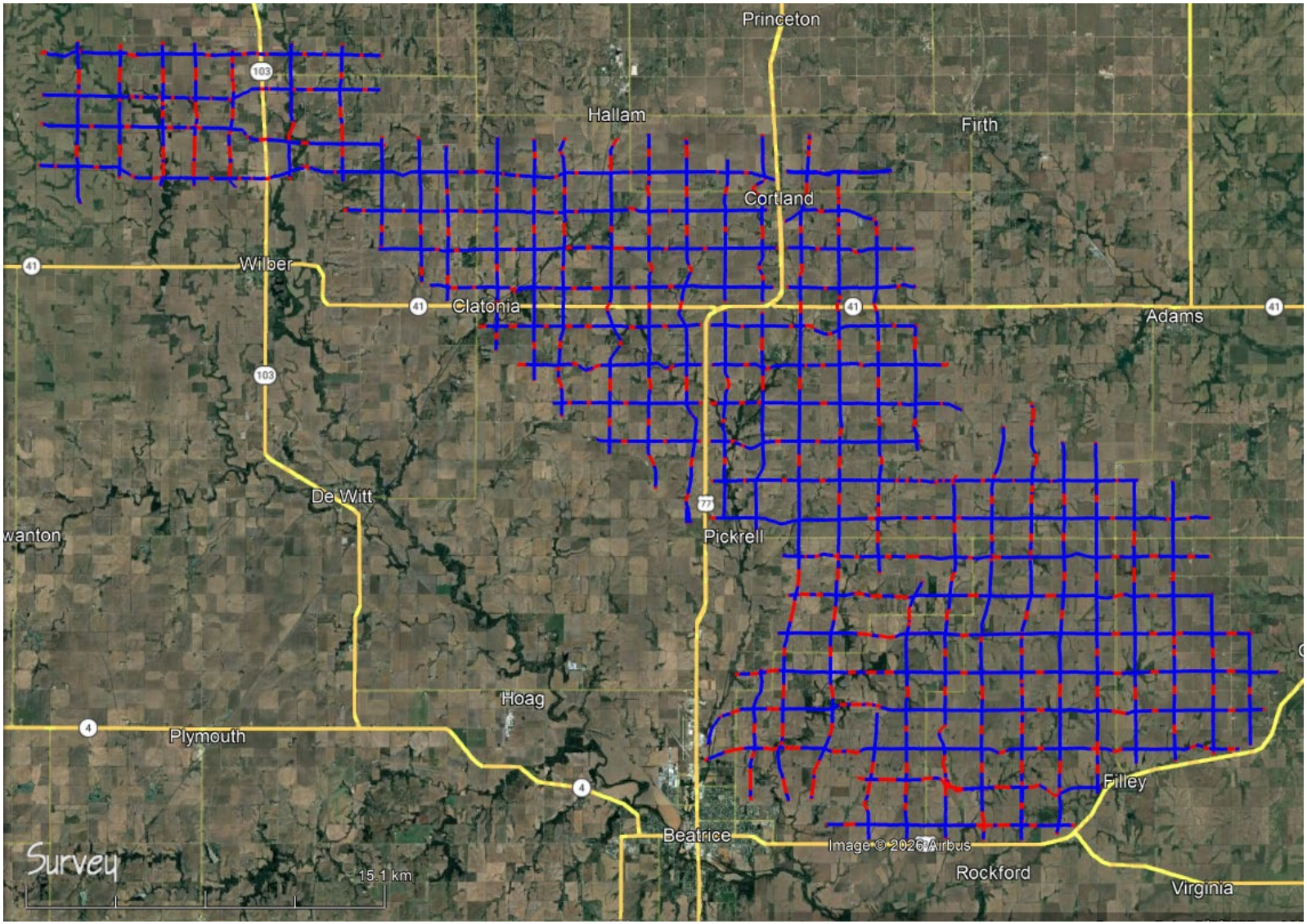


Figure 4-14. Locations of inverted data (blue lines) along the AEM flight lines (red lines) on the LBBNRD 2025 AEM survey area in Google Earth. Where blue lines are not present indicates decoupled (removed) data. Google Earth kmz's of the inverted data locations as well as the "as-flown" flight lines are included in Appendix 3\KMZ.

4.4.5 Magnetic Field Data

As discussed above, the SkyTEM 304 includes a Total Field magnetometer. The magnetic Total Field data can yield information about infrastructure as well as geology. Figure 4-15 shows the residual magnetic Total Field (RMF) intensity data for the LBBNRD AEM survey area after correcting for diurnal drift and removing the International Geomagnetic Reference Field (IGRF). This data is used in decoupling efforts.

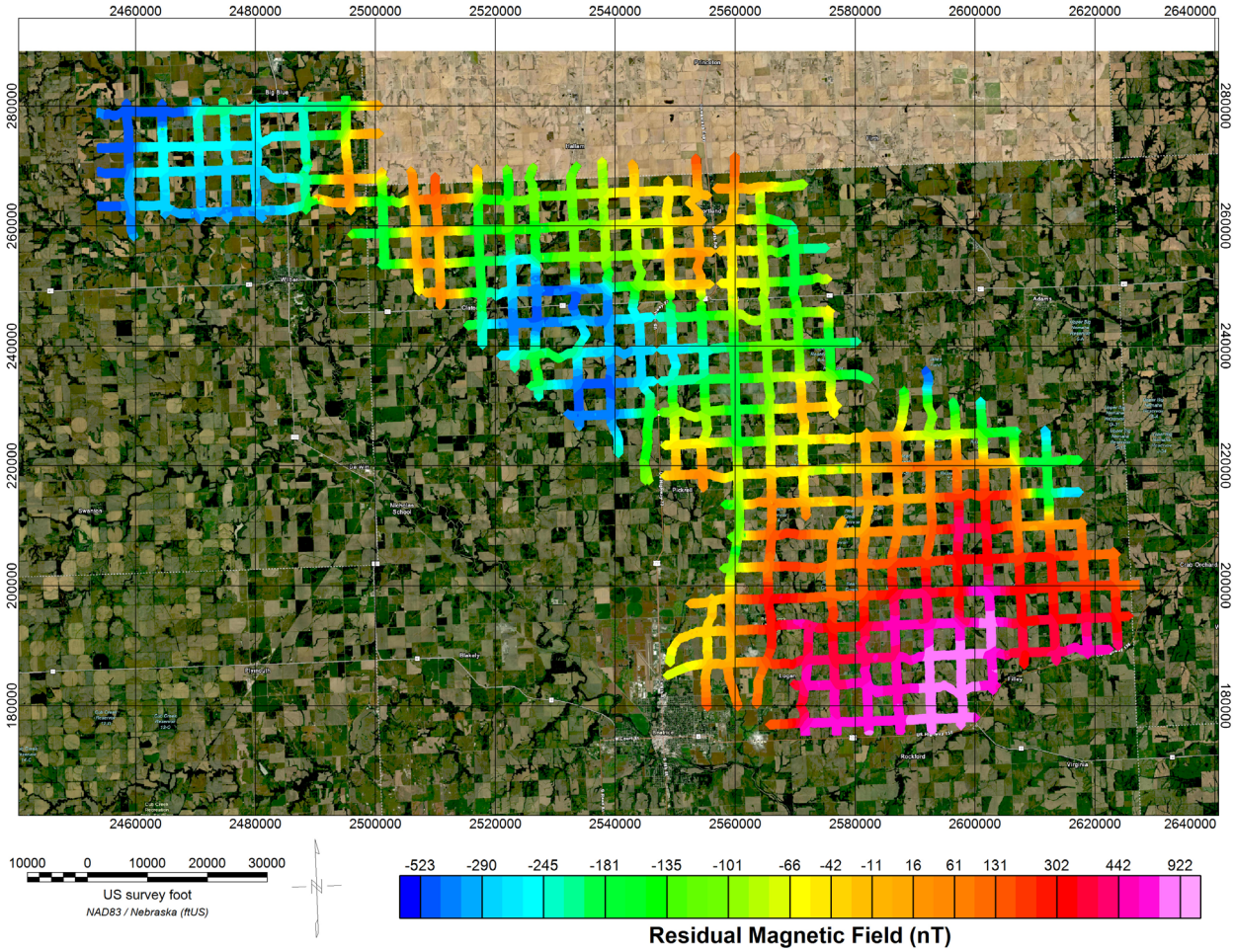


Figure 4-15. Residual magnetic Total Field intensity data for the LBBNRD 2025 AEM survey area corrected for diurnal drift, with the International Geomagnetic Reference Field (IGRF) removed. Projection is Nebraska State Plane NAD83, feet.

4.5 Spatially-Constrained Inversion

Following the initial decoupling and LCI analysis, Spatially-Constrained Inversions (SCI) were performed. SCIs use EM data along, and across, flight lines within user-specified distance criteria (Viezzoli et al., 2008).

The LBBNRD 2025 AEM data were inverted using a 40-layer model structure. The SCI inversions used smooth models, each with a starting resistivity of 10 Ohm-m (equivalent to a 10 ohm-m halfspace). The thicknesses of the first layers of the models were about 6.6 ft (2 m) with the thicknesses of the consecutive layers increasing approximately by a factor of 1.01. The depths to the bottoms of the 39th layers were set to 325.0 ft, with thicknesses up to about 21.6 ft. The thicknesses of the layers increase with depth (Table 4-3 and Figure 4-16) as the resolution of the EM technique decreases. The spatial reference distance, ***s***, for the inversion constraints was set to 328 ft (100 m) with a power law falloff of 0.75. The vertical and lateral constraints, ***ResVerSTD*** and ***ResLatStD***, were set to 2.4 and 1.4, respectively, for all layers.

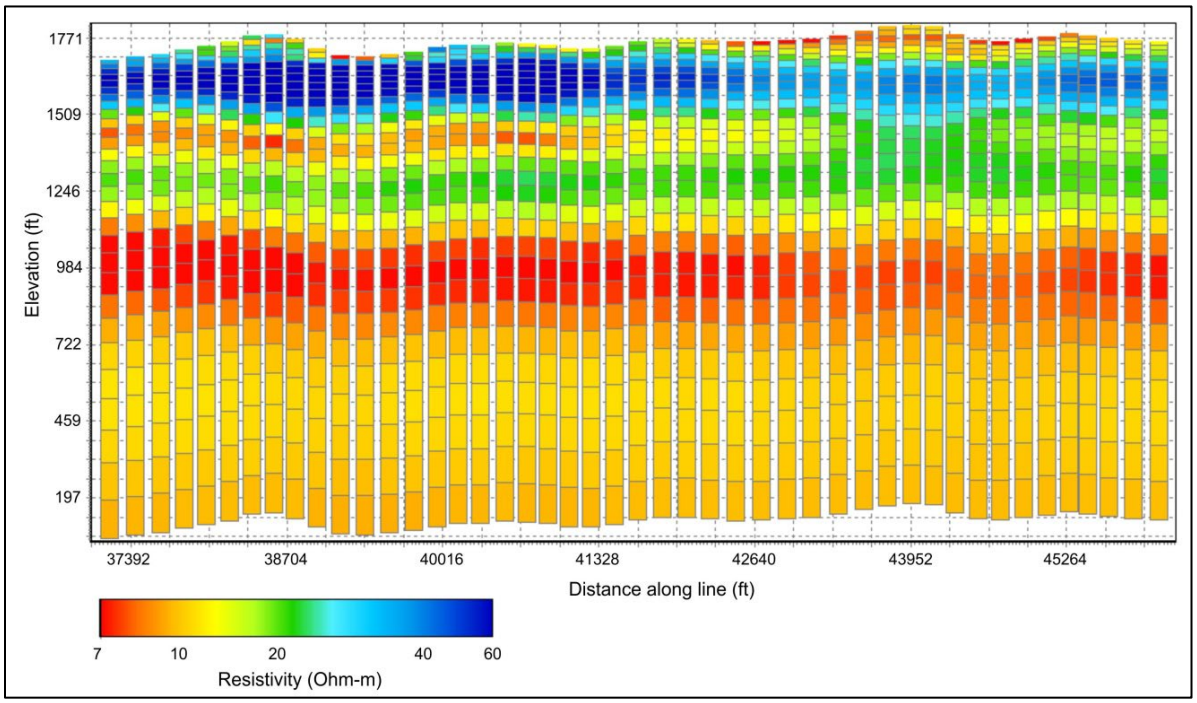


Figure 4-16. An example of an AEM profile illustrating increasing model layer thicknesses with depth.

In addition to the recovered resistivity models, the SCIs also produce data residual error values (single sounding error residuals) and Depth of Investigation (DOI) estimates. The data residuals compare the measured data with the forward modeled response of the individual inverted models (Christensen et al., 2009). The DOI provides a general estimate of the depth to which the AEM data are sensitive to changes in the resistivity distribution at depth (Christiansen and Auken, 2012). Two DOI's are calculated: an "Upper" DOI at a cumulative sensitivity of 1.2 and a "Lower" DOI set at a cumulative sensitivity of 0.6. A more detailed discussion on the DOI can be found in Asch et al. (2015).

Table 4-3: Thickness and depth to bottom for each layer in the Spatially Constrained Inversion (SCI) AEM earth models. The thickness of the model layers increase with depth as the resolution of the AEM technique decreases.

Layer	Depth to Bottom (ft)	Thickness (ft)	Depth to Bottom (m)	Thickness (m)	Layer	Depth to Bottom (ft)	Thickness (ft)	Depth to Bottom (m)	Thickness (m)
1	6.6	6.6	2.0	2.0	21	276.6	23.0	84.3	7.0
2	13.5	6.9	4.1	2.1	22	301.2	24.6	91.8	7.5
3	21.0	7.5	6.4	2.3	23	327.1	25.9	99.7	7.9
4	28.9	7.9	8.8	2.4	24	355.0	27.9	108.2	8.5
5	37.4	8.5	11.4	2.6	25	384.5	29.5	117.2	9.0
6	46.3	8.9	14.1	2.7	26	415.7	31.2	126.7	9.5
7	55.8	9.5	17.0	2.9	27	449.2	33.5	136.9	10.2
8	65.9	10.2	20.1	3.1	28	484.9	35.8	147.8	10.9
9	76.8	10.8	23.4	3.3	29	522.7	37.7	159.3	11.5
10	88.3	11.5	26.9	3.5	30	563.0	40.4	171.6	12.3
11	100.7	12.5	30.7	3.8	31	606.0	43.0	184.7	13.1
12	113.9	13.1	34.7	4.0	32	651.9	45.9	198.7	14.0
13	127.6	13.8	38.9	4.2	33	700.5	48.6	213.5	14.8
14	142.4	14.8	43.4	4.5	34	752.3	51.8	229.3	15.8
15	158.1	15.7	48.2	4.8	35	807.5	55.1	246.1	16.8
16	174.9	16.7	53.3	5.1	36	866.2	58.7	264.0	17.9
17	192.9	18.0	58.8	5.5	37	928.9	62.7	283.1	19.1
18	212.0	19.0	64.6	5.8	38	995.5	66.6	303.4	20.3
19	232.3	20.3	70.8	6.2	39	1066.3	70.9	325.0	21.6
20	253.6	21.3	77.3	6.5					

Figure 4-17 presents a histogram of the LBBNRD 2025 SCI inversion data/model residuals and a map of data to model error residuals comparison is presented in Figure 4-18.

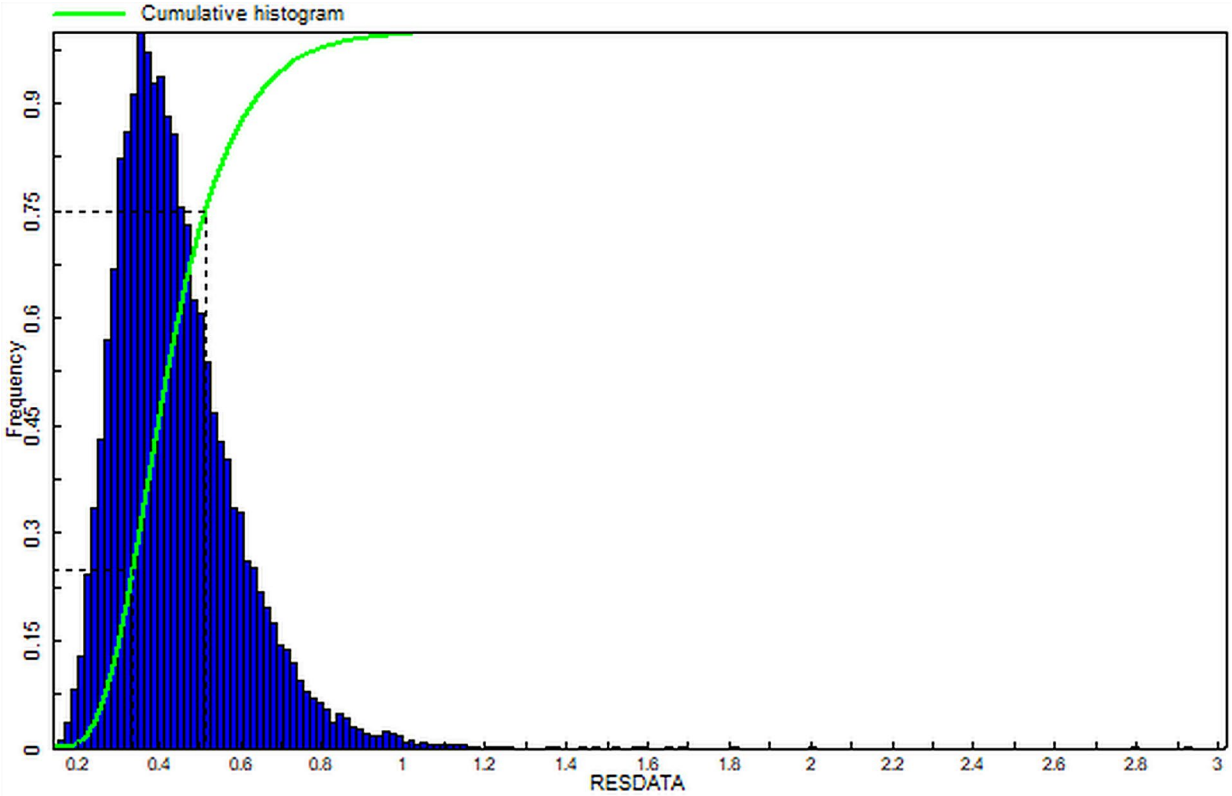


Figure 4-17. Data/model residual histogram for the LBBNRD 2025 SCI inversion results.

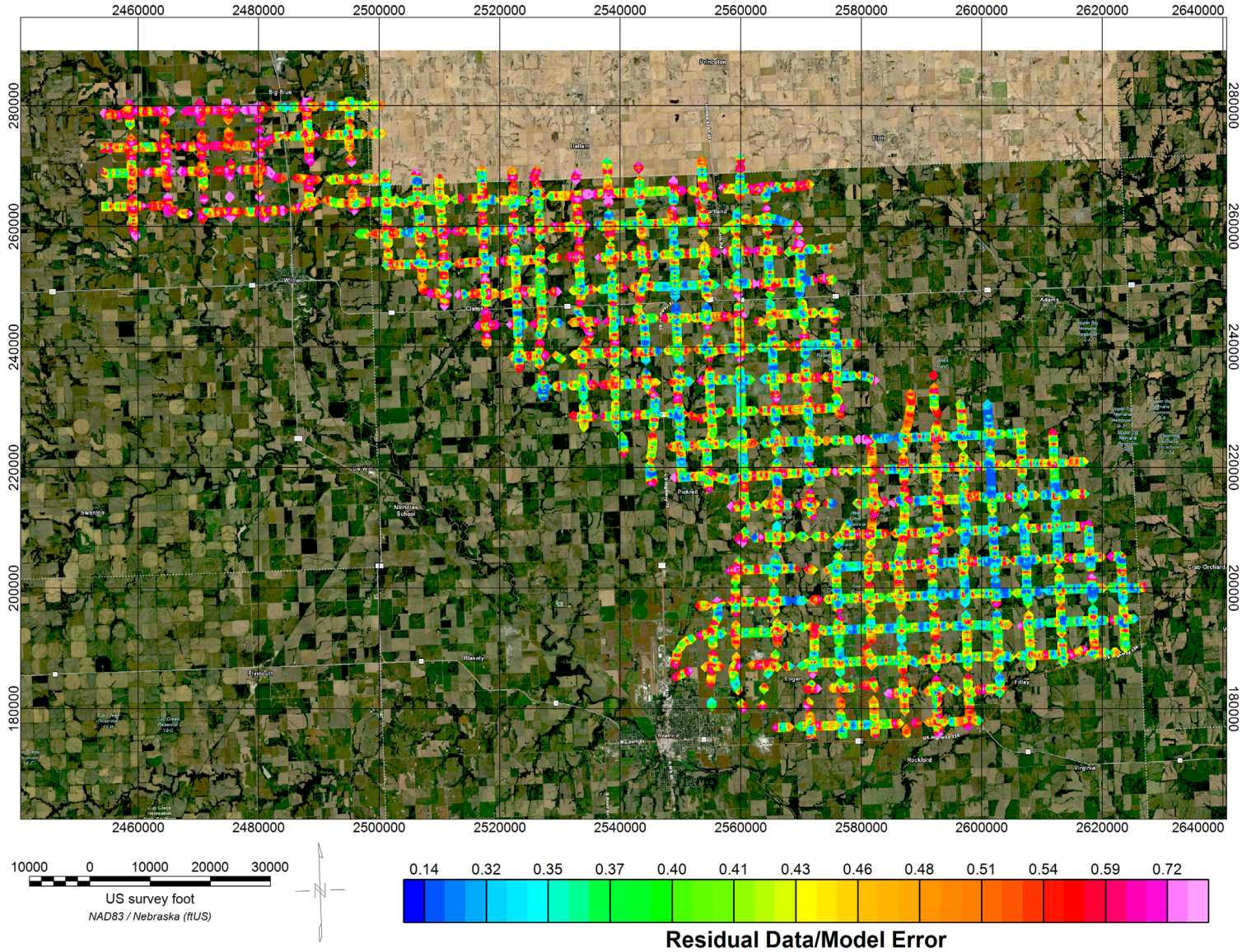


Figure 4-18. Map of data-inversion model residuals for the LBBNRD 2025 SCI inversion results. Projection is Nebraska State Plane NAD83, feet.

5 AEM Results and Interpretation

This section provides the details involved in the interpretation of the LBBNRD 2025 AEM data and inversion results.

5.1 Interpretative Process

5.1.1 Merging AEM Flight Lines

After the inversion process, flight lines from the 2025 LBBNRD AEM data set were combined to create continuous lines from lines flown in two parts due to infrastructure and or flight planning. These continuous lines allow for improved viewing and interpretation of the AEM inversions results across the LBBNRD area. A compiled table listing the originally flown lines from the AEM inversions and the newly combined lines are shown in Table 5-1. Line L100042 was removed from the database as it is a repeat of line L100043. Line 190161 was removed as it was a duplicate of the end of the line L190160. This table would be used if referring to the original as-flown lines within the raw acquired data and the inverted data sets. Figure 5-1 presents a map showing the merged segments where the lines were connected.

Table 5-1. LBBNRD 2025 AEM lines merged.

Direction	Original Line 1	Original Line 2	New Line
E-W	100071	100072	100070
E-W	100102	100103	100105
E-W	100201	100202	100203
N-S	190251	190252	190253

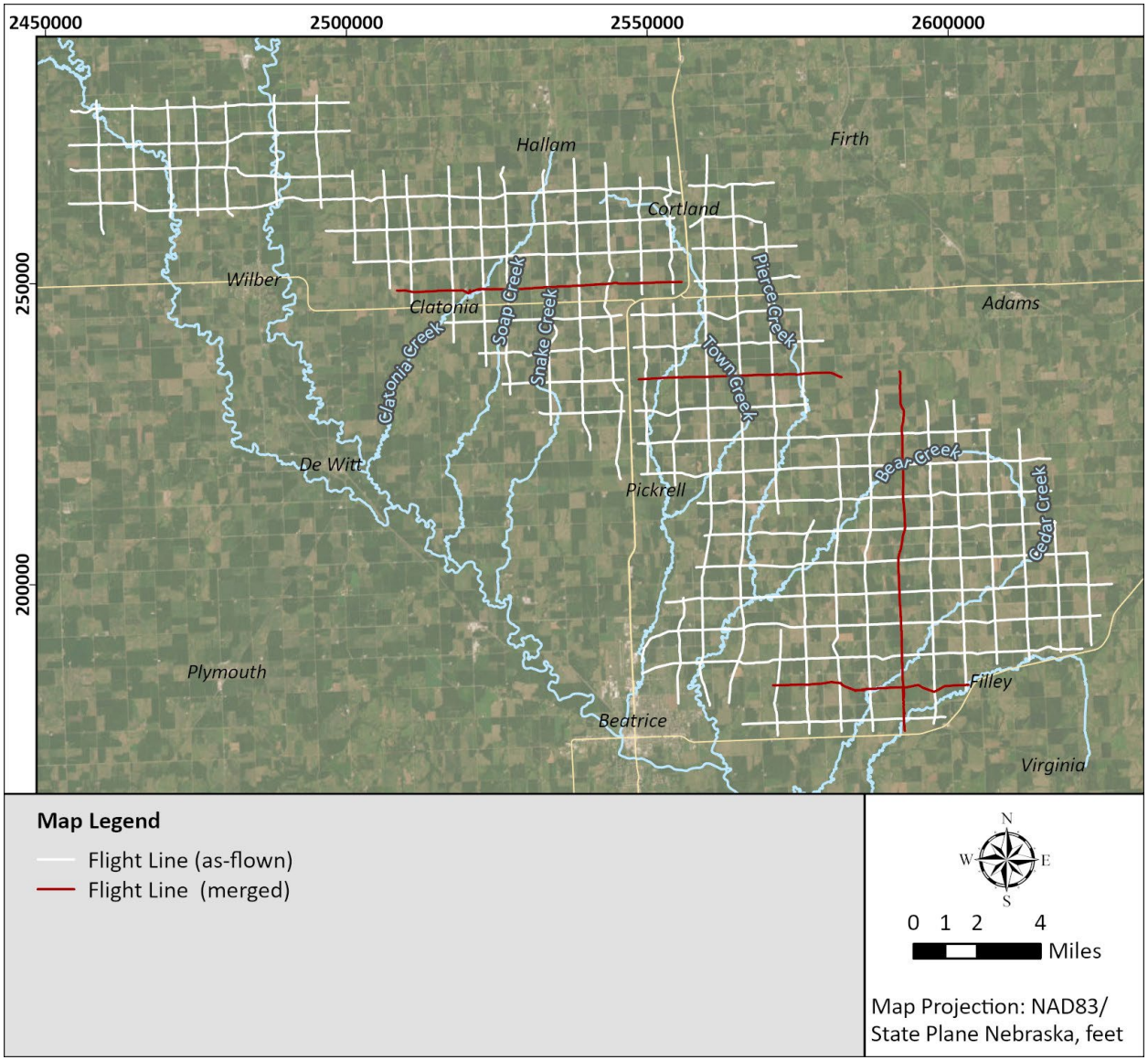


Figure 5-1. The flight lines and the connected merged lines for the 2025 LBBNRD AEM survey.

5.1.2 Construction of the Project Digital Elevation Model

To ensure that the elevation used in the project is constant for all the data sources (i.e., boreholes and AEM) a ground surface Digital Elevation Model (DEM) was downloaded and processed for the 2025 LBBNRD survey (Figure 5-2). The raster dataset was downloaded from the National Map Data Download Application (U.S. Geological Survey, 2026) at a resolution of 1/3 arc-second or approximately 30 ft. The native geographic coordinates are North American Datum of 1983 (NAD 83) and the elevation values are referenced to the North American Vertical Datum of 1988 (NAVD 88). The original 30 ft resolution was resampled to 300 ft and project products such as 2D grids and 3D voxel products were snapped to this 300 ft resolution. The map in Figure 5-2 of the ground surface DEM shows a vertical relief of 485 ft with a minimum elevation of 1080 ft and a maximum elevation of 1565 ft and an average elevation of 1322 ft. This DEM was used to reference all elevations within the AEM and borehole datasets.

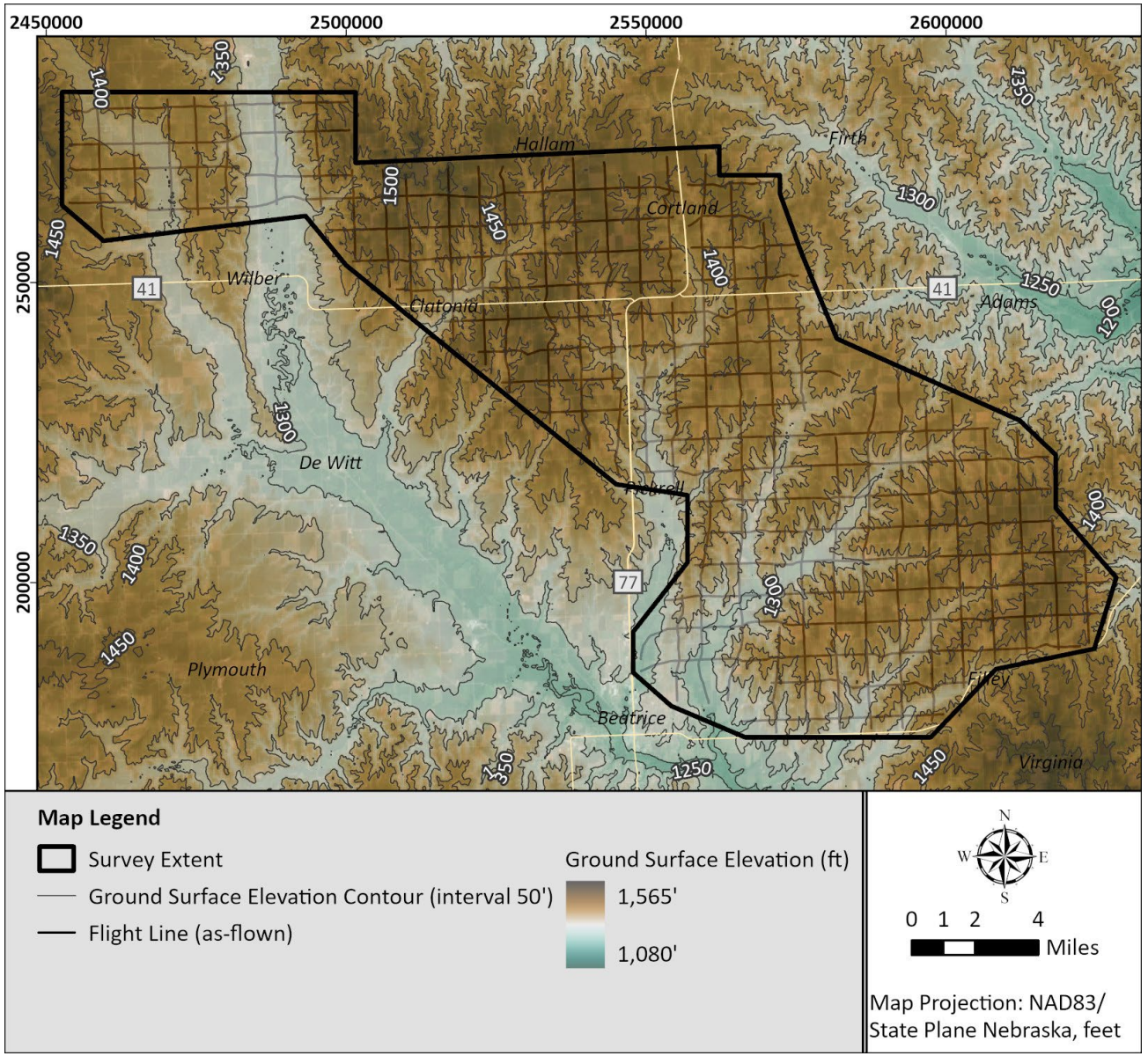


Figure 5-2. Map of the ground surface Digital Elevation Model (DEM) for the 2025 LBBNRD AEM survey.

5.1.3 Borehole-Only Surface of the Bedrock

As a guide in the interpretation of the AEM, a bedrock surface was prepared using CSD and NE-DWEE borehole logs in combination with published geologic maps. For conciseness, the bedrock surface interpolation process is described in the following list:

Data used:

- Most up to date NE-DWEE and CSD borehole data downloaded from the Nebraska GeoCloud (2026)
- NE-DWEE borehole processing
    - Extracted NE-DWEE boreholes within 1 mile of the planned flight lines.
    - Extracted project ground surface elevation to the NE-DWEE boreholes.
    - In a spreadsheet, categorized each borehole's lithology description as either 'Bedrock' or 'Unconsolidated' based on the description type.
        - For example:
            - Sandstone, Shale, Siltstone, Limestone, Chalk = 'Bedrock'
            - Clay, silt, gravel/boulders, etc. = 'Unconsolidated'
    - Extracted the depth/elevation of the first 'Bedrock' encountered for each borehole.
    - Saved the extracted data as a new working table.
- CSD borehole processing
    - Extracted CSD boreholes within 1 mile of planned flight lines.
    - Extracted project ground surface elevation to the CSD boreholes.
    - Used the stratigraphy table associated with the CSD borehole database to determine the depth/elevation of the first encountered 'Bedrock'.
    - Added the CSD borehole bedrock depths to the working table.

Borehole bedrock elevation interpolation:

- Converted the working table of NE-DWEE and CSD bedrock boreholes into a point shapefile.
- Interpolated the borehole point shapefile into a continuous raster dataset using the kriging geostatistical model and exported to a 300 ft cell size grid, snapped to the project ground surface DEM.
- Calculated the residuals of the actual measured top of bedrock elevation to the interpolated top of bedrock elevation.
- Reviewed any borehole where the residual was > 30 ft or < -30 ft. The value of 30 was used because it is a general representation of the degree of error while logging a borehole with mud rotary drilling techniques as it is approximately one drill stem length. Flagged and reviewed those boreholes that appeared to be anomalous.
    - After review, removed logs from the point shapefile that appeared to be inaccurate (i.e. bedrock was denoted at a depth inconsistent with surrounding wells).
- Re-interpolated the point shapefile following the same kriging geostatistical model and snapped to the 300 ft project ground surface DEM.
    - The final borehole shapefile used for interpolation of the borehole-only bedrock surface contained 403 data points and is depicted in Figure 5-3 below.

The bedrock surface was used as a guide in the interpretation of the bedrock within the AEM data profiles described next.

5.1.4 Interpretative 2D Profiles

After final combination of the AEM data, characterization of the subsurface was performed in cross-section format using Datamine Discover Profile Analyst (Datamine, 2026). During interpretation, the horizontal and vertical scale of the profiles were adjusted to facilitate viewing. The color scale of the resistivity data was also adjusted to illuminate subtle differences in the resistivity structure within the inverted AEM resistivity data related to the area being interpreted.

The first step in the interpretation is digitizing the contacts between the geologic units including: Quaternary (***Q***), Cretaceous Greenhorn and Graneros (***Kgg***), Cretaceous Dakota Group (***Kd***), and the undifferentiated Permian Chase Group, Permian Council Grove Group, Permian Admire Group, and Pennsylvanian Wabaunsee Group (***P***). The interpretive process benefited from the use of CSD and NE-DWEE, which combined provided lithologic, stratigraphic, and geophysical information. The interpretations were simultaneously checked against the CSD's Nebraska bedrock geology maps (Burchett, 1986 and Burchett and Pabian, 1992) and the geological outcrop map (Burchett et al., 1972). However, horizontal extents of geologic units may differ from Burchett (1986) and Burchett and Pabian (1992) due to the final interpretation of the AEM.

The interpretation began with picking the ***Kgg***/***Q***, the ***Kd***/***Q***, and ***P/Q*** contacts. These three contacts combine to form the bedrock surface. The borehole-only bedrock surface was mapped on the profiles and was used as a guide for the interpretation. The interpretation of the ***P***/***Kd*** and ***Kd***/***Kgg*** contacts included examining the AEM profile sections for contrasts in the electrical resistivity between model layers and using the borehole logs and the borehole-only bedrock. Three specific combinations of these surfaces will produce continuous layer interfaces: 1) The elevation of the of top of the ***Kgg*** is only the ***Kgg***/***Q*** interface; 2) The elevation of the top of the ***Kd*** is the result of ***Kd***/***Kgg*** + ***Kd***/***Q***; and 3) The elevation of the top of the ***P*** is the result of ***P***/***Kd*** + ***P***/***Q***. Many of the CSD and NE-DWEE borehole logs stop at the ***P*** due to that stratigraphic unit not being considered an aquifer since it is composed predominantly of limestone and shale.

For the profiles, the clipping distance from the flight line, or maximum distance from the flight line at which a borehole is displayed on the profile, was set independently for the CSD boreholes and the NE-DWEE boreholes. Typically, the CSD clipping distance was set to 2,640 ft, and the NE-DWEE boreholes was set to 1,320 ft. Both the ***Kd*** and the ***P*** can be challenging to interpret due to the variable nature of the limestone and shale of the ***P***, the presence of very low resistivities due to the presence of elevated total dissolvable solids (TDS) welling up into the ***Kd***, and the often lack of electrical contrast with the variable electrical resistivity of the ***Kd***. This is the reason the borehole-only surfaces were used as references in the interpretation of the ***Kd/Q***, ***P***/***Kd*** and ***P/Q*** contacts.

The interpretation of the ***Kd***/***Kgg*** and ***Kd/Q*** contacts included examination of the CSD and NE-DWEE boreholes and comparison with the AEM resistivities. The borehole information is critical in the

determination of an estimated top of the ***Kd***. The following borehole log characteristics were used to locate the top of the ***Kd***: 1) ***Kd*** is indicated on the CSD borehole stratigraphic logs; 2) There is an indication of sandstone, siltstone, or shale in the CSD borehole lithology logs; 3) There is an indication of sandstone, siltstone, shale in the NE-DWEE lithology logs; and 4) There is a resistivity change or layer indicating ***Q*** loess or till deposits.

Patterns in the resistivity were also used to match the difference in the ***Q*** and the ***Kd***. In the areas of coarse ***Kd*** deposits and Quaternary ***Q*** deposits, the interpretation is more challenging due to a lack of resistivity contrast. Resistivity zone patterns were used to match these areas and continuations of the ***Kd*** from under the low resistivity loess/till deposits were used to estimate the contact.

The interpretation of the ***P***/***Kd*** and ***P/Q*** contacts included examination of the CSD borehole stratigraphy logs and NE-DWEE lithology logs in comparison to the AEM resistivities. The borehole information is critical in the determination of an estimated top of the ***P***. The following borehole log characteristics were used to locate the top of the ***P***: 1) the shallowest elevation for ***P*** or older formations/groups was identified, then extracted from the CSD borehole stratigraphic logs; and 2) there is a resistivity change or layer indicating ***Q*** loess or till deposits, or ***Kd*** materials.

It should be noted that the tops of the ***Kd*** and ***Kgg***, as interpreted, are estimates. This is due to the challenge of both the lithology interpretation of drill cuttings of the ***Kd*** and the low electrical resistivity contrast. Throughout this report both the ***Kgg*** and ***Kd*** will be shown as dashed lines and care needs to be exercised in the use of the interpreted top of these surfaces. Generally, for all profiles, the inversion DOI was inspected during interpretation. And, the white areas within the profiles are zones that were cut from the AEM data due to EM-coupling from infrastructure or areas that were not flown due to FAA regulations were interpreted across the data gap.

East-west flight line L100011, presented in Figure 5-4, is approximately 8.5-miles-long and is the most northwestern line in the survey. Sub-cropping ***Kgg*** is observed on the western end underlain by the ***Kd***. Many boreholes indicate coarse materials and high resistivities. This includes CSD Test Hole 01-CS-2019. A moderate resistor is also noted in the lower ***Kd*** section, and this is most likely comprised of sands and some finer grained materials. The Estimated Saline Water Level (ESWL) is indicated by the dashed purple line is present within the ***Kd***. Regions within the ***Kd*** have been denoted as “Fresh ***Kd***” and “Saline ***Kd***” in the profiles. This surface was generated by a <7 ohm-m threshold, where the elevation of the top of the first cell at or below 7 ohm-m was extracted, a smoothing filter was added to remove noisy areas. These low resistivities are not unique to high TDS waters and fine grain sediments, like clays, can be conductive as well. For AEM methods to tease apart geologic features, a contrast in the electrical resistivity model needs to be observed and differentiating clay layers from saline water intrusions can be difficult, if not impossible. However, we know that the ***P*** should be resistive due to the carbonate makeup in this area.

East-West flight line L100070, presented in Figure 5-5, is approximately 8.5-miles-long. Many NE-DWEE-registered wells can be seen along the profile, and much of the interpreted ***Kd*** is observed along the line with several of the lithology logs indicating sandstone. The ESWL is just at the bottom of the ***Kd*** on the western end of the line. There is limited high resistivity materials within the ***Q*** section.

North-south line L190191, presented in Figure 5-6, is approximately 17.5-miles-long and shows interpreted contacts for both ***P***/***Kd*** and ***Q***/***P***. The AEM and the NE-DWEE registered wells both indicate that the ***Kd*** is present and the borehole-only top of ***P*** surface was used as guide to pick the ***P***/***Kd*** and ***Q***/***P*** boundary. This profile shows a deep ***Q*** paleochannel on the south end as well the edge of another channel on the northern end. Many wells are completed in these areas. The ESWL can be observed below the ***Kd*** contact.

North-south line L190271, presented in Figure 5-7, is approximately 9.5-miles-long and on the eastern side of the survey across the paleochannel. This profile shows the ESWL surface well below the ***Q*** materials within the ***P***. Again, the AEM and the NE-DWEE registered wells indicate areas of increased coarse-grained materials. However, the paleochannel contains much less higher resistivity materials as compared with Figure 5-6.

The above examples illustrate the interpretive process that was used on the profiles provided within this report. All the flight lines are presented in *Appendix 1 – 2D Profiles* with the resulting hydrogeological interpretations. Details for each flight line are presented as well as the corresponding CSD and NE-DWEE registered wells within the specified distances.

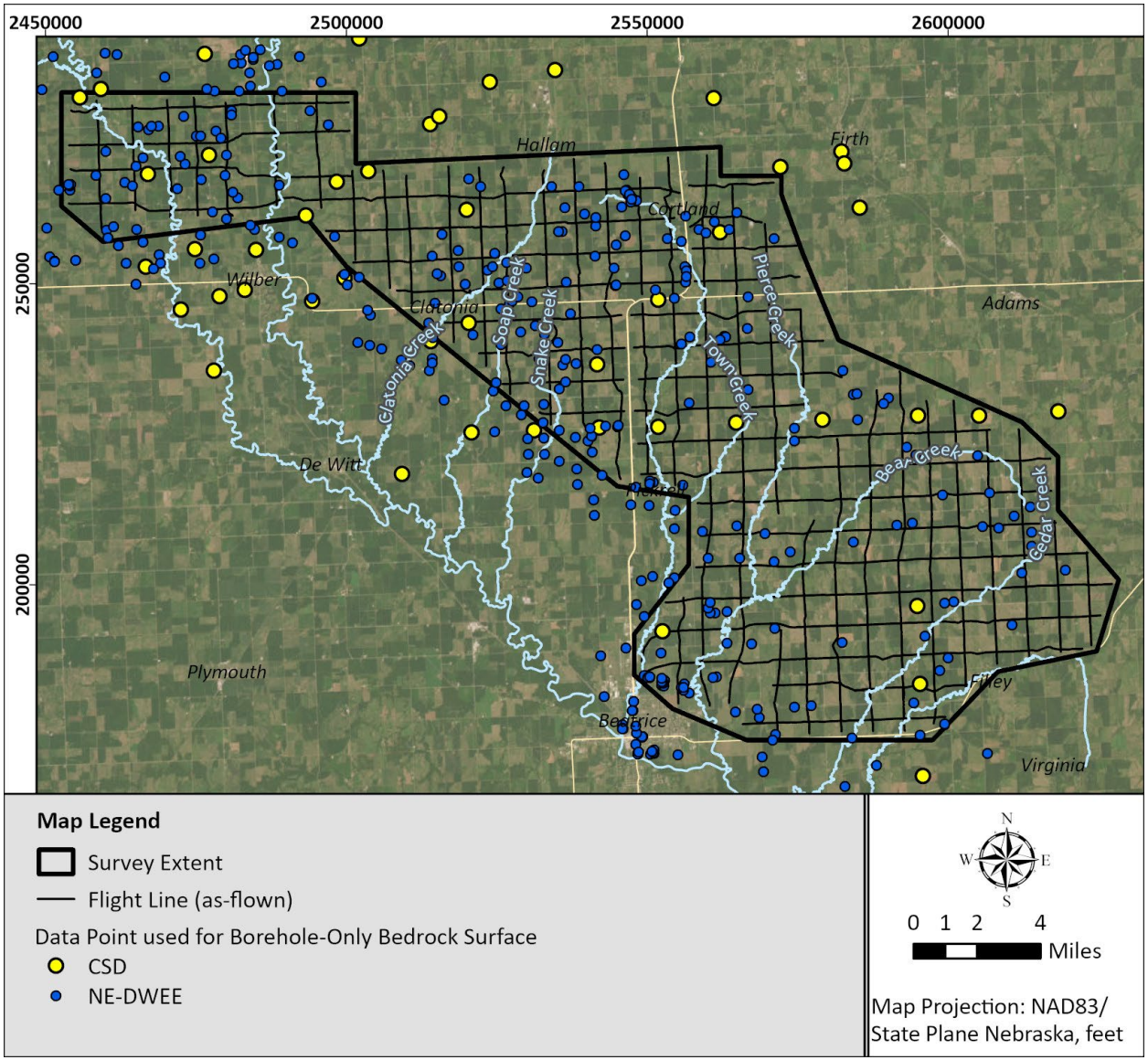


Figure 5-3. Map of the project boundary showing the data points used to interpolate the bedrock surface elevation. This "borehole only" interpolated bedrock surface was used as a guide in the interpretation of the AEM data. The projection is NAD83 State Plane Nebraska (feet).

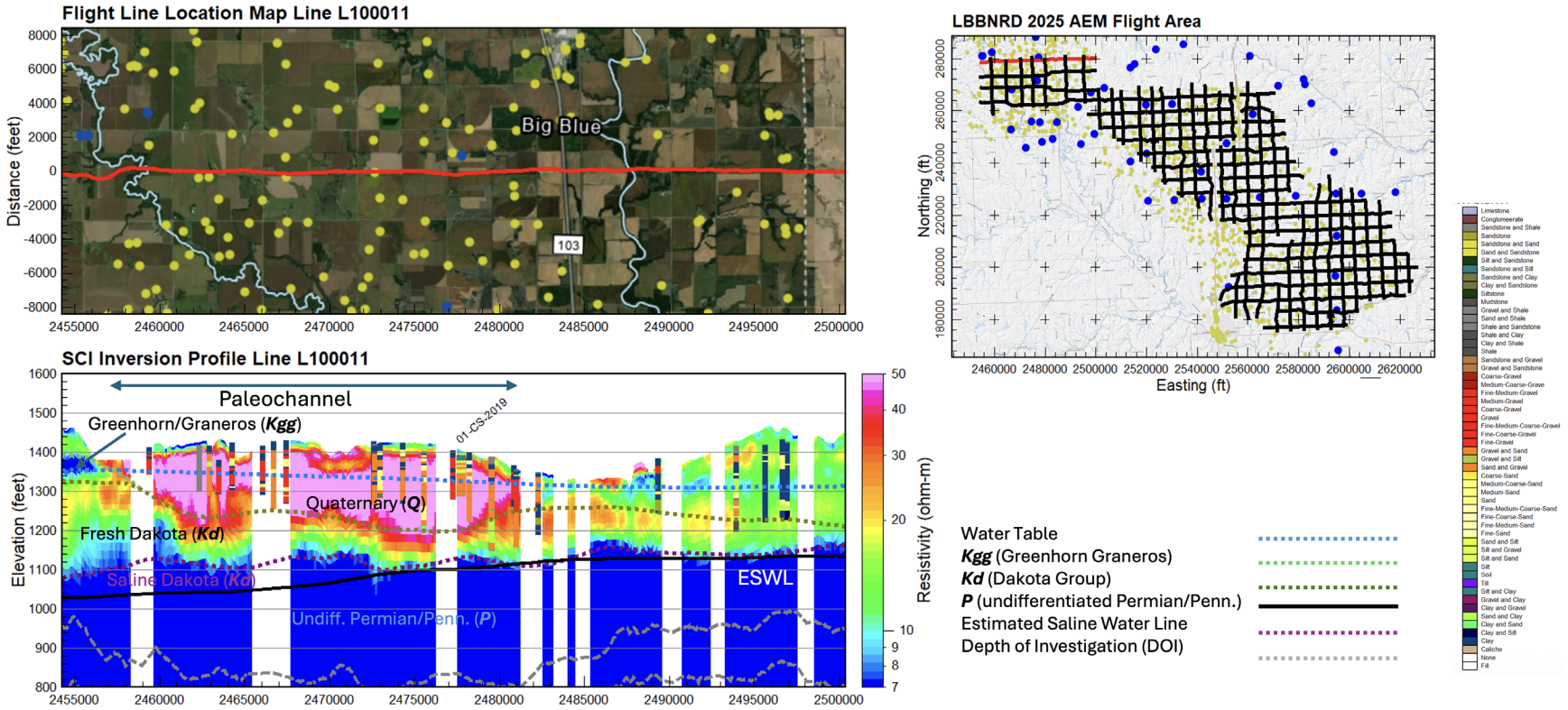


Figure 5-4. 8.5-mile-long southwest-northeast line L100011. The top right map displays the flight lines as black lines and the selected flight line shown in the profiles as a red line. Blue dots indicate CSD test holes and olive dots are the NE-DWEE registered wells. Lithology from CSD and NE-DWEE registered boreholes within 1,320 feet are projected on the flight line. Gaps in the profile are due to EM decoupling from infrastructure or areas that were not flown due to FAA regulations. Projection is NAD83 State Plane Nebraska (feet), the vertical datum is NAVD88 (feet).

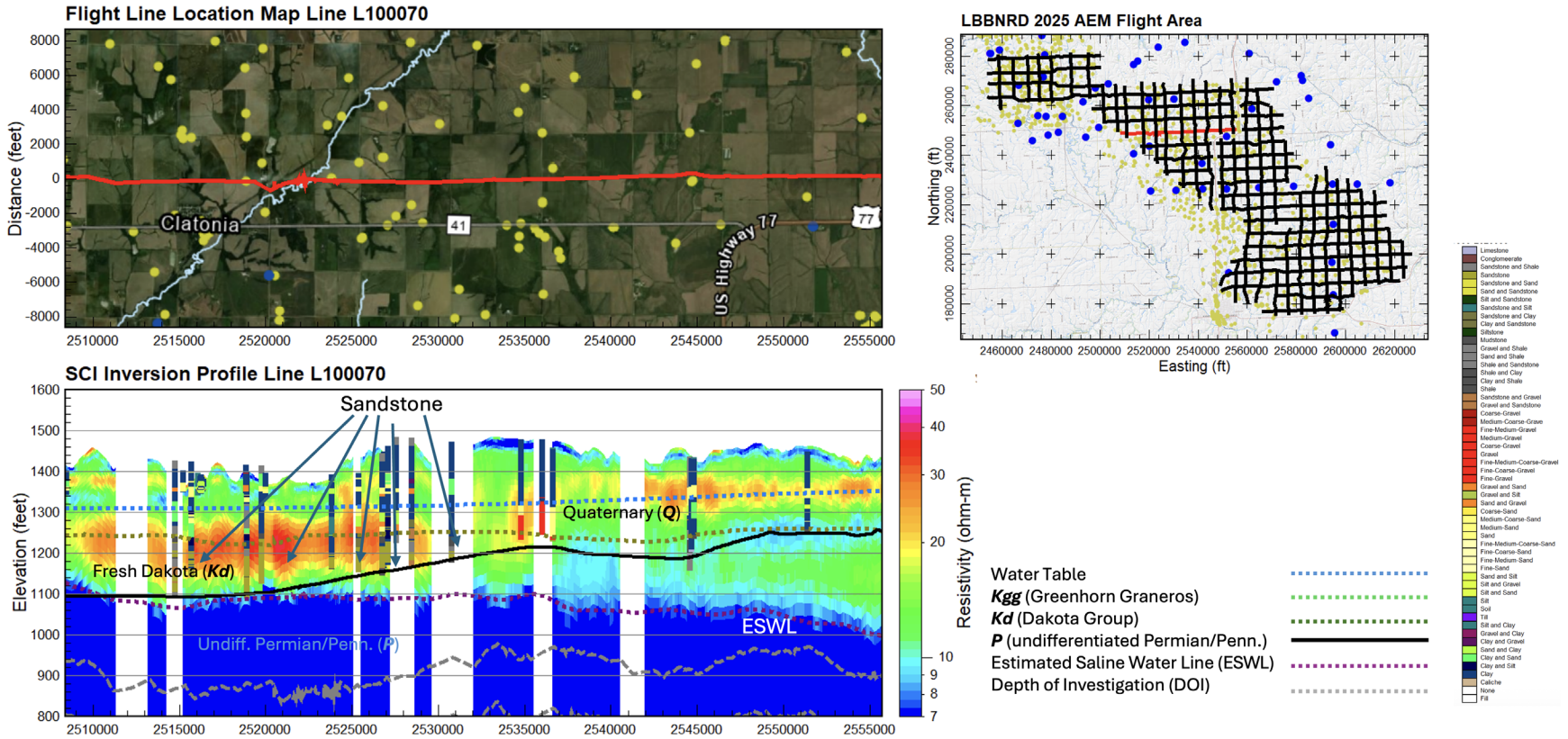


Figure 5-5. 8.5-mile-long east-west line L100070. The top right map displays the flight lines as black lines and the selected flight line shown in the profiles as a red line. Blue dots indicate CSD test holes and olive dots are the NE-DWEE registered wells. Lithology from CSD and NE-DWEE registered boreholes within 1,000 feet are projected on the flight line. Gaps in the profile are due to EM decoupling from infrastructure or areas that were not flown due to FAA regulations. Projection is NAD83 State Plane Nebraska (feet), the vertical datum is NAVD88 (feet).

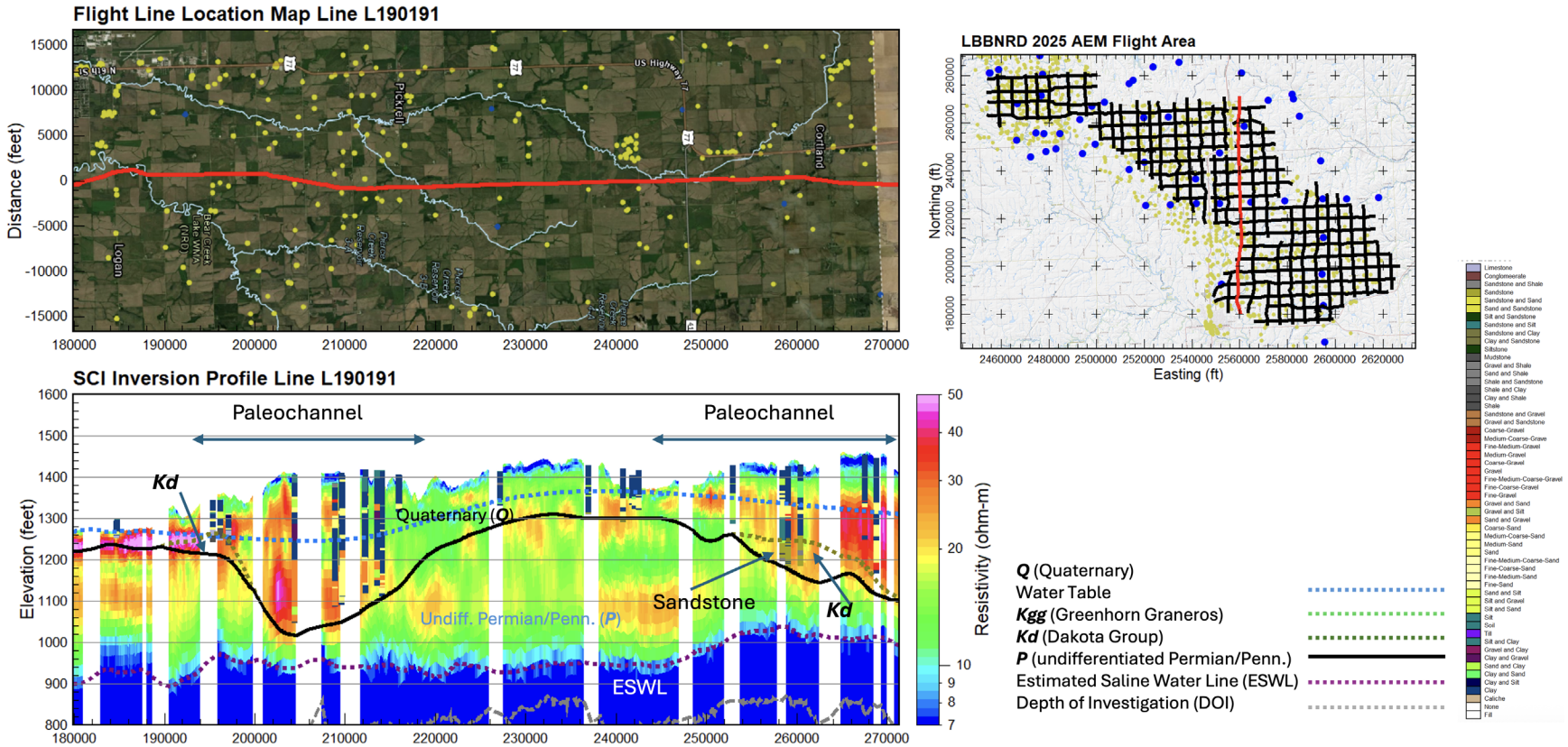


Figure 5-6. 17.5-mile-long north-south line L190191. The top right map displays the flight lines as black lines and the selected flight line shown in the profiles as a red line. Blue dots indicate CSD test holes and olive dots are the NE-DWEE registered wells. Lithology from CSD and NE-DWEE registered boreholes within 1,000 feet are projected on the flight line. Gaps in the profile are due to EM decoupling from infrastructure or areas that were not flown due to FAA regulations. Projection is NAD83 State Plane Nebraska (feet), the vertical datum is NAVD88 (feet).

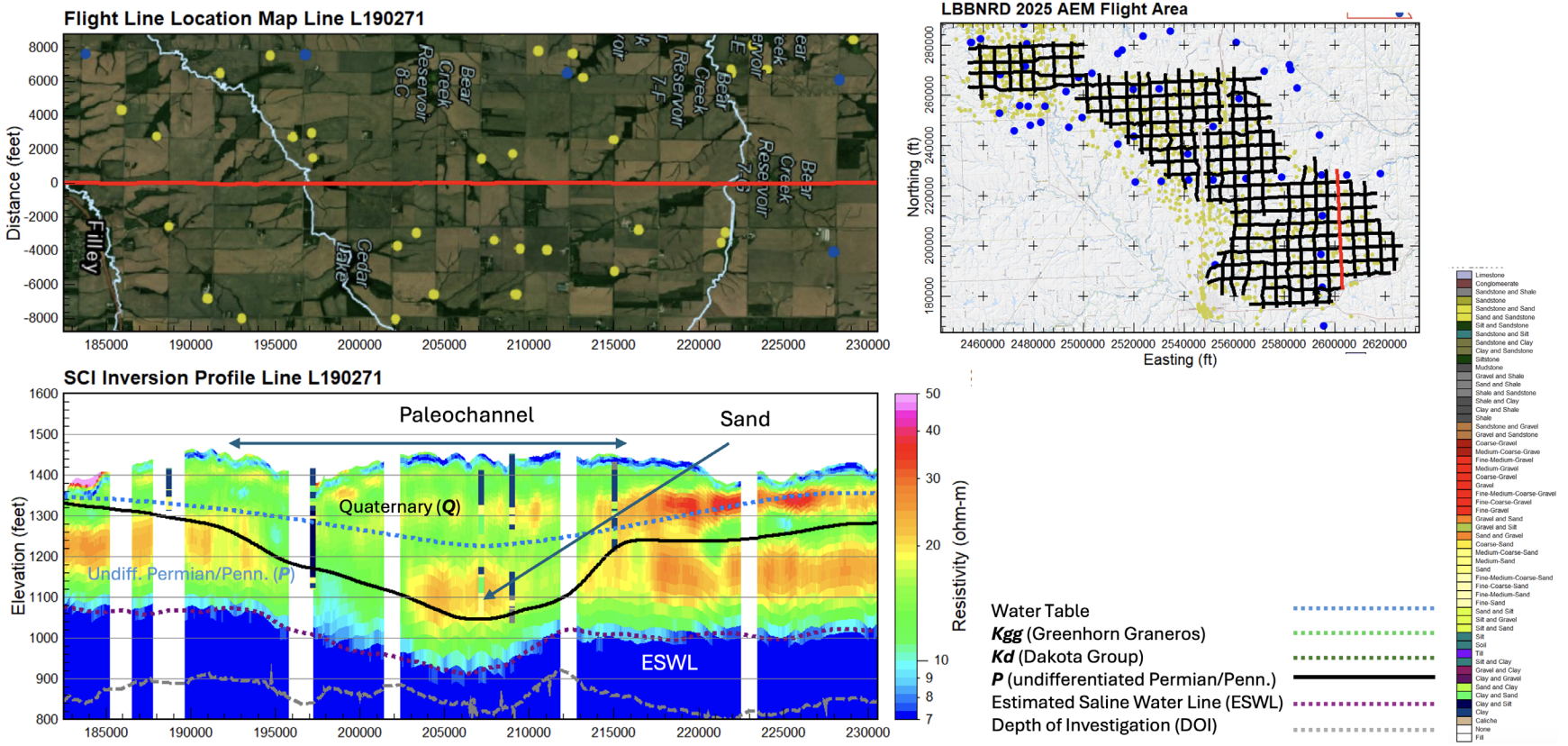


Figure 5-7. 9.5-mile-long north-south line L190271. The top right map displays the flight lines as black lines and the selected flight line shown in the profiles as a red line. Blue dots indicate CSD test holes and olive dots are the NE-DWEE registered wells. Lithology from CSD and NE-DWEE registered boreholes within 1,000 feet are projected on the flight line. Gaps in the profile are due to EM decoupling from infrastructure or areas that were not flown due to FAA regulations. Projection is NAD83 State Plane Nebraska (feet), the vertical datum is NAVD88 (feet).

5.1.5 Interpretative Surface Grids

After the AEM data were interpreted, the interpretations (i.e., points with elevations that represent the top of specific geologic units) were extracted into a GIS shapefile so that continuous raster surfaces could be developed. Please note that the terms grid, surface, and raster are used interchangeably, and all refer to a continuous dataset made up of cells, with each cell being a 300 ft by 300 ft area, where each cell contains elevation data representative at that cell location.

In addition to the AEM data interpretation points, CSD and NE_DWEE boreholes with elevation data were considered during the surface interpolation process. The number of points used for the interpolation of the top of ***Kgg***, ***Kd***, and ***P*** surfaces are displayed in Table 5.2.

Table 5-2. Number of data points used to interpolate the elevation of the top of *Kgg*, *Kd,* and *P* surfaces.

Geologic Unit	# of AEM Data Points	# of CSD Boreholes	# of NE-DWEE Points
Top of Bedrock	**2,406**	**170**	**47**
Bottom of Cretaceous Greenhorn-Graneros (*Kgg*)	**15**	**0**	**1**
Bottom of Cretaceous Dakota Group (*Kd*)	**361**	**0**	**3**

The elevation point data were interpolated for each geologic unit into a continuous surface using the kriging geostatistical model and exported to 300 ft cell size resolution raster datasets. The surfaces were corrected with the 300 ft resolution ground surface DEM so that each surface was restrained to less than or equal to the DEM minus 3' elevation.

Figures 5-8, Figure 5-9, and Figure 5-10 present maps displaying the top elevation surfaces of the ***Kgg***, ***Kd*** and ***P*** within the 2025 LBBNRD AEM survey area, respectively. Using the top elevation grids for the ***Kgg***, ***Kd***, and ***P*** units, a top of bedrock elevation surface was produced by mosaicking, or stitching, the three grids together. Figure 5-11 is a map of the elevation of the top of bedrock surface within the 2025 LBBNRD AEM survey area.

Each top elevation surface was subtracted from the DEM to calculate the depth (in feet) to the top of each surface. Figure 5-12, Figure 5-13, Figure 5-14, and Figure 5-15 present maps displaying the depth to the tops of the ***Kgg***, ***Kd***, ***P***, and bedrock, respectively.

Total thickness for the ***Q***, ***Kgg***, and ***Kd*** were calculated using the top of elevation surfaces and DEM in ESRI's raster calculator. Table 5-3 summarizes the raster calculator input and output for each thickness calculation. The output was set to 'snap' to the 300 ft DEM and then was clipped to each geologic unit extent.

Table 5-3. Summary of the input into ESRI's raster calculator and the resultant output.

Raster Calculator Input	Output Result
DEM – Bedrock	Q Thickness
Top of *Kgg* - Top of *Kd*	*Kgg* Thickness
Top of *Kd* - Top of *P*	*Kd* Thickness

Figure 5-16, Figure 5-17, and Figure 5-18 present maps displaying the total thickness of ***Q***, ***Kgg***, and ***Kd***, respectively.

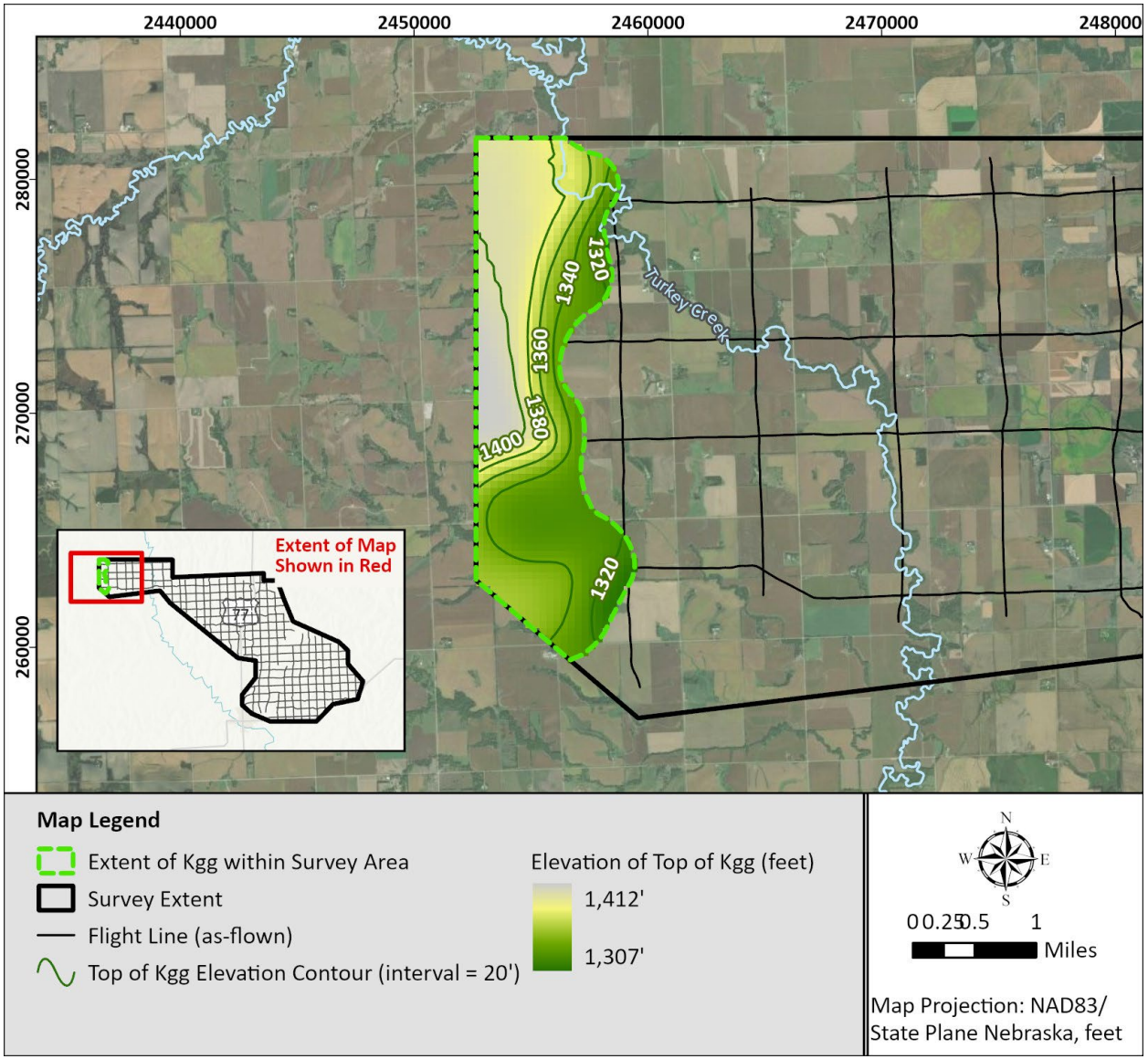


Figure 5-8. Map displaying the elevation of the top of the Cretaceous Greenhorn/Graneros (*Kgg*) Group. The extent of the *Kgg* within the survey area is shown in bright green. Map projection is NAD83 State Plane Nebraska (feet).

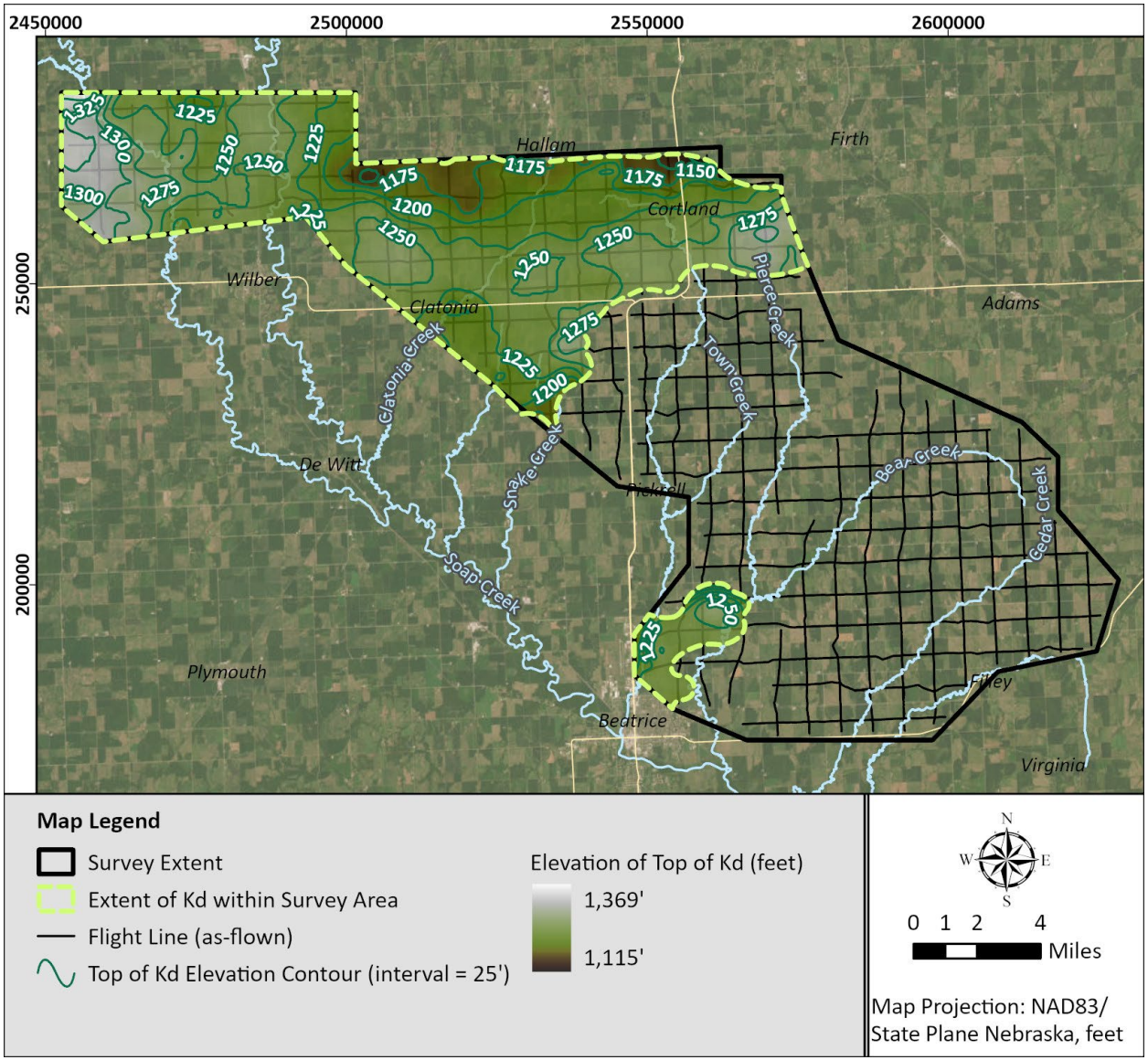


Figure 5-9. Map displaying the elevation of the top of the Cretaceous Dakota (*Kd*) Group. The extent of the *Kd* within the survey area is shown in bright green. Map projection is NAD83 State Plane Nebraska (feet).

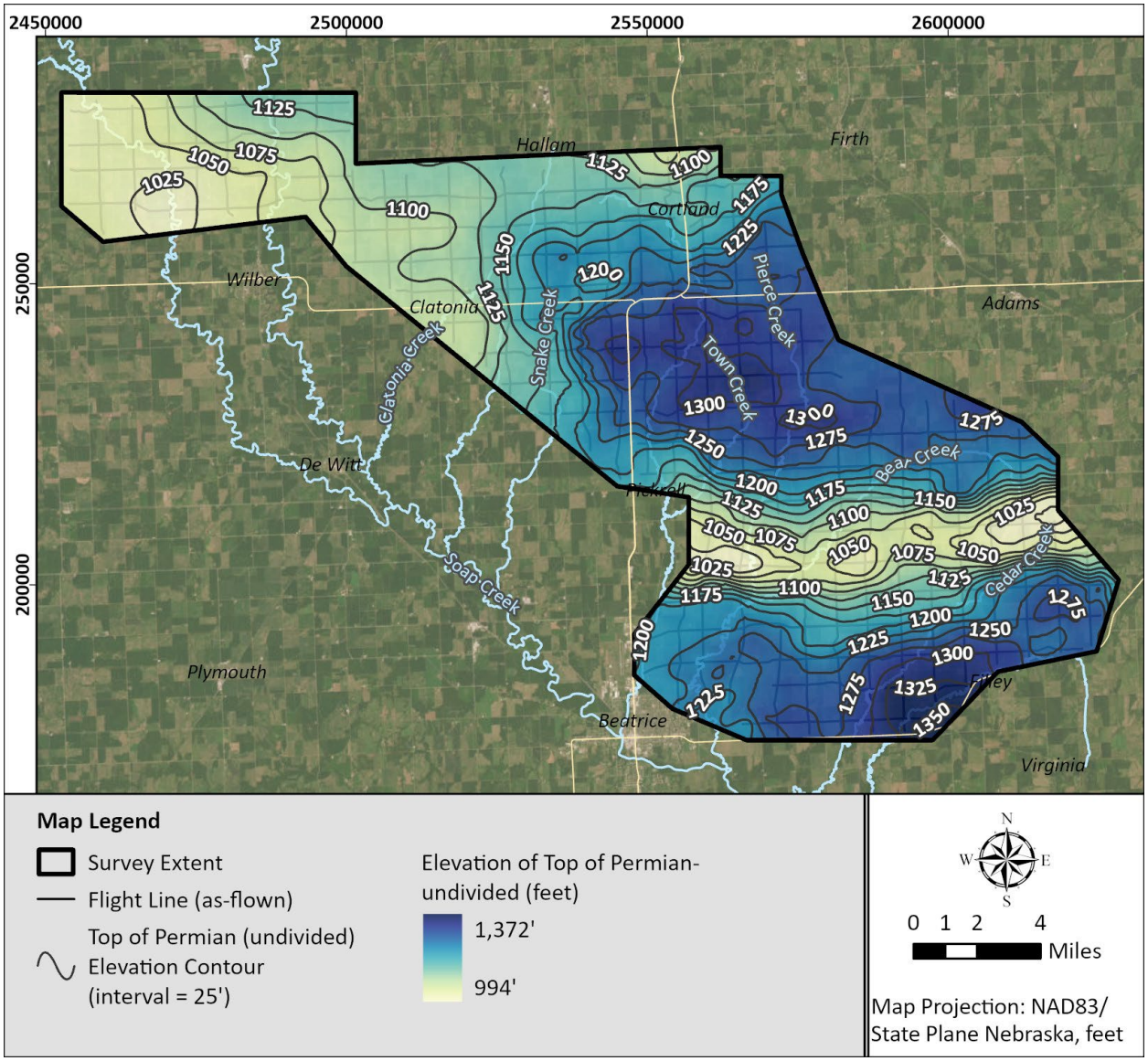


Figure 5-10. Map displaying the elevation of the top of undifferentiated Permian units. Map projection is NAD83 State Plane Nebraska (feet).

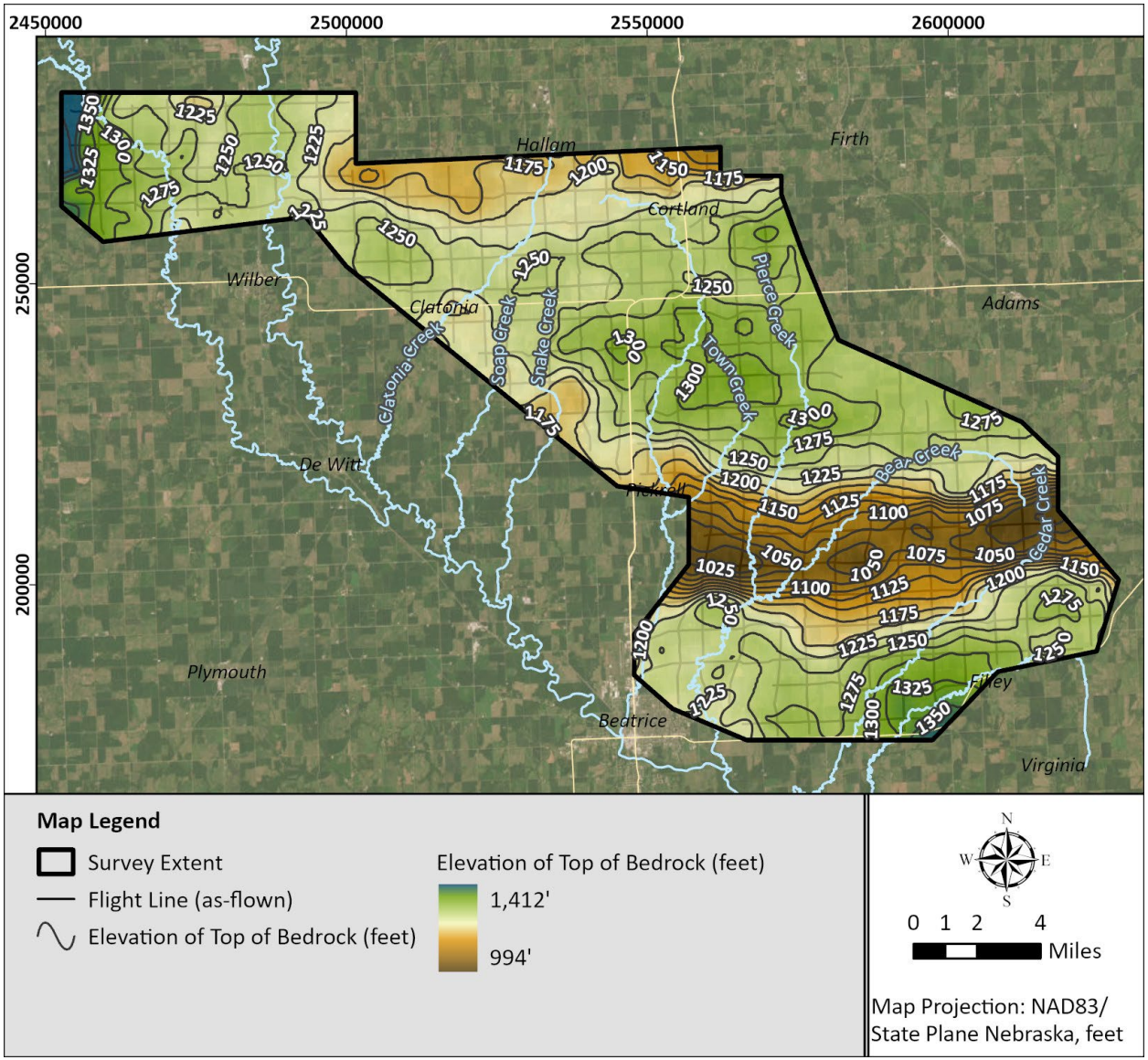


Figure 5-11. Map displaying the elevation of the top of bedrock. Map projection is NAD83 State Plane Nebraska (feet).

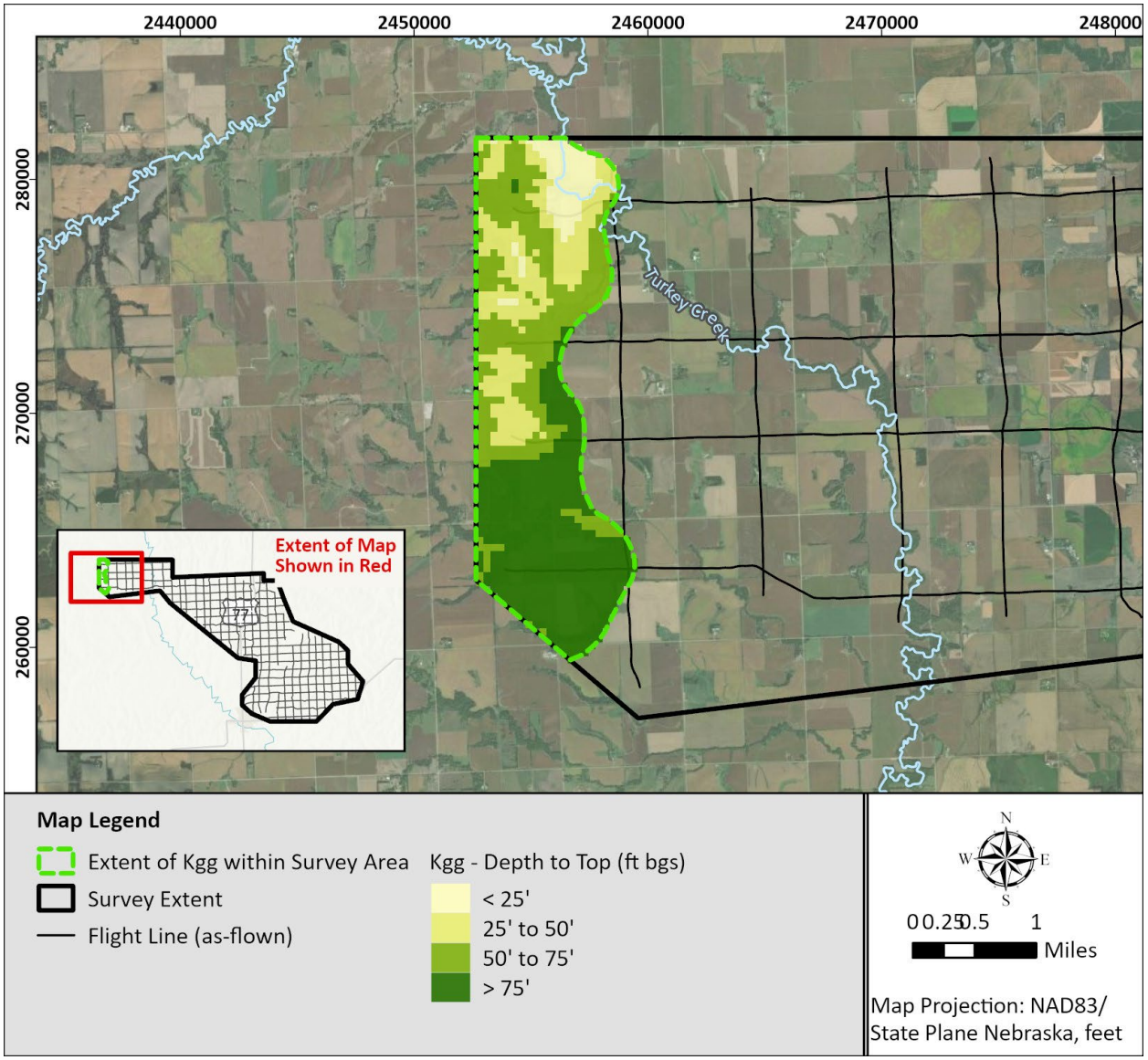


Figure 5–12. Map displaying the depth to the top of Cretaceous Greenhorn/Graneros (*Kgg*) Group. The extent of the *Kgg* within the survey area is shown in bright green. Map projection is NAD83 State Plane Nebraska (feet).

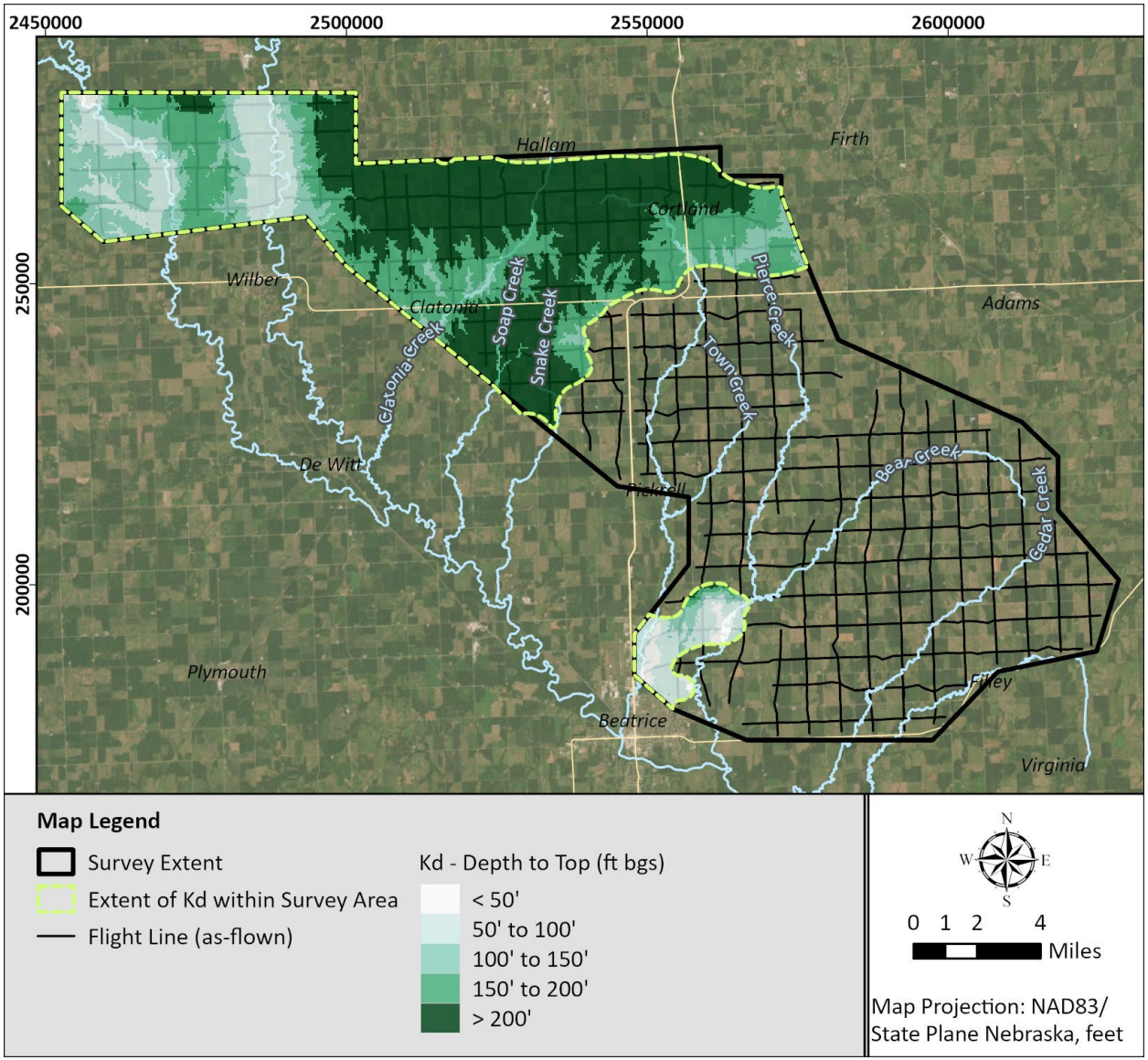


Figure 5-13. Map displaying the depth to the top of Cretaceous Dakota (*Kd*) Group. The extent of the *Kd* within the survey area is shown in bright green. Map projection is NAD83 State Plane Nebraska (feet).

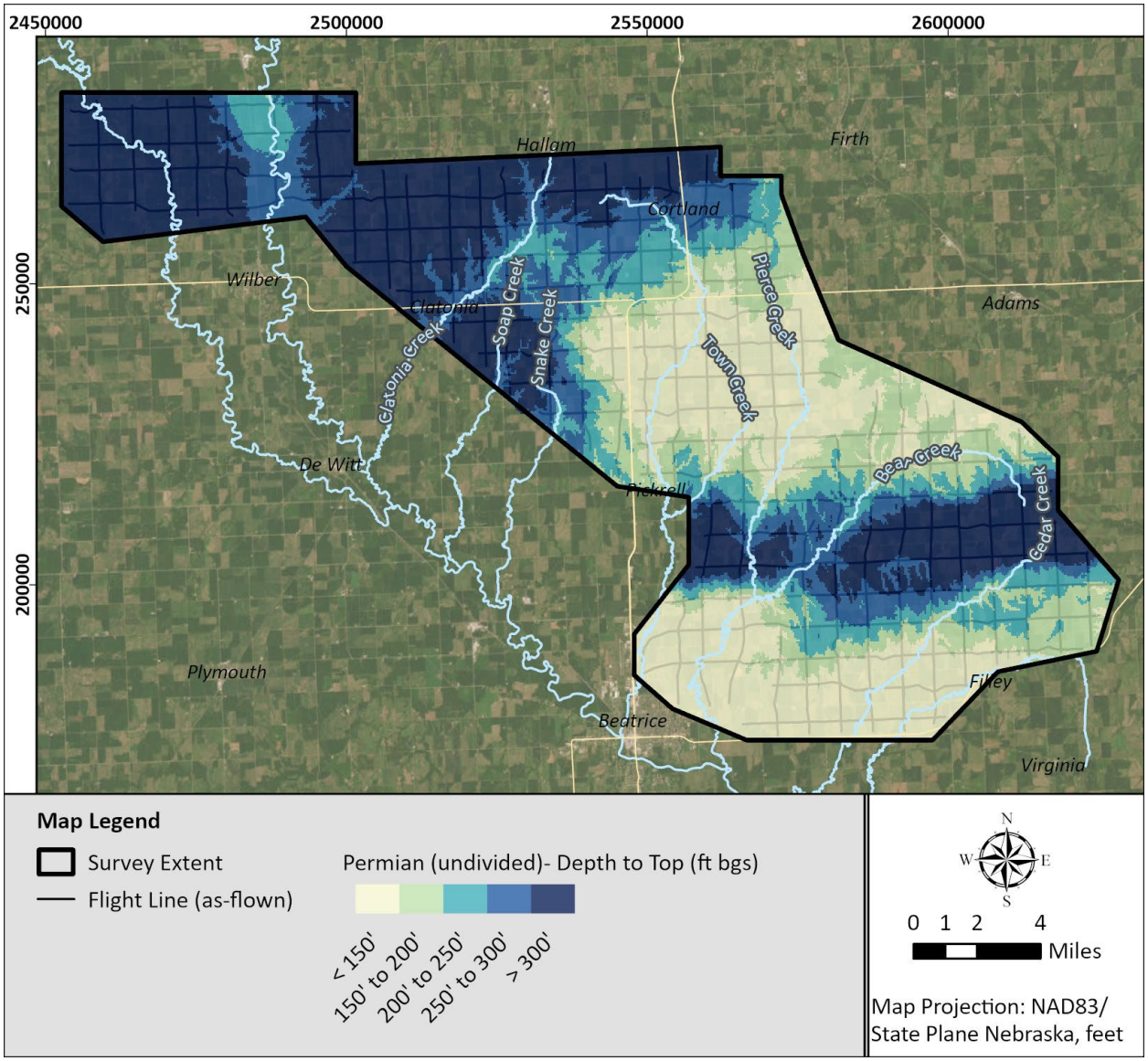


Figure 5-14. Map displaying the depth to the top of undifferentiated Permian units. Map projection is NAD83 State Plane Nebraska (feet).

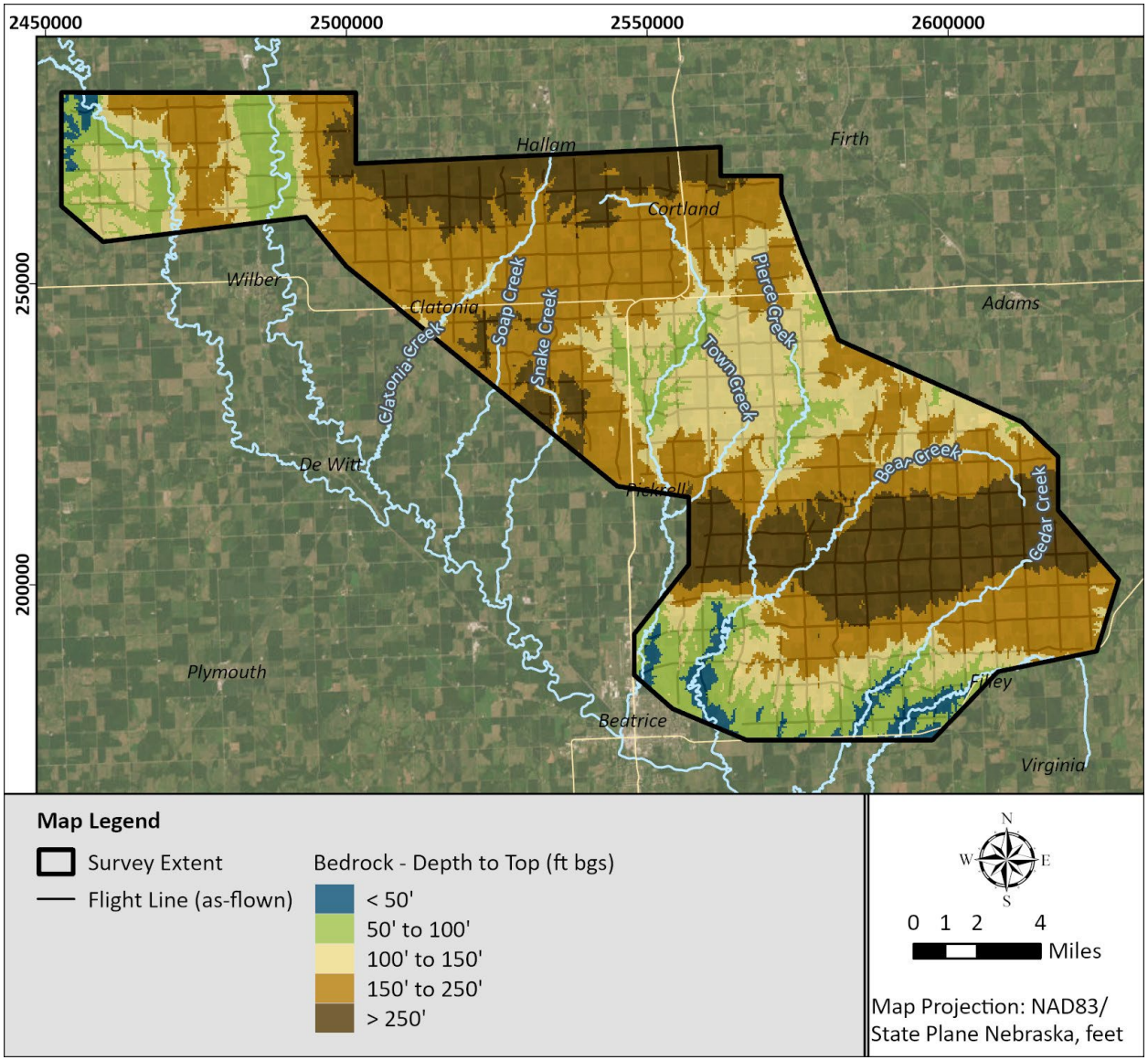


Figure 5-15. Map displaying the depth to the top of bedrock. Map projection is NAD83 State Plane Nebraska (feet).

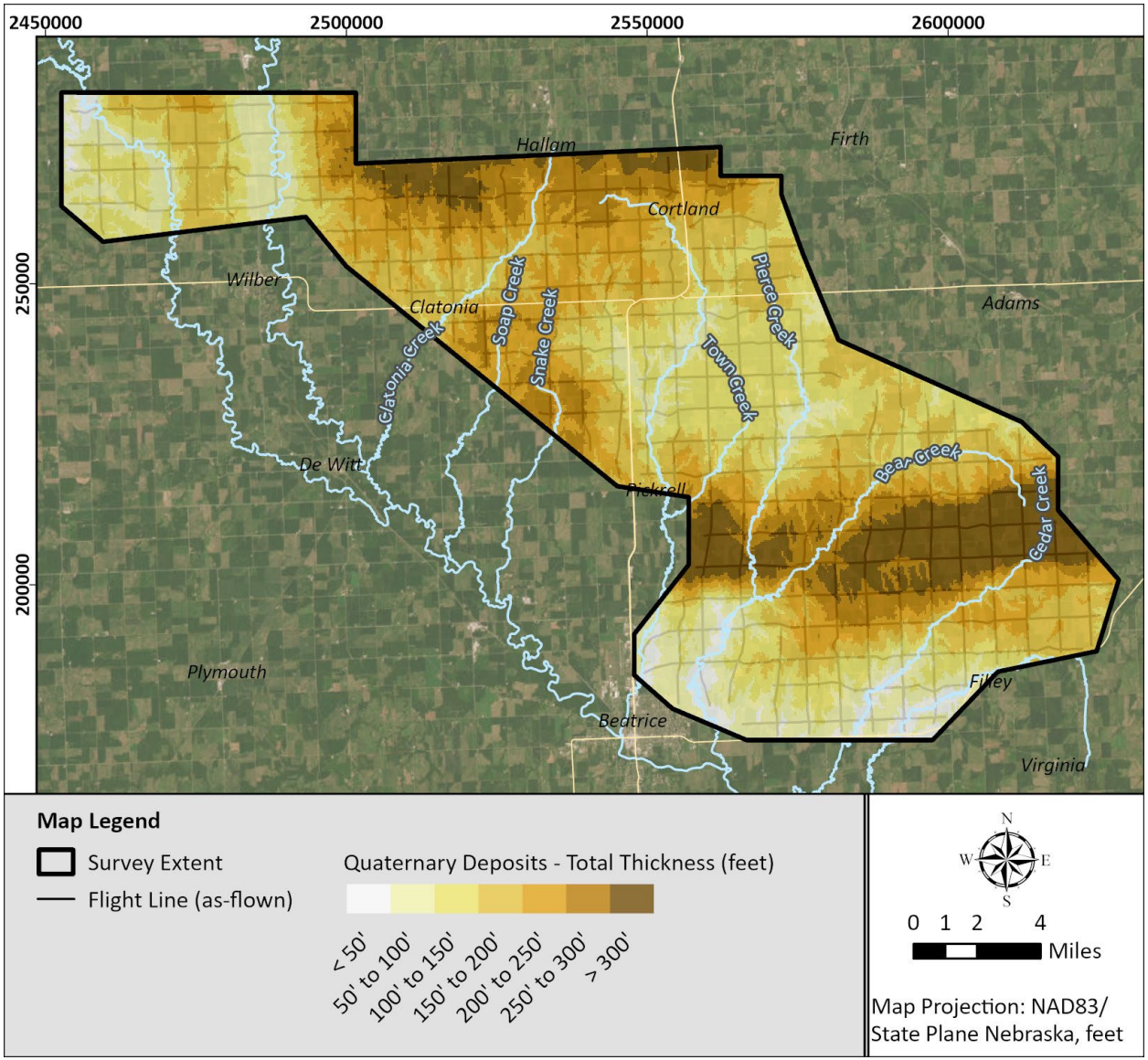


Figure 5–16. Map of displaying the total thickness of the Quaternary (*Q*) material. Map projection is NAD83 State Plane Nebraska (feet).

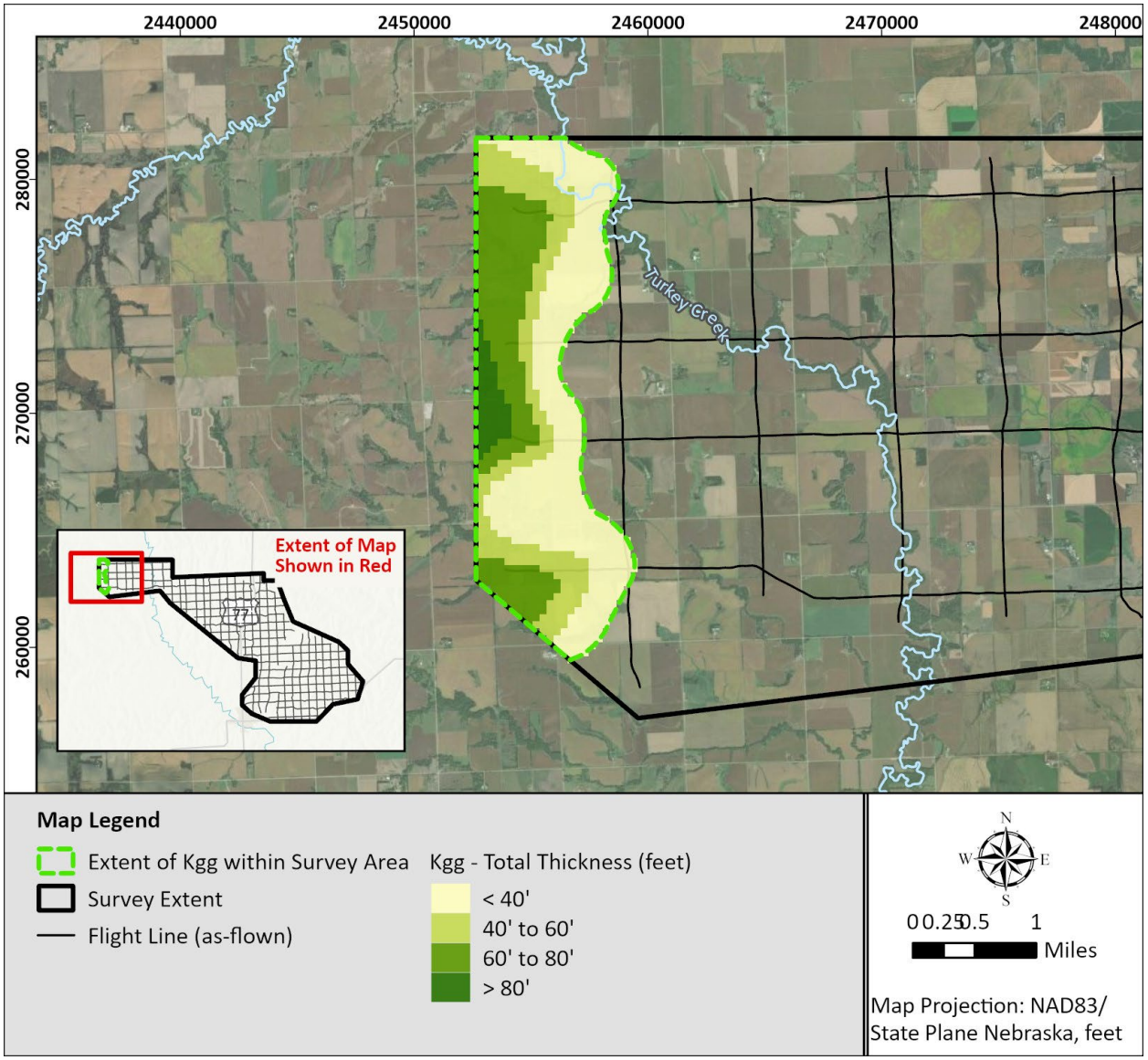


Figure 5-17. Map of displaying the total thickness of the Cretaceous Greenhorn/Graneros (*Kgg*) material. Map projection is NAD83 State Plane Nebraska (feet).

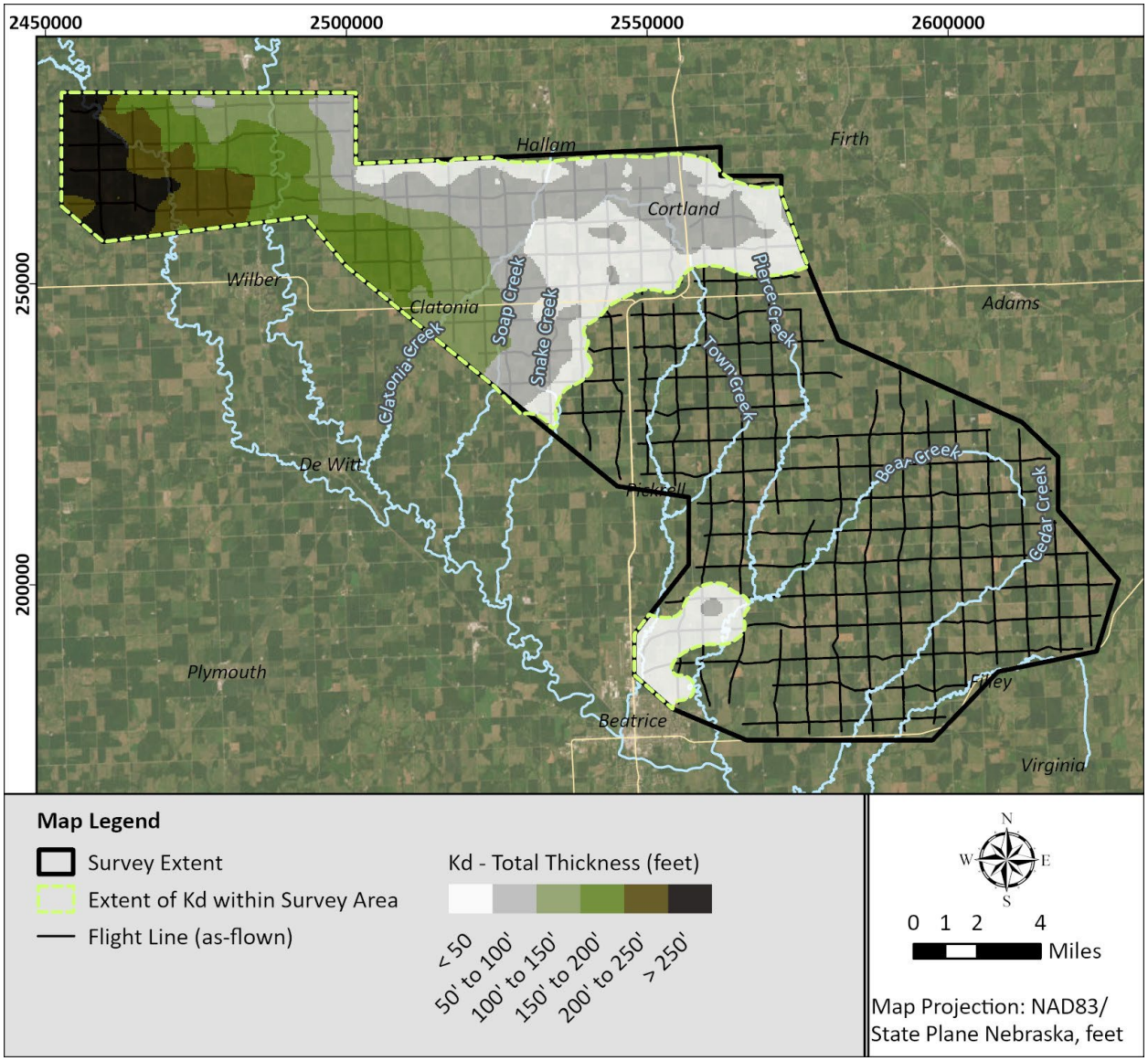


Figure 5-18. Map displaying the total thickness of Cretaceous Dakota (*Kd*) Group. The extent of the *Kd* within the survey area is shown in bright green. Map projection is NAD83 State Plane Nebraska (feet).

5.1.6 Water Table

To assist in the approximation of the saturated materials along the surveyed AEM flight lines, a water table was created. Water level data were provided by LBBNRD as shapefiles, including *MonWell_Levels* and *Irrigation_Levels.* These two shapefiles provided a robust, consistent dataset of historic water levels and most useful to this project were the water level readings from Spring 2025 *(Personal Communication, Tyler Weishahn, January 2026)*. Wells from the shapefiles within and adjacent to the survey area were extracted into a single dataset for interpolation into a continuous raster surface.

To add control for the interpolated surface, "stream points" were digitized along the Big Blue River in the south and the Middle Branch Big Nemaha River in the north. The ground surface elevation was extracted to each point to represent the water level at that location.

Additional control was needed in areas where data gaps existed in the monitoring and irrigation well datasets. NE-DWEE well water levels were hand-selected to add to the water level dataset based on location (i.e., where data gaps exist) and age (no wells older than 1999 were used, with the exception of well ID 58404 [G-050882]). Two wells, ID 58404 and ID 175433 (G-139724) were measured by LBBNRD on February 26, 2026, to confirm the static water level in the southeast area of the survey area (*Personal Communication, Tyler Weishahn, 02/26/2026*). These two data points were key to developing a more realistic water table south of the deepest part of the paleochannel in the southeast of the survey area.

After these four datasets were compiled (two datasets from LBBNRD, hand-selected NE-DWEE wells, and stream points), a surface was interpolated using the kriging geostatistical method in ArcGIS Pro. The interpolated surface was smoothed with the focal statistics tool, then the accuracy of the surface was checked by calculating the residual values for the data points used in the interpolation (i.e., water level in point dataset minus water level at that location extracted from interpolated surface). All residuals were +/- 6 ft. The final surface was corrected with the project ground surface DEM so that no part of the water table surface was higher in elevation than the ground surface. Figure 5-19 below displays the water table elevation surface along with the control points used to interpolate the surface. The water table elevation was subtracted from the project ground surface DEM to determine the depth to the top of the water table. Figure 5-20 displays the elevation of (left image) and depth to (right image) the water table in feet with contours for reference.

The saturated thickness of ***Q***, ***Kgg***, and ***Kd*** were calculated using both the mosaic tool and raster calculator with the water table, top of bedrock, and top of ***Kd*** and ***P*** surfaces. Figure 5-21, Figure 5-22, and Figure 5-23 are maps displaying the total saturated thickness of ***Q, Kgg,*** and ***Kd***, respectively.

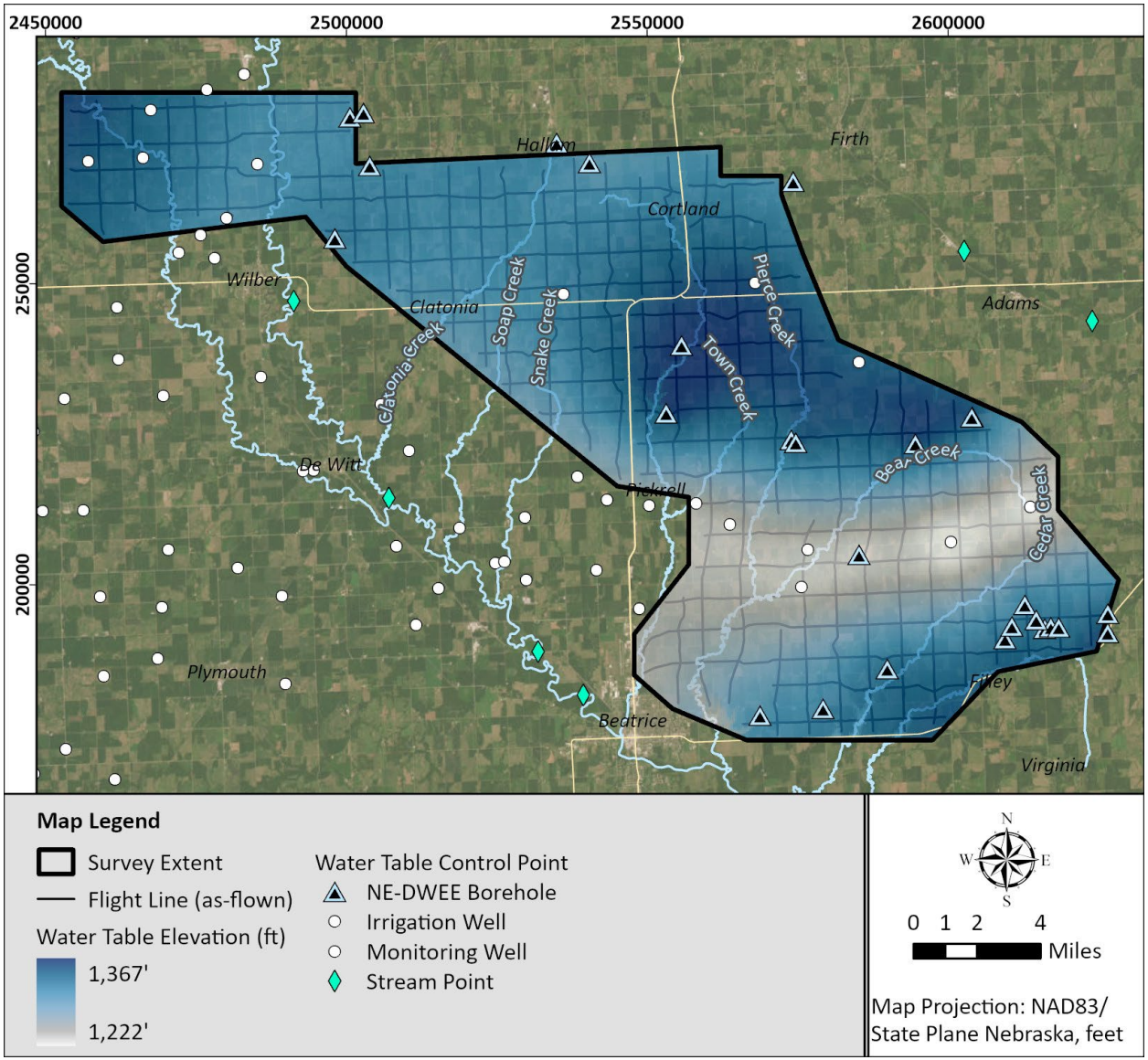


Figure 5-19. Map of water table elevation surface and the control points used to interpolate the surface. The projection is NAD83 State Plane Nebraska (feet).

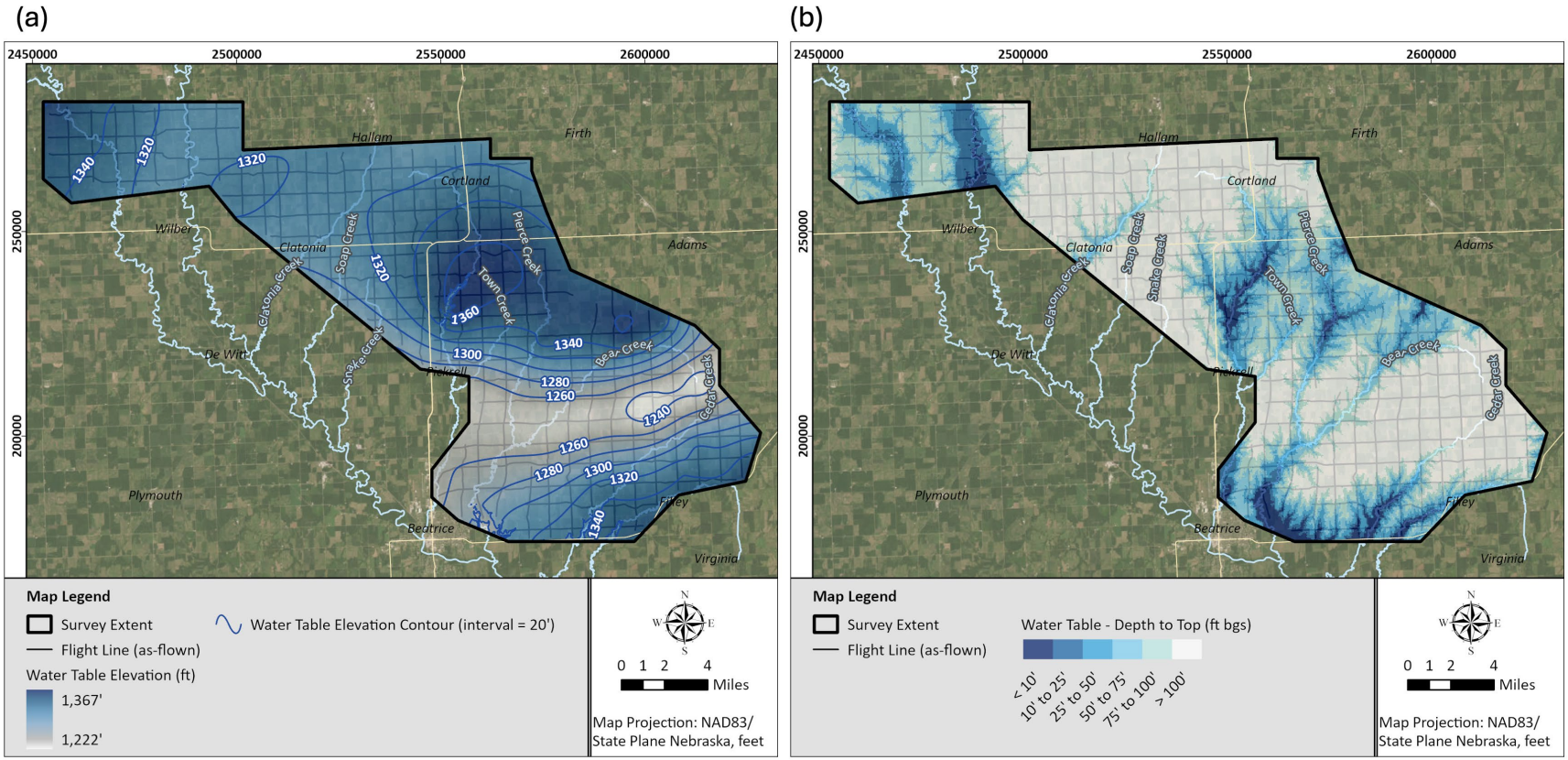


Figure 5-20. Map showing the (a) elevation and (b) depth of and to the water table (ft bgs). The projection is NAD83 State Plane Nebraska (feet).

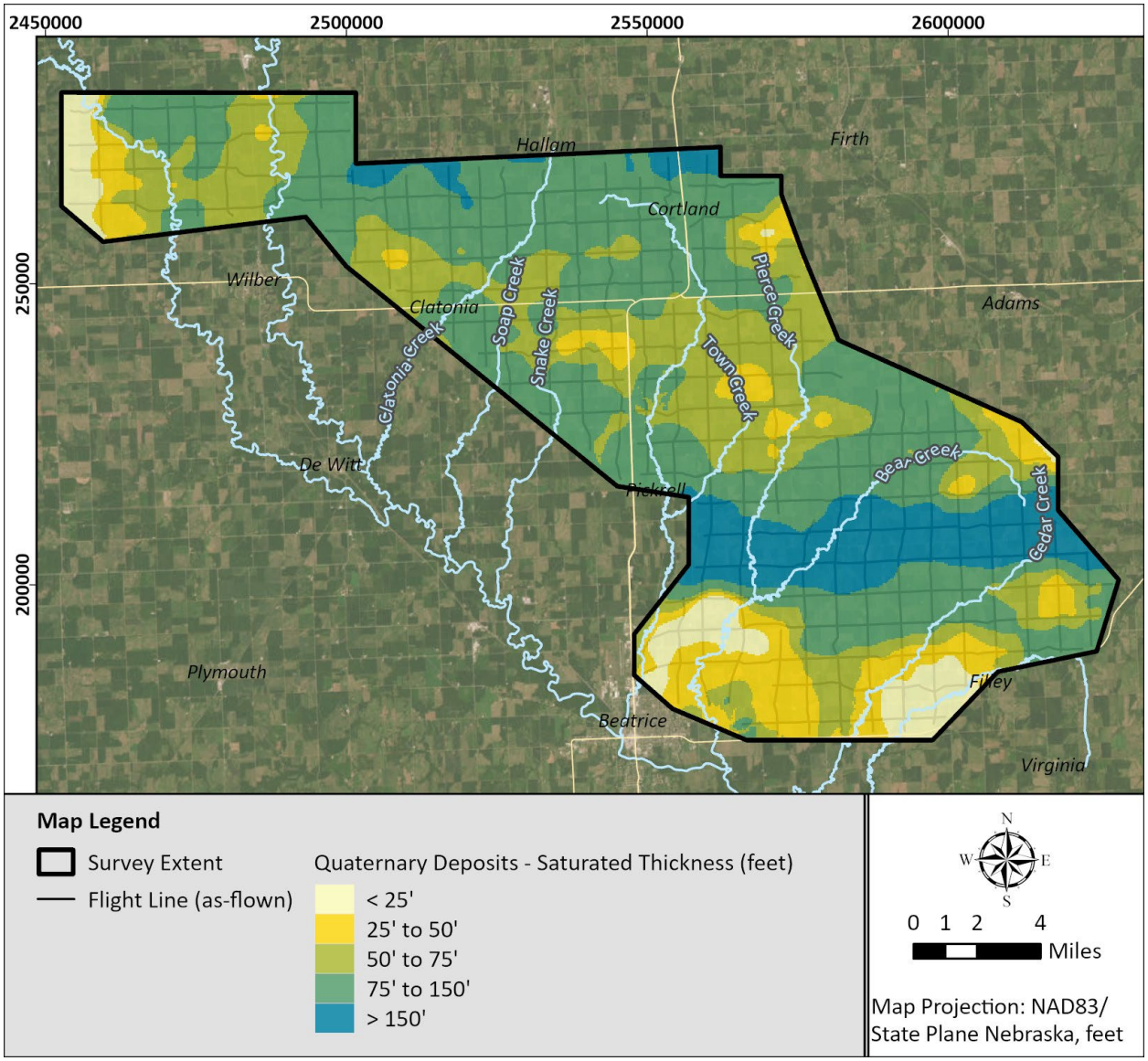


Figure 5-21. Map displaying the saturated thickness of the Quaternary (*Q*) materials. The projection is NAD83 State Plane Nebraska (feet).

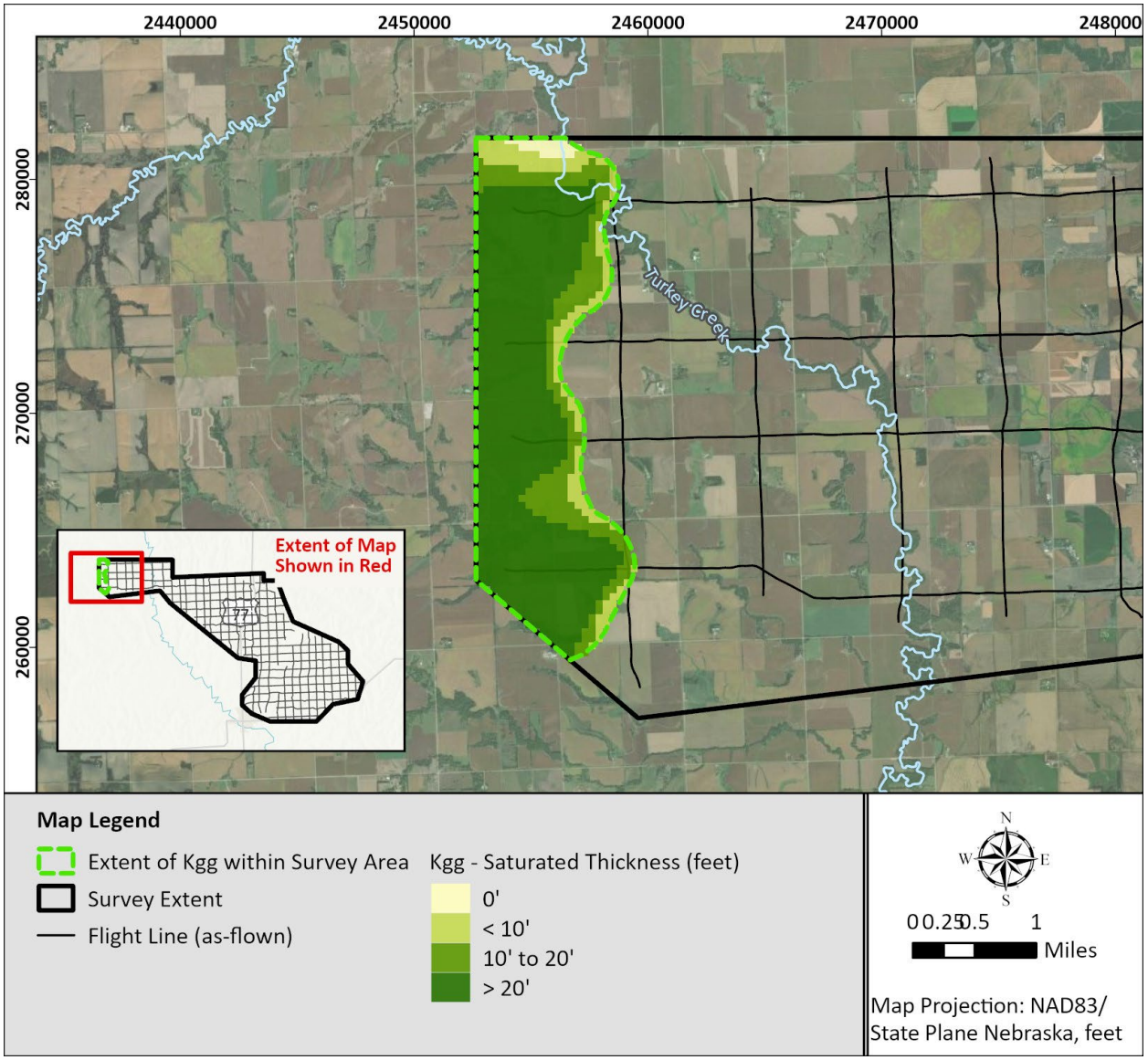


Figure 5-22. Map displaying the saturated thickness of the Cretaceous Greenhorn and Graneros (*Kgg*) Group. The extent of the *Kgg* within the survey area is shown in bright green. Map projection is NAD83 State Plane Nebraska (feet).

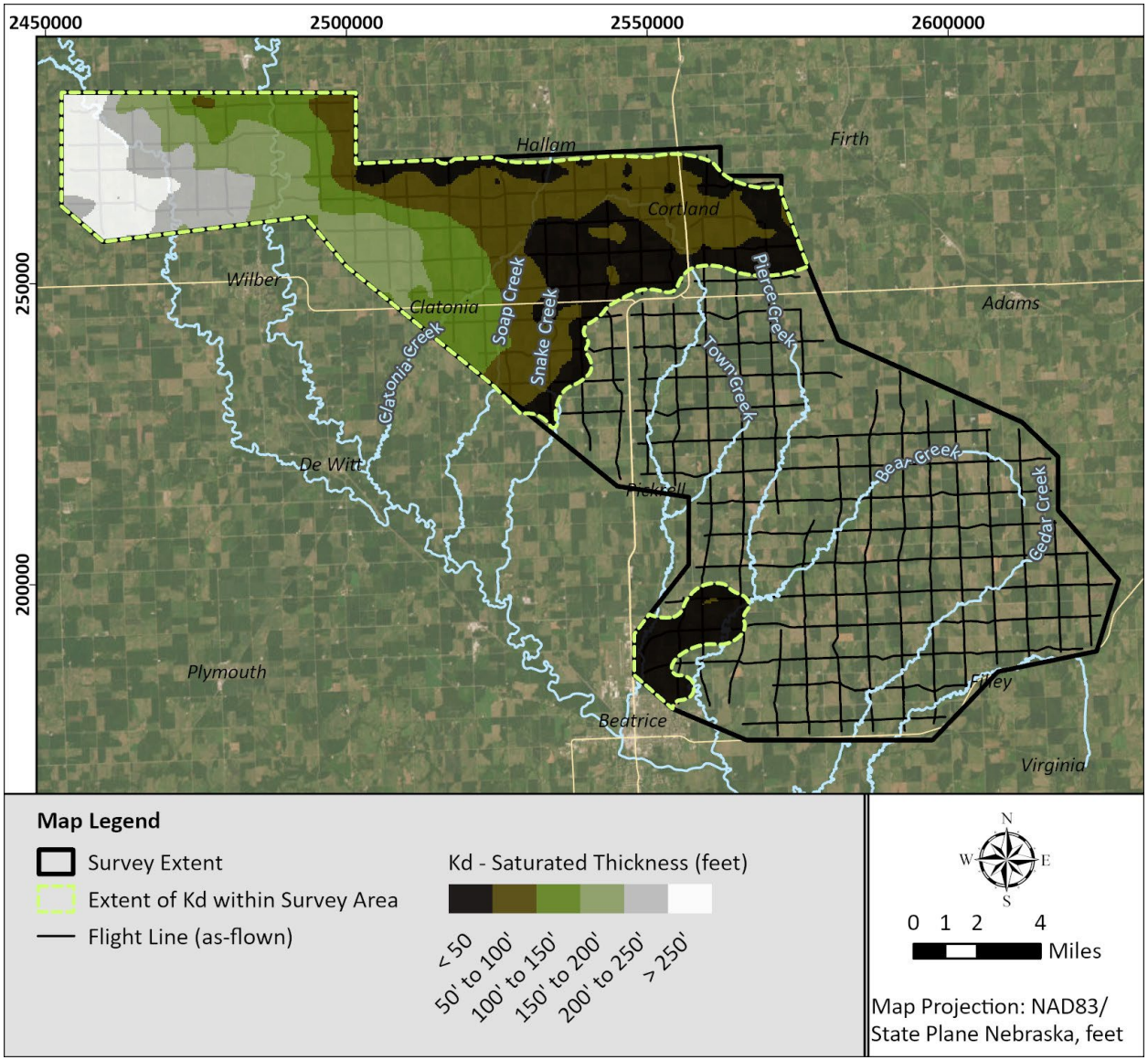


Figure 5-23. Map displaying the saturated thickness of the Cretaceous Dakota (*Kd*) Group. The extent of the *Kd* within the survey area is shown in bright green. Map projection is NAD83 State Plane Nebraska (feet).

5.1.7 Transmissivity Maps

The transmissivity (**T**), or the ability of an aquifer to transmit water, of the unconsolidated saturated material was calculated. The transmissivity, as discussed above in Section 2.2, was calculated using the equation:

$$T = K * b$$

where **K** is the hydraulic conductivity (ft/sec) and **b** is the saturated aquifer thickness (ft).

The **K** values used to calculate transmissivity within the 2025 LBBNRD survey area were determined based on Fetter (1988, Table 4.6). The Fetter (1988) table lists ranges of **K** values based on material type. LBBNRD project **K** values were selected from the table based on known material type determined through AEM interpretation. Table 5-4 lists the **K** values that were used to calculate transmissivity for the LBBNRD survey area and represent the middle of the range given in the Fetter (1988) table for each material type:

Table 5-4. Summary of Hydraulic Conductivities, K, used to calculate transmissivities.

Q Deposits Material Type	K used for Transmissivity calculation (ft/sec)
Marginal	**1.7×10^{-5} (Silty sands, fine sands)**
Aquifer and Coarse	**1.7×10^{-3} (Well-sorted sands glacial outwash)**

The transmissivity of each saturated material type (marginal; and aquifer and coarse aquifer) for ***Q*** were calculated separately and then added together to determine the overall transmissivity of saturated materials for marginal, aquifer, and coarse aquifer materials.

The resultant raster datasets were compared to the values displayed in "Transmissivity of Principal Aquifer Lincoln and Nebraska City Quadrangles, Nebraska" (Summerside and Myers, 2005). The comparison showed that the AEM-derived values were relatively similar to the values in the published map in Summerside and Myers (2005), but showed more detail and variation. This is to be expected because the AEM data provided a more expansive data coverage to calculate the transmissivity.

Figure 5-24 displays the range of transmissivities for the ***Q*** marginal, aquifer, and coarse aquifer saturated materials in the 2025 LBBNRD AEM survey as compared to the digitized contours from Summerside and Myers (2005). Figure 5-25 presents the same data but without the Summerside and Myers (2005) contours.

It is apparent that the transmissivity results indicate a likely paleochannel feature in the subsurface of the 2025 LBBNRD AEM survey area.

5.1.7.1 Transmissivity of the Cretaceous Dakota Group (Kd)

Using a similar approach as was used to calculate transmissivity maps for the ***Q***, an attempt was made to estimate the transmissivity of the ***Kd*** aquifer. In review of the literature in the area of eastern Nebraska, there are few references on the transmissivity within the ***Kd***. Many of the wells in the ***Kd*** do not extend to the bottom of the aquifer. According to Divine (2014), the highest transmissivity calculated in the Dakota aquifer in neighboring Lancaster County (greater than 10,000 gpd/ft) is generally under and around Lincoln, Nebraska. Also, in Divine (2014) it is pointed out that historic aquifer tests performed at wells near Antelope Creek, also within Lancaster County, were used to calculate transmissivity values that ranged from 56,000 gpd/ft to 72,000 gpd/ft. O'Connor (1987) has a **K** value of 5.56×10^{-4} feet/sec. This value is from northeastern Nebraska, north of the Platte River. The second value, from southwestern Iowa from Gannon and Vogelgesang (2015), is 6.48×10^{-4} feet/sec. We elected to use the average of the two values of 6.02×10^{-4} feet/sec. The saturated thickness of the ***Kd***, using the > 18 ohm-m threshold, was used, composed of cemented sand and sand dominant material along with the sand/silt dominant materials.

Unlike the ***Q***, we have no map for the ***Kd*** to compare with as in Summerside and Myers (2005) that can be used to adjust our values as pumping tests are almost nonexistent within the ***Kd***. This is estimation of the ***Kd*** transmissivity and needs to be used carefully and as a guide and not as a firm value.

Figure 5-26 is the estimated transmissivity calculated for the ***Kd*** using the estimates above for the materials over 18 ohm-m or the sand dominant materials.

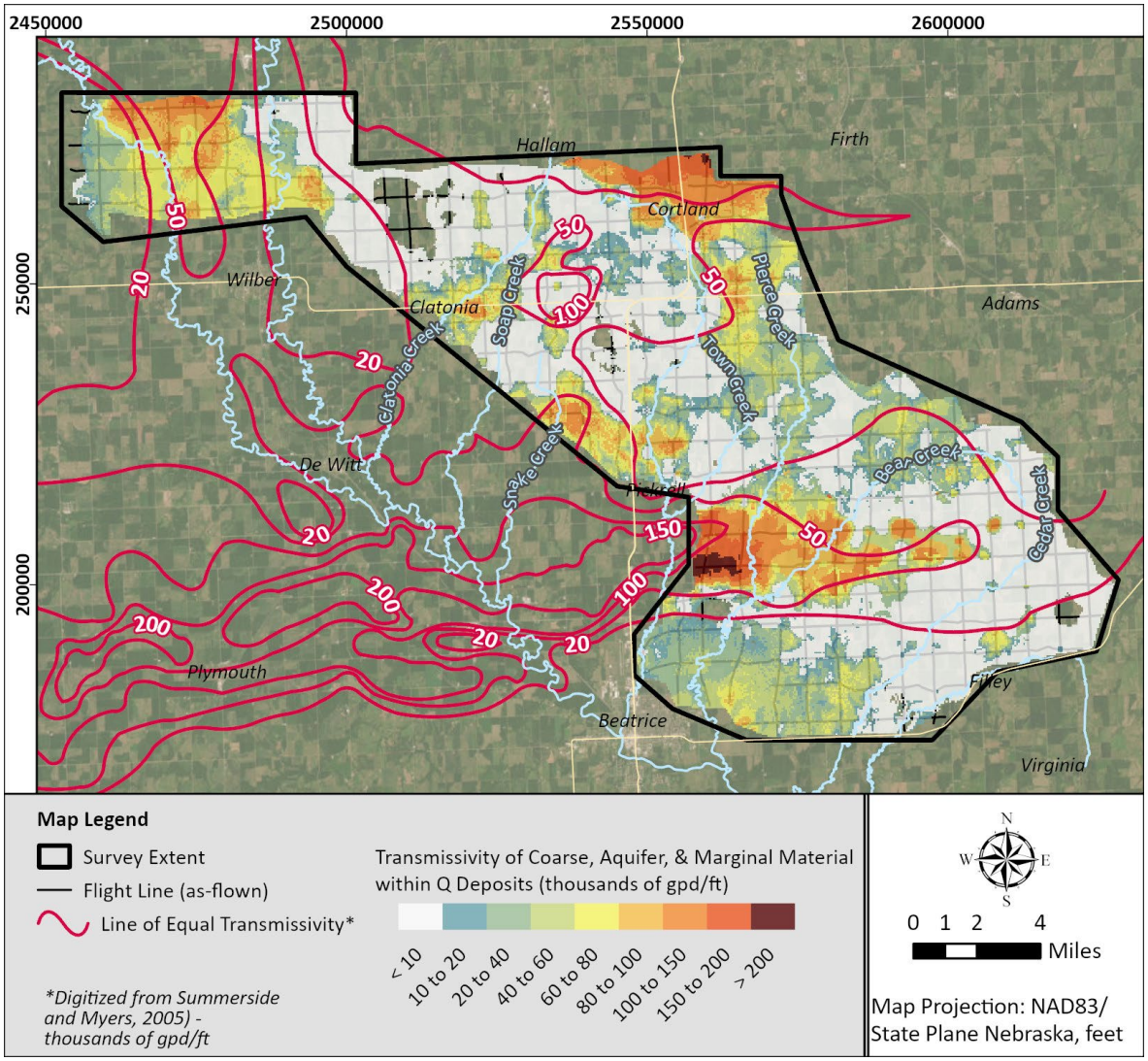


Figure 5-24. Map of the calculated transmissivities within the marginal, aquifer, and coarse aquifer materials of the *Q* deposits in the LBBNRD 2025 AEM survey area with an overlay of digitized contours from Summerside and Myers (2005). Flight lines are depicted as black lines and published transmissivity contours were digitized and added to the map for a visual comparison. The map projection is NAD83 State Plane Nebraska (feet).

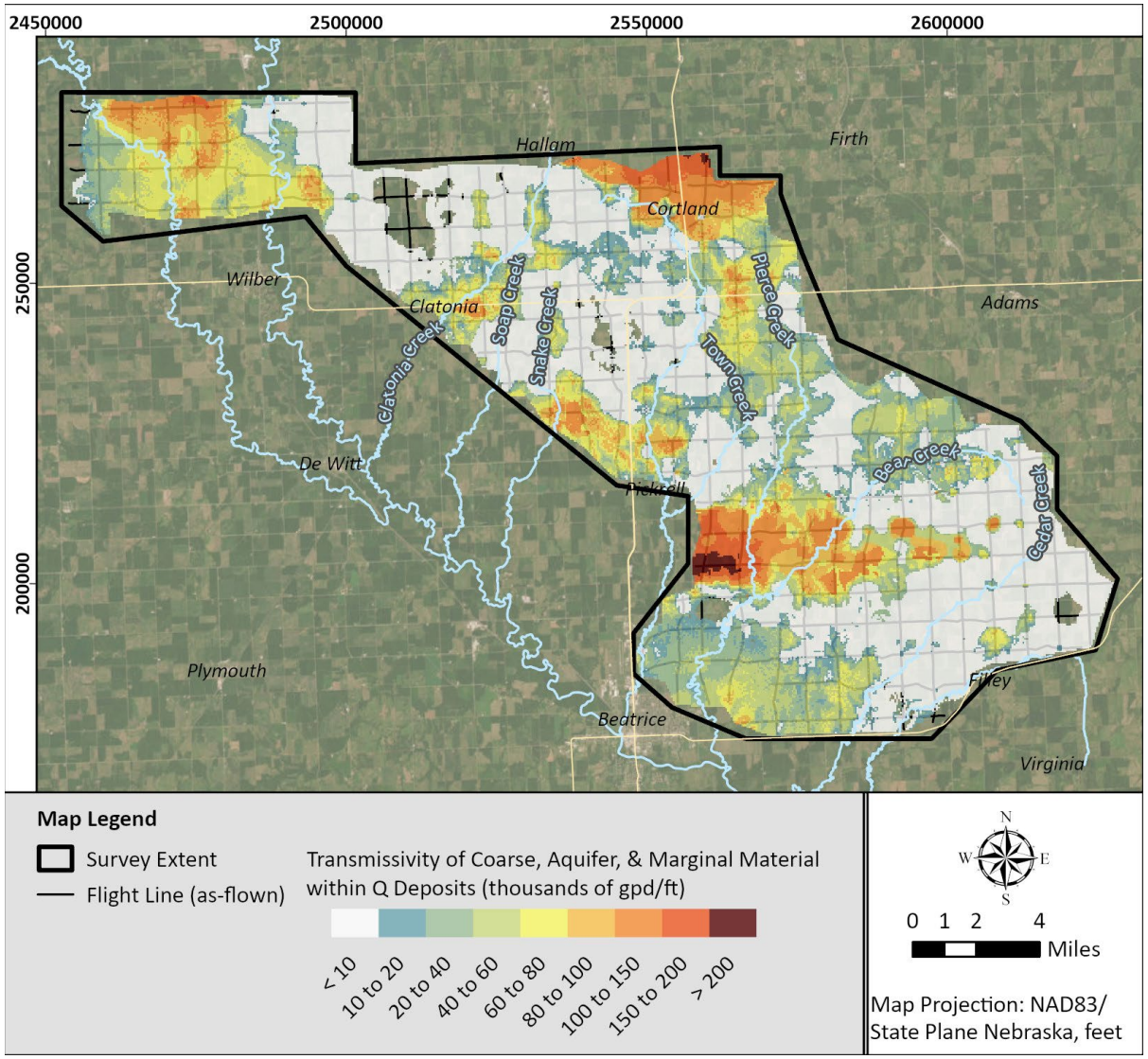


Figure 5-25. Map of the calculated transmissivity within the marginal, aquifer, and coarse aquifer material of the *Q* deposits in the LBBNRD 2025 AEM survey area without the Summerside and Myers (2005) transmissivity contours. Flight lines are depicted as black lines. The map projection is NAD83 State Plane Nebraska (feet).

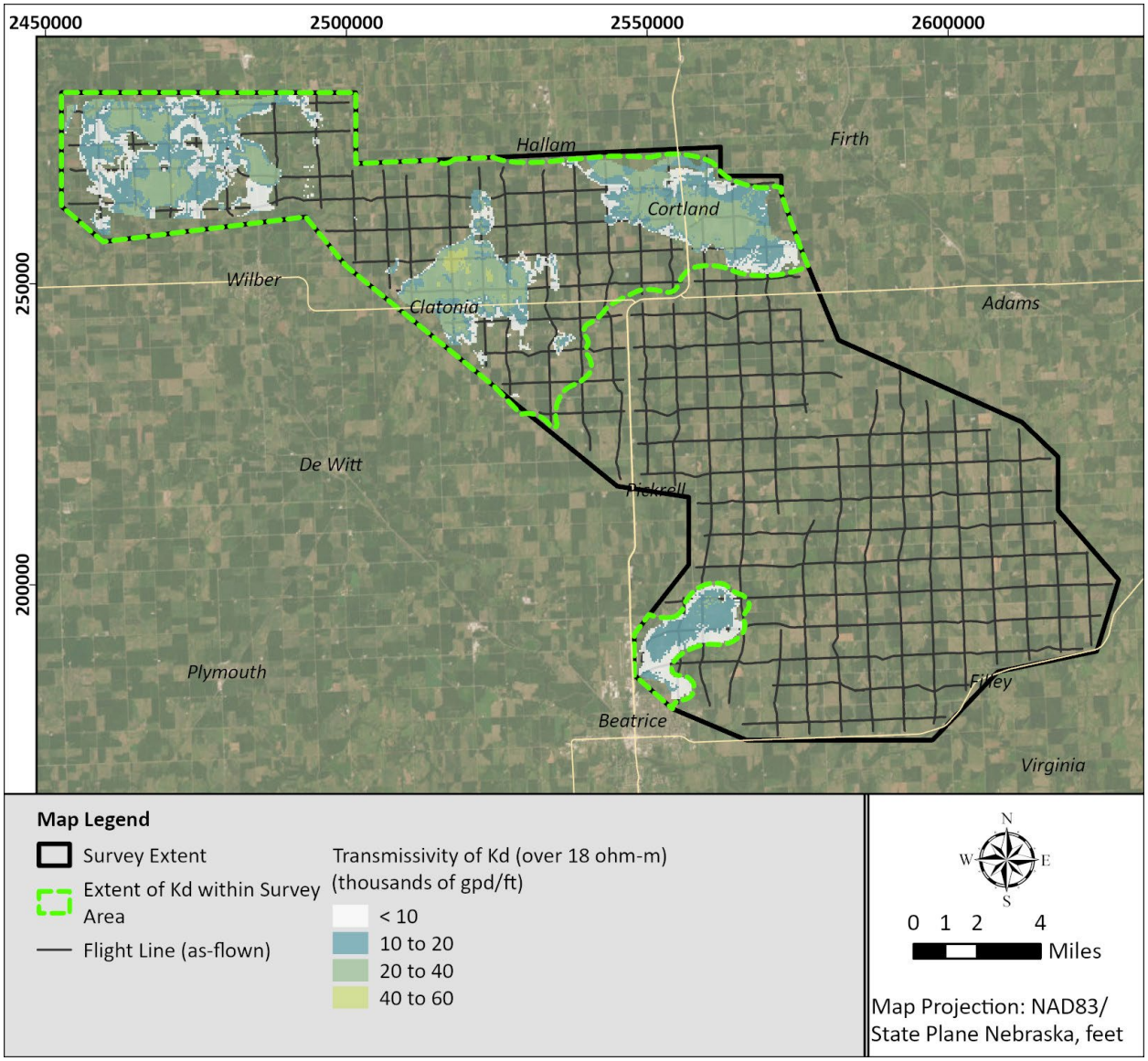


Figure 5-26. Map of the calculated transmissivity within Cretaceous Dakota Group (*Kd*) deposits over > 18 ohm-m "Sand Dominant Materials" in the LBBNRD 2025 AEM survey area. Flight lines are depicted as black lines. The map projection is NAD83 State Plane Nebraska (feet).

5.1.8 Specific Capacity Maps

An estimate of specific capacity was made for the Nebraska Department of Water, Energy, and Environment (NE-DWEE) wells based on the following:

- Screen data (i.e. depth of top and bottom of the screen interval) were extracted from the Nebraska GeoCloud (2026) and data such as static water level, pumping water level, and well yield were extracted from the NE-DWEE well shapefile for NE-DWEE wells located within the survey area.
- Screen top and bottom depths/elevations were compared to the depth/top elevation of bedrock surface (constructed from the AEM data) for each well.
- Based on the comparison, each well was designated with a "completion aquifer" (either ***Q***, Bedrock, or completed in both). For example, if the top of a well screen was below the bottom of ***Q*** deposits, then the well was designated as "Bedrock".
- For the wells without a screen interval, but included data to calculate specific capacity, the bottom of the well was reviewed to determine the completion aquifer.
    - If the total depth of a well was less than the top of bedrock, then it was considered a ***Q*** well
- After the well was designated with a completion aquifer, the Specific Capacity was calculated for each well based on the equation:
    - SC = pumping rate / drawdown (pumping water level minus static water level)
- The calculated Specific Capacity values are only as accurate as the pumping data provided in the NE-DWEE dataset (i.e., the well logs). The Specific Capacity values should be considered as approximate, but they do give a helpful, general overview of well production rates.
    - There were 513 NE-DWEE wells with the data required to calculate Specific Capacity and assign the well to a completion aquifer. Over 400 of those wells were designated as completed within the ***Q*** deposits; over 30 were designated as completed within bedrock (***Kd***); less than 10 were designated as dually completed; and over 60 were designated as undetermined because there wasn't enough screen information to distinguish which aquifer the well was completed in.

Figure 5-27 displays the transmissivity of saturated marginal, aquifer, and coarse aquifer material of ***Q*** along with the Specific Capacity of wells screened within the ***Q*** deposits. Figure 5-28 presents saturated thickness of ***Kd*** over 18 ohm-m with the Specific Capacity of wells screened within the ***Kd***. Figure 5-29 presents saturated thickness of ***Kd*** over 35 ohm-m with the Specific Capacity of wells screened in the ***Kd***.

5.1.9 Geologic Map Updates

Based on the addition of AEM data within the 2025 LBBNRD survey area, minor refinements were made to the published geologic maps (Burchett, 1986, Burchett and Pabian, 1992), specifically to the extent of the ***Kgg*** and ***Kd***. The refinements made to both extents were based on the resistivity of the material and "picks" based on the AEM resistivity models made during the interpretation portion of the project. Figure 5-30 is a map displaying the published geologic map (Burchett, 1986) and the refined extent.

5.1.10 3D Interpretative Voxel Grids

A voxel grid was completed for the LBBNRD 2025 AEM survey area. The voxel grids were made using a 300 feet grid cell size and the model layer thickness (from Table 4-3). A minimum curvature method was used within Datamine Discover PA (Datamine Discover, 2026). All layers were referenced to their depth from the surface and then projected on the area DEM.

After the grid was calculated, the grid was split at the interpreted top of bedrock (***P***/***Q***, ***Kd***/***Q***, ***Kgg***/***Q*** interfaces) to yield a Bedrock voxel and a ***Q*** voxel. The Bedrock Voxel was subdivided at the ***Kd***/***Kgg*** interface to yield a ***Kgg*** voxel and a ***Kd***+***P*** voxel. The ***Kd***+***P*** voxel was then split at the ***P***/***Kd*** interface yielding voxels for both the ***Kd*** and the ***P***. All these subdivisions and splits used the surface elevation grids discussed above in Section 5.1.5. The resulting voxel grids can be used to explore the distribution of the aquifer materials within the area in 3D. Specifically, these grids can allow for visual inspection of the volume of materials above the bedrock as well as surface materials.

The Quaternary (***Q***) and ***Kd*** materials can also be separated by thresholds developed for four lithology classes (see Section 5.2.1 and Section 5.2.2 below). Utilizing the voxel grids of the ***Q*** and ***Kd***, analysis can be made of the thickness of the different materials within the section. Additionally, the ***Q*** and ***Kd*** voxel can be split into unsaturated and saturated portions utilizing the LBBNRD Spring 2025 water table (Section 5.1.6).

Figure 5-31 is an exploded diagram of the plot of the stratigraphy of the area, including the ***Q, Kd,*** and ***P***, looking to the north. The voxel grids can be found in *Appendix 3-Deliverables**Voxel*.

The voxel model was also used to develop the depth to the saline water by using a threshold on the resistivity of 7 ohm-m. Additionally, the upper iso-surface was smoothed by a 3x3 cell filter and then was also run through a low pass filter to remove jitter on the surface. Figure 5-32 is a depth to the top of the interpreted saline water.

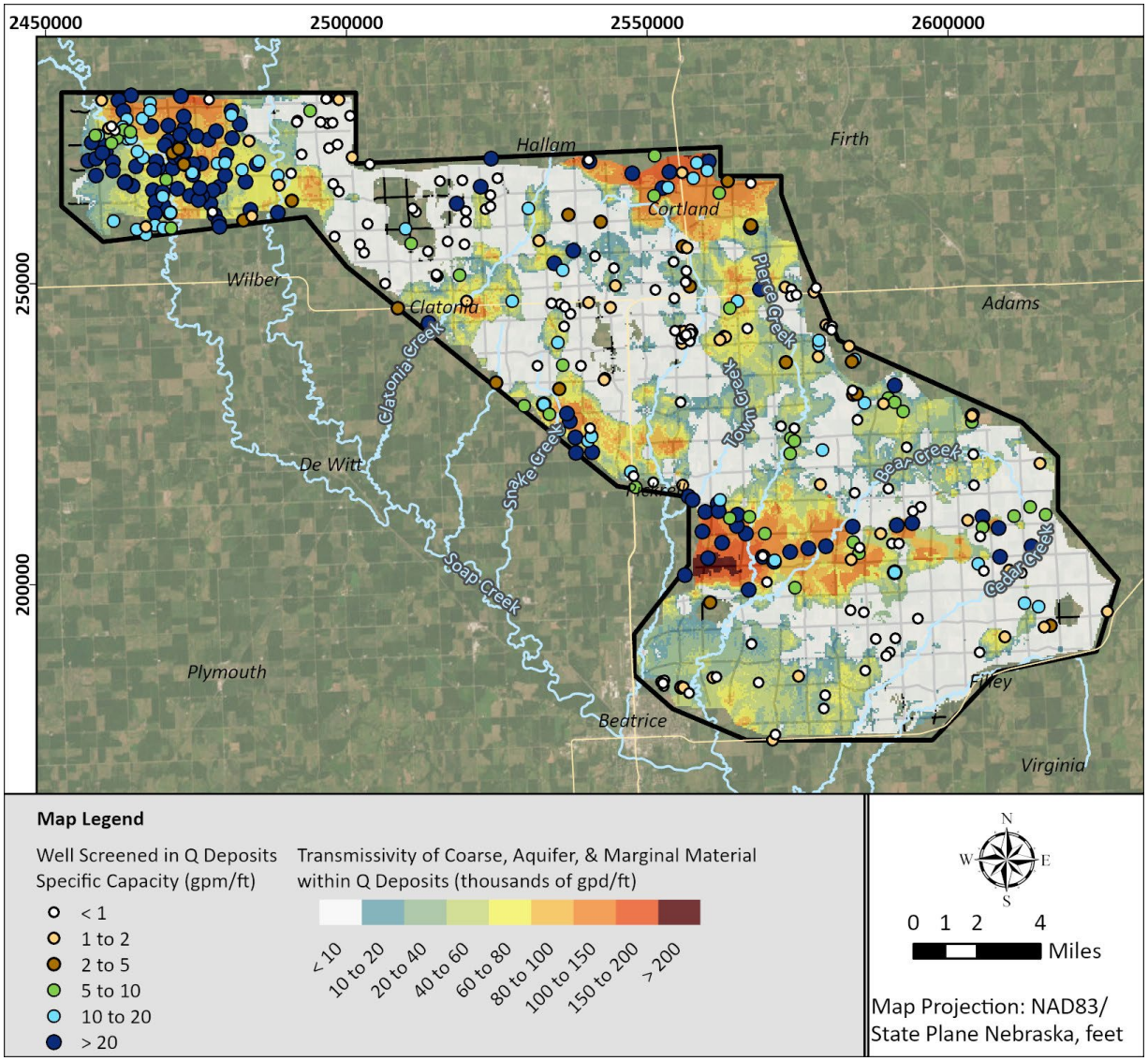


Figure 5-27. Map of the calculated transmissivities within the saturated Coarse, Aquifer, and Marginal materials within the *Q* deposits along with the specific capacity of the NE-DWEE wells designated as being completed within the *Q* deposits based on screen interval. Flight lines are depicted as black lines. The map projection is NAD83 State Plane Nebraska (feet).

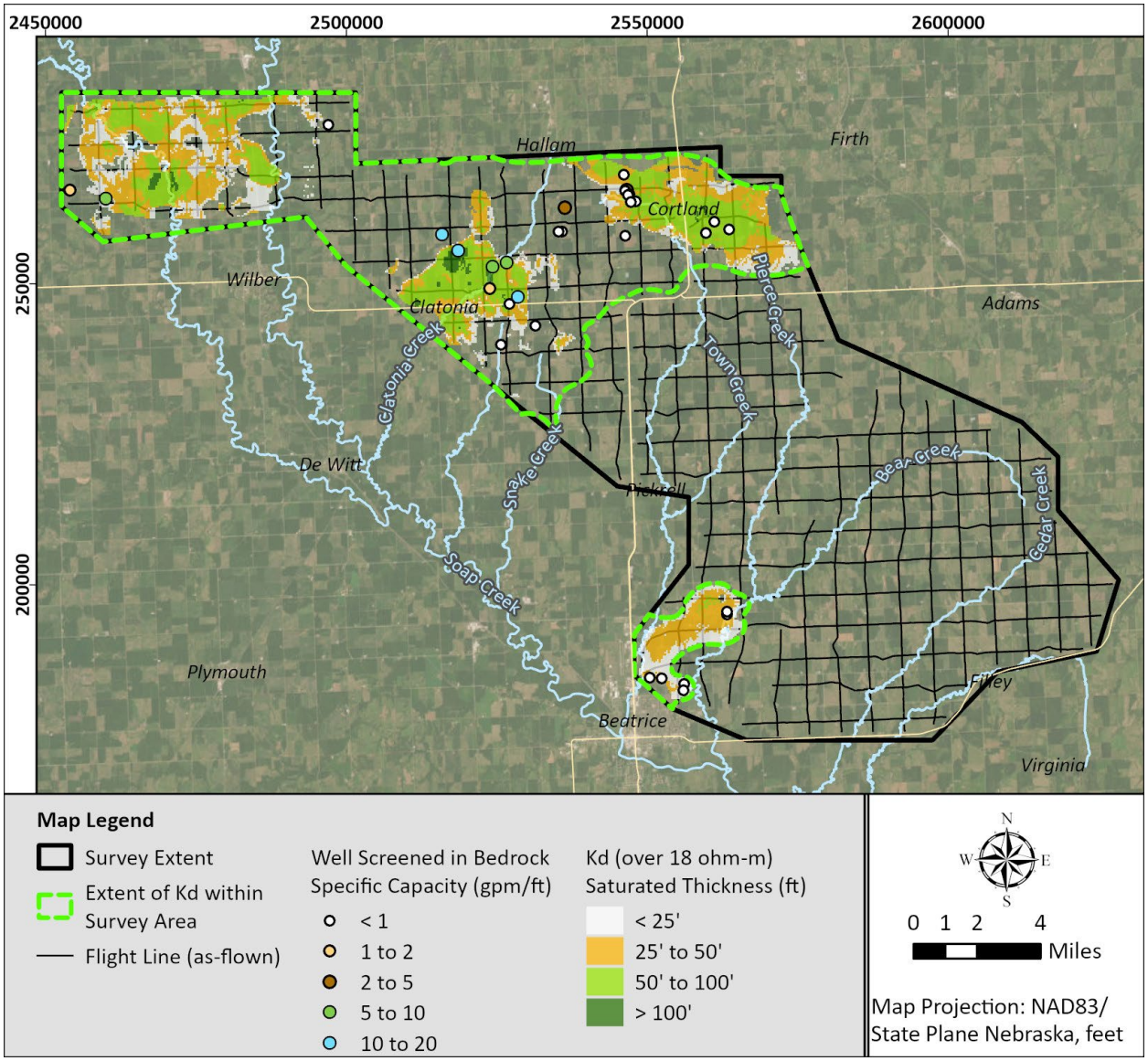


Figure 5-28. Map of saturated *Kd* (over 18 ohm-m) along with the specific capacity of the NE-DWEE wells screened within the *Kd*. Flight lines are depicted as black lines. The map projection is NAD83 State Plane Nebraska (feet).

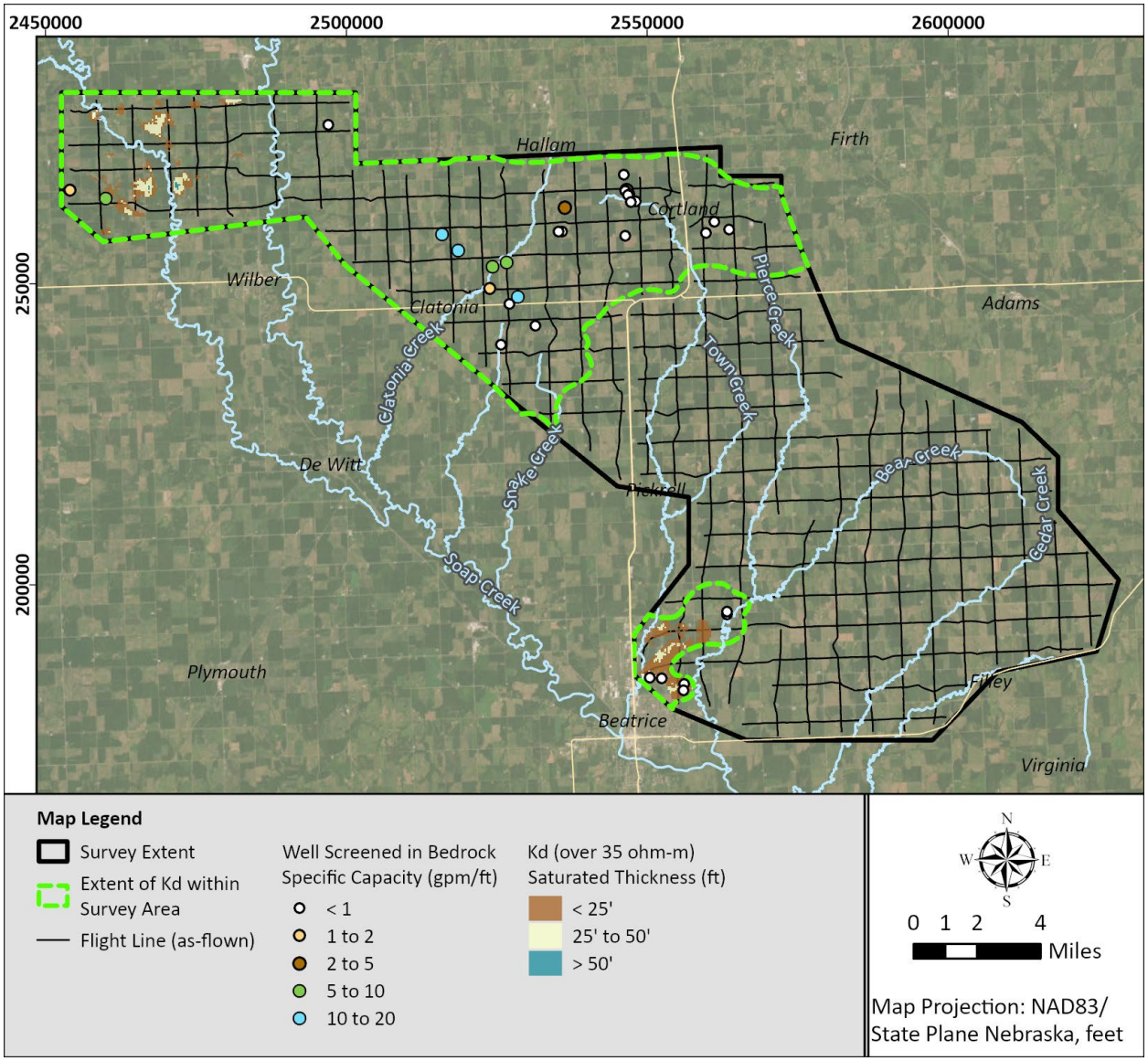


Figure 5-29. Map of saturated *Kd* (over 35 ohm-m) along with the specific capacity of the NE-DWEE wells screened within the *Kd*. Flight lines are depicted as black lines. The map projection is NAD83 State Plane Nebraska (feet).

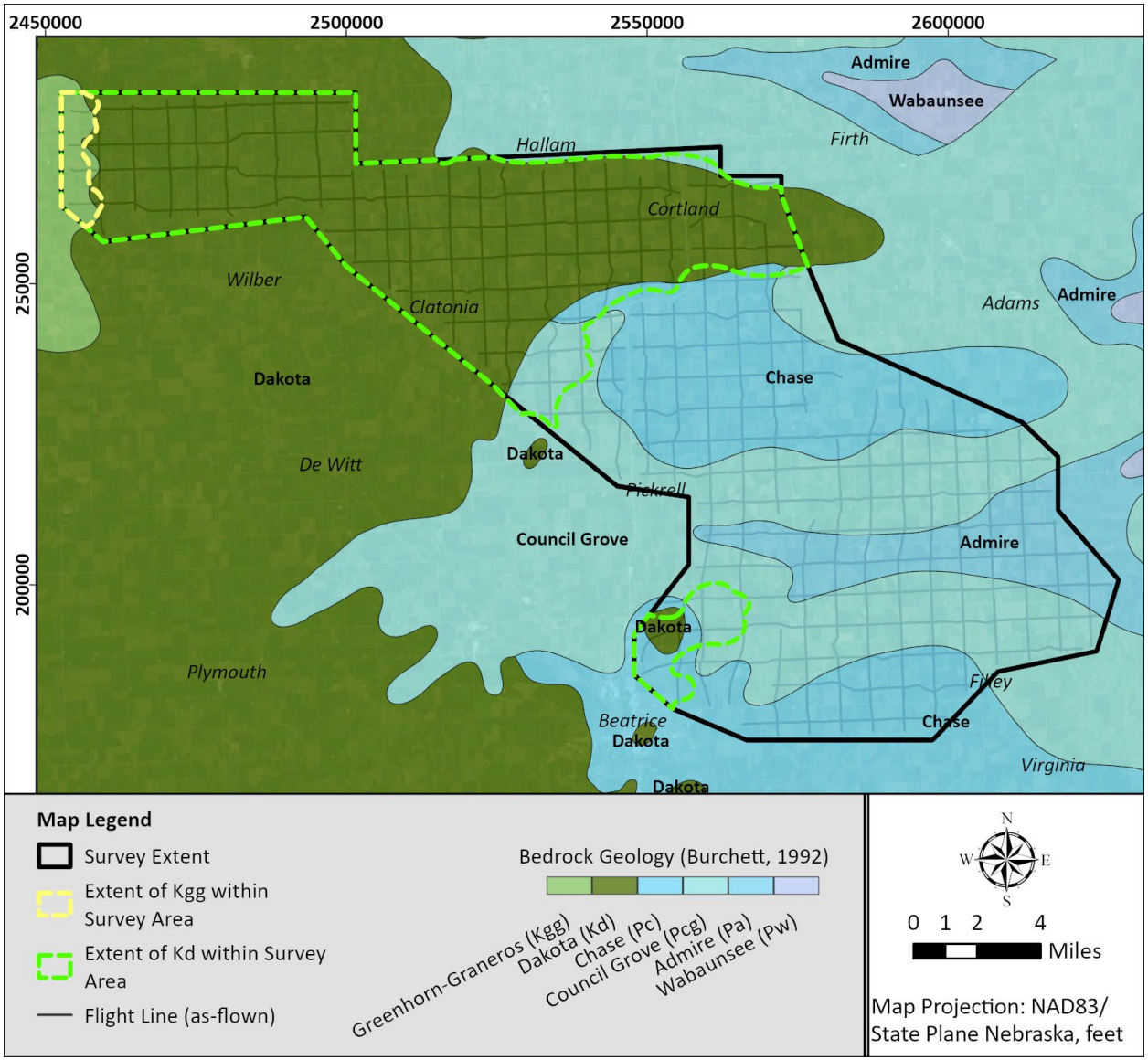


Figure 5-30. Map of geologic units by Burchett (1986) and Burchett and Pabian (1992) with the refined extent of *Kd* shown in bright green and *Kgg* shown in yellow. Flight lines are depicted as black lines. The map projection is NAD83 State Plane Nebraska (feet).

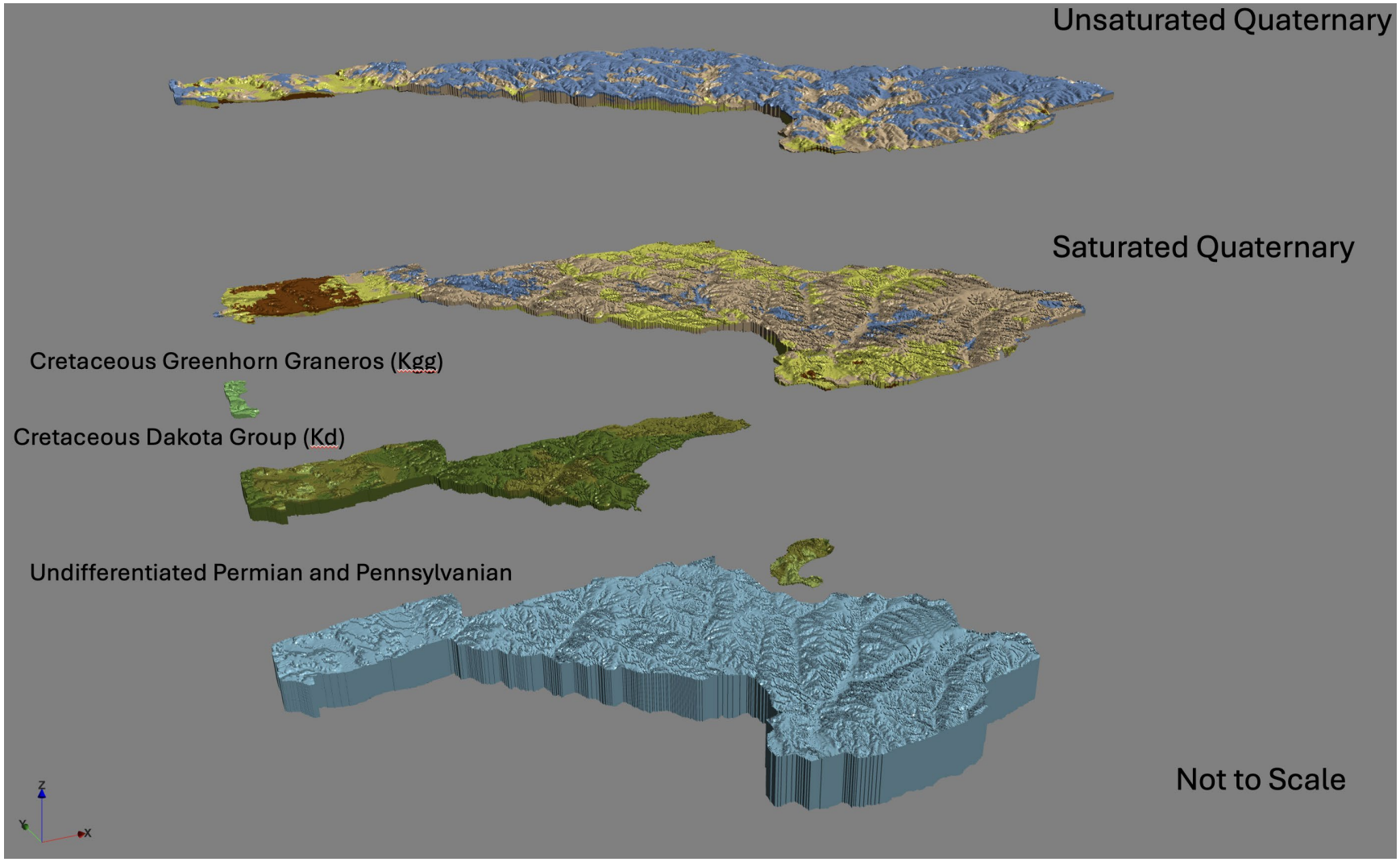


Figure 5-31. Exploded 3D Voxel model of the stratigraphy of the LBBNRD 2025 AEM area showing unsaturated and saturated Quaternary (*Q*) and Cretaceous Dakota Group (*Kd*) material and undifferentiated Permian Chase Council Grove and Admire Groups (*P*). Not to scale.

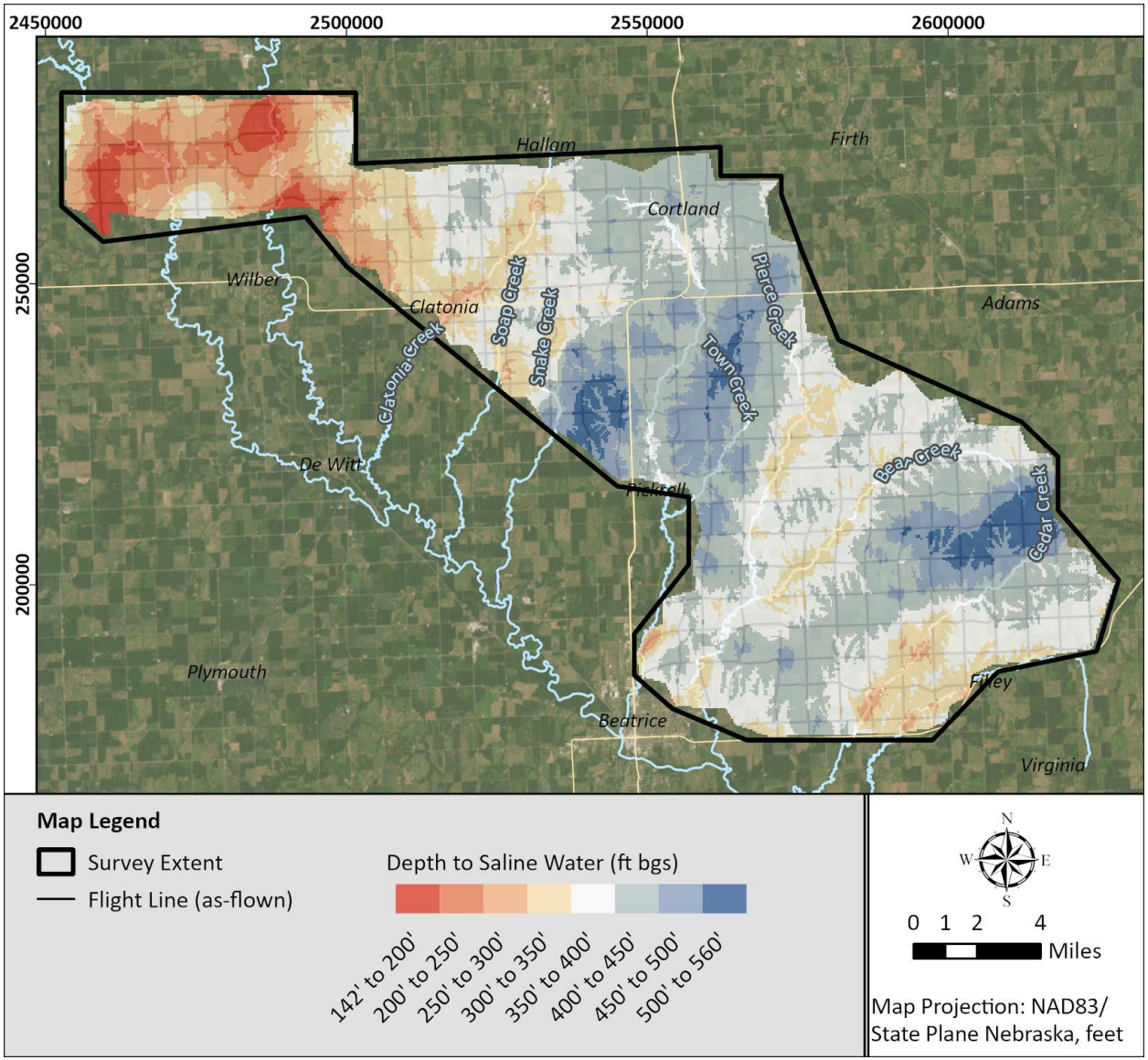


Figure 5-32. Interpreted depth to the top of the saline water interface. The map projection is NAD83 State Plane Nebraska (feet).

5.2 Comparison of AEM Inversion Resistivity to Borehole Geophysical Resistivity Logs

Three geophysical logs existed in the CSD database within the 2025 LBBNRD AEM survey area. These included *01-CS-2019, 03-CS-2019*, and *01-LBB-2023*. These logs included a combination of at least one 16-inch Short Normal, 64-inch Long Normal, and/or Lateral log.

A critical examination of the absolute values of the resistivity needs to include an awareness of errors in calibration and in the proper operation of the equipment. Many of the early 1940-1980's electric logs were paper logs that were scanned and digitized and then included in the database. There is a long-standing issue with using geophysical logs as ground truth when comparing to AEM acquisition systems and inversions that are well calibrated using modern techniques. Throughout much of the geophysical logging at the time it was acquired, the relative deflections of the resistivity measurements were all that was required or expected from a geophysical log. Operators were seldom trained in the proper operation of a calibrated sonde or in the ability to recognize high contact resistance of a cable head. This has led to many geophysical logs that are uncalibrated within the CSD database. Note that these logs still have scientific merit in their ability to relatively indicate an increase or a decrease in the formation resistivity. The logs used herein are for qualitative comparison to the AEM because detailed calibration and corrections would need to be carried out for the resistivity values in the logs to be directly used as numerical constraints in the inversion of the AEM data (Ley-Cooper and Davis, 2010).

In order to compare the E-logs to the AEM data, a 1,500-foot search radius was used around *01-CS-2019* and *03-CS-2019* and any AEM soundings within that distance were averaged and a mean and standard deviation was calculated. For 01-LBB-2023, a 2,700-foot search radius was used. Figure 5-33 presents a graph of the three wells' 16-inch Short Normal resistivity logs plotted with the inverted AEM average resistivity and standard deviation within the specified distances. The logs show an agreement in the shape of the resistivity curves with a much higher magnitude of the well logs. The log from *01-LBB-2023* (left) shows the same shape but a higher magnitude. The log from *01-CS-2019* (center) has much more detail as compared with the AEM. However, the higher magnitude in both indicates a high resistivity area. The log from *03-CS-2019* (right) displays a much different magnitude and may be the result of lateral variations in the lithology. Some of these changes may be related to local variations over the 1,500-2,700 feet interval but look to also be related to instrument calibration.

Figure 5-34 through Figure 5-36 are plots of the borehole geophysics on the closest AEM survey line. The geophysical log is plotted on the same color scale as the AEM and are within specified distance of the flight line. The lithology is indicated on the center of the E-Log. As was observed in Figure 5-33, the shape is similar but the resistivity is higher than the AEM levels.

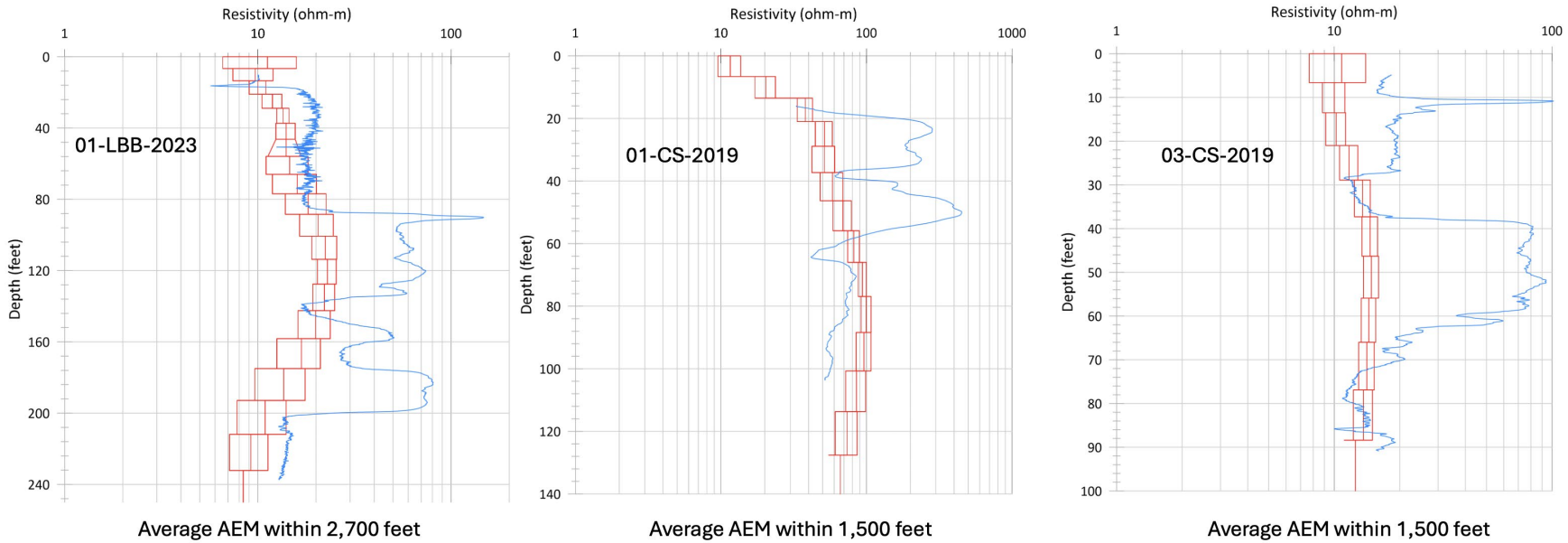


Figure 5-33. Graph of the three 16-inch normal resistivity log values (blue line) and the inverted airborne electromagnetic average resistivity values and errors bars of one standard deviation (red line) within 1,500 feet of 01-CS-2019 and 03-CS-2019 and 2,700 feet for 01-LBB-2023.

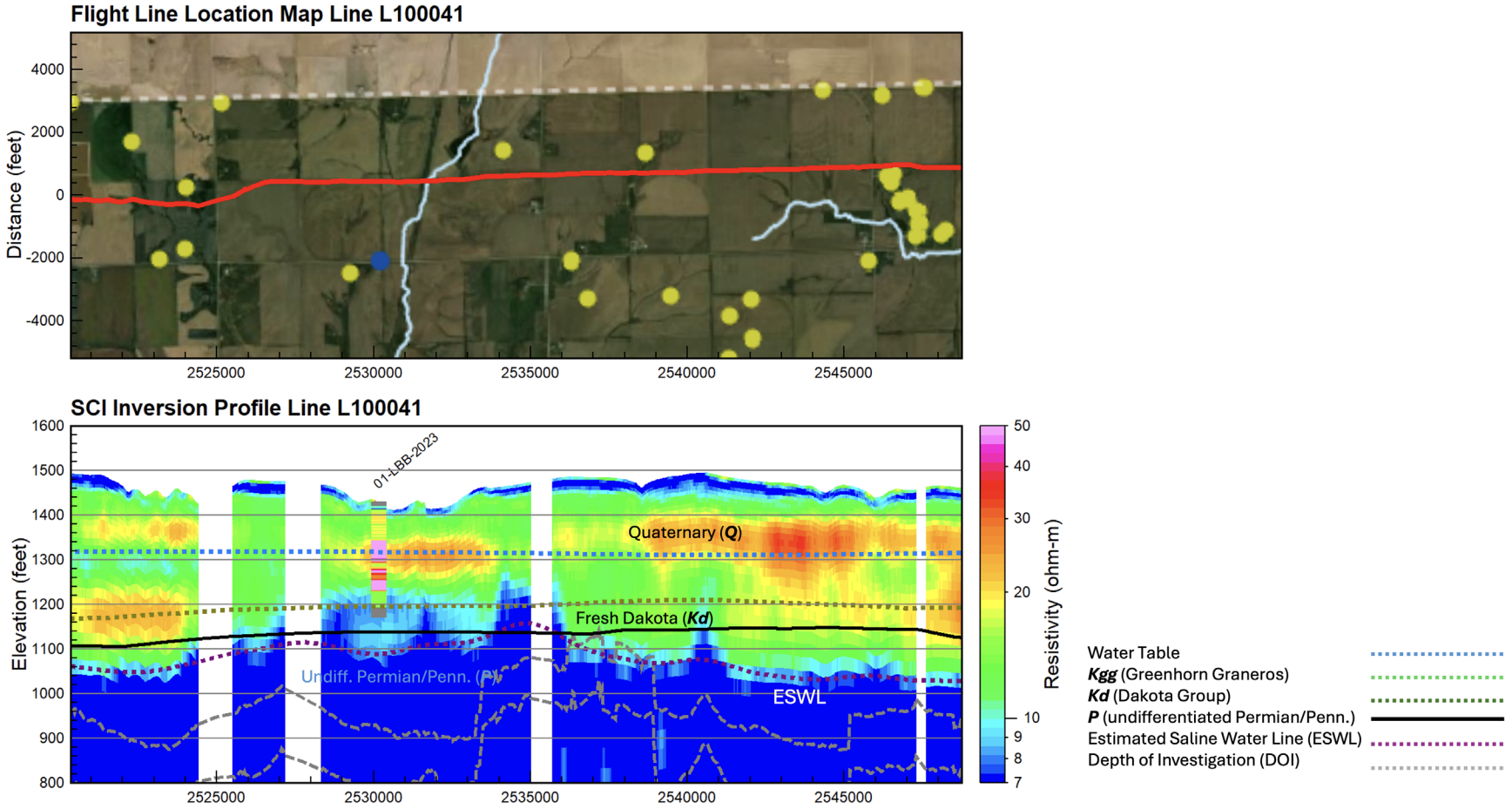


Figure 5-34. A segment of survey line L100041. Resistivity and lithology from CSD test hole 01-LBB-2023 within 2,700 feet. Gaps in the profile are due to EM decoupling from infrastructure or areas that were not flown due to FAA regulations. Projection is NAD83 State Plane Nebraska (feet), the vertical datum is NAVD88 (feet).

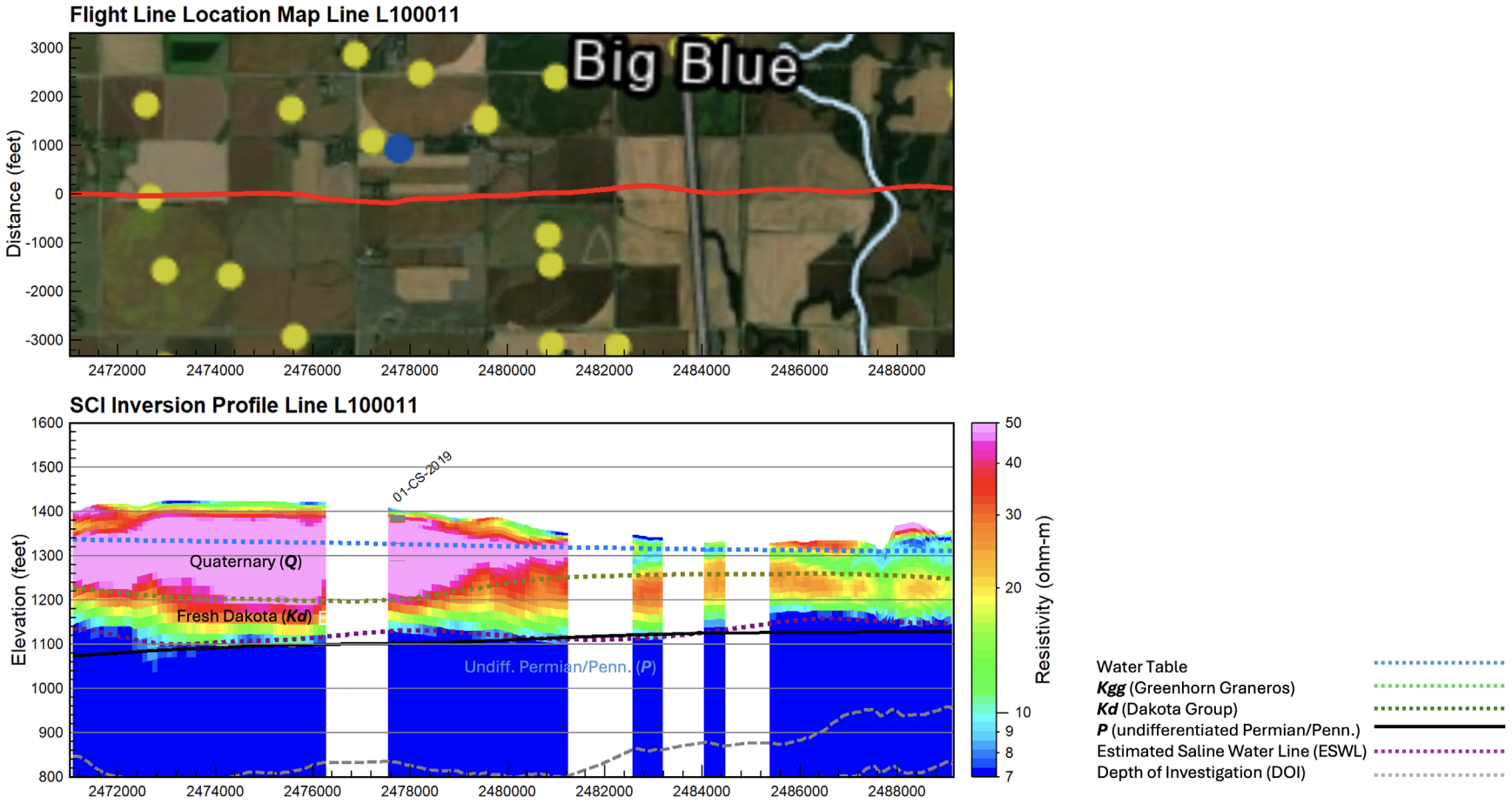


Figure 5-35. A segment of survey line L100011. Resistivity and lithology from CSD test hole 01-CS-2019 within 1,500 feet. Gaps in the profile are due to EM decoupling from infrastructure or areas that were not flown due to FAA regulations. Projection is NAD83 State Plane Nebraska (feet), the vertical datum is NAVD88 (feet).

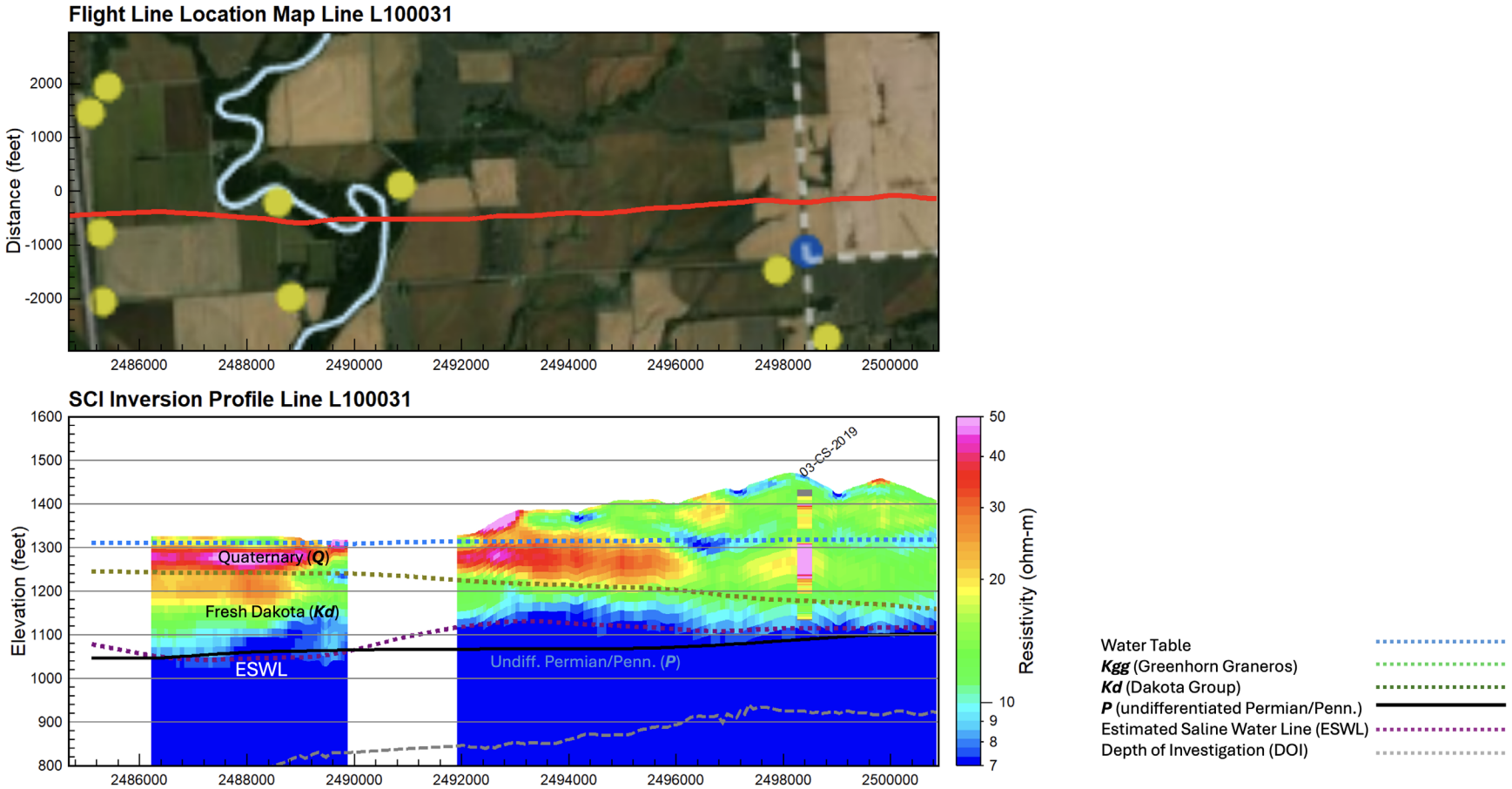


Figure 5-36. A segment of survey line L100031. Resistivity and lithology from CSD test hole 03-CS-2019 within 1,500 feet. Gaps in the profile are due to EM decoupling from infrastructure or areas that were not flown due to FAA regulations. Projection is NAD83 State Plane Nebraska (feet), the vertical datum is NAVD88 (feet).

5.2.1 Resistivity Relationship in the Quaternary Aquifer System

A critical aspect of a geophysical survey is assessing the nature of the material detected by the geophysical method applied in the investigation. Regarding the 2025 LBBNRD AEM survey area, assessment of the sediment character in the Quaternary (***Q***) aquifer system is required to determine the overall composition of the major categories used to define the aquifer and aquitards. This is typically done by utilizing the borehole geophysical logs associated with lithology.

In the LBBNRD 2025 AEM survey area there are four geophysical logs to complete this analysis, but they are of the older type that were digitized from paper logs and are not calibrated. Unlike the work that was presented in Carney et al. (2015), uncalibrated logs are inadequate within the LBBNRD 2025 AEM survey area. An assessment of the resistivity thresholds used to characterize non-aquifer, marginal, aquifer, and coarse aquifer materials was conducted using a comparison to the lithologies in the well logs and the AEM resistivity. This allowed for the characterization of the ranges of resistivities present in the ***Q*** units described in this report. It was determined that the Carney et al. (2015) report adequately mapped the aquifer materials that were interpreted for this project; therefore, the analysis presented in Carney et al. (2015) was used for the categorization of the Quaternary aquifer system within the LBBNRD survey area. The ***Q*** aquifers were broken down by resistivity for aquifer materials (less than 12 ohm-m for non-aquifer material, 12-20 ohm-m for marginal aquifer material, 20-50 ohm-m for aquifer material, and greater than 50 ohm-m for coarse aquifer material). Figure 5-37 is a plot of the color bar used and the resistivity ranges for the four aquifer material types.

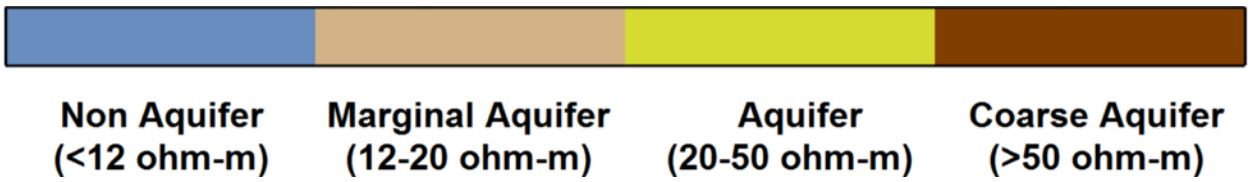


Figure 5-37. Plot displaying the resistivities by major Quaternary (*Q*) aquifer material color categories used in the LBBNRD 2025 AEM survey: blue- non-aquifer materials, tan- marginal aquifer materials, yellow- aquifer materials, brown- coarse aquifer materials (Carney et al., 2015).

5.2.2 Resistivity Relationship in the Cretaceous Dakota Group Aquifer System

As discussed above, a critical aspect of a geophysical survey is assessing the nature of the material detected by the geophysical method applied in the investigation. Regarding the 2025 LBBNRD AEM survey area, assessment of the sediment character in the Cretaceous Dakota Group (***Kd***) aquifer system, or as sometimes referred to as the Maha Aquifer (Divine and Sibray, 2017), is required to determine the overall composition of the major categories used to define the aquifer and aquitards.

The ***Kd*** within the LBBNRD was split into four parts based on empirical comparisons to lithology logs. 0-3 ohm-m was classified as Shale/Clay Dominant materials, 3-18 ohm-m as Siltstone/Silt Dominant materials, 18-35 ohm-m Sand/Silt Dominant, and 35 ohm-m and greater as Sandstone/Sand Dominant materials. These are splits that were used in the 2023 LBBNRD and 2024 LBBNRD reports from AGF (2024a) and AGF (2025). Additional unpublished work in the Nebraska ***Kd*** using AEM data has led to a better understanding of the resistivity versus lithology with the ***Kd***.

Lacking the quality geophysical well logs in the ***Kd*** that exist in the ***Q***, it is difficult to produce a more robust statistical distribution of the resistivity versus lithology as was done for the ***Q*** materials (Carney et al., 2015). Figure 5-38 is an image of the color scale that was used in the interpretation of the ***Kd***.

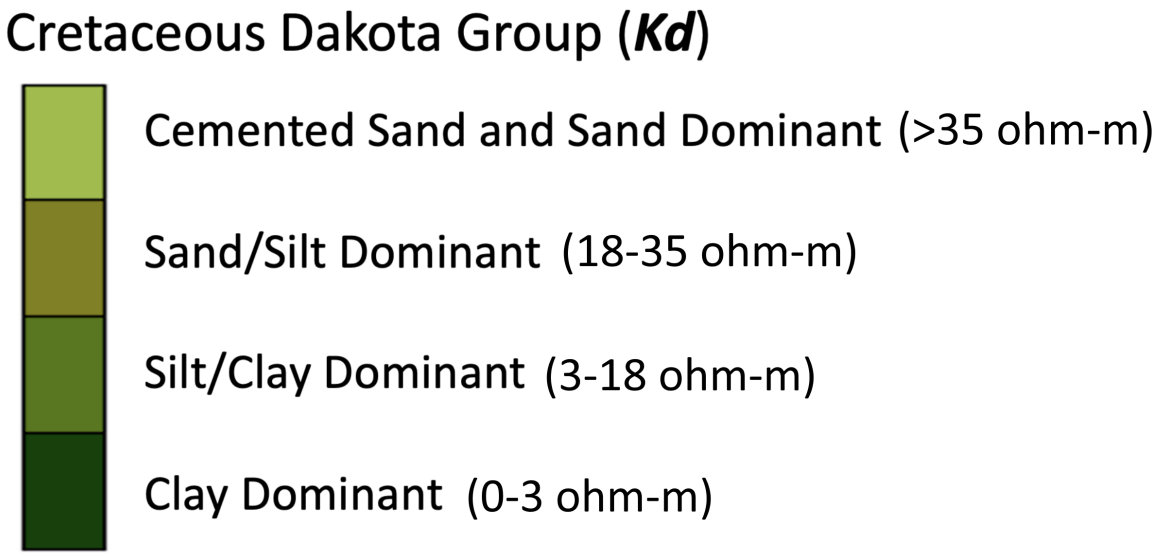


Figure 5-38. Plot displaying the Cretaceous Dakota Group (*Kd*) resistivities by dominant material and the color categories used in the LBBNRD 2025 AEM survey.

5.3 Hydrogeological Framework of the LBBNRD 2025 AEM Survey Area

The priority for this survey was to build a detailed hydrogeologic framework to better understand the aquifers within the areas of northwest Gage and southeast Saline counties within the LBBNRD. The end goal is to establish a scientific-based approach to defining new management boundaries.

The AEM reveals variability of the aquifer materials within the Quaternary (***Q***) and Cretaceous Dakota Group (***Kd***) deposits, which provide the groundwater supply, and their spatial relationship to each other and the surface water. These spatial relationships can provide insight into groundwater supply in the AEM survey area. The Permian Chase Group (***Pc***) and Permian Council Grove Group (***Pcg***) are under much of the survey area and beneath the ***Q*** and ***Kd***. The ***Pcg*** underlies the ***Q*** in the eastern side of the survey area. The ***Pcg*** also underlies the ***Pc***. There is a very small amount of Pennsylvanian Admire Group (***IPa***) on the very far eastern end of the survey area according to Burchett (1986) that has not been interpreted or broken out. There is a thin remnant of the Cretaceous Greenhorn and Graneros (***Kgg***) on the far western edge of the survey overlying the ***Kd***. The term bedrock in this report represents the Cretaceous bedrock units of the ***Kgg***, ***Kd,*** and the undifferentiated Permian (***P***) units. The ***Kd*** is on the western half of the survey area. Figure 5-39 is the revised geology map of the area based on the interpretation of the AEM. This figure is based on Burchett and Pabian (1992) with modifications due to the higher resolution AEM data. The ***Q*** is expressed in the resistivity color scale as shown in Section 5.2.1 to present locations of aquifer materials composed of non-aquifer (blue color in figures), marginal aquifer (tan color in figures), aquifer (yellow color in figures), and coarse aquifer materials (brown color in figures). The ***Q*** materials are composed predominantly of preglacial alluvial deposits and glacial outwash and till with a loess cover in some areas. The ***Kd*** is expressed in the resistivity color scale as shown in Section 5.2.2 representing cemented sand and sand dominant, sand/silt dominant, slit clay dominant, and clay dominant. The ***Kd*** is consolidated, semi-consolidated, and non-consolidated fluvial and deltaic sediments.

Figure 5-40 and Figure 5-41 are 3D fence diagrams and present the overall distribution of ***Q***, ***Kgg***, ***Kd***, and ***P*** (as described in Section 2) across the LBBNRD 2025 AEM survey area. The ***Q*** aquifer materials can generally be characterized by alluvial/outwash materials in a paleochannel through the eastern side of the survey area. There is just a small remnant of the ***Kgg***. This looks to be composed entirely of the Graneros Shale with the Greenhorn Limestone eroded off; the Graneros is an aquiclude or confining layer. The ***Kd*** in the western half of the survey area is directly deposited on the ***P*** units. The ***Kd*** is composed of consolidated and semi-consolidated clay, silt, sand, sandstone, siltstone, and shale. The deposits are in fluvial deposits associated with the delta front that existed east of the survey area and underwent multiple regression and transgressive sequences in the Cretaceous (Witzke et al., 1983).The undifferentiated Permian groups (***P***) are impermeable shale and limestone, and they are considered aquicludes, or boundaries to groundwater flow, that are present throughout the survey area. The combined top of ***P*** surface can be considered the bottom of the aquifer. Within the ***Kd*** and ***P*** units saline water exists at depth and is widespread in the LBBNRD area of Nebraska (Korus et al., 2013). Figure 5-42 presents an exploded 3D voxel model of the unsaturated ***Q***, unsaturated ***Kgg***, saturated ***Q,*** saturated ***Kd***, and undifferentiated ***P*** units.

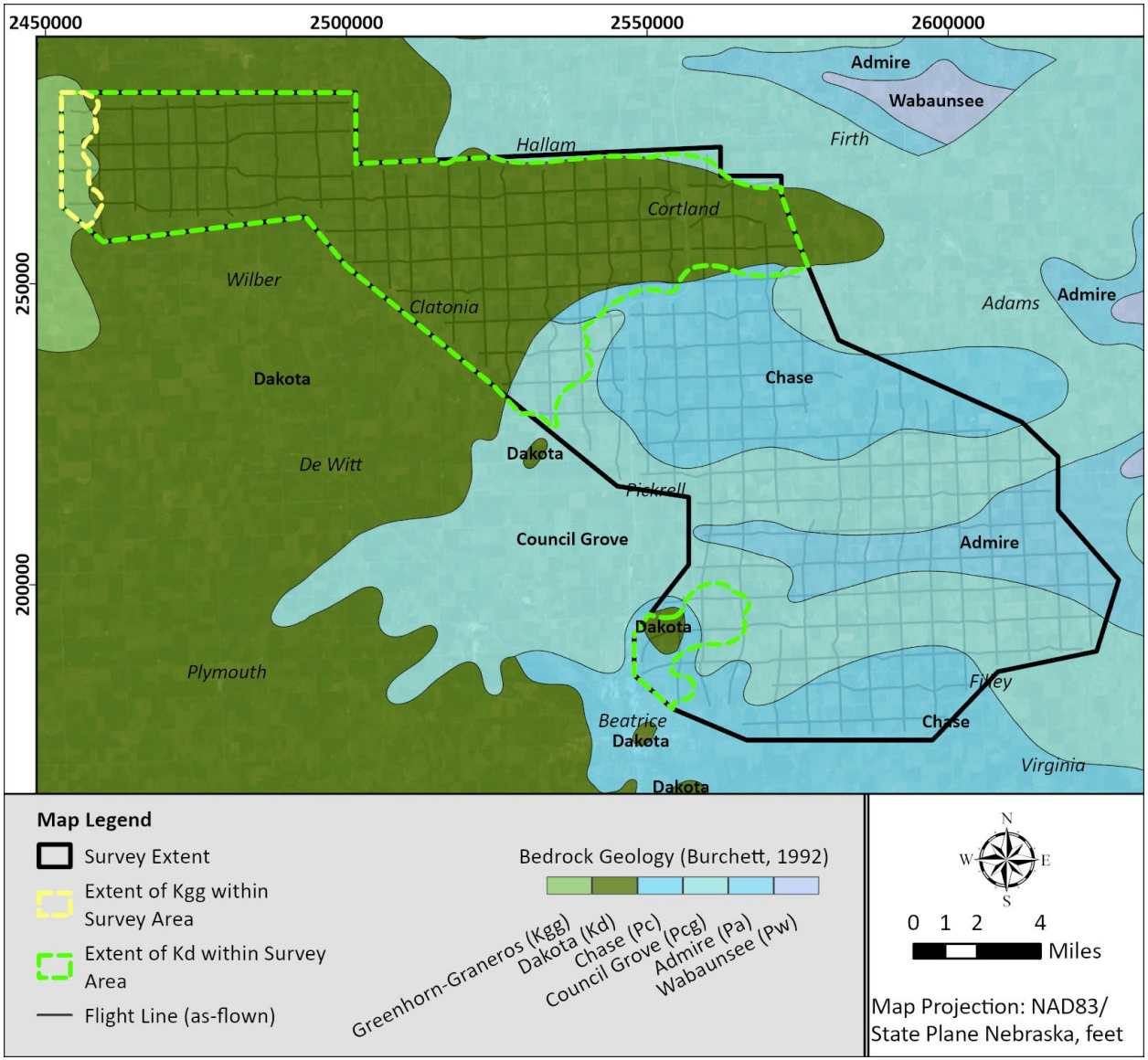


Figure 5-39. Bedrock map of the survey area modified from Burchett and Pabian (1992) using the LBBNRD 2025 AEM survey results.

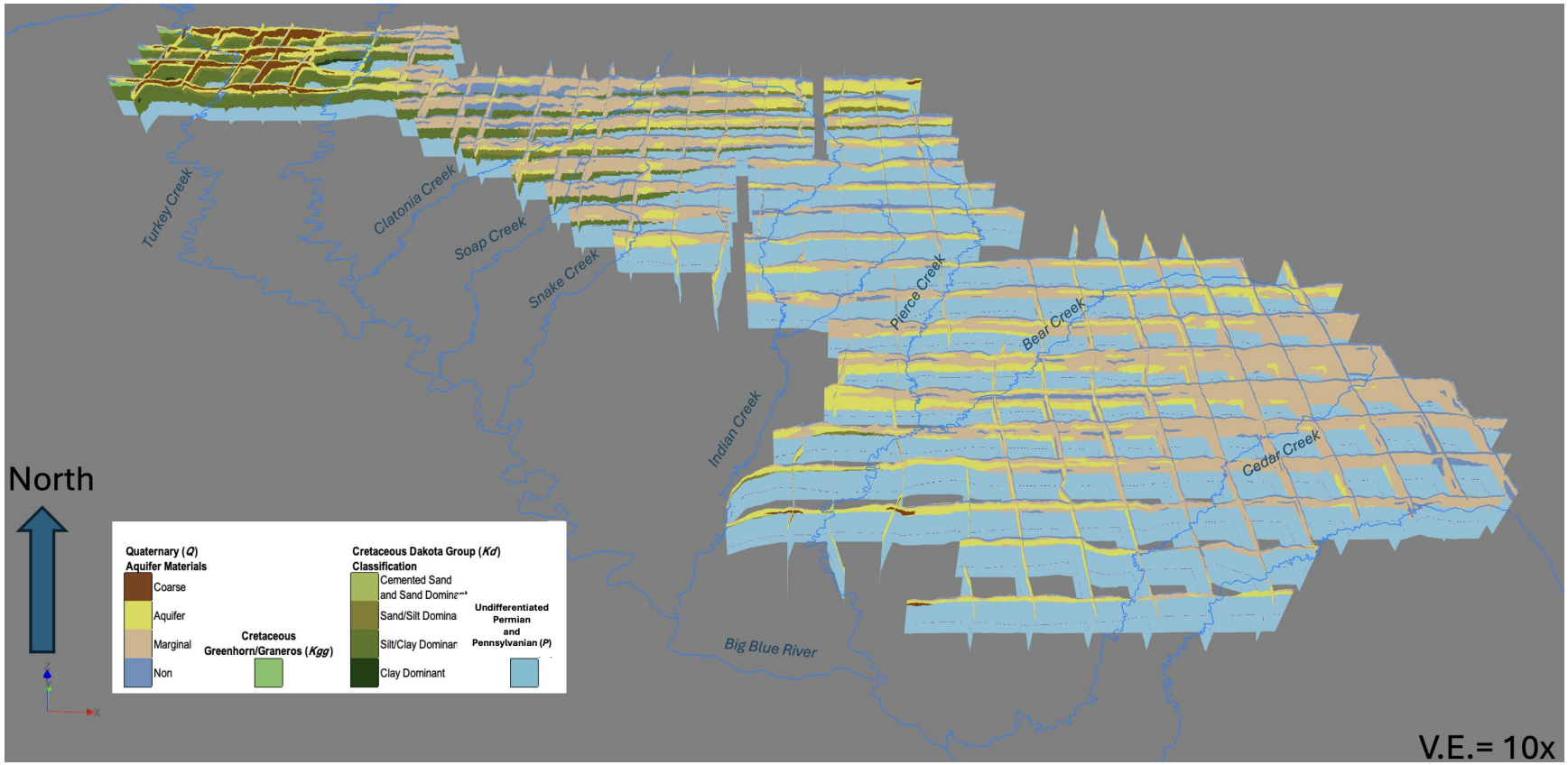


Figure 5-40. 3D Fence Diagram looking to the north of the interpreted distributions of aquifer material within the LBBNRD 2025 AEM survey area. V.E.=10x.

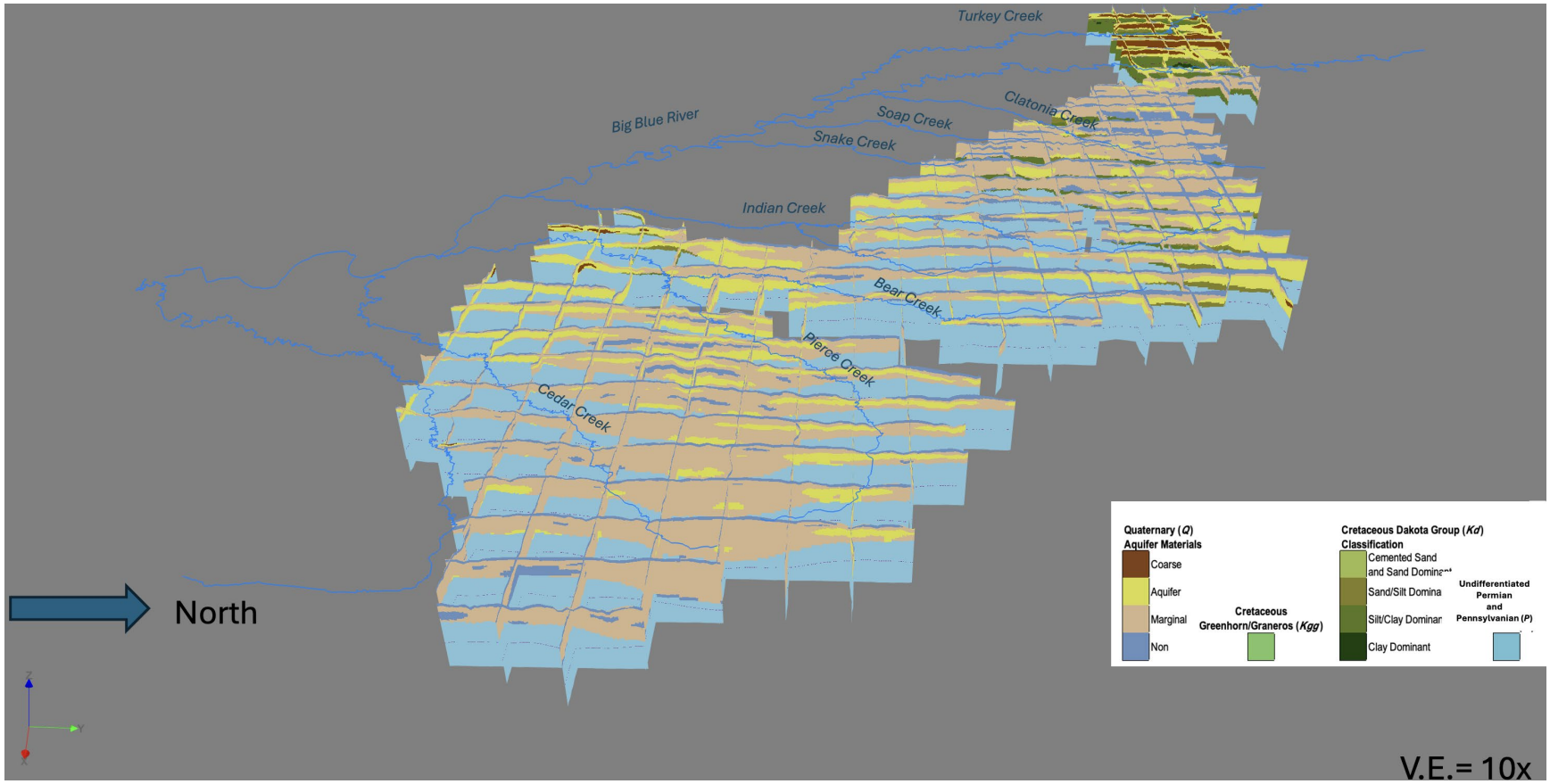


Figure 5-41. 3D Fence Diagram looking to the north of the interpreted distributions of aquifer material within the LBBNRD 2025 AEM survey area. V.E.=10x.

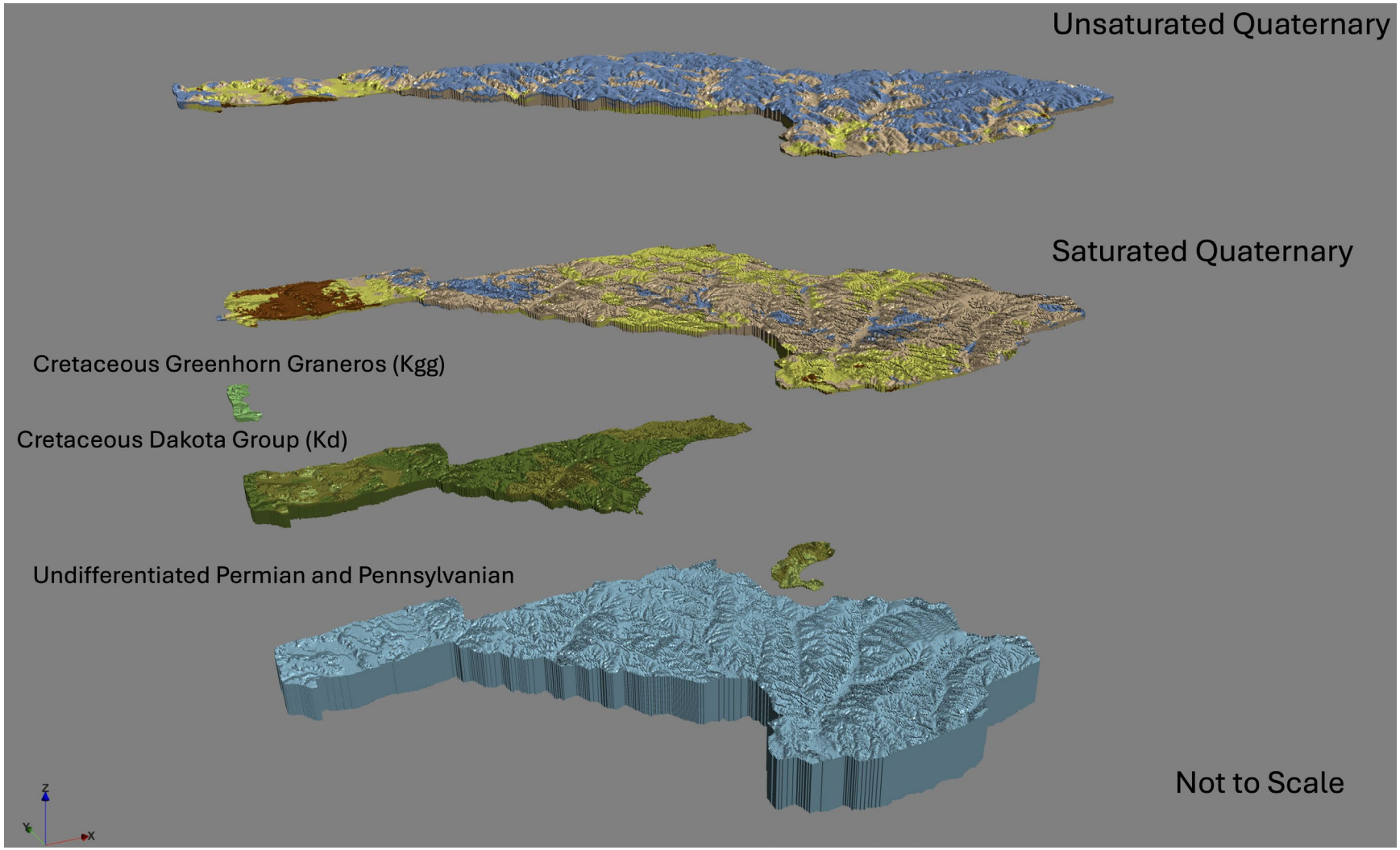


Figure 5-42. 3D exploded voxel model looking north of the LBBNRD 2025 AEM survey area showing Quaternary (*Q*) unsaturated and saturated, Cretaceous Greenhorn and Graneros (*Kgg*), and Cretaceous Dakota Group (*Kd*) saturated, and the undifferentiated Permian/Pennsylvanian Groups (*P*). Not to scale.

5.3.1 The Hydrogeology of the Quaternary

The Quaternary (***Q***) materials of the LBBNRD 2025 AEM survey area are predominantly composed of two zones: 1) the alluvial sediments dominated by sands and gravels of the paleovalleys, and 2) the glacial deposits of till, outwash and loess deposits. The total thickness of the ***Q*** (including both zones of ***Q***) is shown in Figure 5-43. The paleochannel is not easily discernable in the ***Q*** total thickness map. The thickness of the ***Q*** is controlled by the topography of the area, but the thicker section of > 250 feet extends in a general east-west trend at the south end of the survey area.

The first zone, mentioned above, is aquifer material in the ***Q*** fluvial paleochannel sediments (yellow color in figures) and coarse aquifer materials (brown color in figures) that indicate sands and gravels of the paleovalley aquifers and the outwash deposits. A 3D view of the voxel model of the total ***Q*** aquifer and coarse aquifer materials (Figure 5-44) shows the distribution of those materials with the undifferentiated Permian (***P***) surface in the background.

As noted above, the second ***Q*** zone is the loess and glacial tills containing silts and clays which make up the marginal aquifer and non-aquifer material and are poor aquifers. Figure 5-45 illustrates the 3D distribution of the marginal (tan color in figures) and non-aquifer (blue color in figures) materials. There are some windows in the till and loess deposits that can be seen in the areas of the Big Blue River and Swan and Turkey creeks drainages. The non-aquifer materials are typically on the upland areas and are composed of the loess deposits.

An enhanced understanding of the distribution of ***Q*** aquifer materials can be gained by an examination of the flight line profiles. East-west trending profile of line L100041, approximately in the top 1/3 of the survey area (Figure 5-46), is a good example of the ***Q*** section crossing the paleochannel deposits on the western and eastern side of the profile. The ***Kgg*** is on the western end of the line and the ***Kd*** thins from the west to the east. On Figure 5-46 the LBBNRD AEM flight area map inset on the upper right indicates all the flight lines as black lines. The line displayed in the profiles is indicated in red and boreholes are indicated as blue dots from the CSD database and small olive dots from NE-DWEE database. The flight line location map on the upper left indicates the flight line location on an air photo, also indicating the borehole locations. The middle profile is the SCI inversion result which shows the results of the inversion as electrical resistivity. Gaps in the resistivity profile are a result of editing areas of EM-coupling out of the data or of areas that were not over flown due to infrastructure. Located on the profile are lithologies indicated on the Nebraska GeoCloud lithology legend from the CSD and NE-DWEE databases that are within 1,320 feet of the flight line. When present on the profile (due to displayed elevation range), the Depth of Investigation (DOI) is indicated by dashed gray lines. The ***Kgg*** and the ***Kd*** are indicated by dashed lines and the top of the ***P*** is indicated by a solid black line. The Spring 2025 LBBNRD water table is indicated by the dashed blue line, and the estimated saline water line is indicated by the dashed purple line.

The interpretation profile on the bottom of Figure 5-46 shows the results of the hydrogeological framework interpretation. Located on the profile are NE-DWEE database boreholes (gray) within 1,000 feet of the flight line with the screen intervals colored (indicated in the legend) with the specific capacity

in gpm/ft. The ***Kgg*** , ***Kd*** , and ***P*** are indicated by the colors in the legend. The Spring 2025 LBBNRD water table is indicated by the dashed blue line. Estimated aquifer materials are represented by the colors in the legend.

The presence of the high electrical resistivity paleochannel deposits is observed in the 'SCI Inversion Profile'. Confirmation is seen in the many NE-DWEE wells within 1,320 feet of the flight line. The low electrical resistivity of the tills and the loess that is overlying the paleochannel can also be observed on the eastern end of the line. Several wells had the information to calculate Specific Capacity (SC) and indicated a higher SC value in the paleochannel deposits. The saturated thickness of the ***Q*** aquifer decreases to the west. On the far west of the line, the ***Kgg*** is covered by a thin loess deposit and forms the edge of the paleochannel.

Examining Figure 5-47, north-south trending line L190191, several features can be seen in the ***Q*** aquifer system. A paleochannel is seen on the south and north end of the line. Remnants of the ***Kd*** is also seen along the line and is indicated in the lithology logs from the NE-DWEE database. Both the southern and the northern paleochannels have sand deposits of aquifer materials where higher SC values are indicated. There is also an area on the south of the line where it crosses Bear Creek and saturated aquifer materials are at the surface.

Figure 5-48 presents north-south trending line L190253 on the eastern third of the flight area. This line crosses the deeper paleochannel/paleovalley and illustrates a glacial outwash deposit on the top of a paleochannel that was eroded into the ***P*** bedrock. This profile also illustrates the confining lithology or layers that are above the deeper paleochannel; these layers are most likely preglacial. A few NE-DWEE wells indicate good SC values in the deepest of the sand deposits.

Using the LBBNRD Spring 2025 water table estimates, saturated thickness can be derived from the data. Figure 5-49 is the total saturated thickness of the ***Q*** and Figure 5-50 is the saturated thickness of the aquifer and coarse aquifer material. These figures illustrate the paleochannel deposits and the paleovalley aquifer in the ***Q*** sediments. As indicated above, the marginal aquifer material class can provide some water but at a much lower rate due to the interlayering of clays and silts.

As a comparison, the ***Q*** marginal and non-aquifer material saturated thickness is indicated in Figure 5-51. The saturated marginal aquifer materials are throughout the area. The saturated non-aquifer materials are more isolated.

Using the calculated transmissivity maps (Section 5.1.7) and plotting the registered wells with specific capacity data for completions within the ***Q***, an image of the ***Q*** aquifer can be better illuminated (Figure 5-52**)**. Most completions within the ***Q*** are within the paleovalley aquifer in the higher transmissive materials. The correlation is excellent with the Specific Capacity values and the position of the AEM estimated transmissivity. This can be compared with what has been previously published about the paleovalley aquifer by overlying transmissivity contours from Summerside and Myers (2005) on the AEM estimated transmissivity map (Figure 5-53). A good general agreement is observed, and more details revealed, by the AEM due to the high density of observations.

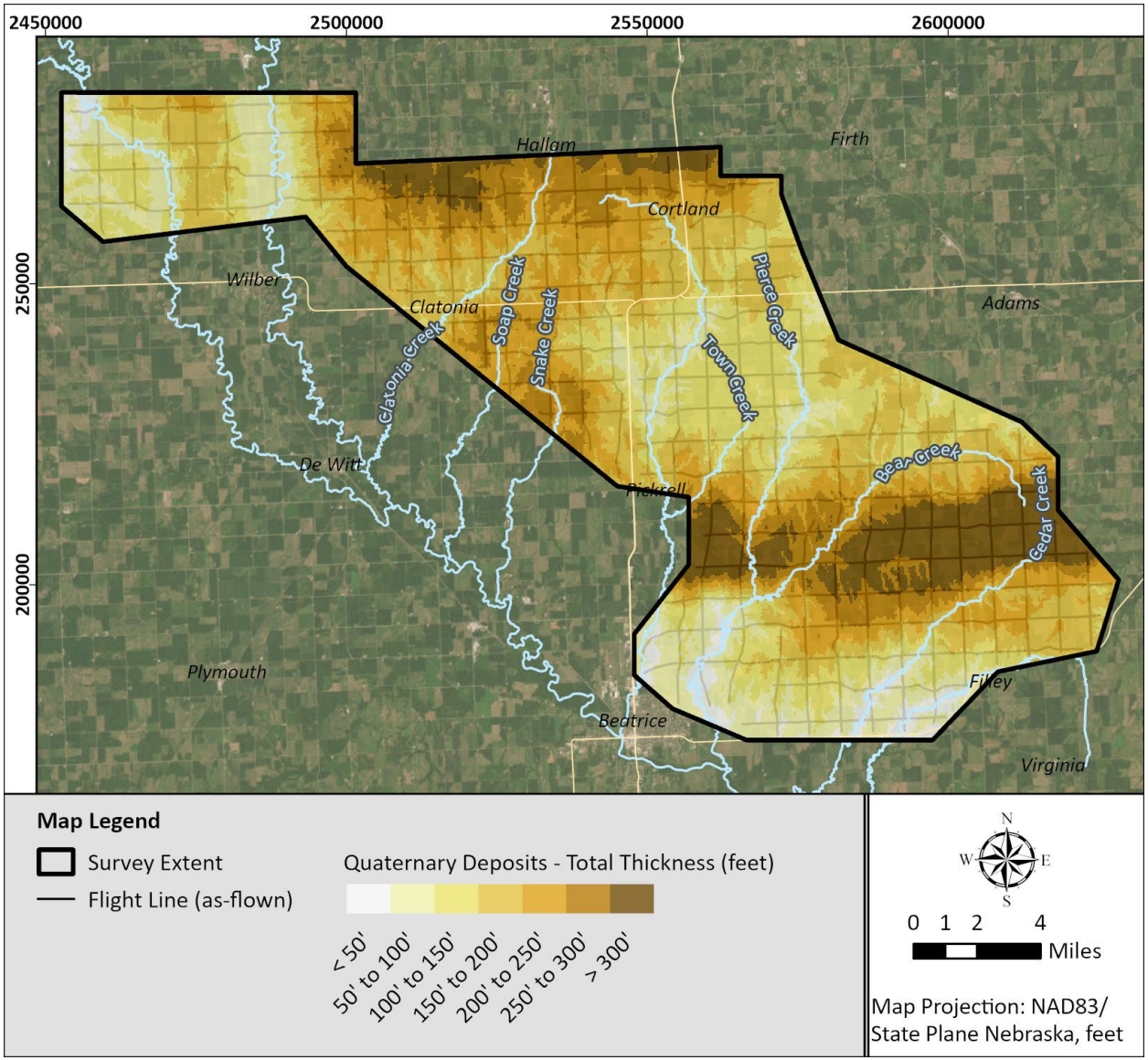


Figure 5-43. Map of the Quaternary (*Q*) total thickness within the LBBNRD 2025 AEM survey area.

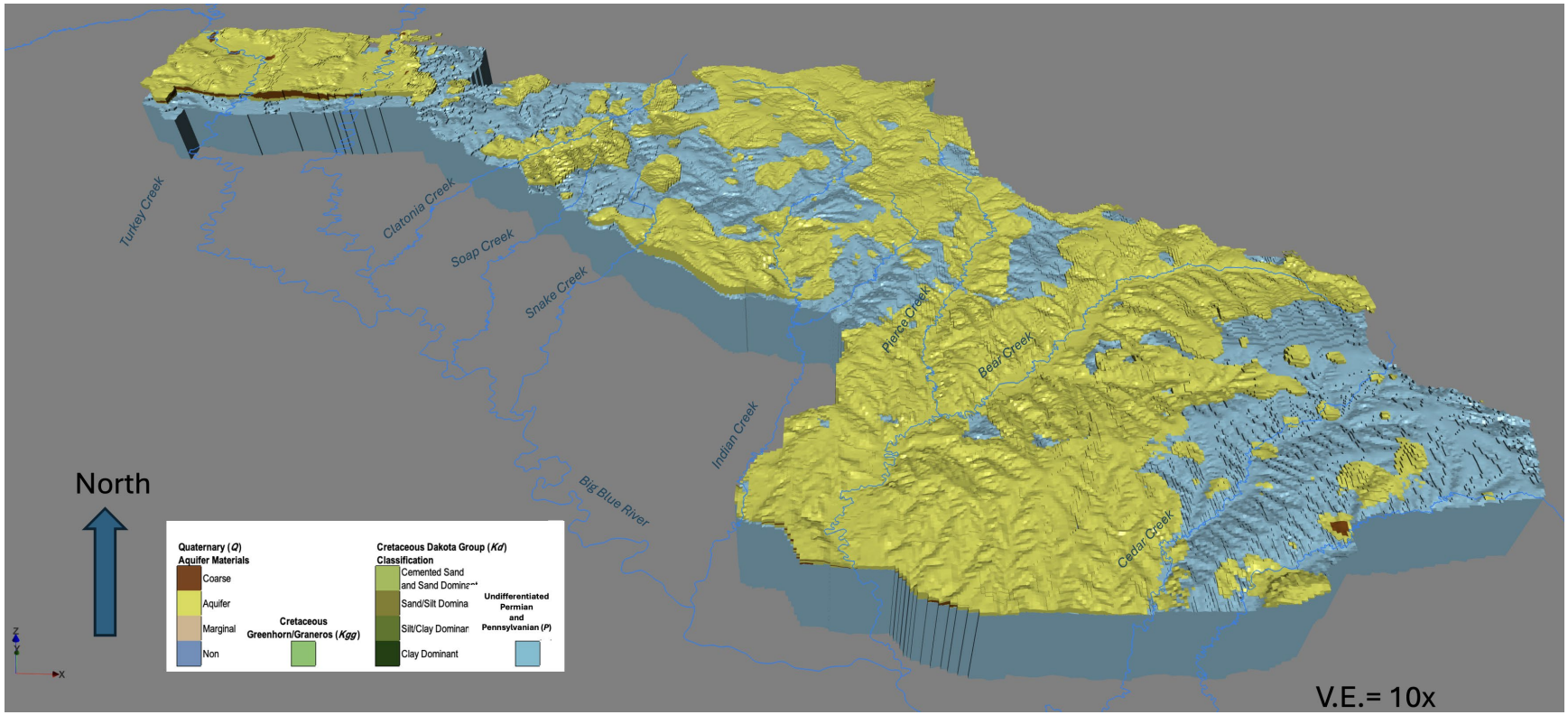


Figure 5-44. 3D Voxel diagram looking to the north of the interpreted distributions of total aquifer and coarse aquifer material of the Quaternary (*Q*) within the LBBNRD 2025 AEM survey area. V.E.=10x.

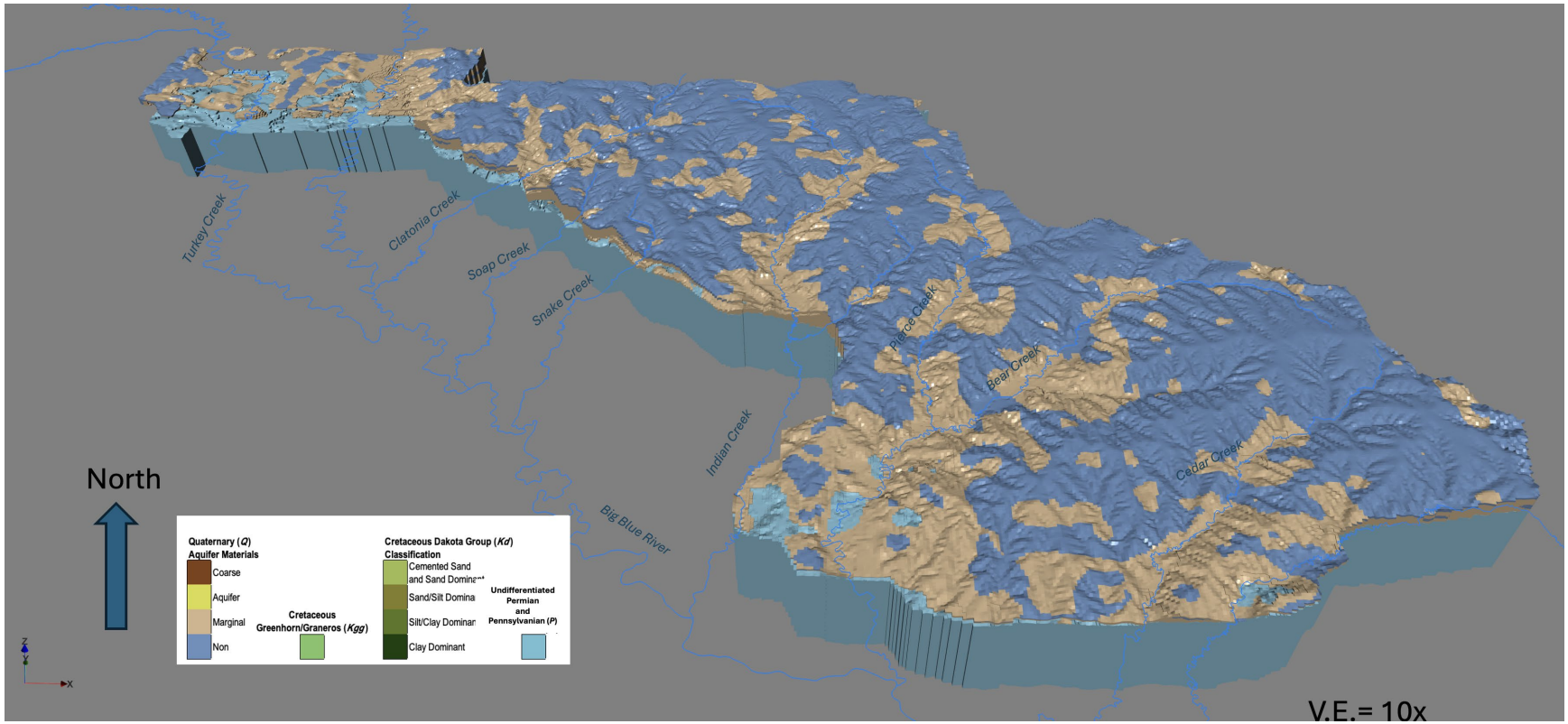


Figure 5-45. 3D Voxel diagram looking to the north of the interpreted distributions of the total non- and marginal-aquifer materials of the Quaternary (*Q*) within the LBBNRD 2025 AEM survey area. V.E.=10x.

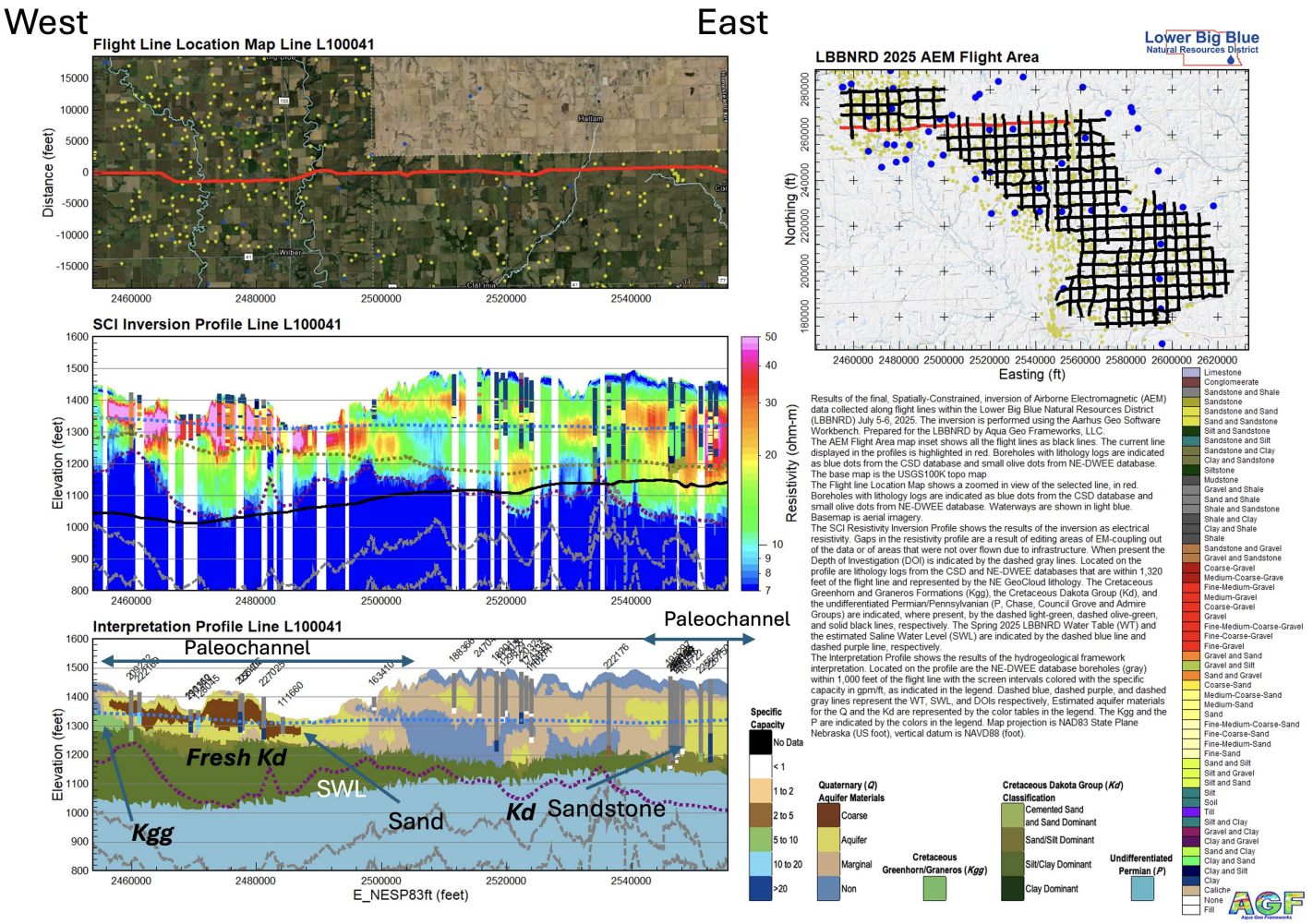


Figure 5-46. East-West AEM flight line L100041. A location map is on the upper right. On the left the top profile shows the air photo along the flight line. The middle profile is the SCI resistivity inversion result showing borehole lithologies and the bottom profile is an interpretative section showing the undifferentiated Permian/Pennsylvanian (*P*), Cretaceous Greenhorn and Graneros (*Kgg*), and Cretaceous Dakota Group (*Kd*), underlying the Quaternary (Q) subdivided into interpreted aquifer materials. Boreholes in the bottom section indicate measured Specific Capacity. The LBBNRD 2025 Spring water table is indicated by the dashed blue line and the estimated saline water (SWL) level is indicated by the dash purple line.

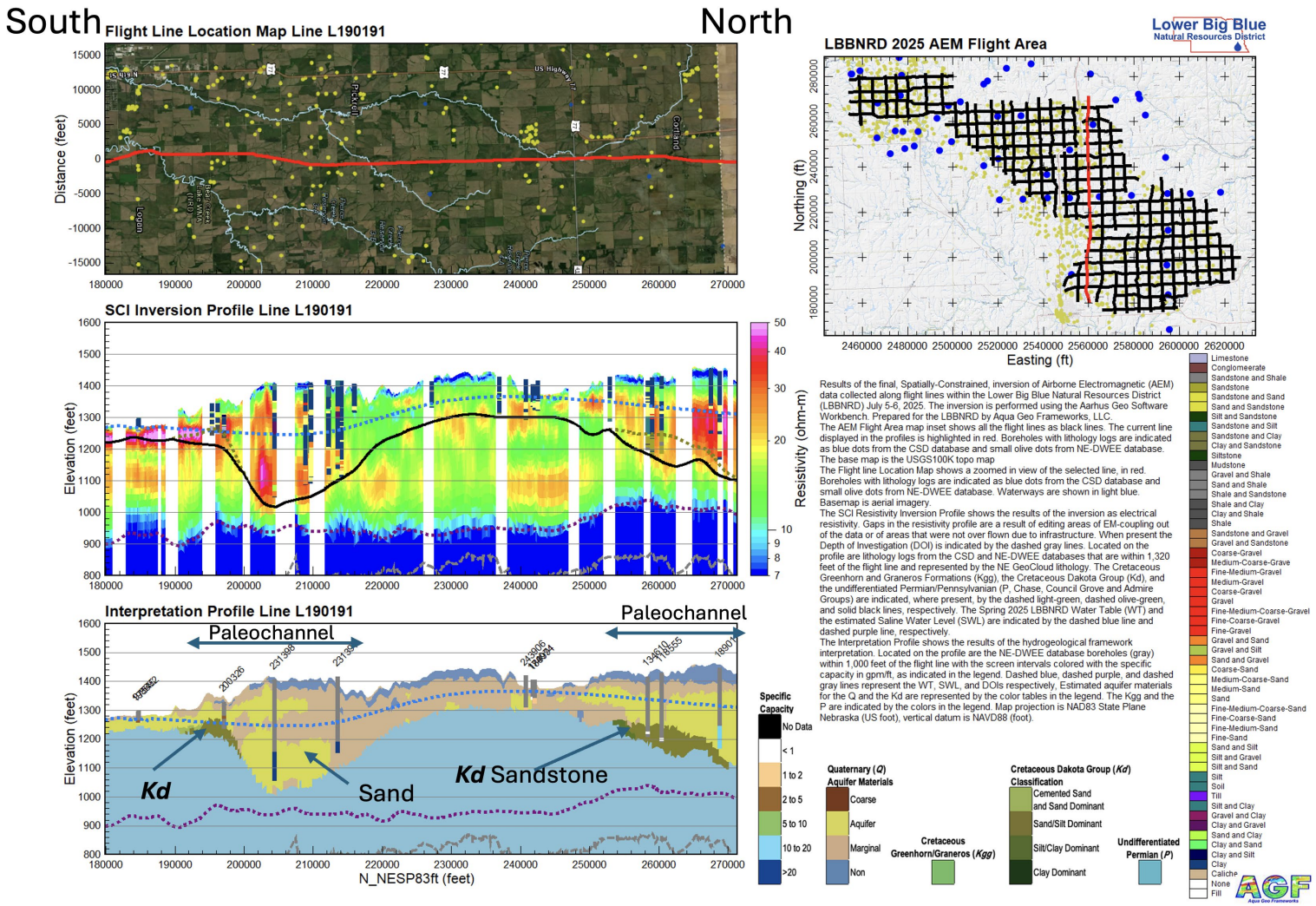


Figure 5-47. North-south AEM flight line L190191. A location map is on the upper right. On the left the top profile shows the air photo along the flight line. The middle profile is the SCI resistivity inversion result showing borehole lithologies and the bottom profile is an interpretative section showing the undifferentiated Permian/Pennsylvanian (*P*), Cretaceous Dakota Group (*Kd*), underlying the Quaternary (Q) subdivided into interpreted aquifer materials. Boreholes in the bottom section indicate measured Specific Capacity. The LBBNRD 2025 Spring water table is indicated by the dashed blue line and the estimated saline water level (SWL) is indicated by the dash purple line.

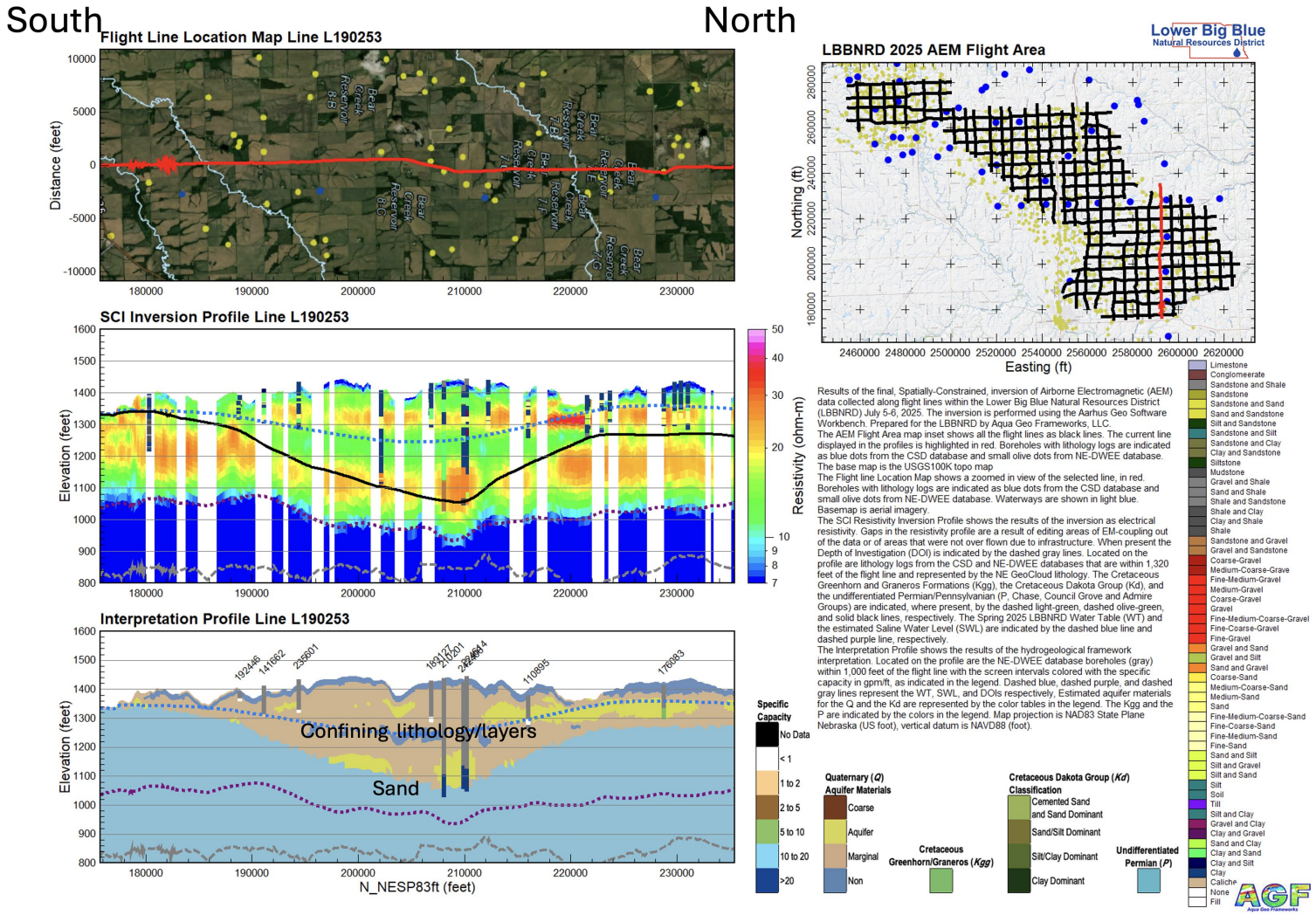


Figure 5-48. North-south AEM flight line L190253. A location map is on the upper right. On the left the top profile shows the air photo along the flight line. The middle profile is the SCI resistivity inversion result showing borehole lithologies and the bottom profile is an interpretative section showing the undifferentiated Permian/Pennsylvanian (*P*), Cretaceous Dakota Group (*Kd*), underlying the Quaternary (Q) subdivided into interpreted aquifer materials. Boreholes in the bottom section indicate measured Specific Capacity. The LBBNRD 2025 Spring water table is indicated by the dashed blue line and the estimated saline water level (SWL) is indicated by the dash purple line.

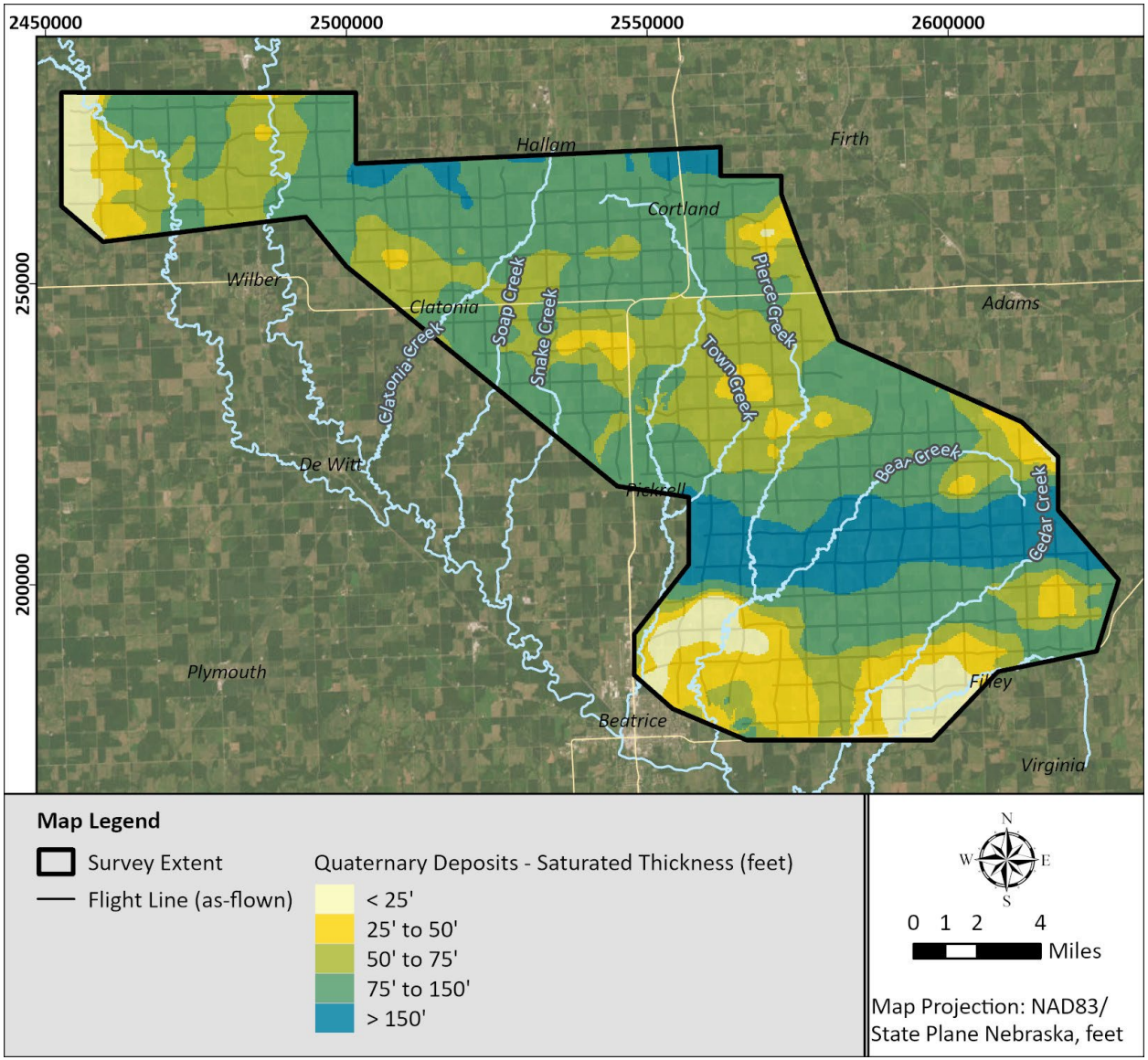


Figure 5-49. Map of the total saturated Quaternary (*Q*) thickness within the LBBNRD 2025 AEM survey area calculated using the Spring 2025 LBBNRD water levels.

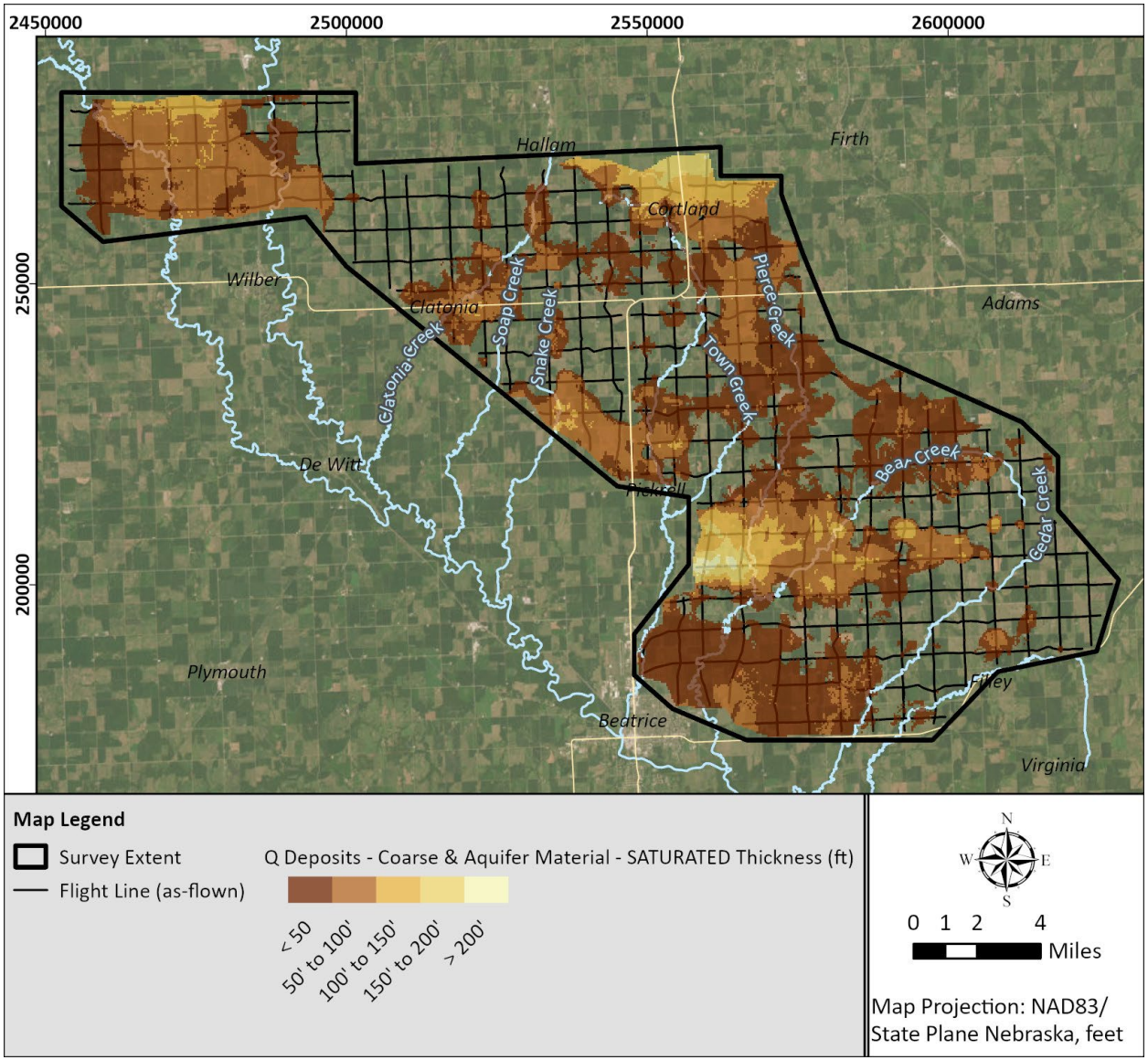


Figure 5-50. Map of the Quaternary (*Q*) aquifer and coarse aquifer material saturated thickness within the LBBNRD 2025 AEM survey area calculated using the Spring 2025 LBBNRD water levels.

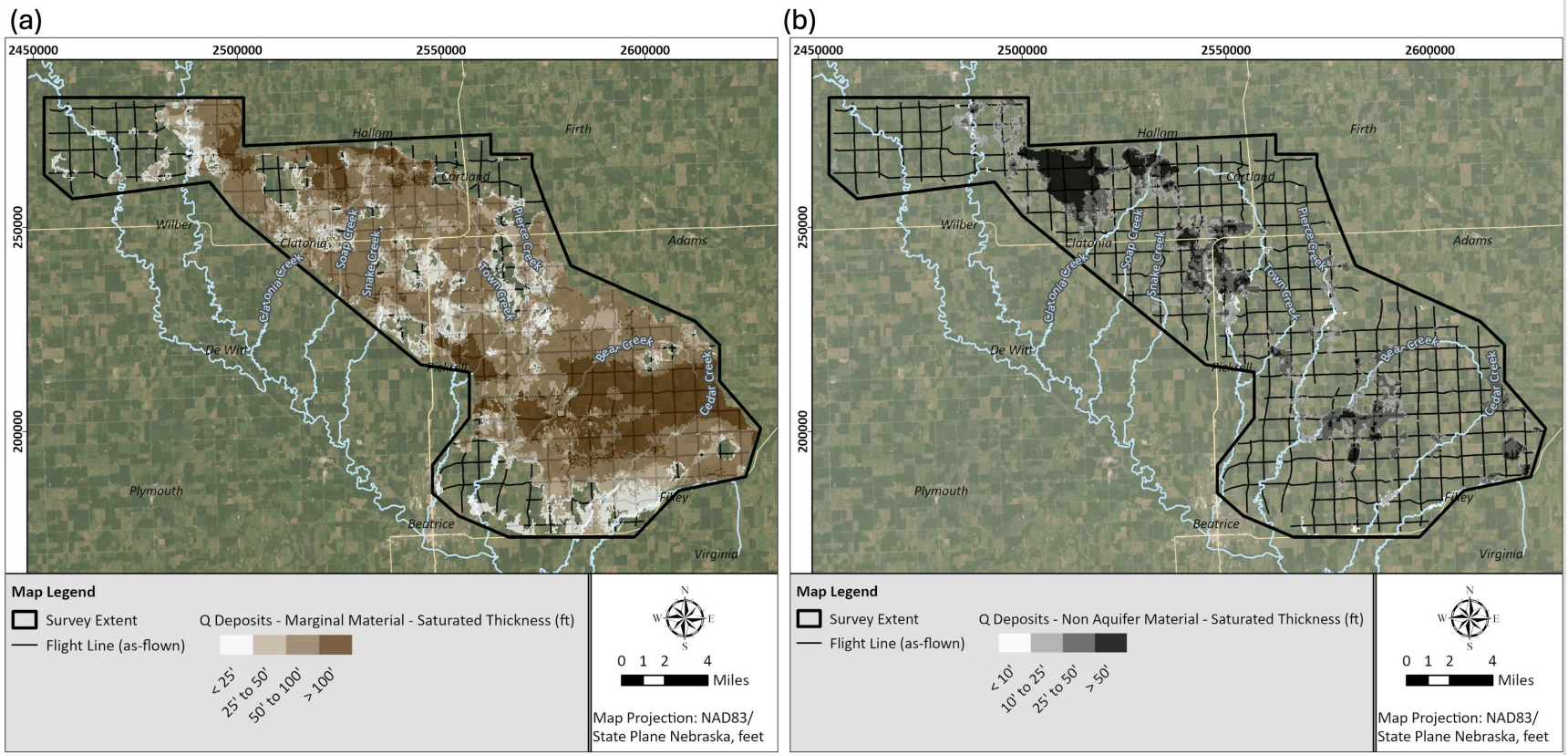


Figure 5-51. Map of the saturated Quaternary (*Q*) marginal aquifer materials (a), and saturated non-aquifer material thickness (b) within the LBBNRD 2025 AEM survey area calculated using the Spring 2025 LBBNRD water levels.

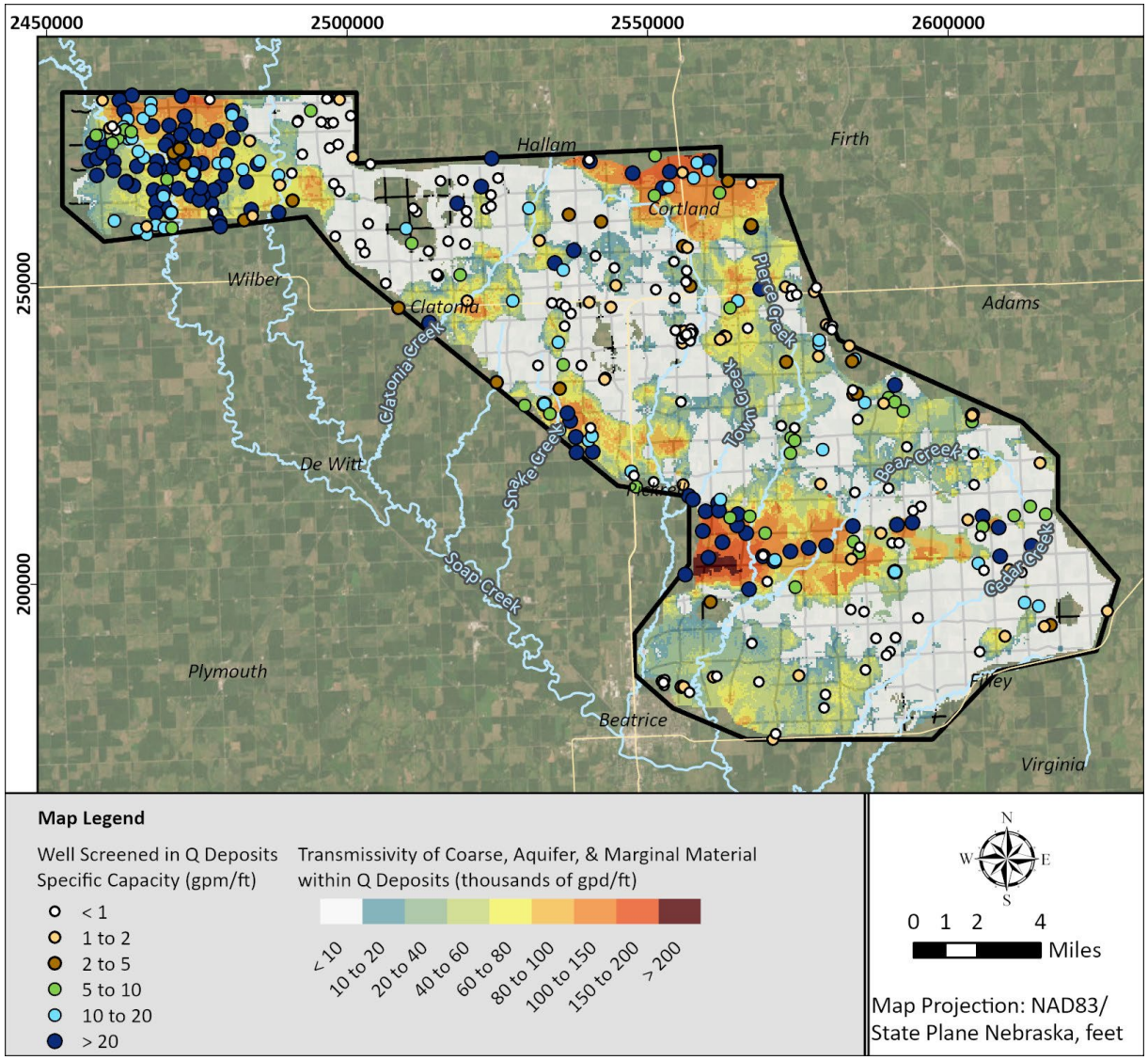


Figure 5-52. Map of the estimated transmissivity (gpd/feet) of the Quaternary (*Q*) marginal aquifer materials, aquifer materials, and coarse aquifer materials within the LBBNRD 2025 AEM survey area. Specific Capacity values from the NE-DWEE registered well database for wells screen in the Q are shown as indicated by the legend.

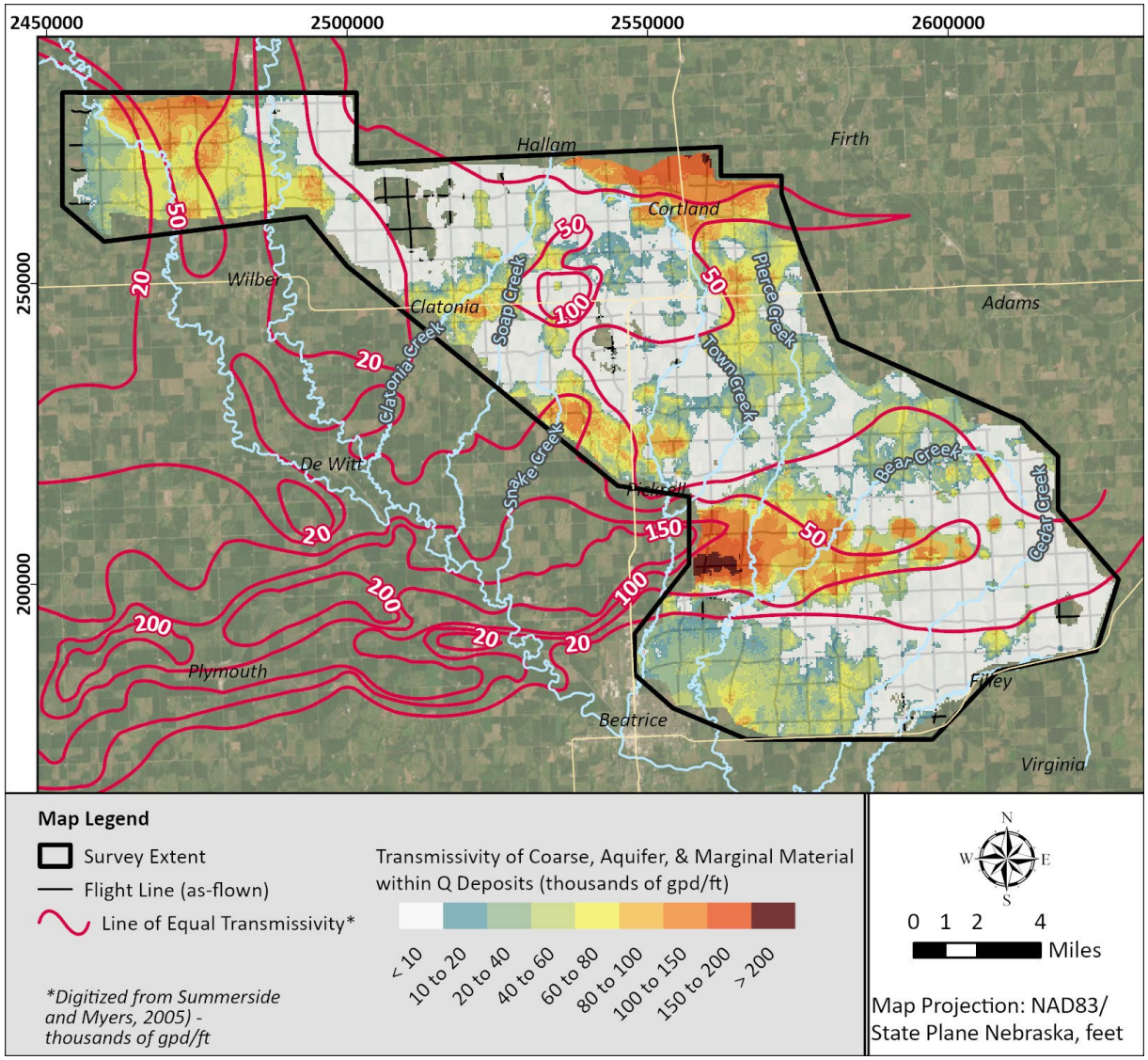


Figure 5-53. Map of the estimated transmissivity (gpd/feet) of the Quaternary (Q) marginal aquifer materials, aquifer materials, and coarse aquifer material transmissivity within the LBBNRD 2025 AEM survey area. Overlain with the transmissivity contours from Summerside and Myers (2005).

5.3.2 Hydrogeology of the Cretaceous Dakota Group

The Cretaceous Dakota Group (***Kd***) is in the western part of the survey area and is directly deposited on the undifferentiated Permian (***P***) units. The ***Kd*** was eroded from the eastern third of the survey area before and during the glacial period. The ***Kd*** is composed of consolidated and semi-consolidated clay, silt, sand, sandstone, siltstone, and shale. The deposits are in fluvial deposits associated with the delta front that existed and underwent multiple regressive and transgressive sequences in the Cretaceous (Witzke et al., 1983).

These materials overlie the undifferentiated Permian (***P***) in the western section of the survey area and serve as the regional aquiclude. A map of the depth to the top of the ***Kd***, is presented in Figure 5-54. The top of the ***P*** influenced the depositional environment of the ***Kd*** due to the control the surface had on the stream gradient at the time of deposition where sediments were deposited. A majority of the ***Kd*** is saturated throughout the survey area (Figure 5-55). The total thickness and the saturated thickness of the ***Kd*** is 0 to > 250 feet as shown in Figure 5-55.

Figure 5-56 is a 3D voxel model looking north showing the distribution of ***Kd*** cemented sand and sand dominant materials along with the sand/silt dominant materials. This represents resistivities > 18 ohm-m. Similarly, Figure 5-57 presents a 3D voxel model, looking north, showing the distribution of ***Kd*** materials with resistivities over 35 ohm-m. This illustrates the limited resistivity materials within the ***Kd***. Figure 5-58 presents a 3D voxel model, looking north, showing the distribution of ***Kd*** materials with resistivities over 18 ohm-m with the estimated saline waters < 7 ohm-m indicated as red-yellow. There are several areas that indicate that saline waters are within the saturated portion of the ***Kd***.

Figure 5-59 presents the profile of east-west Line L100041, that has been previously examined in this report, in the north of the survey area. The lithologies of the wells on the west and east end indicated sandstone within the ***Kd***. There are wells competed in the sandstones (>18 ohm-m) with specific capacity (SC) value from 5 to 10 gpm/ft and lower. The middle area of the profile shows the surface of the estimated saline waters.

Figure 5-60 is a map of the saturated thickness of the sandstone and sand dominant and sand/silt dominant > 18 ohm-m and the SC of the wells which are completed in the ***Kd***. There is a correlation of the > 18 ohm-m materials to the location of higher SC values for wells completed in the ***Kd***. There are a few wells that fall outside this zone and the depth of the screens are in the silt clay dominate ***Kd***. Figure 5-61 is a profile along east-west trending line L1000061 and it shows several wells completed within the ***Kd***. Wells in the center of the profile have SC of 10 to 20 and 5 to 10 gpd/ft within the area of Sand and Silt Dominant materials. The well on the eastern side in the thin ***Kd*** that is Silt/Clay Dominant the SC is < 1 gpd/ft. Figure 5-62 is a north-south profile along line L190201 that shows a couple areas of remnant ***Kd***. The wells have SC of <1 gpm/ft. These are not very good wells due to the thin nature of the ***Kd*** and the short screens. The transmissivity maps were explained in (Section 5.1.7) for the ***Kd***; the transmissivity map is an estimate based on the limited data. When the SC values from the NE-DWEE registered wells are placed on the ***Kd*** AEM estimated transmissivity map (Figure 5-63), a good general agreement is observed, with the exception of some of the well discussed above.

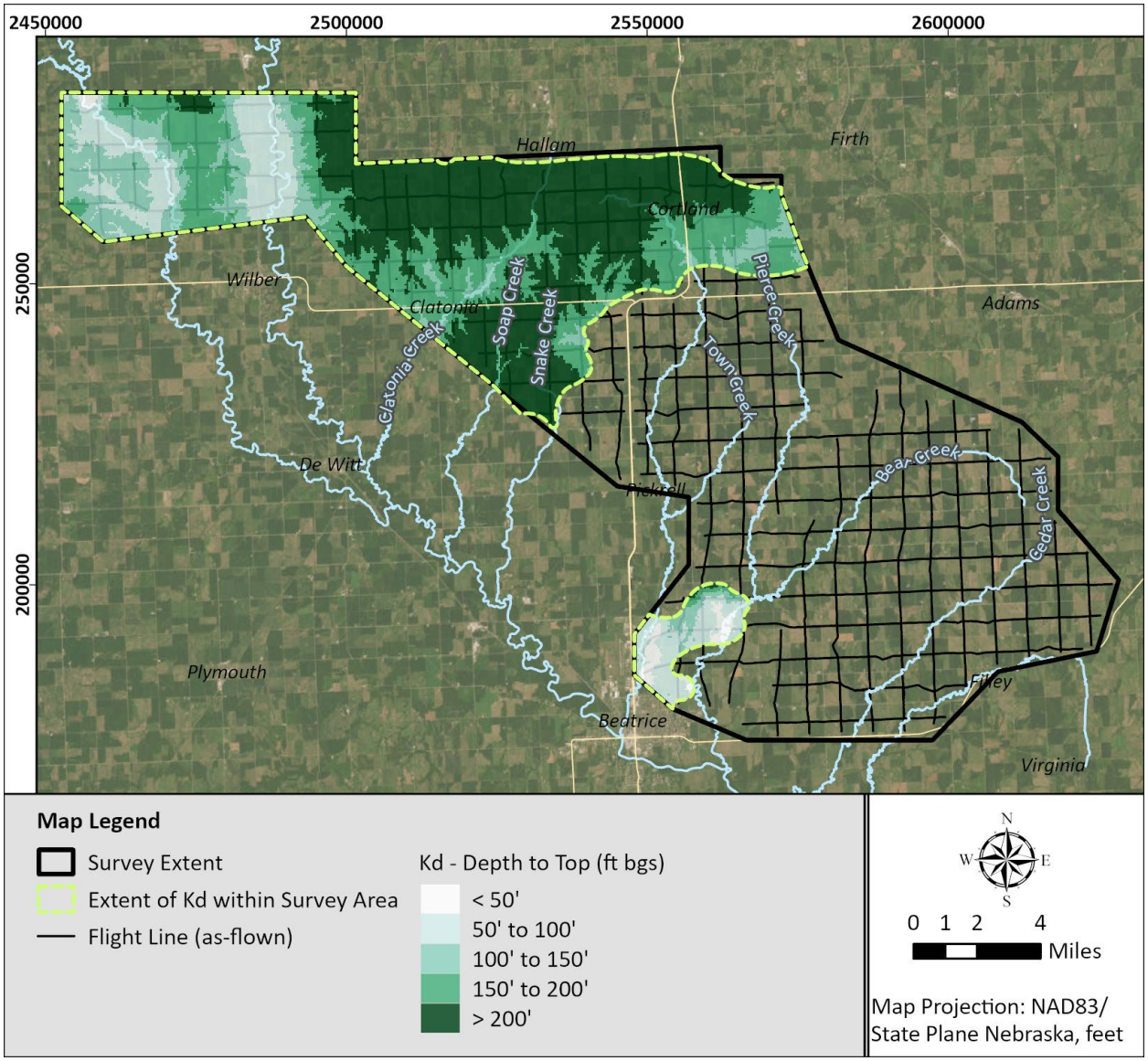


Figure 5-54. Map of the depth to the top of Cretaceous Dakota Group (*Kd*).

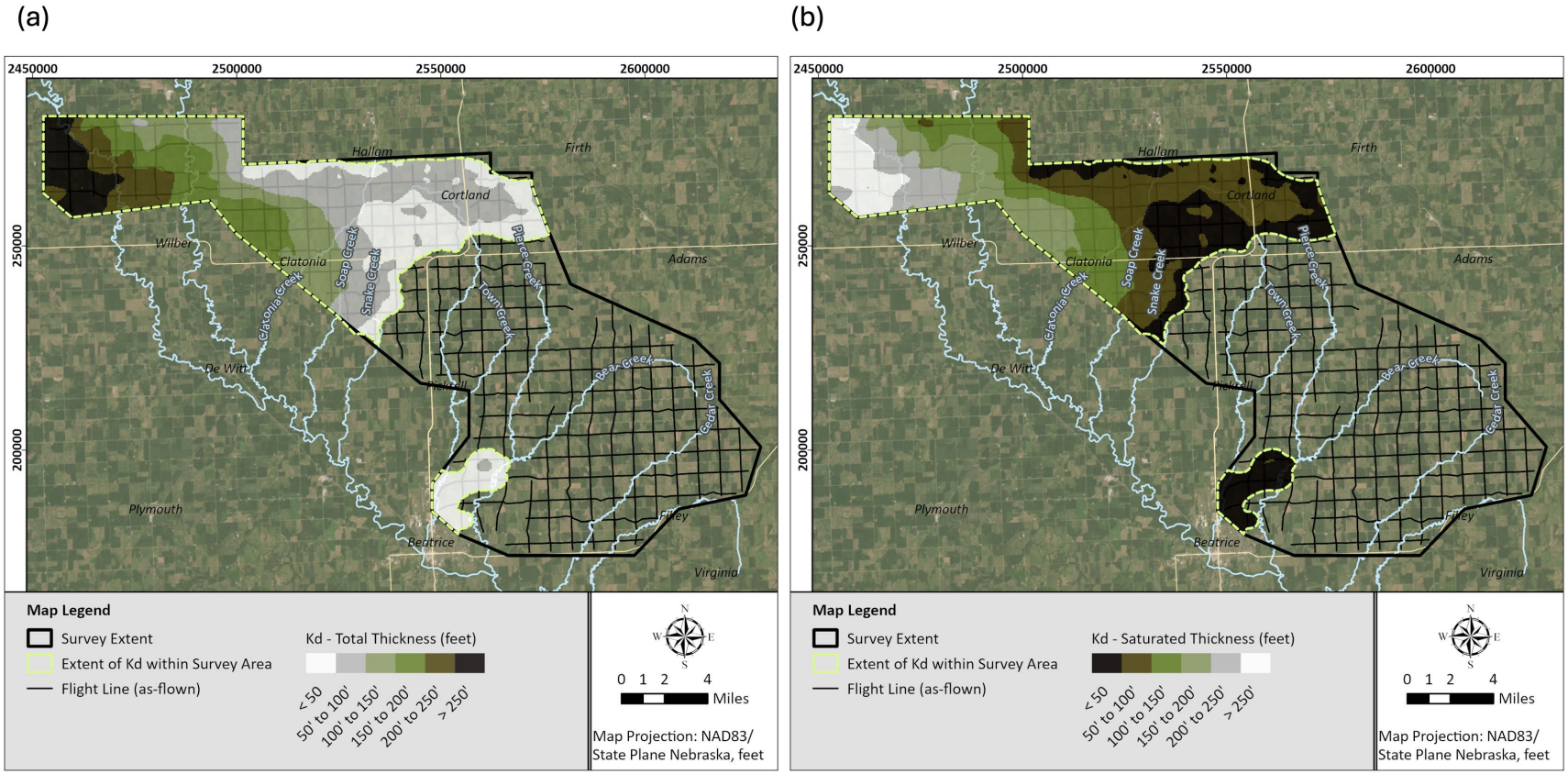


Figure 5-55. Map of the total thickness (a) and the of the saturated thickness (b) of the Cretaceous Dakota Group (*Kd*).

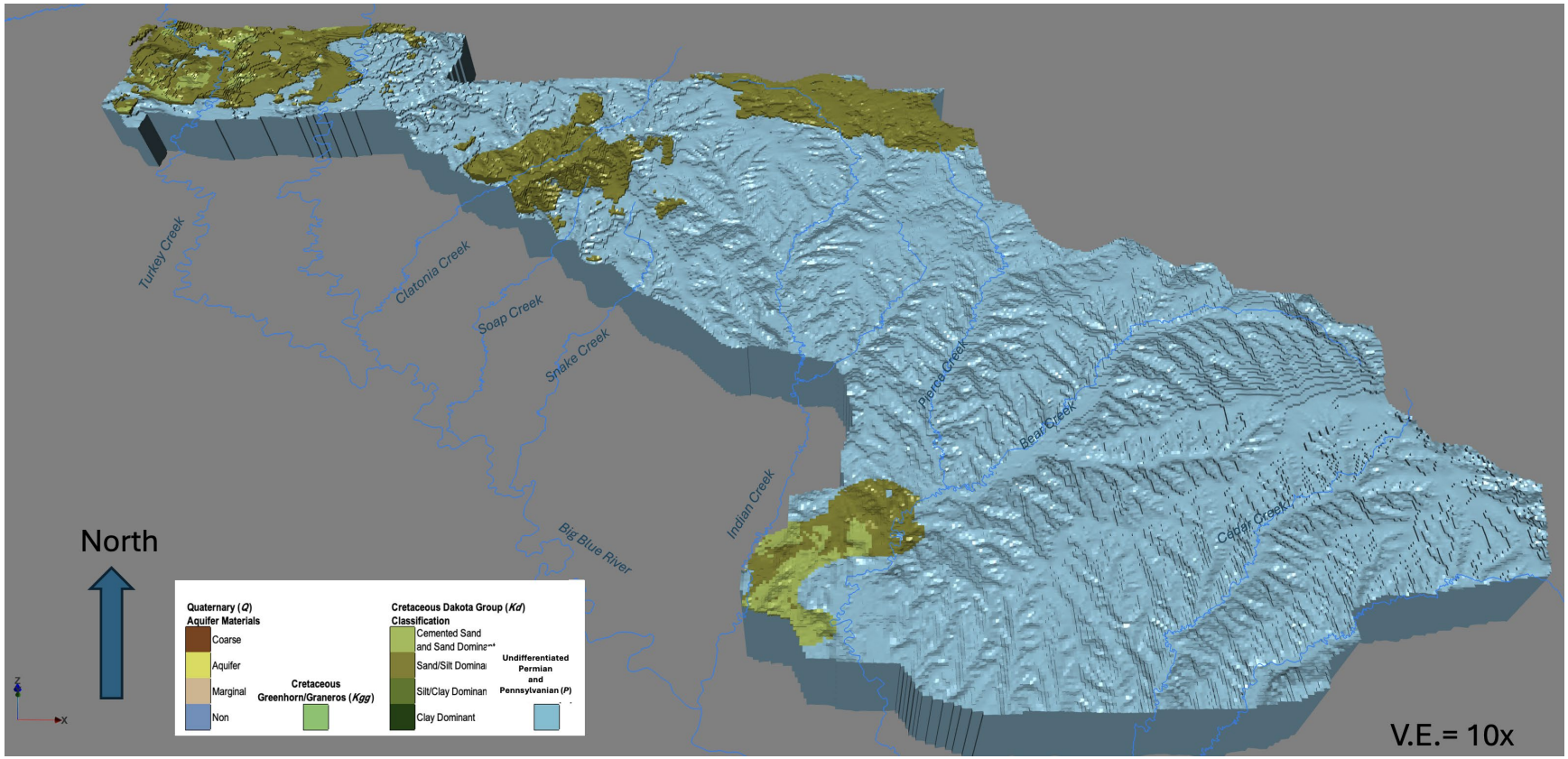


Figure 5-56. 3D Voxel diagram looking to the north of the interpreted Cretaceous Dakota Group (Kd) distributions of cemented sand and sand dominant as well as sand and silt dominant material > 18 ohm-m within the LBBNRD 2025 AEM survey area. V.E.=20x.

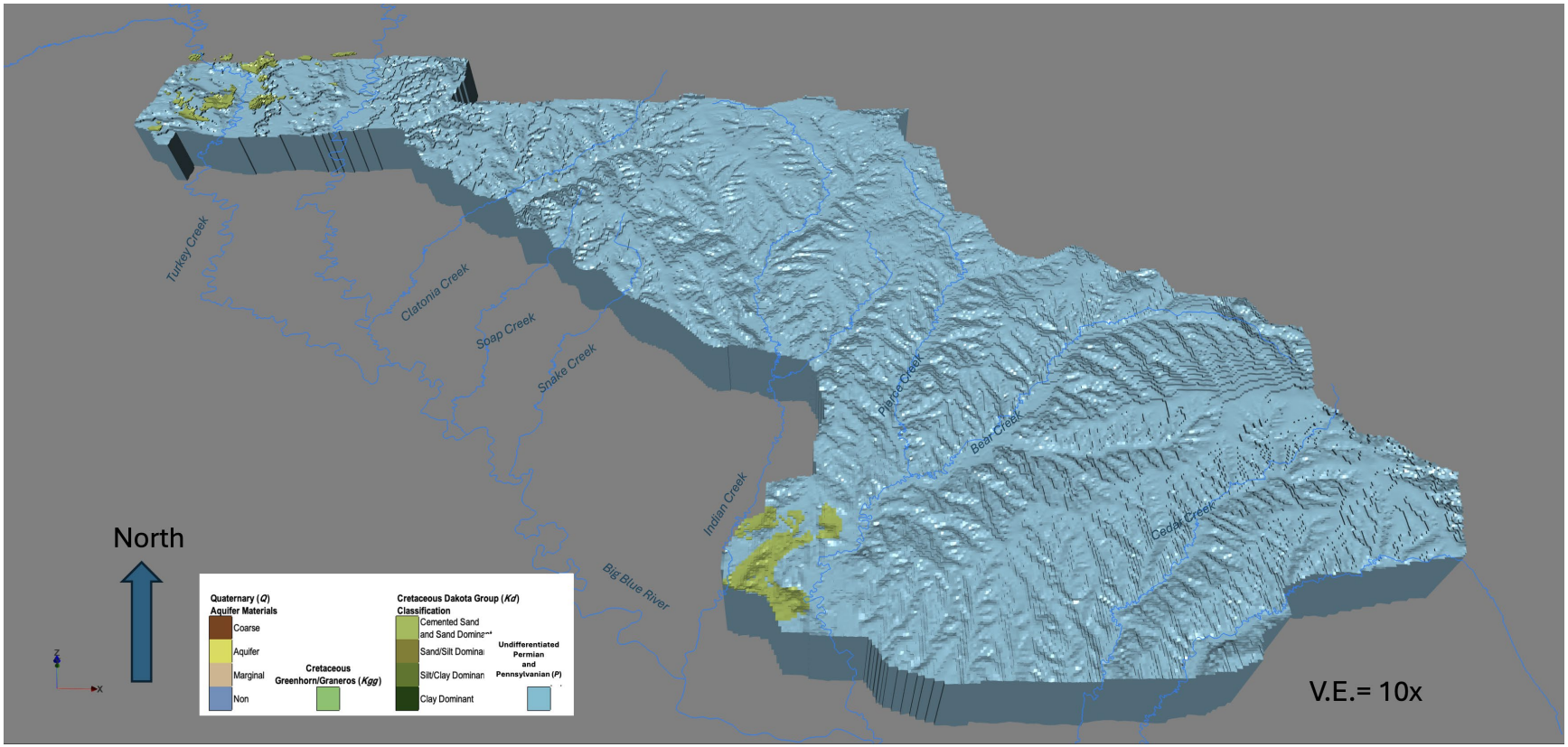


Figure 5-57. 3D Voxel diagram looking to the north of the interpreted Cretaceous Dakota Group (*Kd*) distributions of cemented sand and sand dominant material > 35 ohm-m within the LBBNRD 2025 AEM survey area. V.E.=20x.

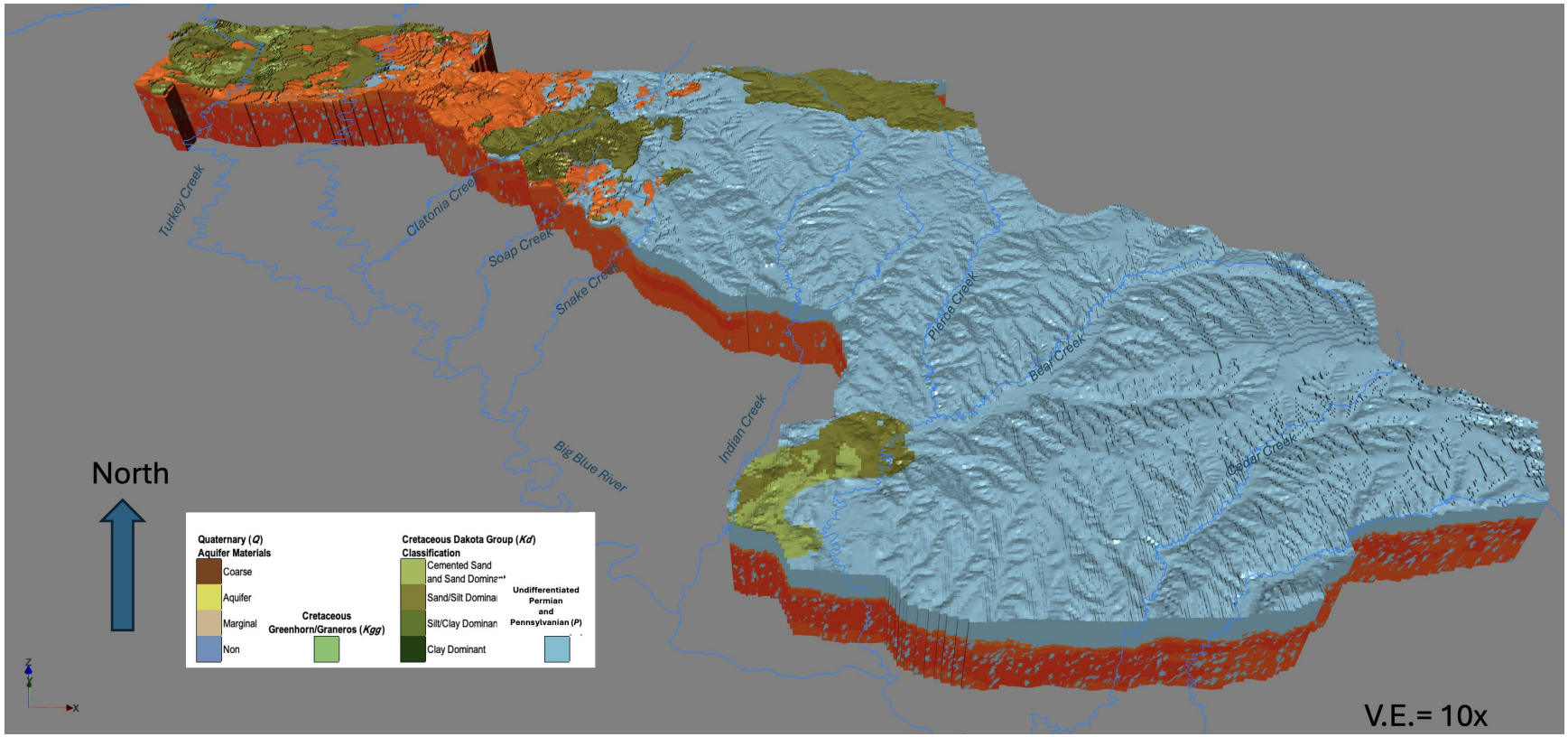


Figure 5-58. 3D Voxel diagram looking to the north of the interpreted Cretaceous Dakota Group (*Kd*) distributions of silt and sand dominant material > 18 ohm-m and the red-yellow area of < 7 ohm-m indicating the estimated saline water within the LBBNRD 2025 AEM survey area. V.E.=10x.

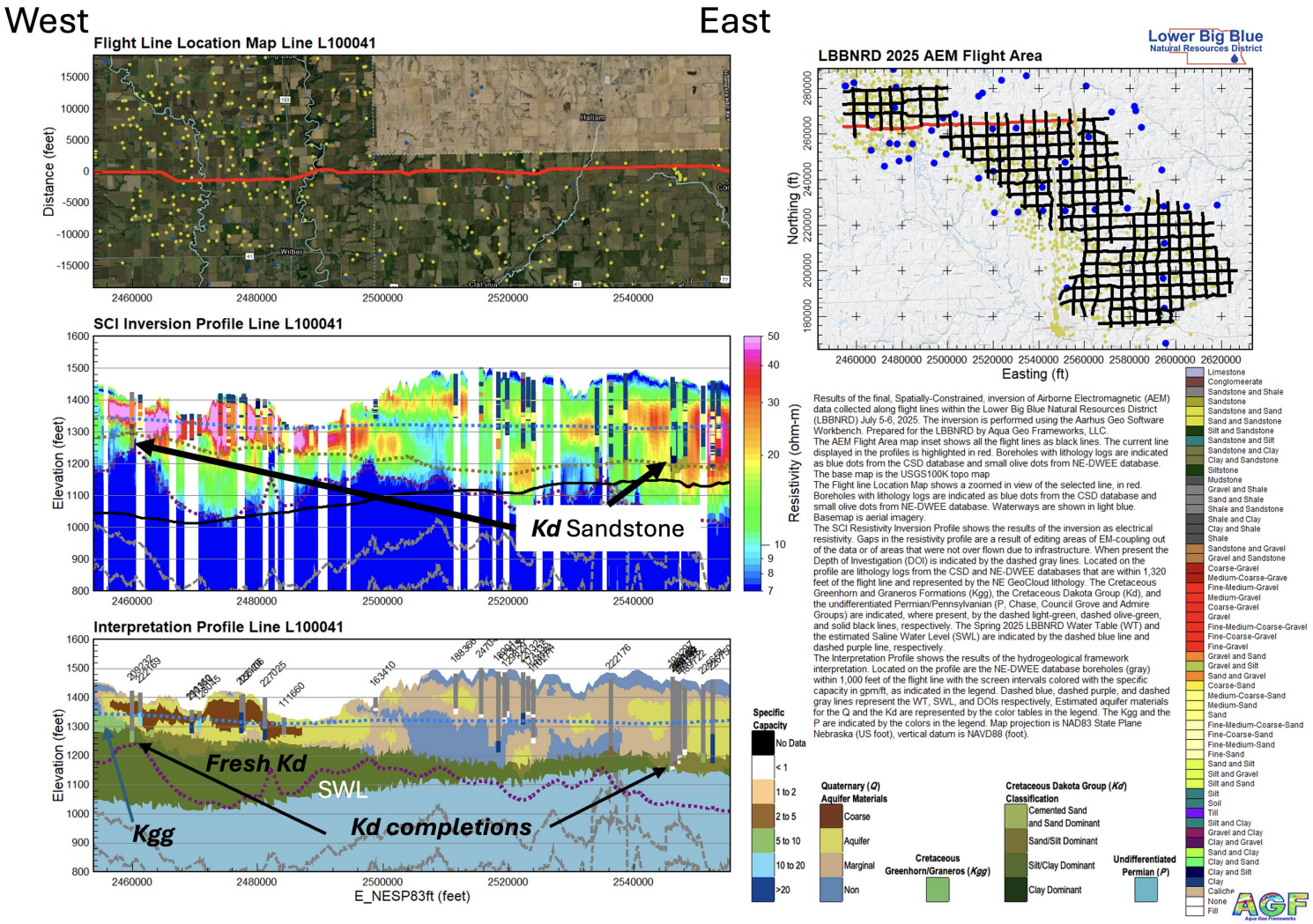


Figure 5-59. East-west AEM flight line L100041. A location map is on the upper right. On the left the top profile shows the air photo along the flight line. The middle profile is the SCI resistivity inversion result showing borehole lithologies and the bottom profile is an interpretative section showing the undifferentiated Permian/Pennsylvanian (*P*), Cretaceous Dakota Group (*Kd*), underlying the Quaternary (*Q*) subdivided into interpreted aquifer materials. Boreholes in the bottom section indicate measured Specific Capacity. The LBBNRD 2025 Spring water table is indicated by the dashed blue line and the estimated saline water level is indicated by the dash purple line.

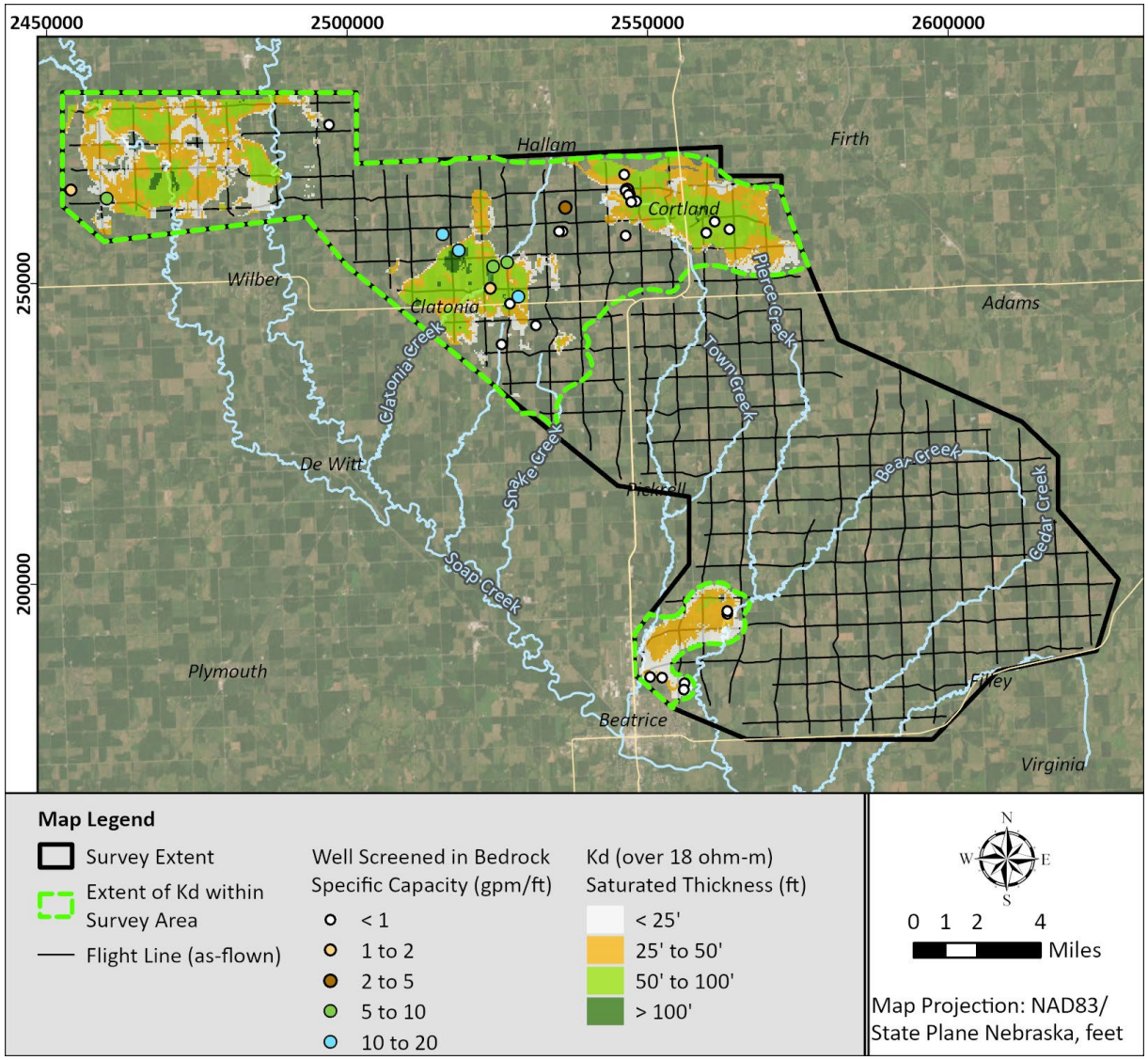


Figure 5-60. Map of the Cretaceous Dakota Group (*Kd*) total saturated thickness of the sandstone and sand-dominant materials within the LBBNRD 2025 AEM survey are with resistivities >18 ohm-m. Specific Capacity values from the NE-DWEE registered well database for wells screen in the Kd are shown as indicated by the legend.

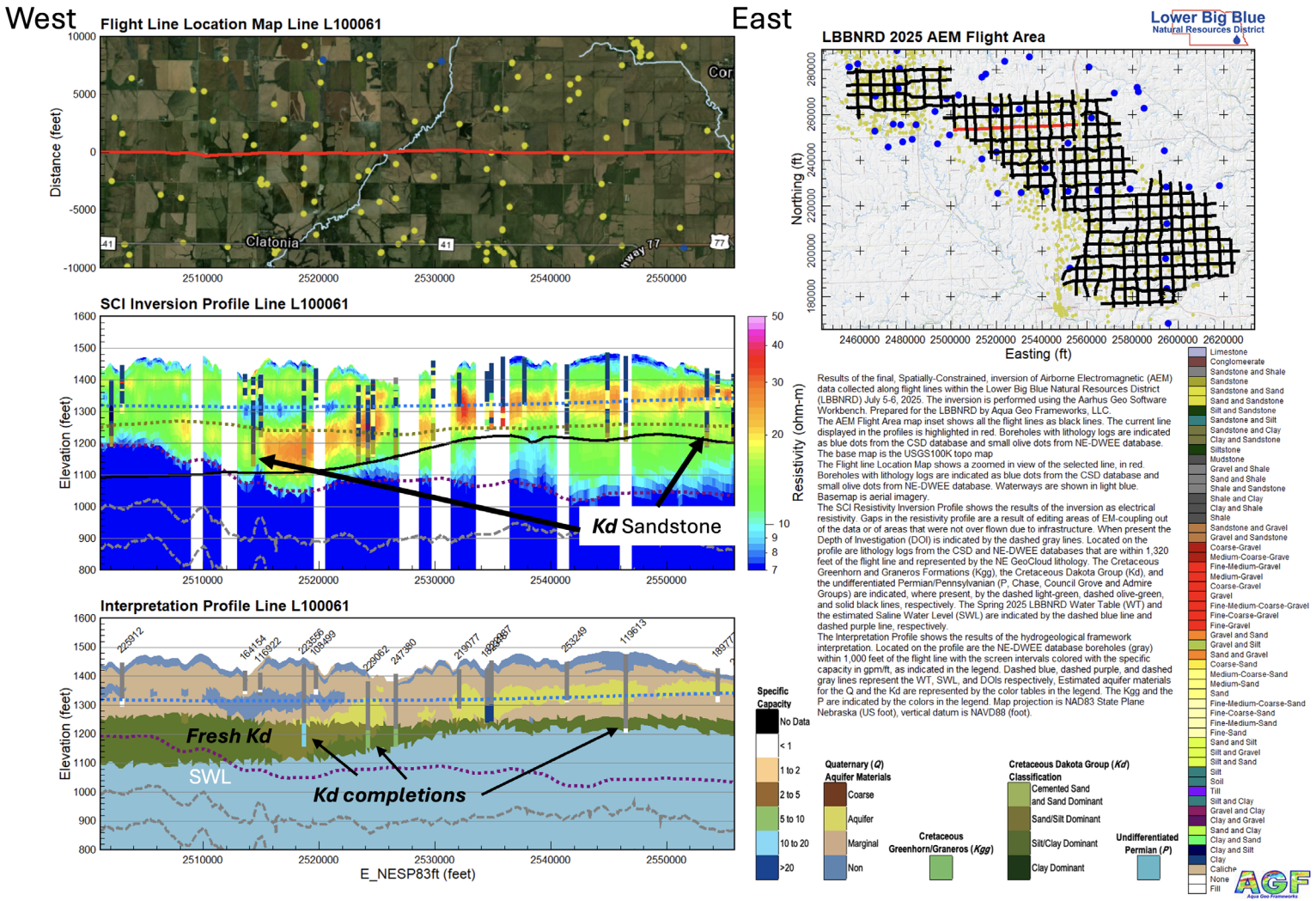


Figure 5-61. East-west AEM flight line L100061. A location map is on the upper right. On the left the top profile shows the air photo along the flight line. The middle profile is the SCI resistivity inversion result showing borehole lithologies and the bottom profile is an interpretative section showing the undifferentiated Permian/Pennsylvanian (*P*), Cretaceous Dakota Group (*Kd*), underlying the Quaternary (*Q*) subdivided into interpreted aquifer materials. Boreholes in the bottom section indicate measured Specific Capacity. The LBBNRD 2025 Spring water table is indicated by the dashed blue line and the estimated saline water level is indicated by the dash purple line.

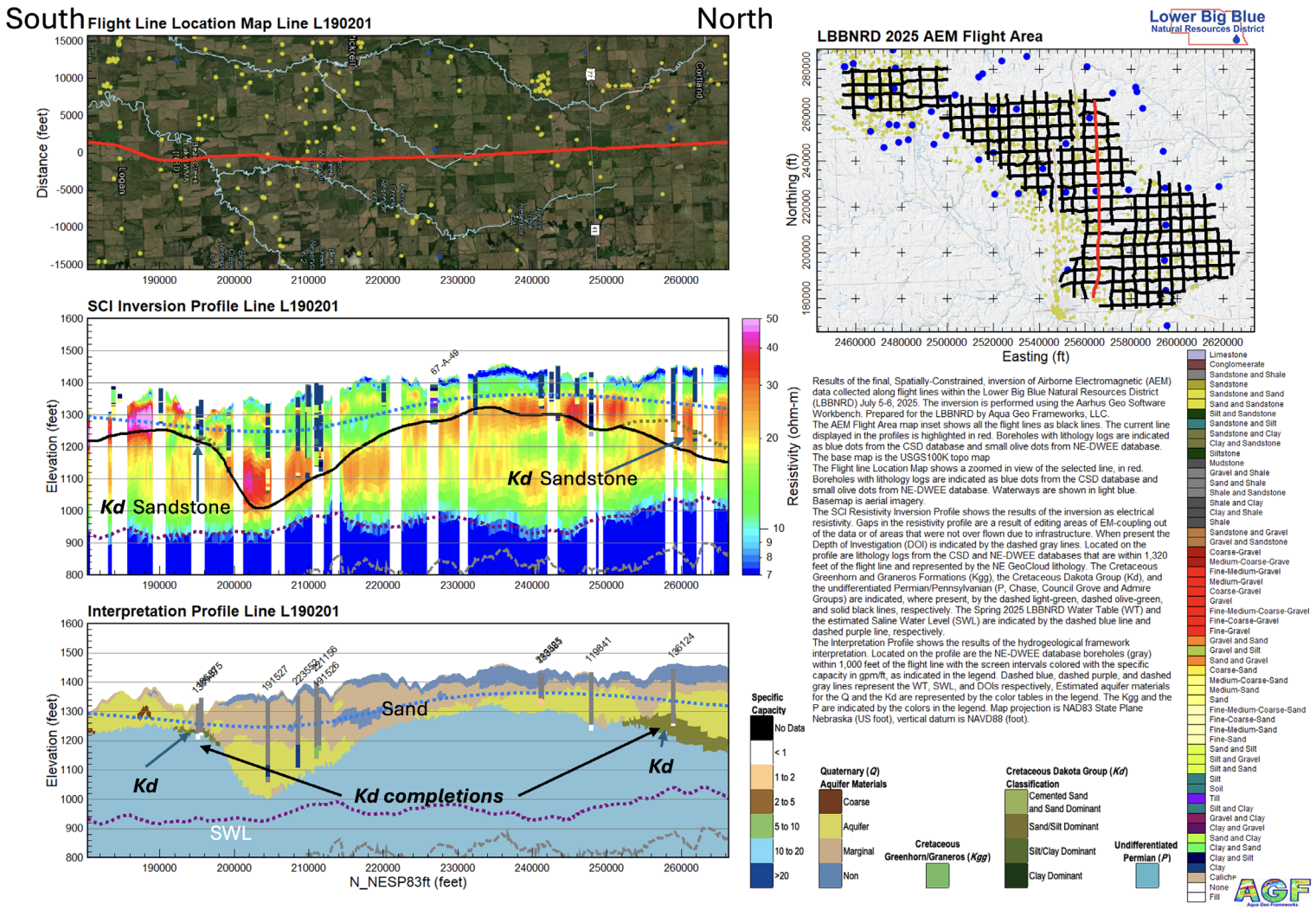


Figure 5-62. North-south AEM flight line L190201. A location map is on the upper right. On the left the top profile shows the air photo along the flight line. The middle profile is the SCI resistivity inversion result showing borehole lithologies and the bottom profile is an interpretative section showing the undifferentiated Permian/Pennsylvanian (*P*), Cretaceous Dakota Group (*Kd*), underlying the Quaternary (*Q*) subdivided into interpreted aquifer materials. Boreholes in the bottom section indicate measured Specific Capacity. The LBBNRD 2025 Spring water table is indicated by the dashed blue line and the estimated saline water level is indicated by the dash purple line.

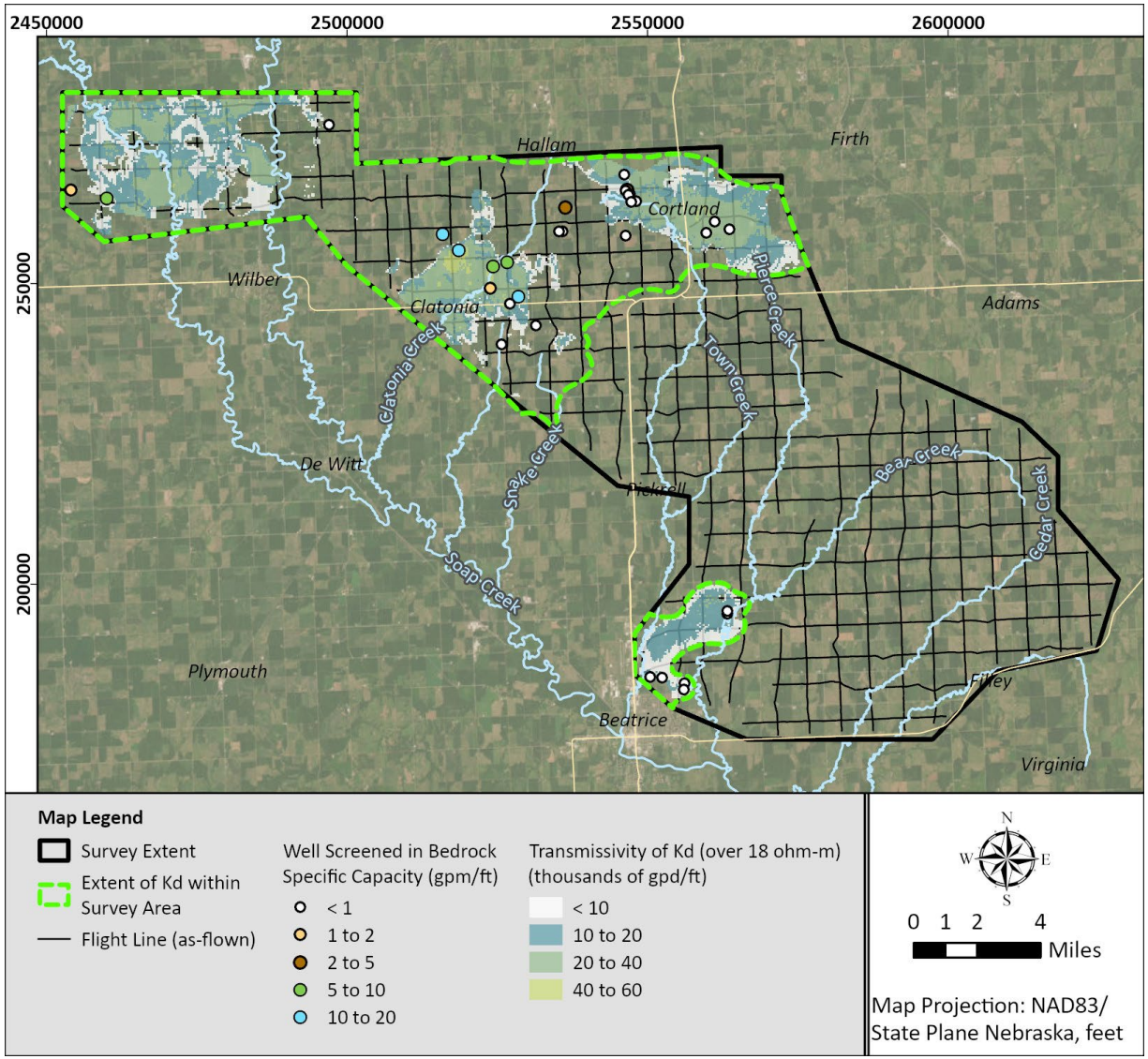


Figure 5-63. Map of the estimated transmissivity (gpd/feet) of the Cretaceous Dakota Group (*Kd*) saturated thickness of the sandstone and sand dominant materials with resistivities > 18 ohm-m within the LBBNRD 2025 AEM survey area. Specific capacity values from the NE-DWEE registered well database for wells screen in the Kd are shown as indicated by the legend.

5.3.3 The Permian/Pennsylvanian Bedrock Hydrology

The Permian bedrock is made up of the Permian Chase Group (***Pc***) and Permian Council Grove Group (***Pcg***), and the Permian Admire Group (***Pa***) which underlies the ***Kd*** (when present) and the ***Q.*** These units are considered aquicludes in this area. There is some use of the fractured limestone within the southern area of Nebraska as an aquifer, but that is not common, and the fractures need to be in hydrogeological connection to a water source, typically a stream or a good aquifer in the ***Q***. Within the survey area there are several wells that are dually completed in both Q and bedrock units (Figure 5-64). Six of these wells that have SC values are within the ***P***, one within the ***Kd,*** and one in the ***Kgg***. For the wells dually completed within the ***P***, it is doubtful that they are producing from the ***P*** but may be serving as a sump for the well and the flow is along the ***Q***/***P*** boundary. For the ***Kd*** well, it is likely that they are also producing some water in the ***Q*** and ***Kd***. For the ***Kgg*** well, again it is doubtful that they are producing from the ***Kgg***; the completion is likely through the ***Kgg*** into the ***Kd***

5.3.4 Groundwater in LBBNRD 2025 AEM Survey Area

As discussed above, the groundwater within LBBNRD 2025 AEM survey area is within the limited alluvial sediments of the present streams, glacial sediments, paleochannel, and paleovalley sediments of the Quaternary (***Q***). There is also groundwater in the fluvial and deltaic sediments of the Cretaceous Dakota Group (***Kd***). The groundwater availability is governed by both the ***Q*** and ***Kd.*** In the western portion of the survey area, the ***Q*** overlies the ***Kd*** and is in hydrogeological connection with the ***Kd***. In general, the ***Q*** groundwater is within paleochannel/paleovalley sediments on the north and the east-west paleovalley covered by outwash sediments in the center with lower yields, and the ***Kd*** groundwater is in the sandstone and sand deposits of the fluvial deposits. Limited wells show completions in both the ***Q*** and the ***Kd***.

Figure 5-65 shows the NE-DWEE specific capacities (SC) of the wells completed within the ***Q*** on the estimated transmissivity (T) of the ***Q*** aquifers. The distribution of the wells with SC data are clearly correlated to the higher T areas. Figure 5-66 shows the NE-DWEE specific capacities (SC) of the wells completed within the ***Kd*** > 18 ohm-m Sandstone/Sand Dominant on the estimated transmissivity (T) of the ***Kd*** aquifers. The distribution of the wells with SC data are clearly correlated to the higher T areas within the ***Kd***.

As was discussed in Section 5.2.2, the calculation of the T is governed by the selection of hydraulic conductivity and the saturated thickness of the unit. Inspecting 3D voxel images of the area can provide more clarification on the location of the wells and the SC in relation to the aquifer materials.

Figure 5-67 is a view from the south looking to the north of the aquifer and coarse aquifer material of the ***Q*** and the > 18 ohm-m sand dominant ***Kd*** with the specific capacity SC (gpm/ft) displayed as sized and colored disks. This figure shows the higher specific capacity wells along the paleovalley aquifer. Note the area displaying no aquifer material (transparent zones), are mostly marginal and non-aquifer material of the ***Q*** as well as the silt and clay dominant materials of the ***Kd***.

One inconsistency that we have observed is on the eastern end of the east-west paleovalley aquifer. The AEM maps moderate resistivities in the paleovalley but there are a few wells that indicate good SC.

Figure 5-68 is of the north-south profile of line L190291, showing the interpretation and the resistivity. The threshold of the aquifer materials is >20 ohm-m; however, the resistivities shown in this area are more on the scale of 17.6 ohm-m. An additional profile was added that shows all the material > 17.5 ohm-m. This encompasses more of the area that the wells indicate good SC. The potential causes of this under estimation of the aquifer materials is as follows: 1) the threshold is too high; 2) the AEM model is not resolving the resistivity under the low resistivity materials above the sands, ultimately smoothing out the resistivity response; 3) the sands are irregular and spatially variable and are not adequately sampled by the line spacing, and 4) the calculated SC values are not indicative of the well performance. It is likely be a combination of factors that is leading to the lower bulk resistivity. The fact is this area is not indicating a large area of resistive materials as compared to other areas of the paleovalley with similar overlying fine grained materials. Looking at the adjacent project area immediately east within the Nemaha Natural Resources District (NNRD). The NNRD paleovalley also indicates low resistivity/fine grained materials (AGF, 2024b). Figure 5-69 is a 3D Fence diagram looking to the west from the NNRD of the paleovalley toward the 2025 and 2024 LBBNRD (AGF, 2025) AEM survey results.

The results of the LBBNRD 2025 survey do match well with the surrounding data sets. Figure 5-70 is a plot of the bedrock elevation of the LBBNRD 2025 survey area combined with the 2024 LBBNRD (AGF, 2025) NNRD (AGF, 2024b) and the Lower Platte South Natural Resources District (LPSNRD) (Lower Platte River Sub-Regional Groundwater Model, in press). The paleovalleys are continuous and consistent across the surveys that were flown from 2007 to 2025. Figure 5-71 is a 3D fence look to the north of the LBBNRD 2025 survey area combined with the 2024 LBBNRD (AGF, 2025) NNRD (AGF, 2024b) including the Sprague and Firth portions of NNRD. The consistency of the interpreted aquifer materials can be observed across the multiple surveys.

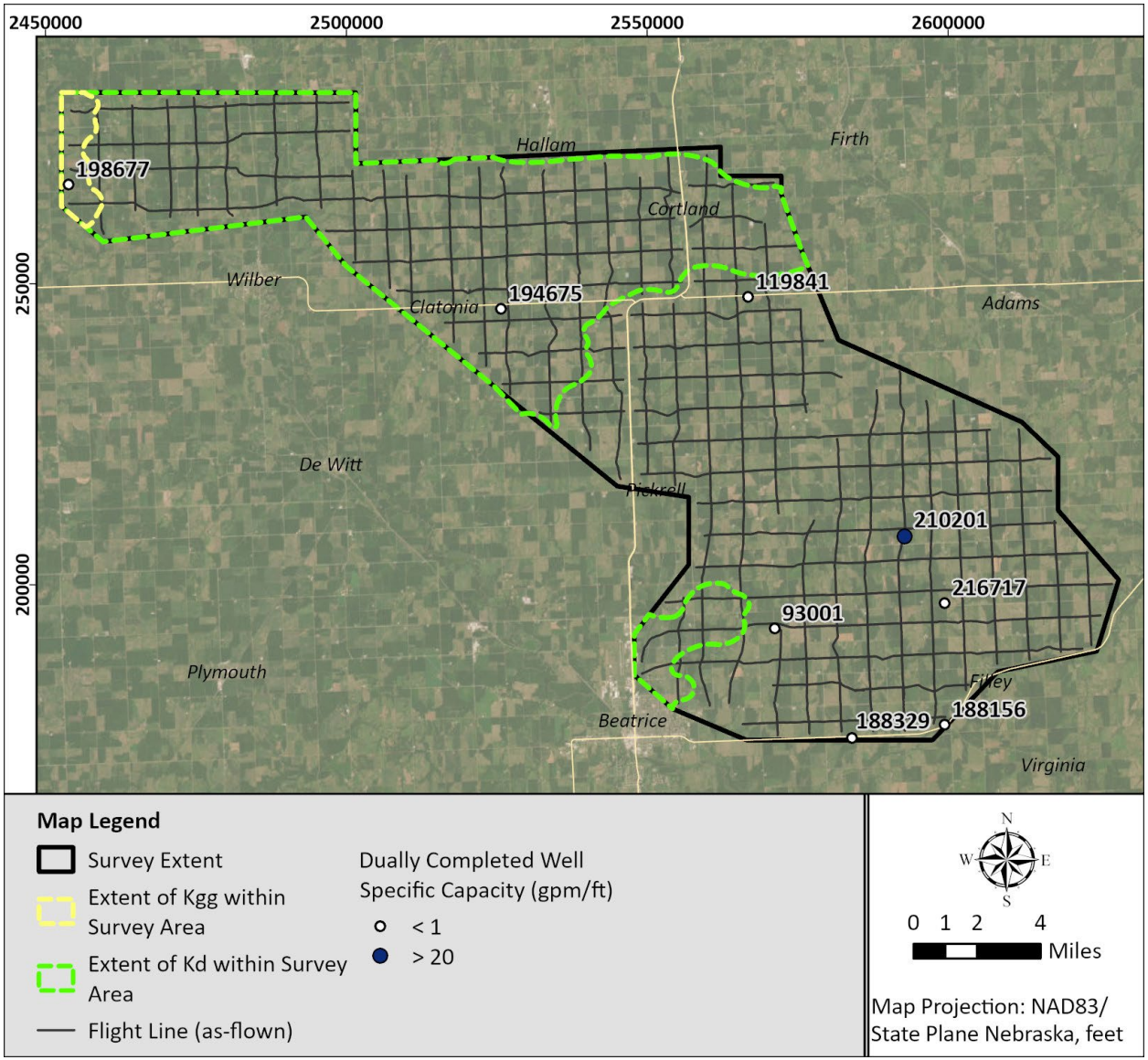


Figure 5-64. Map of the extent of the bedrock units (Cretaceous Greenhorn/Graneros (*Kgg*), Cretaceous Dakota Group (*Kd*), Undifferentiated Permian/Pennsylvanian (*P*) and the NE-DWEE wells that are dually completed in the Quaternary (*Q*) and the bedrock units.

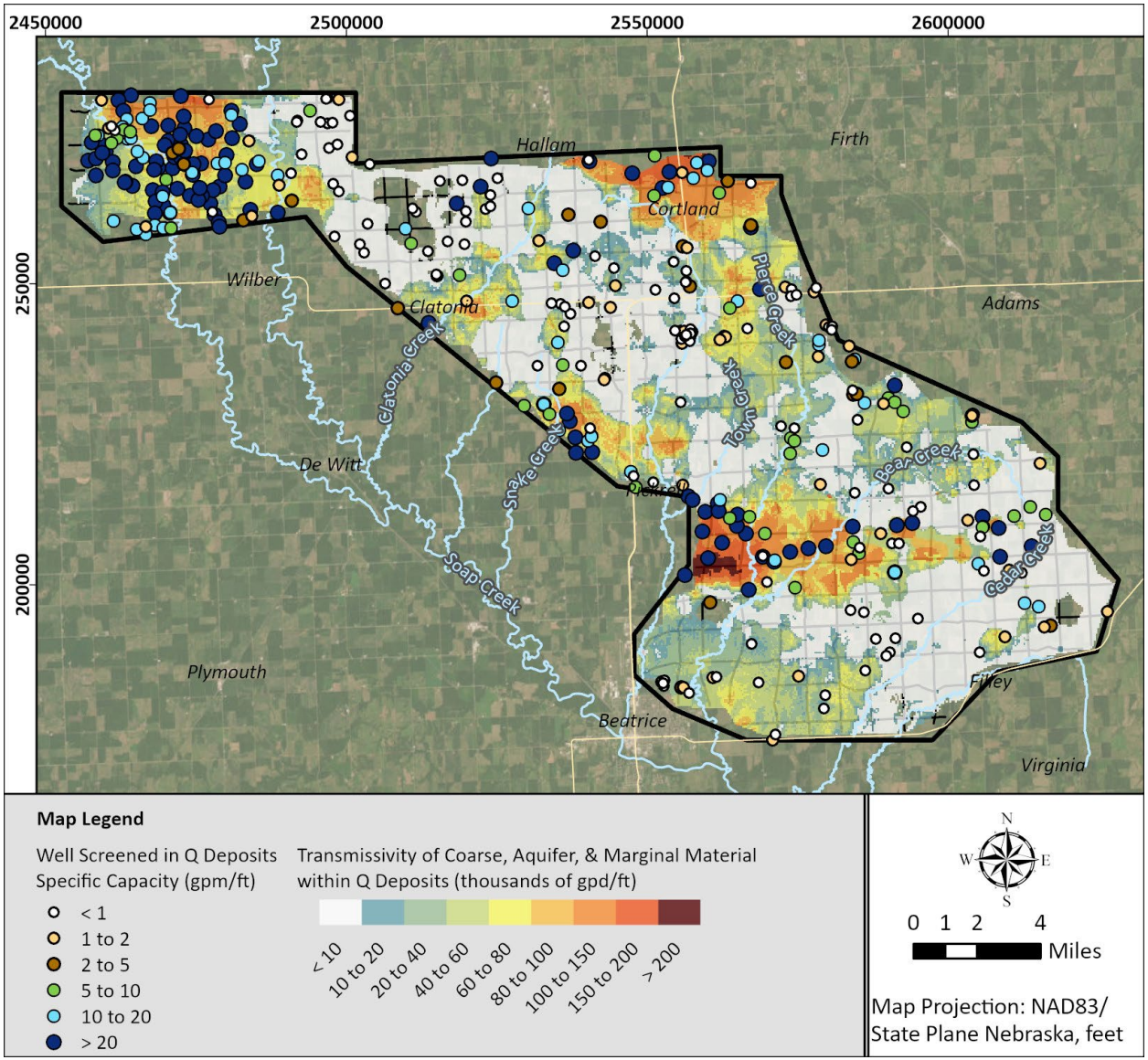


Figure 5-65. Map of the estimated Transmissivity (T) (gpd/ft) of the Quaternary (*Q*) coarse, aquifer, and marginal aquifer materials with the Specific Capacity (SC) of the NE-DWEE registered wells completed within the *Q*.

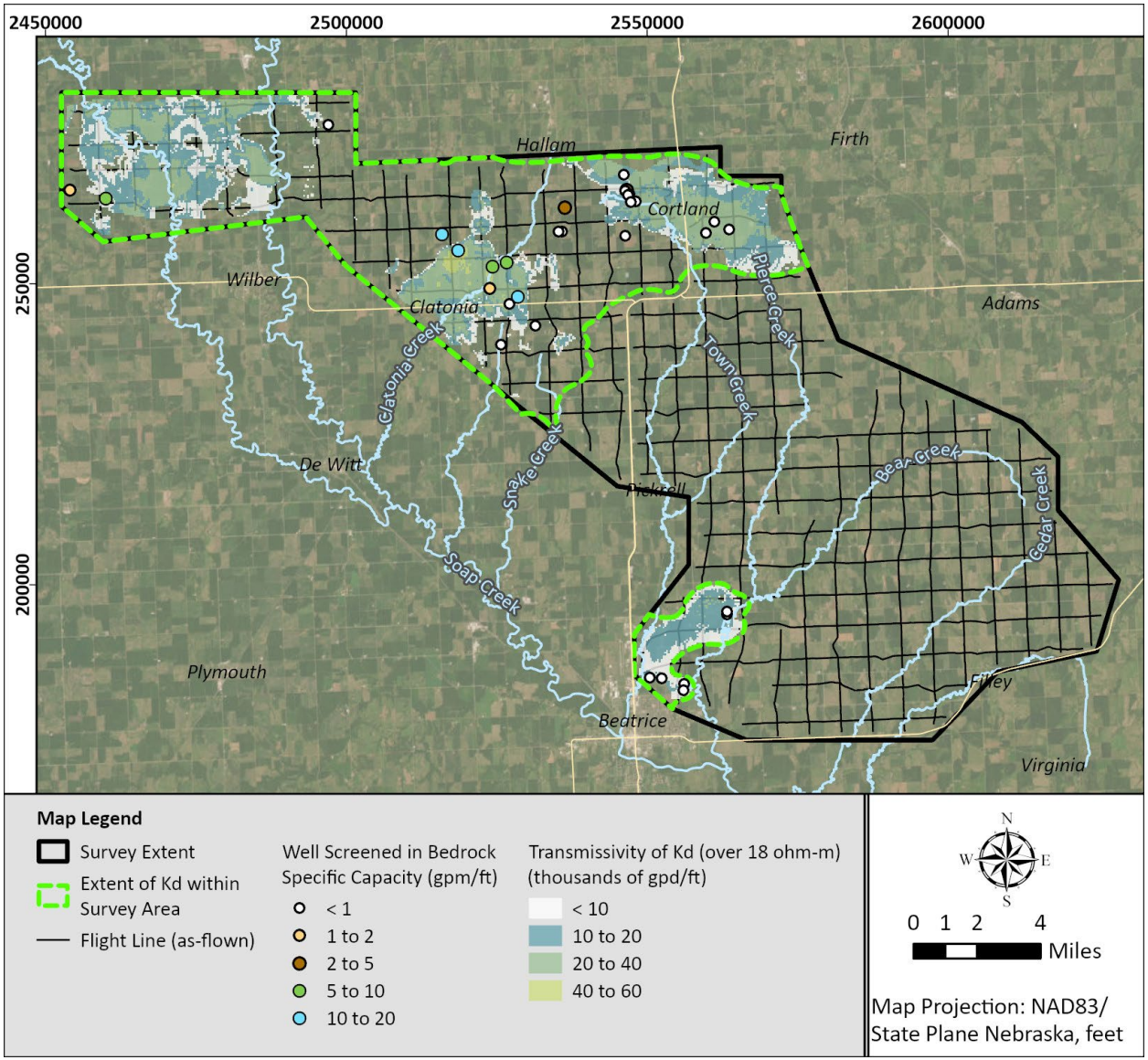


Figure 5-66. Map of the saturated Transmissivity (T) (gpd/ft) Cretaceous Dakota Group (*Kd*) with resistivities >18 ohm-m cemented sand and sand dominant with the Specific Capacity (SC) of the NE-DWEE registered wells completed within the *Q* and *Kd*.

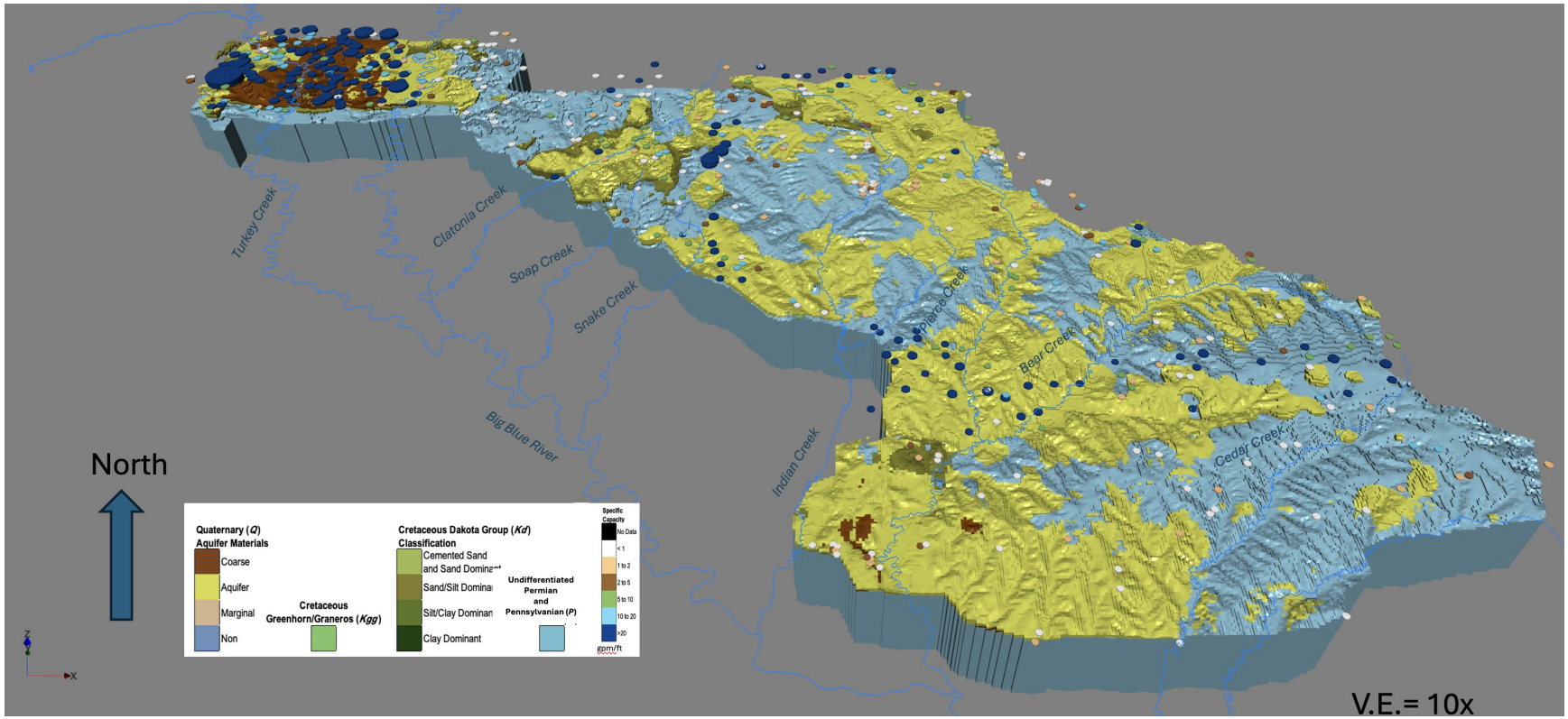


Figure 5-67. 3D voxel model of the saturated Quaternary (*Q*) coarse and aquifer materials plus the saturated Cretaceous Dakota Group (*Kd*) with resistivities > 18 ohm-m cemented sand and sand dominant material with the Specific Capacity (SC) of the all NE-DWEE registered wells completed within the area. V.E. =10x.

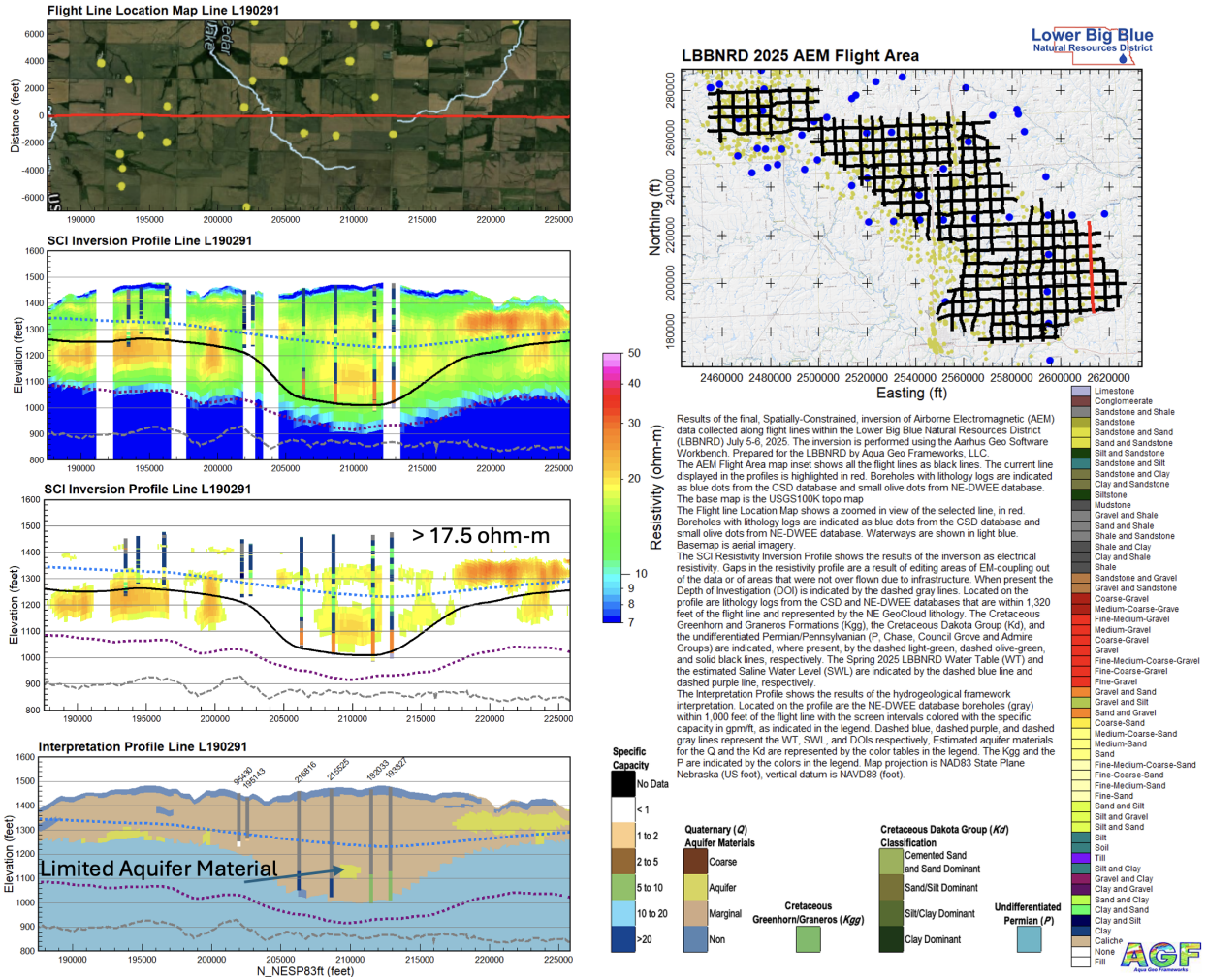


Figure 5-68. North-south AEM flight line L190291. A location map is on the upper right. On the left the top profile shows the air photo along the flight line. The second from the top profile is the SCI resistivity inversion result showing borehole lithologies, the third from the top profile is a thresholded view of material > 17.5 ohm-m. and the bottom profile is an interpretative section showing the undifferentiated Permian/Pennsylvanian (*P*), Cretaceous Dakota Group (*Kd*), underlying the Quaternary (*Q*) subdivided into interpreted aquifer materials. Boreholes in the bottom profile indicate measured Specific Capacity. The LBBNRD 2025 Spring water table is indicated by the dashed blue line and the estimated saline water level is indicated by the dash purple line.

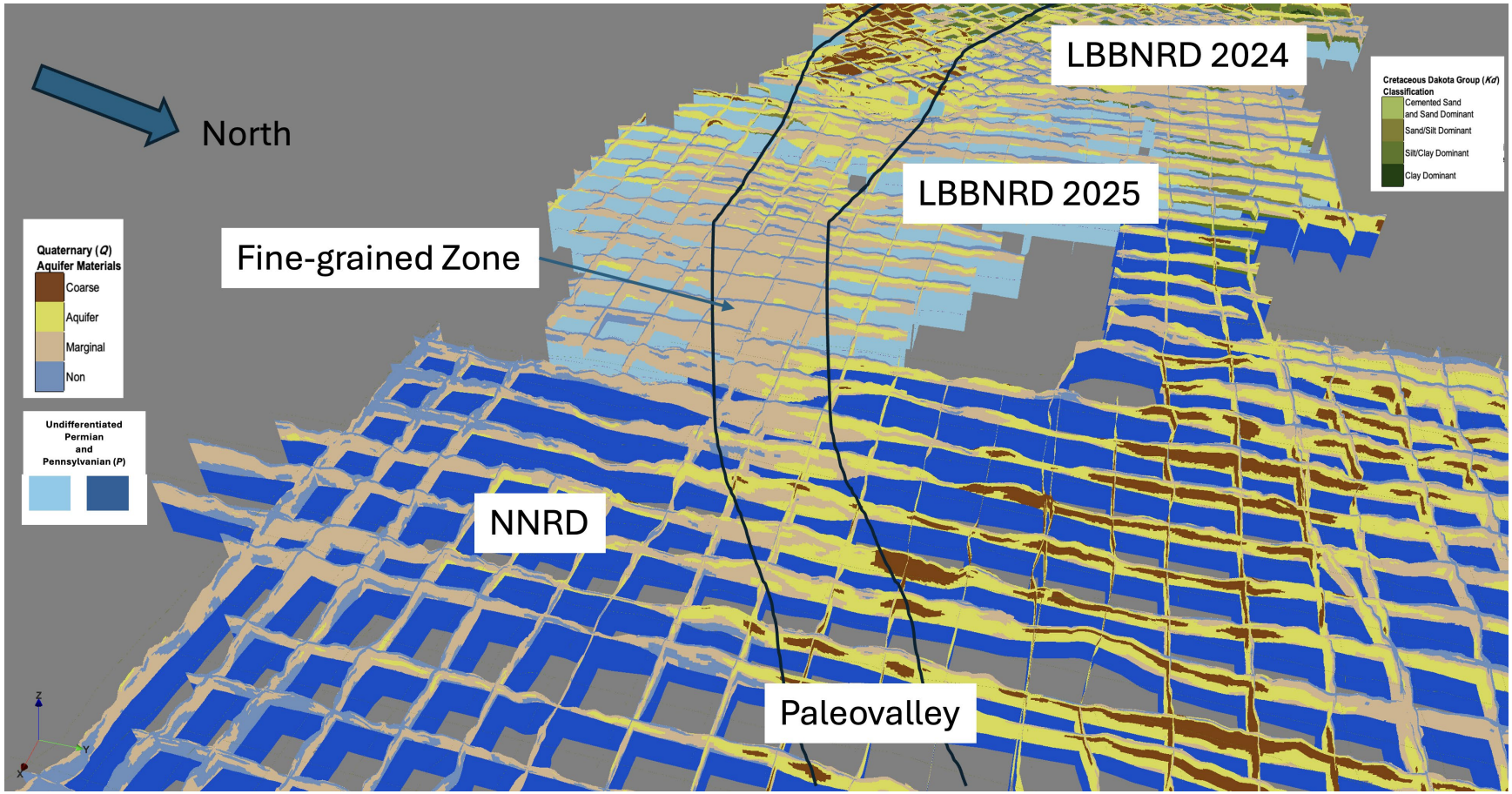


Figure 5-69. 3D Fence Diagram looking to the west of the interpreted distributions of aquifer material within the NNRD (AGF, 2024b), LBBNRD 2024 (AGF, 2025) and LBBNRD 2025 AEM survey area. V.E.=10x.

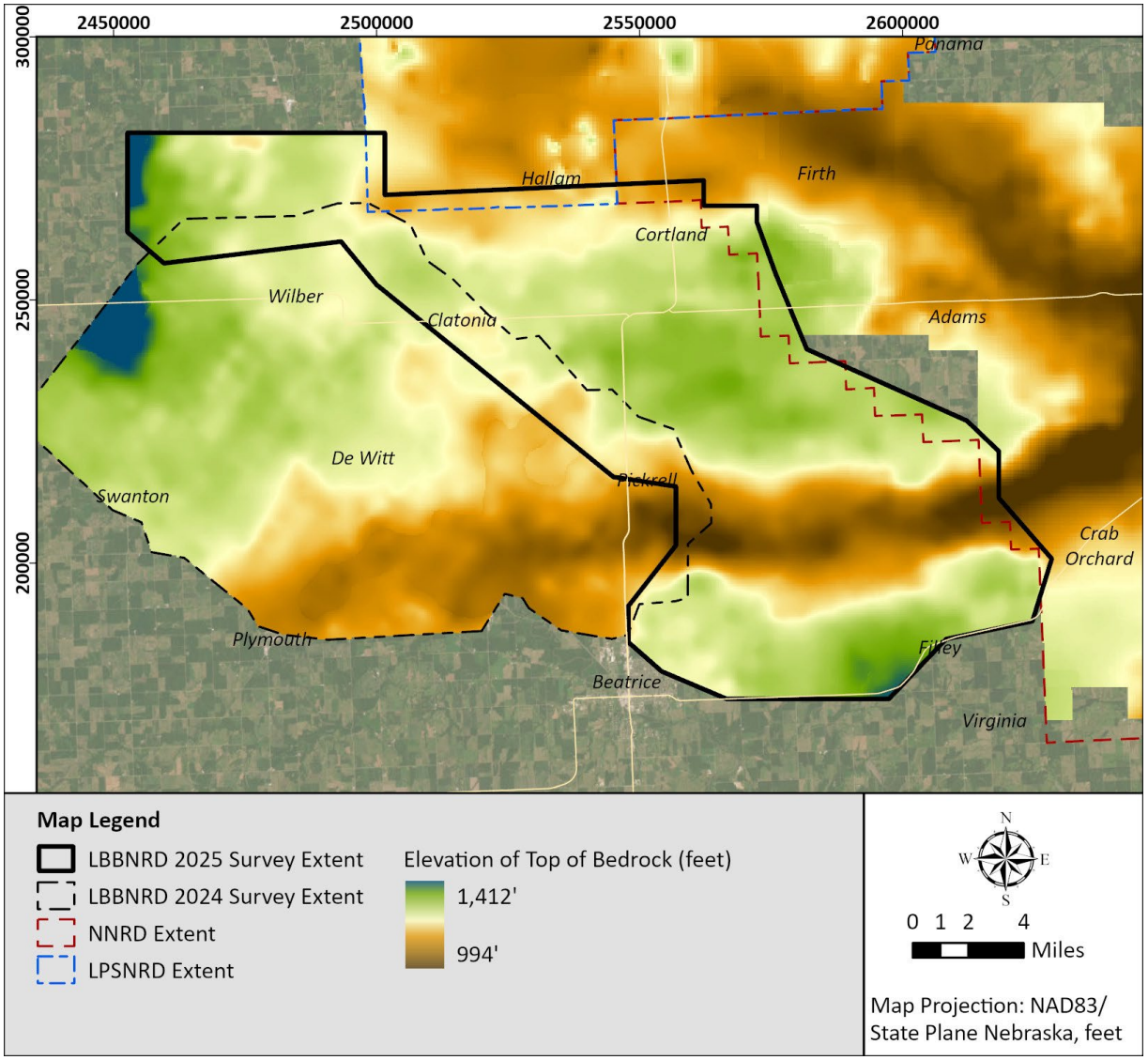


Figure 5-70. Map of the elevation of the bedrock in the area of the LBBNRD 2025 survey including the adjacent bedrock elevation surfaces from the 2024 LBBNRD (AGF, 2025), NNRD (AGF, 2024b) and the Lower Platte South Natural Resources District (LPSNRD) (Lower Platte River Sub-Regional Groundwater Model, in press).

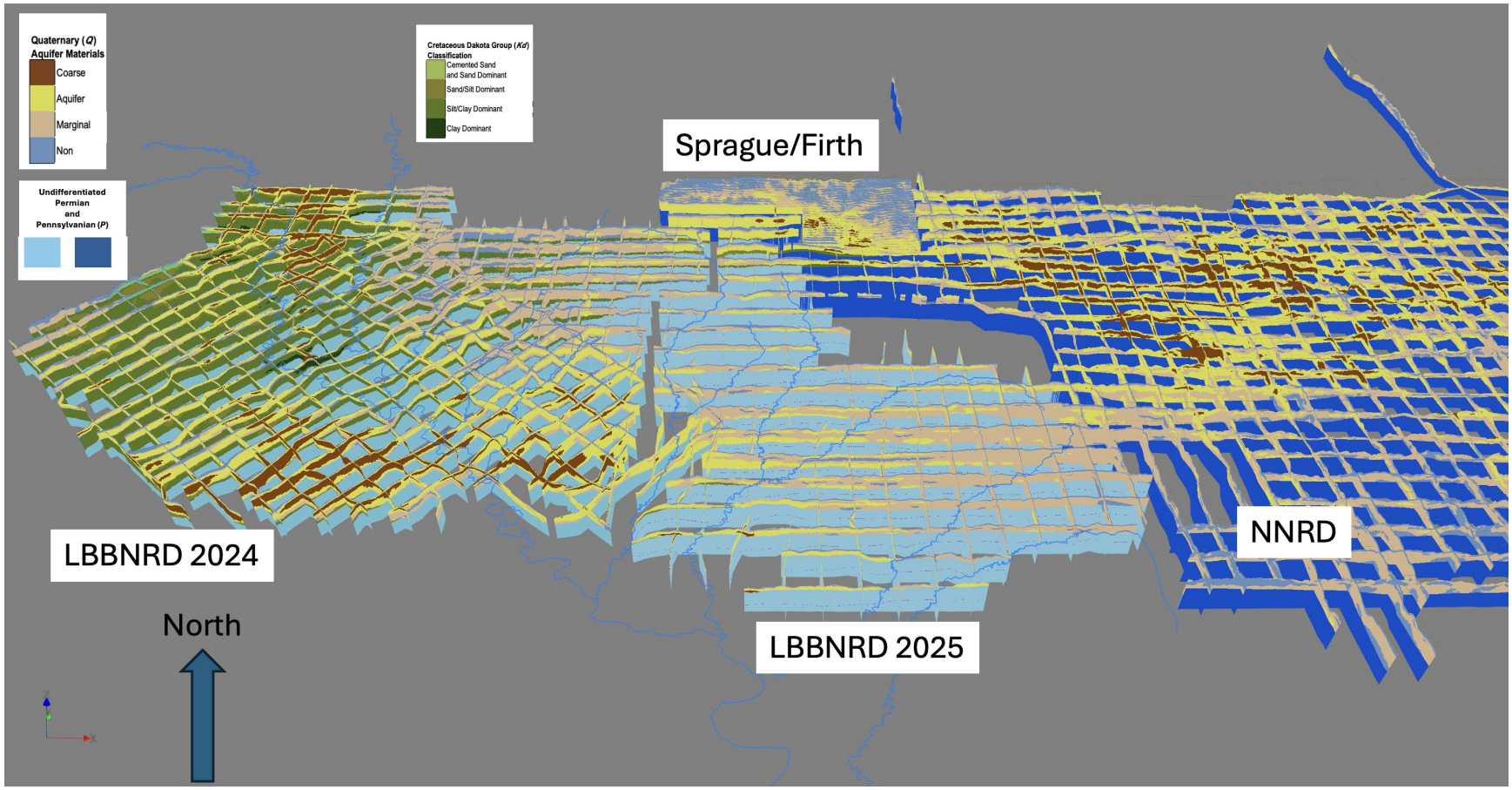


Figure 5-71. 3D Fence Diagram looking to the north of the interpreted distributions of aquifer material within the NNRD (AGF, 2024b), LBBNRD 2024 (AGF, 2025) and LBBNRD 2025 AEM survey area. V.E.=10x.

5.3.5 Estimation of Aquifer Volume/Water Storage for the 2025 LBBNRD AEM Survey Area

Three-dimensional digital representation of the subsurface resulting from the AEM method provides users the ability to estimate total unsaturated and saturated aquifer volume and the amount of extractable water more accurately. An area of approximately 254.51 square miles (approximately 162,884.51 acres) of AEM data were collected in the LBBNRD 2025 AEM survey as shown by the map of 'as flown' flight lines in Figure 1-2.

The criteria for determining the basis of the range of resistivity values used in calculating the volumes of interpreted aquifer material for both ***Q*** and ***Kd*** are provided in Section 5.2. The resistivity ranges for ***Q*** interpreted non-aquifer, marginal aquifer, aquifer, and coarse aquifer materials are also found in Section 5.2.1. The resistivity ranges for the ***Kd*** include clay dominant, silt/clay dominant, sand/silt dominant, and cemented sand and sand dominant materials are also found in Section 5.2.2. The mapped deposits of the ***Q*** and ***Kd*** provide information from which the volumes of selected aquifer materials combined with estimated average values for porosity and specific yield are the best estimates for calculation of aquifer volume in acre/ft, groundwater in storage in acre-ft, and extractable water in acre-ft. The area beneath the survey area included in these calculations and represented in Figure 1-2 were created in Datamine PA explorer, version 2025, Release Build 20.0.40 (Datamine Discover, 2026).

All aquifer materials including non-aquifer material, marginal aquifer material, aquifer material, and coarse aquifer material are used for calculating the groundwater in storage volume and the extractable water volumes for the survey area. Reported values of the average porosity for aquifer materials present are based on values from Freeze and Cherry (1979). Clay porosity ranges from 40%-70%, silt ranges from 35%-50%, sand ranges from 25%-50%, and gravel is from 25%-40%. Conservative estimates for the porosity values used in these calculations within the survey area are 40% for non-aquifer material, 35% for marginal aquifer material, 22% for the aquifer material, and 25% for the coarse aquifer material.

Specific yield values for all ***Q*** aquifer materials were selected by estimating values from Heath (1983). Specific yield for non-aquifer materials was chosen at 0.02 (Heath, 1983) and for marginal aquifer materials a value of 0.05 was selected (Heath, 1983). The specific yield value for aquifer material is 0.20 (Heath, 1983). While coarse aquifer materials exist as localized deposits in the survey area, estimates of specific yield for the coarse aquifer material is 0.19 (Heath, 1983). The aquifer and marginal aquifer materials represent the dominant material types by total volume for groundwater storage in the survey area. For specific yield, maps of the area would be improved if new maps were produced using this new AEM survey information plus the addition of aquifer tests or other methods of gaining new data including Nuclear Magnetic Resonance (NMR) surveys to capture aquifer characteristics including: mobile water, total porosity, and hydraulic conductivity.

All ***Kd*** aquifer materials including clay dominant, silt/clay dominant, sand/silt dominant, and cemented sand and sand dominant materials were used for calculating the groundwater in storage volume and the extractable water volumes for the survey area. Values for the ***Kd*** are problematic at best due to the limited reported values. Thus, information from Freeze and Cherry (1979), O'Conner (1987), Dominico

and Schwartz (1998), Fetter (1988), Gannon and Vogelgesang (2015), and Divine and Sibray (2017) was used to estimate volumes. These publications indicate that clay dominant porosity ranges from 35%-60%, clay/silt dominant material ranges from 35%-60%, sand/silt dominant material ranges from 25%-50%, and cemented sand and sand dominant material is from 5%-40%. The conservative estimates for the ***Kd*** porosity values used in these calculations within the survey area are 40% for Clay dominant material, 40% for clay/silt dominant material, 30% for the sand/silt material, and 35% for the cemented sand and sand dominant material.

Specific yield values for all ***Kd*** aquifer materials were selected by estimating values. Specific yield for clay dominant materials was chosen at 0.01 (Heath, 1983) and for clay/silt materials a value of 0.05 was selected (Heath, 1983). The specific yield for the sand/silt dominant is 0.08 (Heath, 1983). The specific yield for the cemented sand and sand dominant material is 0.10 (Heath, 1983). The aquifer and marginal aquifer materials represent the dominant material types by total volume for groundwater storage in the 2025 LBBNRD AEM survey area. For specific yield, maps of the area would be improved if new maps were produced using this new AEM survey information plus the addition of aquifer tests or other methods of gaining new data including Nuclear Magnetic Resonance (NMR) surveys to capture aquifer characteristics including: mobile water, total porosity, and hydraulic conductivity.

Table 5-5 shows the results of calculations of the amount of groundwater in storage calculated by volume of the saturated ***Q*** materials multiplied by the estimated porosity and estimated specific yield. 33% of the ***Q*** materials are saturated.

The values in the Table 5-5 are for the saturated (based on the LBBNRD Spring 2025 water table) ***Q*** aquifer (saturated) materials, and have a total volume of **14,460,190** acre-ft. The estimated volume of groundwater in storage for ***Q*** aquifer material is **4,507,005** acre-ft. The estimated extractable volume of groundwater in ***Q*** aquifer materials is **1,397,951** acre-ft.

There is only a small portion of the ***Kd*** that is unsaturated based on the LBBNRD 2025 Spring water table. The values in the Table 5-6 are for the saturated ***Kd*** materials and have a total volume of **7,213,844** acre-ft which is 100% of the total ***Kd***. The estimated volume of groundwater in storage for ***Kd*** is **2,749,752** acre-ft. The estimated extractable volume of groundwater in ***Kd*** aquifer materials is **400,208** acre-ft. Note that these numbers exclude some of the estimated saline waters.

A useful calculation would be combining the saturated ***Q*** and ***Kd*** of all materials. Again, this is using the LBBNRD Spring 2025 water table and the assumed values for the porosity and specific yield as discussed above for Table 5-5 and Table 5-6. The total estimated volume of the saturated ***Q*** and ***Kd*** aquifer materials is **21,674,033** acre-ft, which is 56.68 % of the total combined ***Q*** and ***Kd*** aquifer materials. The total groundwater in storage is **7,256,757** acre-ft. The total groundwater in storage is **1,798,159** acre-ft.

As stated above, these estimates are based on the water table map as calculated from the LBBNRD Spring 2025 water levels (Section 5.1.6). Also, these volumetric estimates consider only the volume of water assumed in the pore spaces of the aquifer material defined by the resistivity threshold levels and do not account for the possible “confined or semi-confined” water under pressure (head above the aquifer). Note that additional analysis of data for the confined, or semi-confined, areas of the AEM

survey area would need to be completed before any designation of these areas can be made. Aquifer testing may be the only way to confidently ascertain the confining condition of the overlying loess.

An estimate of the area that may be confined can be provided by looking at the unsaturated ***Q*** non-aquifer material and marginal aquifer material thicknesses (Figure 5-72). This volume of water would add to the values reported in Table 5-5 and Table 5-6. However, too much uncertainty exists in developing an average level of head above the top of the aquifer across the entire project area, as well as defining a representative storativity term for the confined or semi-confined aquifers. Thus, the volumes listed in Table 5-5 and Table 5-6 are conservative estimates and the amount released from the decline in pressure is not considered.

Table 5-5. Volumes for Saturated Quaternary (*Q*) aquifer materials underlying the LBBNRD 2025 AEM survey area.

Q Aqufer Material	Average Porosity	Average Specific yield	Aquifer Volume (ft3)	Aquifer Volume (Acre-Ft)	Groundwater Potential in Storage Volume (acre-ft)	Extractable Potential Water Volume (Acre-ft)
Coarse > 50 ohm-m	0.25	0.19	15,214,623,451	349,280	87320	66363
Aquifer 20-50 ohm-m	0.22	0.20	193,914,889,399	4,451,673	979368	890335
Marginal 12-20 ohm-m	0.35	0.05	368,846,715,149	8,467,555	2963644	423378
Non 0-12 ohm-m	0.40	0.02	51,909,652,238	1,191,682	476673	17875
			Totals:	**14,460,190**	**4,507,005**	**1,397,951**

Table 5-6. Volumes for Saturated Cretaceous Dakota Group (*Kd*) aquifer materials underlying the LBBNRD 2025 AEM survey area.

Kd Aqufer Material	Average Porosity	Average Specific yield	Aquifer Volume (ft3)	Aquifer Volume (Acre-Ft)	Groundwater Potential in Storage Volume (acre-ft)	Extractable Potential Water Volume (Acre-ft)
Cemented Sand and Sand Dominant >35 ohm-m	0.35	0.10	2,429,922,656	55,783	19524	5578
Sand/Silt Dominant 35-18 ohm-m	0.3	0.08	57,933,307,422	1,329,966	398990	106397
Silt/Clay Dominant 18-3 ohm-m	0.4	0.05	250,417,365,990	5,748,792	2299517	287440
Clay Dominant < 3 ohm-m	0.4	0.01	3,454,432,155	79,303	31721	793
			Totals:	**7,213,844**	**2,749,752**	**400,208**

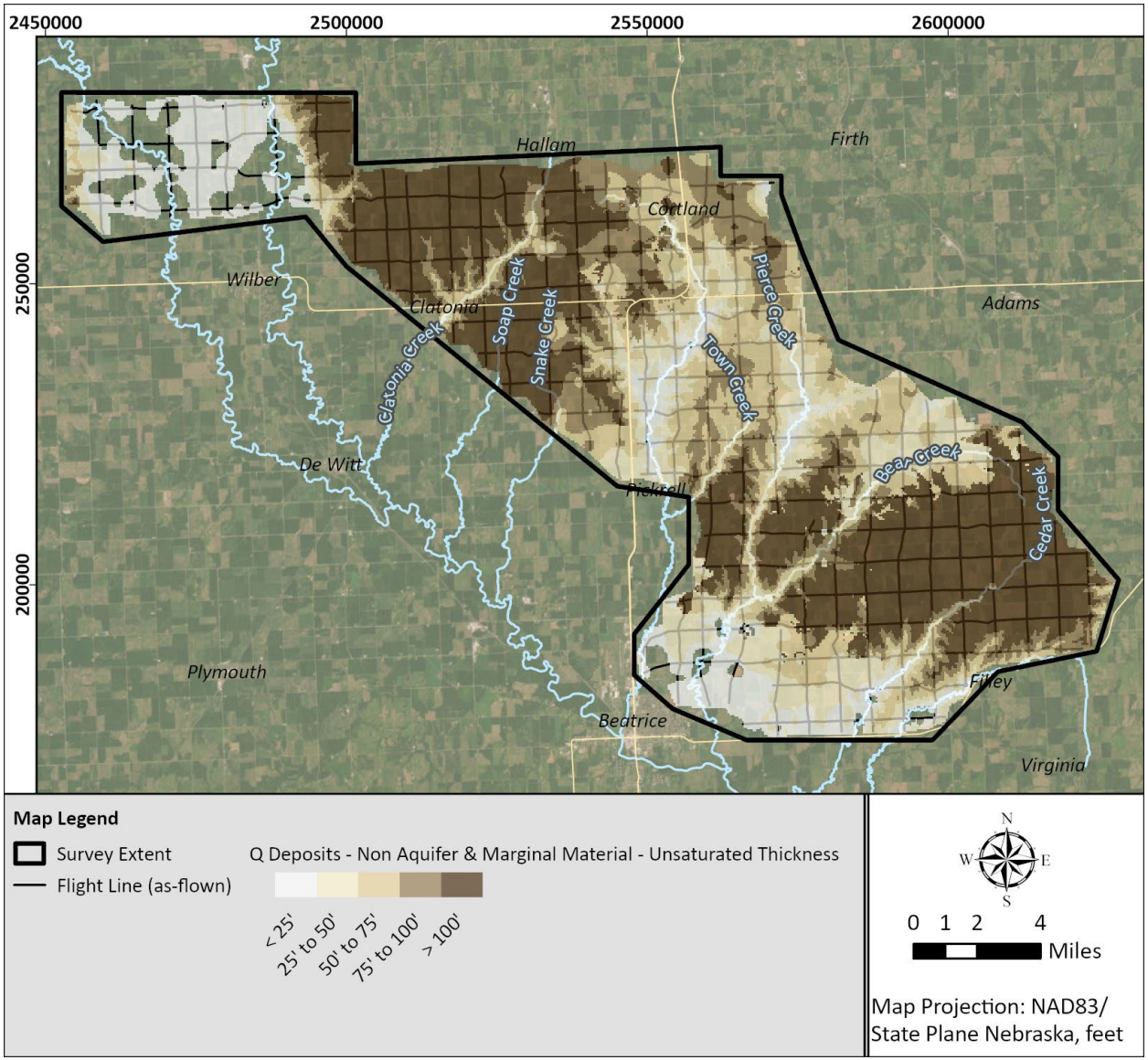


Figure 5-72. Map of the Non- and Marginal-Aquifer materials within the unsaturated portion of the Quaternary (*Q*) potentially creating a confined aquifer beneath.

5.3.6 Groundwater Quality in the LBBNRD 2025 AEM Survey Area

The primary contaminants of concern throughout the LBBNRD are nitrates. As such, the LBBNRD annually samples dedicated monitoring wells and registered irrigation wells for nitrate analysis. The AEM provided information on the near surface materials in the LBBNRD AEM survey area. Near surface occurrences of sandy soils and sand deposits (aquifer materials) provide conduits for contaminants to migrate into the groundwater.

Using the 3D interpretation of the AEM, a near surface occurrence of the aquifer materials map can be generated. Using the water quality data collected by the LBBNRD (Personal Communication, Tyler Weishahn, January 2025), the data was overlain on the aquifer material map of the unsaturated non- and marginal aquifer material. Illustrated in Figure 5-73 is the correlation of nitrate samples and the areas of the non- and marginal aquifer. There is a correlation with some of the sample locations to the areas in the northwest of the survey area in the areas on missing or areas of < 25 feet of non- and marginal aquifer materials. These would be areas of thinner clay layers. However, there is a weak to no correlation in many of the other areas of the survey in Figure 5-73.

Additionally, when the thickness of the unsaturated coarse- and aquifer-materials are plotted with the nitrate values (Figure 5-74), a correlation to some of the locations in the northwestern area can be seen with near surface coarse and aquifer materials. There is a weak correlation in the rest of the survey area. The nitrates distribution in the area is controlled by several factors. It is not just controlled on the surface materials and may also be related to groundwater flow.

As discussed in the interpretation of the AEM, within the ***Kd*** and the ***P*** units of the LBBNRD 2025 AEM survey area a low resistivity layer of < 7 ohm-m is interpreted as a regional saline water interface. The interface is shallow in the center of the survey area near the Big Blue River and areas of Turkey Creek in the northwestern part of the survey. The shallowest area is 142 feet. These areas would need to be confirmed with water quality sampling but there is a high probability that these areas contain saline waters. Clay layers can impact this estimation due to the similar resistivity values. It is also possible that the saline water is at the level of a clay layer and that the clay layer is impeding the upward migration of the deeper saline waters. Care would need to be exercised in drilling to not penetrate any confining clay layers. Figure 5-75 is a map of the depth of the estimated saline waters. The area of shallow saline water is seen in the center of the survey area with the deepest areas up to 560 feet.

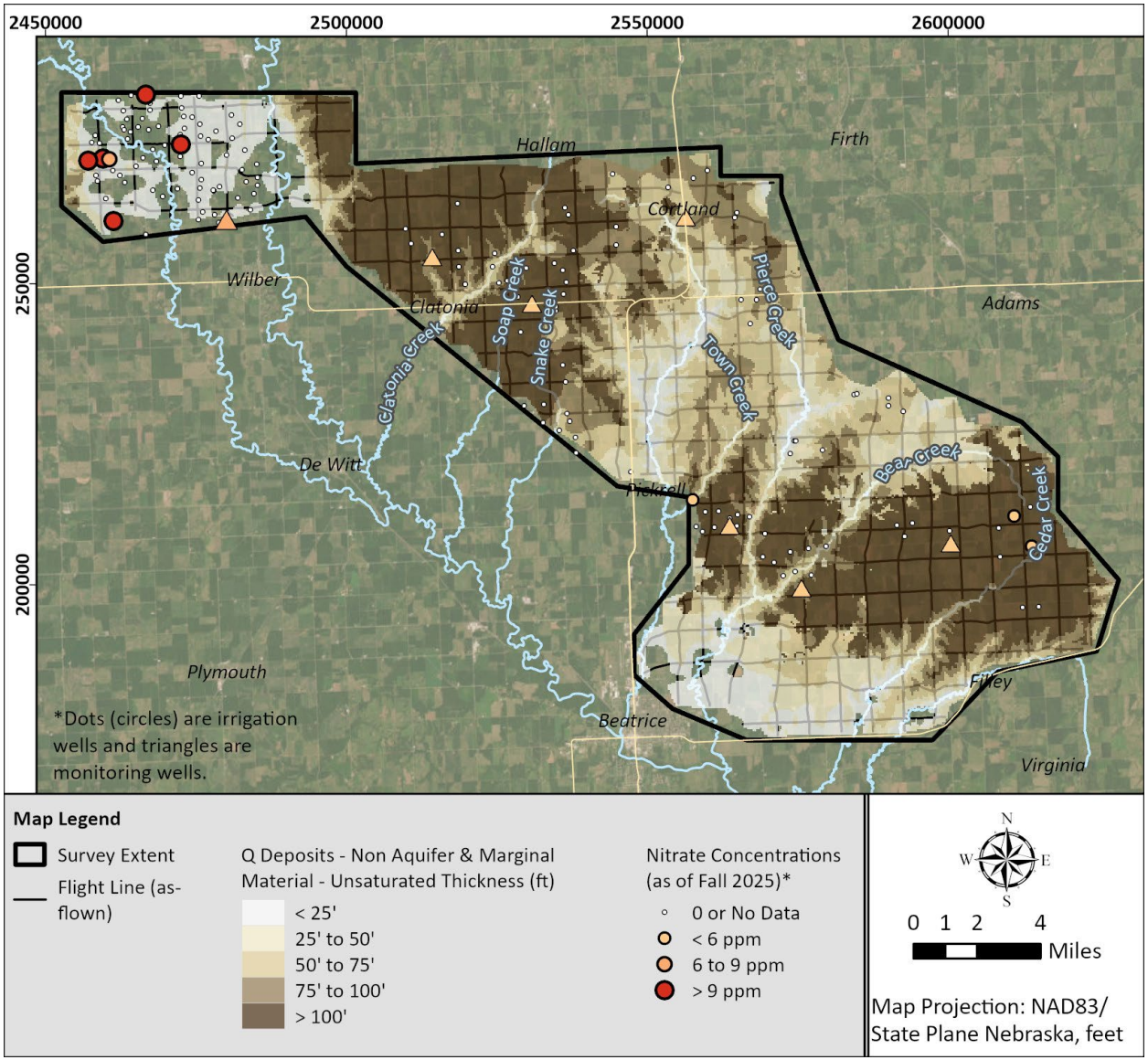


Figure 5-73. Map of the thickness of the unsaturated non- and marginal-aquifer material and the LBBNRD nitrate samples.

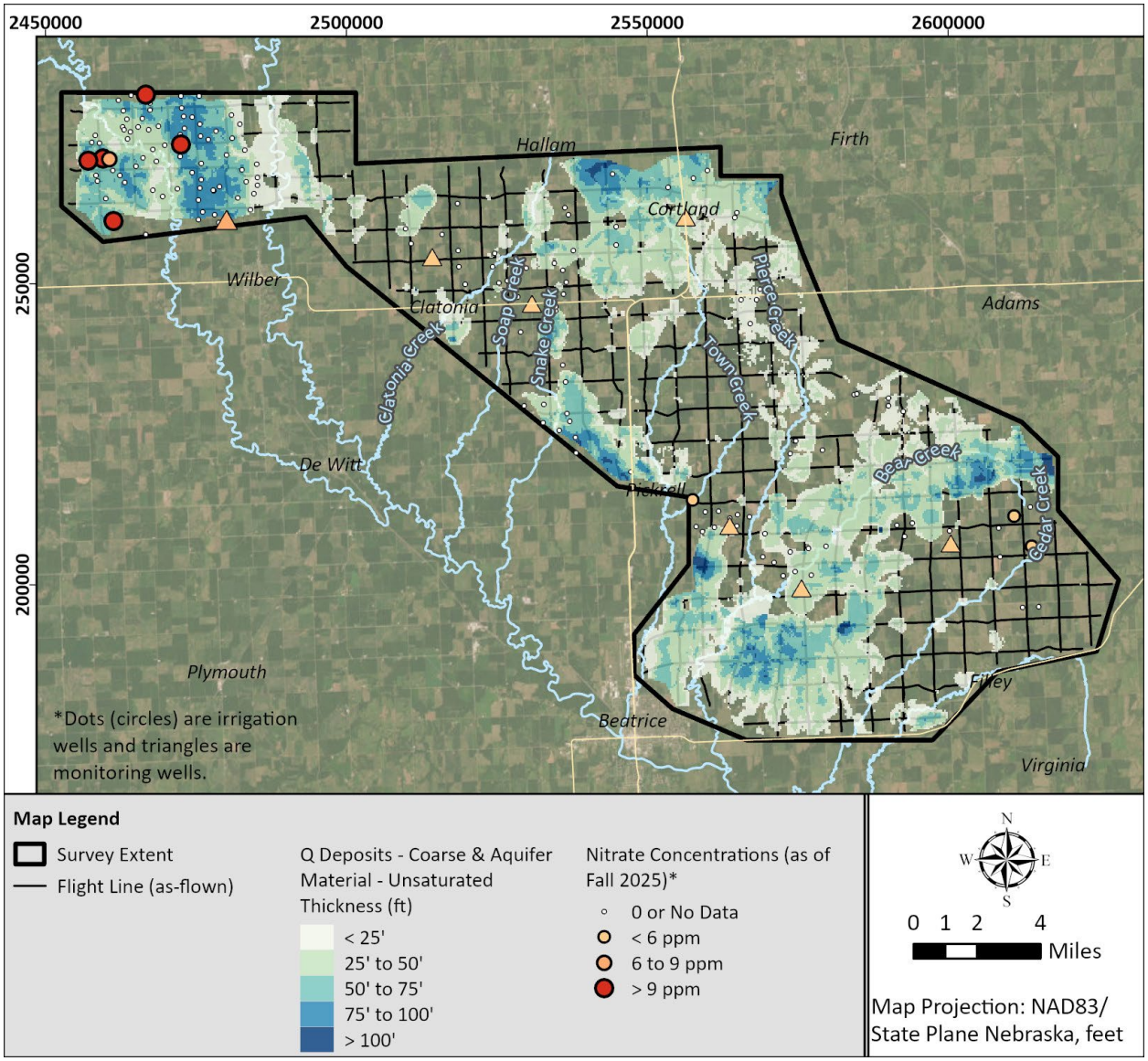


Figure 5-74. Map of the thickness of the unsaturated coarse- and aquifer-material and the LBBNRD nitrate samples.

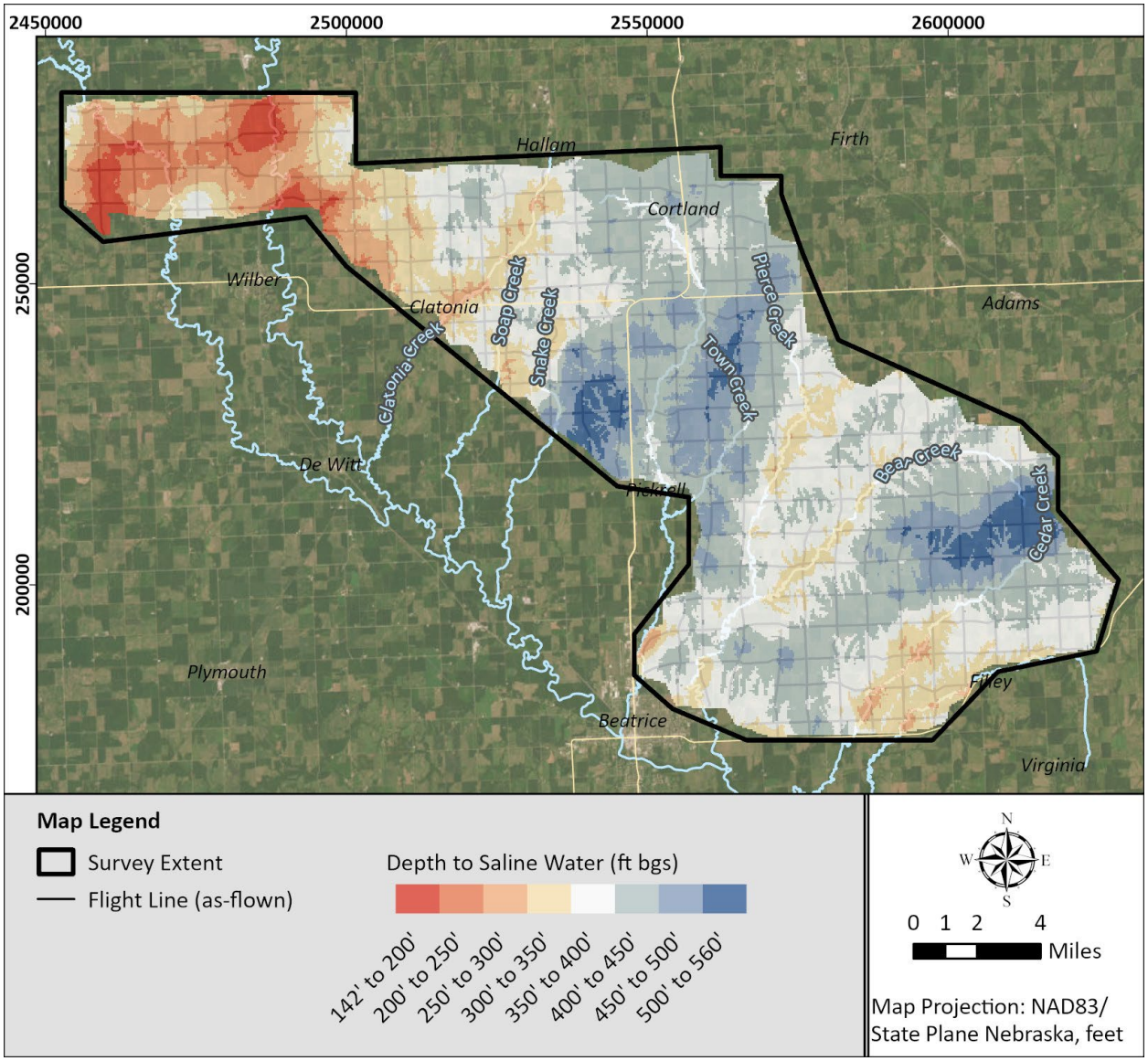


Figure 5-75. Map of the depth to the estimated saline water based on the < 7 ohm-m cutoff.

5.3.7 Recharge in ***the LBBNRD 2025 AEM Survey Area***

An important question that is required to be assessed in any groundwater availability study is the location of recharge sites. The AEM has the unique ability to map the near-surface aquifer materials as indicated above to help determine potential areas of recharge.

Using a similar approach to what was utilized in the water quality section (Section 5.3.6), near surface ***Q*** materials composed of coarse and aquifer material were mapped using the following criteria: 1) Greater than 6 feet thickness of coarse and aquifer material; 2) The top of the coarse and aquifer material is less than or equal to 3 feet below the ground surface; and 3) There is greater than 10 feet of depth between the top of the coarse and aquifer material and the top of the bedrock. These criteria are based on the idea that a recharge area within the survey area would require relatively thick coarse and aquifer material close to ground surface, with bedrock deep enough to allow for water to recharge to depth.

Figure 5-76 is the map of the thickness of the coarse and aquifer material that meet those criteria. Many of these areas are along the stream where the till and loess have been eroded away exposing the deeper coarse and aquifer material. One area of caution that needs to be observed is the high topography feature between the Big Blue River and Turkey Creek. This area may be difficult to use as a recharge site. Figure 5-77 is a 3D voxel plot of the near-surface aquifer materials.

Examining the profiles can help to understand the 3D connections of the near-surface materials to the deeper aquifer. Figure 5-78 is an east-west profile of line L100011. Areas of potential recharge exist along this profile near Turkey Creek that have coarse and aquifer materiel that is currently unsaturated and surface exposure. A recharge area target map has been developed to help identify areas that could be investigated in the future for recharge locations (Figure 5-79).

Utilizing the above maps to target recharge areas can be done. However, it is imperative that accurate test holes are used to assess the geological materials which may include sonic cores. Any possible thin clay layers that were not detected with the AEM or may have been missed in the test hole drilling may be detected by calibrated borehole geophysical induction logs. Infiltration tests also need to be conducted to fully evaluate recharge rates.

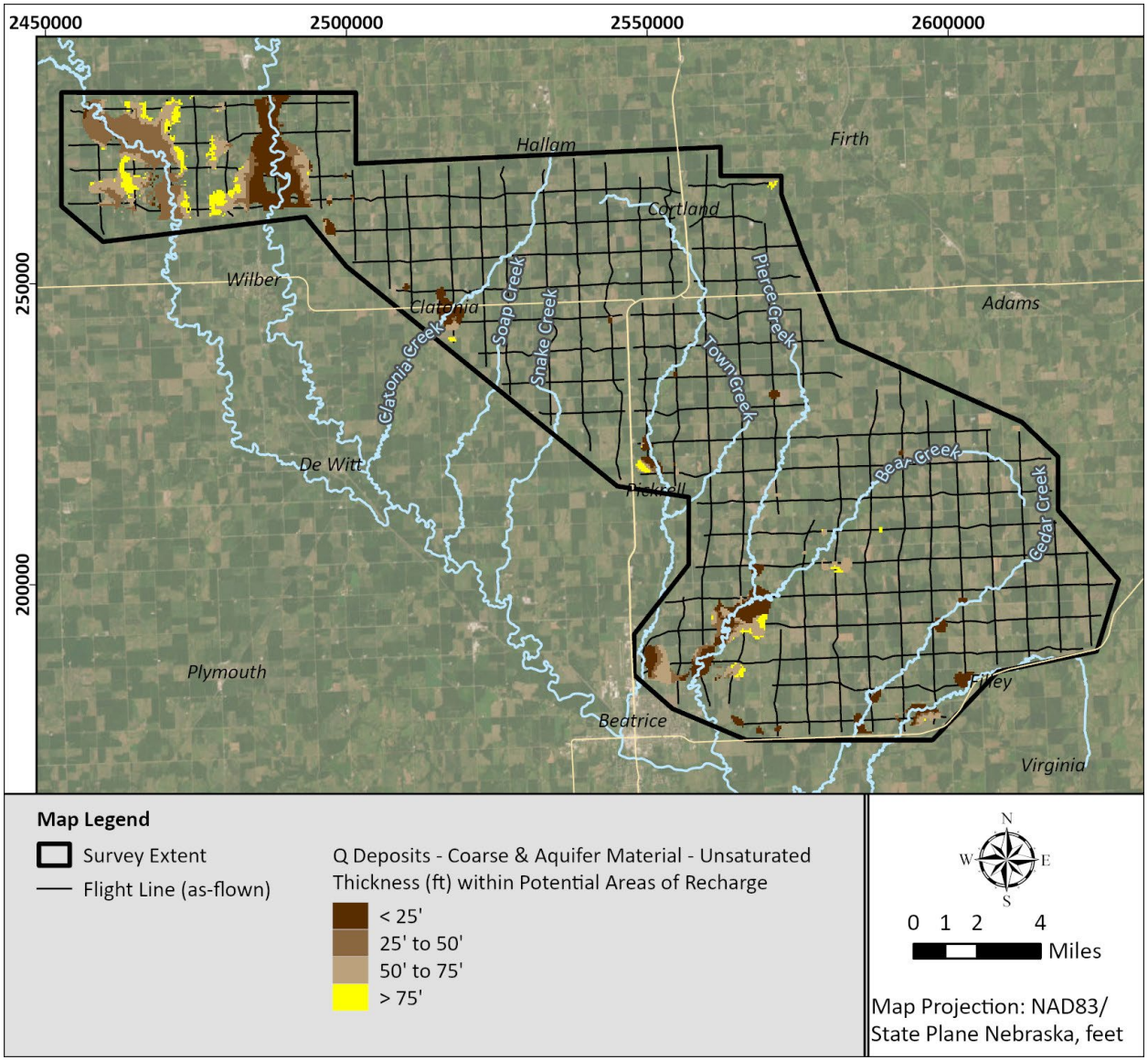


Figure 5-76. Map of the thickness of the unsaturated coarse and aquifer material that is in the near surface that may provide recharge pathway to lower aquifers.

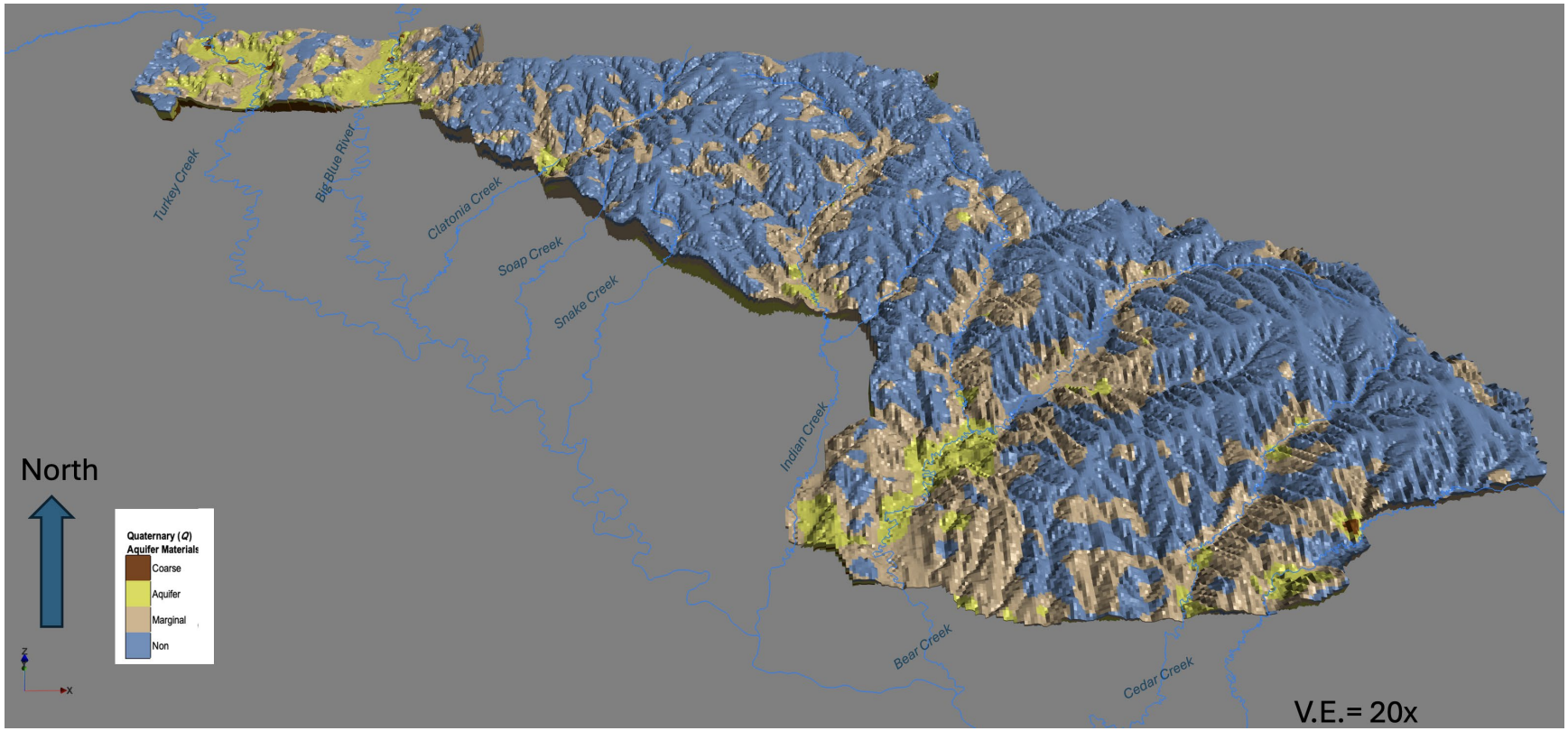


Figure 5-77. 3D voxel plot of the near-surface aquifer materials looking to the north. V.E=20x.

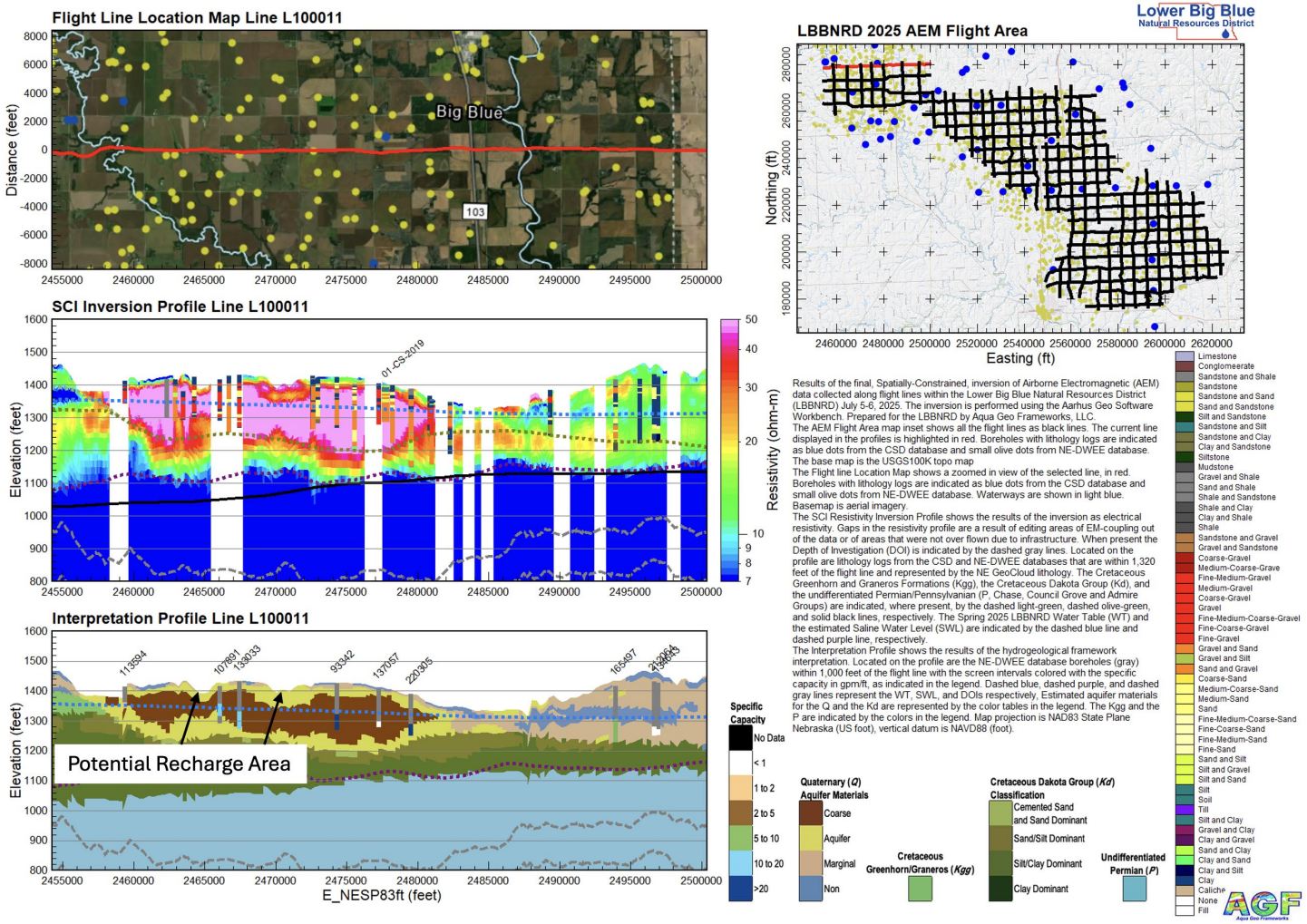


Figure 5-78. Northeast-southwest AEM flight line L100011. A location map is on the upper right. On the left the top profile shows the air photo along the flight line. The middle profile is the SCI resistivity inversion result showing borehole lithologies and the bottom profile is an interpretative section showing the undifferentiated Permian/Pennsylvanian (*P*), Cretaceous Dakota Group (*Kd*), Cretaceous Greenhorn/Graneros (*Kgg*) underlying the Quaternary (*Q*) subdivided into interpreted aquifer materials. Boreholes in the bottom section indicate measured Specific Capacity. The LBBNRD 2025 Spring water table is indicated by the dashed blue line and the estimated saline water level is indicated by the dash purple line.

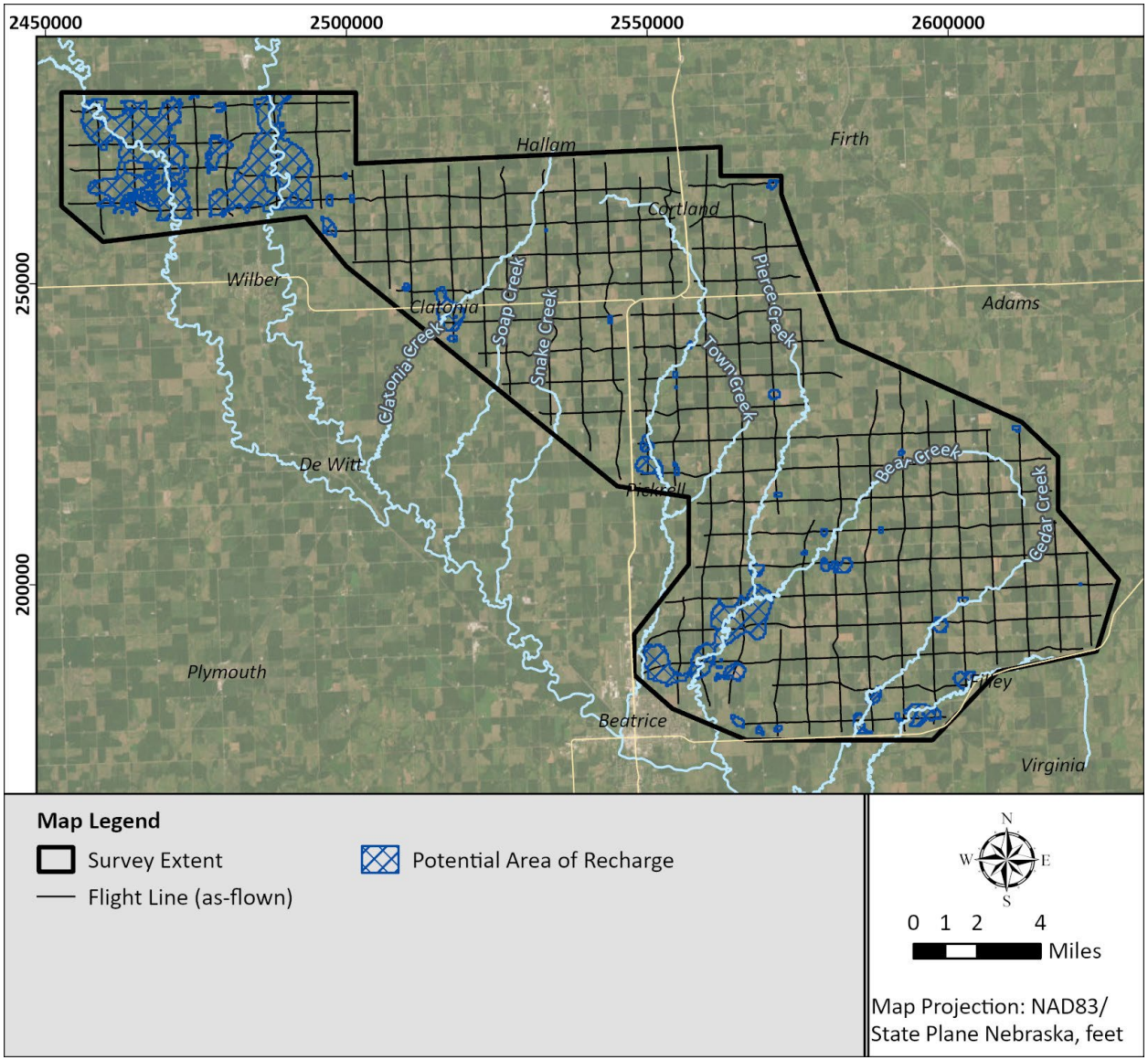


Figure 5-79. Map of the potential recharge locations based on the presence of Coarse and Aquifer materials in the near surface with connections to the deeper aquifers.

5.4 New Understanding of AEM Framework Applied to Water Management Efforts in in the LBBNRD 2025 AEM Survey Area

All management plans can be improved as new information is gathered and considered for modifying the management practices. Much of this study was focused on the determination of the groundwater availability within the LBBNRD AEM survey area. Previous mapping was based on surficial mapping and limited test hole drilling coupled with monitoring well networks. While this provided some understanding of the hydrogeology it raised more questions.

The important findings of this AEM survey that can have an impact on the management of the area are related to the estimated shape and configuration of the aquifers. Examples are estimates of both the ***Q*** and the ***Kd*** aquifers transmissivities as was determined in this study. The ***Q*** transmissivity map is also in general agreement with the map produced by Summerside and Myers (2005). The AEM provides a much higher resolution view of the area as compared with the previous mapping, but that is expected and the goal of this study.

Additionally, estimates of the transmissivity of the ***Kd*** aquifer were produced. The uncertainties in the hydrogeological parameters used in the ***Kd*** transmissivity estimates need to be acknowledged, but the maps can serve as a starting point to the understanding of the area.

Determining the areas that are impacted by nitrates due to the configuration of the near-surface materials is critical. These same areas can also be targets for recharge. The maps produced in this study can guide both management of nitrate control areas as well as allow implementation of recharge projects.

5.5 Key AEM Findings

5.5.1 Boreholes

Information from boreholes was used to analyze the Airborne Electromagnetic (AEM) inversion results. These included Nebraska Conservation Survey Division (CSD) information on 53 test holes containing lithology and stratigraphic information, and three (3) test holes containing geophysical information. Nebraska-Department of Water, Energy, and Environment (NE-DWEE) wells totaled 1,213 registered well records containing usable lithology information. These boreholes were essential in the interpretation of the AEM.

5.5.2 Digitizing Interpreted Geological Contacts

Characterization and interpretation of the subsurface was performed in cross-section and in derived surface grid formats. Contacts between the geologic units were digitized in 2D including the Quaternary (***Q***), Cretaceous Greenhorn and Graneros (***Kgg***), Cretaceous Dakota Group (***Kd***), and the undifferentiated Permian (***P***) composed of the Permian Chase (***Pc***) and Permian Council Grove Groups (***Pcg***), and Permian Admire (***IPa***). The interpretive process benefited from the use of CSD and NE-DWEE borehole logs. Geological outcrop maps previously published were also used on the far western side of the survey area, but all outcrops were outside the survey area. Surface grids of the interpreted geologic formations were then produced. Each flight line profile with interpretation including the Quaternary/Cretaceous Dakota Group aquifer material mapping is included in the appendices as well as interpretative surface grids.

5.5.3 Resistivity/Lithology Relationship

Assessment of the sediment character in both the Quaternary (***Q***), Cretaceous Greenhorn and Graneros (***Kgg***), Cretaceous Dakota Group (***Kd***) aquifer system, and the undifferentiated Permian/Pennsylvanian bedrock was conducted to determine the overall composition of the major categories used to define the aquifer and aquitards in the survey area. A numerical assessment of the resistivity thresholds within the ***Q*** was used to characterize non-aquifer (<12 ohm-m), marginal (12-25 ohm-m), aquifer (25-50 ohm-m), and coarse sand-rich intervals (>50 ohm-m) material. The ***Kgg*** was only present on the far western edge of the survey area and composed of the Graneros Shale with low resistivities in the range of 12 ohm-m. The ***Kgg*** is a confining layer and is not considered an aquifer. The ***Kd*** within the LBBNRD AEM survey area was split into four parts based on empirical comparisons to lithology logs. The four parts were classified as follows: 1) 0-3 ohm-m as Shale/Clay Dominant materials; 2) 3-18 ohm-m as Siltstone/Silt Dominant materials; 3) 18-35 ohm-m as Sand/Silt Dominant; and 4) 35 ohm-m and greater as Sandstone/Sand Dominant materials. This is the same distribution used in the pervious report from the AEM in the LBBNRD in 2023 and 2024 (AGF, 2024a; AGF, 2025). The undifferentiated Permian/Pennsylvanian bedrock varied greatly but generally had moderate resistivities in the range of 15-30 ohm-m except for the areas that contain saline waters; these areas had resistivities <7 ohm-m. The shallowest area that contains saline waters is 142 feet.

5.5.4 Hydrogeological Framework of the LBBNRD 2025 AEM Survey Area

The AEM reveals considerable variability in the Quaternary (***Q***) and Cretaceous Dakota Group (***Kd***) deposits across the AEM survey area. The groundwater within the LBBNRD 2025 AEM survey area is within the limited alluvial sediments of the present streams, glacial sediments, and the paleovalley sediments of the ***Q***. There is also groundwater in the fluvial and deltaic sediments of the ***Kd***. The actual groundwater availability is dependent upon the material type of both the ***Q*** and ***Kd***. In the western third of the survey area, the ***Q*** overlies the ***Kd*** and is in hydrogeological connection with the ***Kd***. In general, the ***Q*** groundwater is available within paleovalley sediments and glacial outwash sediments, and the ***Kd*** groundwater is available in the sandstone and sand deposits of the fluvial/delta deposits. Some NE-DWEE wells are completed in both the ***Q*** and the ***Kd***.

An estimated Transmissivity (**T**) map was developed for the ***Q*** aquifers. This is related to the thickness of the saturated aquifer material and the estimated hydraulic conductivities. Most of the higher Specific Capacity (**SC**) values calculated from the NE-DWEE well database are within the higher estimated **T** values of the paleovalley and thick glacial outwash.

The AEM successfully mapped the limited sand rich deposits of the ***Kd***. Some of the ***Kd*** completed wells are in this sand dominant region that has electrical resistivity > 35 ohm-m; these would be the sand dominant materials of the fluvial deposits. While most of the ***Kd*** is saturated, the low yielding shales, siltstone, silts, and clays reduce the actual Specific Yield of the ***Kd*** wells. There is also an area within the ***Kd*** that displays a very low resistivity range that is related to saline waters.

An estimated **T** map was developed for the ***Kd*** in the 2025 LBBNRD AEM survey area using the thickness of the sand dominant materials and hydraulic conductivities from published references (e.g., O'Connor (1987) and Gannon and Vogelgesang (2015)) in the area of eastern Nebraska and western Iowa. The values compare well with the neighboring Lancaster County (Divine, 2014). This map can be helpful, but needs to be used with caution due to the lack of local hydrogeological information on the ***Kd***.

5.5.5 Estimation of Aquifer Volume and Water in Storage in the LBBNRD AEM Survey Area

The values for the saturated Quaternary (***Q***) aquifer (based on the LBBNRD spring 2025 water table) and Cretaceous Dakota Group (***Kd***) aquifer volumes were calculated. Three-dimensional digital representation (3-D Voxel model) of the subsurface resulting from the AEM interpretation allowed the total saturated aquifer volume and the amount of extractable water to be estimated more accurately. An area of approximately 254.51 square miles (approximately 162,884.51 acres) of AEM data were collected in the LBBNRD 2025 AEM survey, and using estimates of porosity and specific yield from the published literature as well as the 3-D Voxel models, the total volume of groundwater in storage and the total volume of extractable groundwater within the saturated ***Q***, ***Kd***, and ***Q*** and ***Kd*** combined were calculated and are as follows:

- ***Q***
    - Total volume of saturated ***Q*** materials: **14,460,190** acre-ft (or approximately 46.61% of total ***Q*** material volume)
    - Estimated groundwater in storage: **4,507,005** acre-ft
    - Estimated extractable volume of groundwater: **1,397,951** acre-ft
- ***Kd***
    - Total volume of saturated ***Kd***: **7,213,844** acre-ft (or approximately 100 % of total ***Kd*** volume)
    - Estimated groundwater in storage: **2,749,752** acre-ft
    - Estimated extractable volume of groundwater: **400,208** acre-ft
- ***Q*** and ***Kd*** combined
    - Total volume of saturated ***Q*** and ***Kd*** combined: **21,674,033** acre-ft (or approximately 56.67% of total ***Q*** and ***Kd*** combined volume)
    - Estimated groundwater in storage: **7,256,757** acre-ft
    - Estimated extractable volume of groundwater: **1,798,159** acre-ft

5.5.6 Groundwater Quality in the LBBNRD 2025 AEM Survey Area

The AEM provided information on the near-surface (unsaturated) materials in the 2025 LBBNRD AEM survey area. Near-surface occurrences of sandy soils and sand deposits (aquifer materials) may provide conduits for contaminants to migrate into the groundwater. Using the 3D interpretation of the AEM, a near-surface occurrence of the aquifer materials 2D grid was generated. A map depicting water quality (nitrate) data collected by the LBBNRD (*Personal Communication, Tyler Weishahn, January 2026*) overlying the near-surface occurrence of aquifer materials grid was made to visually determine if there is a correlation between the near-surface material type and water quality. While there is a low correlation of the water quality to the near-surface materials, other mechanisms and groundwater flow may be contributing to the nitrate distribution.

The AEM survey detected an area of low resistivity of < 7 ohm-m and is interpreted as a regional saline water interface. The interface is shallow in the northwestern corner of the survey area near the Big Blue River and Turkey Creek. The shallowest area is 142 feet. This area would need to be confirmed with water quality sampling but there is a high probability that these areas contain saline waters. Clay layers can impact this estimation due to the similar resistivity values. It is also possible that the saline water is at the level of a clay layer and that the clay layer is impeding the upward migration of the deeper saline waters. Care would need to be exercised in drilling to not penetrate any confining clay layers.

5.5.7 Potential Recharge Zones within the LBBNRD 2025 AEM Survey Area

Using the AEM near-surface (unsaturated) 2D grid of the coarse and aquifer materials, a map was developed to assist in identifying and investigating areas where these materials could be used for recharge. Many of these areas are along the streams where the till and loess have been eroded away exposing the deeper coarse aquifer and aquifer material and may be considered windows into these deeper aquifer materials.

Utilizing the recharge target map to locate recharge areas can be done. However, it is imperative that accurate test holes, which may include sonic cores, are used to assess the geological materials. Any possible thin clay layers that were not detected with the AEM or may have been missed in the test hole drilling may be detected by calibrated borehole geophysical induction logs and natural gamma. Infiltration tests also need to be conducted to fully evaluate recharge rates. Additionally, determining the areas that are impacted by nitrates due to the configuration of the near-surface materials is critical because these same areas can also be targets for recharge due to the nature of the material type. The maps produced in this study can guide both management of nitrate control areas as well as allow implementation of recharge projects.

5.5.8 Using AEM Results to Implement Groundwater Management

All management plans can be improved as new information is gathered and considered for modifying the management practices. Much of this study was focused on the determination of the groundwater availability within the LBBNRD AEM survey area. Previous mapping was based on surficial exposures and limited test hole drilling coupled with monitoring well networks. While this provided some understanding of the hydrogeology, the AEM provides a much higher resolution of the aquifer configuration. The important findings that can have an impact on the management of the area are related to the estimated shape and configuration of the aquifers. Examples of these estimates are the transmissivity (**T**) maps that were made of both the ***Q*** and the ***Kd*** aquifers as part of this study. The hydraulic conductivity values used to estimate the ***Q*** transmissivity were based on the known material type (established with interpretation of the AEM) present within the survey area. The estimated transmissivity produced a **T** map that is in general agreement with the map produced by Summerside and Myers (2005). The AEM-produced **T** map provides a much higher resolution view of the area as compared with the previous mapping, but that is expected and is the goal of this study. The hydraulic conductivity value used to estimate the transmissivity of the ***Kd*** aquifer was based on an average of two published values. The uncertainties in the hydrogeological parameters used in the ***Kd*** transmissivity estimates need to be acknowledged, but the map can serve as a starting point to the understanding of the area.

5.6 Recommendations

Recommendations provided to the LBBNRD in this section are based on the interpretation and understanding gained from the addition of the AEM data to existing information and from discussions with the LBBNRD about their management challenges.

5.6.1 Additional AEM Mapping

The aquifer maps provided in this report represent the detailed hydrogeologic framework developed for the LBBNRD 2025 AEM survey area. The AEM interpretations used to create the aquifer maps match well with the CSD and NE-DWEE borehole lithologic, stratigraphic, and/or geophysical logs. It is recommended that additional areas be flown in the LBBNRD so that these aquifer maps may be broadened to cover a larger geographic extent. Additional survey flight lines can be of a reconnaissance nature to begin with but, later, closely spaced lines or "block flights" should be collected over project areas such as well fields, well head protection areas, and/or areas of detailed recharge projects to develop more detailed frameworks. The line spacing for the block flights should be on the order of 0.25 mile (1,320 ft). It is important to note that AEM data is not meant to replace existing data, such as borehole lithology or aquifer tests, but to provide a framework in which to place the existing hydrogeological data. Therefore, AEM mapping can assist with targeting areas where more expensive technologies including borehole drilling can be implemented, especially when a block flight is flown over an area.

Future AEM mapping projects could potentially be done in cooperation with the neighboring NRDs to get details on the continuous aquifer system that is shared in the area. The Little Blue NRD is a great example of an NRD the LBBNRD can partner with to share an AEM mapping project. A benefit for partnering with other NRDs is to have a combined comprehensive estimate of groundwater storage capacity, which may be calculated by understanding the aquifer characteristics through AEM interpretation.

5.6.2 Siting new test holes and production wells

The AEM framework maps and profiles provided in this report give insight into the 3D relationship between current test holes and production groundwater wells and the material in which they are drilled into. At the time of this report, the current available lithology data for the LBBNRD area was used to help build the framework maps and profiles. It is recommended that the results from this report be used to site new test holes, monitoring wells, and/or water supply wells. Based on more data, the AEM framework maps and profiles provide detail in areas where the previously existing data may have been more regional in nature; this enables better decision-making when siting new wells.

The location of any future water supply wells can also use the results in this report to guide development of new water supply wells. Planners should locate wells in areas of greatest saturated thickness with the least potential for non-point source pollution.

5.6.3 Aquifer testing and borehole logging

Aquifer tests are recommended to improve estimates of aquifer characteristics. A robust aquifer characterization program is highly recommended at the state, regional (NRD's), and smaller municipal levels. Aquifer tests can be designed based on the results of AEM surveys and existing production wells.

Additional test holes with detailed, functional, and well calibrated geophysical logging for aquifer characteristics is highly recommended. The few test holes with calibrated geophysical logs in the LBBNRD survey area were inadequate. The borehole geophysical logs provided for this investigation demonstrate that additional calibrated and verified geophysical logs are required in the LBBNRD.

Examples of additional logging would be borehole flow meter logs and geophysical logs including gamma, neutron, electrical, and induction logs. Detailed aquifer characteristics can be accomplished with nuclear magnetic resonance logging (NMR). This is a quick and effective way to characterize porosity and water content, estimates of permeability, mobile/bound water fraction, and pore-size distributions with depth. This is very cost effective when compared to traditional aquifer tests.

5.6.4 Groundwater Management: Control Areas, Recharge areas

The hydrogeologic framework in this report provides the location and extent of high transmissive and saturated aquifers. Conversely, it also shows areas where high-capacity wells may be limited due to the aquifer characteristics. It is recommended that these areas be used to define the control areas based on empirical data of the AEM coupled with water quality and groundwater levels. The geospatial data products delivered with this report can be directly opened in ESRI's ArcGIS Pro and can be used to provide guidance in the establishment on control areas. These data can also be invaluable to the producers/developers within the area in replacing wells and drilling new wells. These data can be used by the LBBNRD in assessing the well permits of the area and assisting the interested parties to drill successful wells.

This study mapped areas that are windows to the deeper aquifers. These areas may be considered for special recharge projects. These areas also may require additional protections to be added to avoid groundwater quality issues due to the direct conduit of the surface to the deeper aquifer systems. Any management decisions that would propose recharge would need to be weighed against current land use and recharge water availability. The low resistivity < 7 ohm-m depth map that is interpreted as a regional saline water interface can be used to provide guidance in well permitting to avoid any potential wells from penetrating a confining clay or to allowing infiltration of saline waters into the Quaternary aquifer system. Utilizing the 3D products including the profiles and maps can allow the staff and board of the LBBNRD to make informed decisions on the management of the water resources within the District.

6 Description of Data Delivered

6.1 Tables Describing Included Data Files

Table 6-1 describes the raw data files included in *Appendix 3_Deliverables \Raw_Data*. As discussed above, five (5) flights were required to acquire the 2025 LBBNRD AEM data (Figure 4-5). Grouped by flight date, there are four (4) data files included in Appendix 3\Raw_Data for each flight. These files have extensions of "*.sps" and "*.skb". The "*.sps" files include navigation and DGPS location data and the "*.skb" files include the raw AEM data that have been PFC-corrections (discussed in Section 4.4.1). Two additional files are used for all the flights. These are the system description and specifications file (with the extension "*.gex") in the GEO subdirectory and the 'mask' file (with the extension "*.lin"), in the MASK subdirectory, which correlates the flight dates, flight numbers, and assigned line numbers.

Table 6-2 describes the data columns in the ASCII *.xyz file *LBBNRD2025_EM_MAG_AUX.xyz*. This file contains the electromagnetic data, plus the magnetic and navigational data, as supplied directly from SkyTEM.

The result of the SCI is included in *LBBNRD2025_AEM_SCI01_INV_v1.xyz* and the data columns of these databases are described in Table 6-3.

The interpretation results are included in the data file *LBBNRD2025_AEMInterp.xyz* in ASCII format. Table 6-4 describes the data columns of those files.

ESRI ArcGIS raster grids of the surfaces (*.tif) that were used in the interpretation (DEM, water table) and derived from the interpretation (top of geological units) of the AEM and borehole are listed in Table 6-5 and stored in the map package in *Appendix 3 - Deliverables\ESRI Products*. Included shapefiles in the map package are listed in Table 6-6.

In addition, a data file, *LBBNRD2025_SCI01_GeoScene.xyz*, with the Nebraska Geocloud format is included in Appendix 3_Deliverables\GeoCloud. The format is listed in Table 6-7.

Finally, Table 6-8 describes the columns in the LBBNRD 2025 AEM 3D voxel files included in this data delivery.

In summary, the following are included as deliverables:

- Raw Data Files - SkyTEM files *.gex, *skb, *.lin (Table 6-1)
- Raw EM Mag data as ASCII *.xyz (Table 6-2)
- SCI inversion as ASCII *.xyz in array column format (Table 6-3)
- Interpretations as ASCII *.xyz (Table 6-4)
- ESRI GIS files – raster grids (*.flt) and ESRI ArcGIS Pro map package (.mpkx) (Table 6-5) and shapefiles (Table 6-6)
- 2D profiles, Surfaces, and 3D fence diagrams of the AEM survey inversion results
- Files compatible with GeoScene 3D and the Nebraska GeoCloud (Table 6-7)
- LBBNRD 2025 AEM 3D voxel files (LeapFrog Compatible) (Table 6-8)
- KMZs for LBBNRD 2025 AEM flight lines (Discussed in Section 6.2).

Table 6-1. Raw SkyTEM data files

File Type	File Name	Description
Data	..NavSys.sps, ...PaPc.sps, ...RawData_PFC.skb, ...PPP.sps	Raw data files included for each flight used in importing to Aarhus Workbench
Geo	20250630_20099_NE_AGF_304_TX29_SKB_Prelim.gex	304M System Description For SKB (raw) and SkyTEM processed (xyz)
	20250630_20099_NE_AGF_304_TX29_XYZ_Prelim.gex	
	20099_SkyTEM_304_28gates_37gates_PLNI_Prelim.alc	
Mask	20099_LBBNRD2025_Production.lin	Production file listing dates, flights, and assigned line numbers
WorkBench XYZ	20250705_20099_YSA_NE_UTM14n.xyz	7/5 XYZ data
	20250706_20099_YSA_NE_UTM14n.xyz	7/6 XYZ data
	20250705_03_L100201_100192_20099_NE_UTM14n.xyz	Reflights of 2 lines

Table 6-2: Channel name, description, and units for LBBNRD2025_EM_MAG_AUX.xyz with DEM, magnetic, DGPS, Inclinometer, altitude, and associated data.

Parameter	Description	Unit
Line	Line Number	
E_UTM14Nm	Easting, NAD83 UTM Zone 14N	Meters [m]
N_UTM14Nm	Northing, NAD83 UTM Zone 14N	Meters [m]
DEM_m	Digital Elevation	Meters [m]
E_NESP83ft	Easting, NAD83 Nebraska State Plane	Feet [ft]
N_NESP83ft	Northing, NAD83 Nebraska State Plane	Feet [ft]
DEM_ft	Digital Elevation	Feet [ft]
Flight	Name of Flight	yyyymmdd.ff
DateTime	DateTime Format	Decimal days
Date	DateTime Format	yyyymmdd
Time	Time UTC	hhmmss.sss
AngleX	Angle (in flight direction)	Degrees
AngleY	Angle (perpendicular to flight direction)	Degrees
Height_m	System Height Measurement Above Ground	Meters [m]
Height_ft	System Height Measurement Above Ground	Feet [ft]
Lon	Longitude, WGS84	Decimal Degrees
Lat	Latitude, WGS84	Decimal Degrees
Alt	DGPS Altitude above sea level (elevation)	Meters [m]
GDSpeedL	Ground Speed	Kilometers/hour [km/h]
LMcurrent	Current, Low Moment	Amps [A]
HMcurrent	Current, High Moment	Amps [A]

LM_Z_dBdt	**Normalized (PFC-Corrected) Low Moment Z-RxCoil values array**	**pV/(m^4*A)**
HM_Z_dBdt	**Normalized (PFC-Corrected) High Moment Z-RxCoil values array**	**pV/(m^4*A)**
HM_X_dBdt	**Normalized (PFC-Corrected) High Moment X-RxCoil values array**	**pV/(m^4*A)**
PLNI	**Power Line Noise Intensity monitor, 60Hz**	**V/m^2**
Bmag_Raw	**Raw Base Station Mag Data filtered**	**nanoTesla [nT]**
INC	**Magnetic Field Inclination**	**Degrees**
DEC	**Magnetic Field Declination**	**Degrees**
Diurnal	**Diurnal Mag Data**	**nanoTesla [nT]**
MAG_Raw	**Raw Mag Data**	**nanoTesla [nT]**
IGRF	**International Geomagnetic Reference Field**	**nanoTesla [nT]**
RMF	**Residual Magnetic Field**	**nanoTesla [nT]**
TMI	**Total Magnetic Intensity**	**nanoTesla [nT]**
RelUnc_LM_Z_dBdt	**Relative uncertainty in LM Z dB/dt**	
RelUnc_HM_Z_dBdt	**Relative uncertainty in HM Z dB/dt**	
RelUnc_HM_X_dBdt	**Relative uncertainty in HM X dB/dt**	

Table 6-3. Channel name, description, and units for LBBNRD2025_AEM_SCI01_INV_v1.xyz with EM inversion results.

/Parameter	Description	Unit
LINE	**Line Number**	
E_NESPCS83ft	**Easting NAD83, Nebraska State Plane**	**Feet (ft)**
N_NESPCS83ft	**Northing NAD83, Nebraska State Plane**	**Feet [ft]**
DEM_ft	**DEM from 100 ft grid NED NAVD88**	**Feet [ft]**
E_UTM14N_m	**Easting NAD83, UTM Zone 14**	**Meters [m]**
N_UTM14N_m	**Northing NAD83, UTM Zone 14**	**Meters [m]**
DEM_m	**DEM from survey**	**Meters [m]**
Alt_m	**Measured altitude of system above ground**	**Meters [m]**
Invalt_m	**Inverted Altitude of system above ground**	**Meters [m]**
Resdata	**Residual of individual sounding**	
ResTotal	**Total residual for inverted section**	
RHO_I_0 through RHO_I_38	**Inverted resistivity of each layer**	**Ohm-m**
RHO_I_STD_0 through RHO_I_STD_38	**Inverted resistivity error per layer**	
SIGMA_I_0 through SIGMA_I_38	**Conductivity**	**S/m**

DEP_TOP_0_ft through DEP_TOP_38_ft	**Depth to the top of individual layers**	**Feet [ft]**
DEP_BOT_0_ft through DEP_BOT_38_ft	**Depth to the bottom of individual layers**	**Feet [ft]**
THK_0_FT through THK_38_FT	**Thickness of individual layers**	**Feet [ft]**
DEP_TOP_0_m through DEP_TOP_38_M	**Depth to the top of individual layers**	**Meters [m]**
DEP_BOT_0_M through DEP_BOT_38_m	**Depth to the bottom of individual layers**	**Meters [m]**
THK_0_m through THK_38_m	**Thickness of individual layers**	**Meters [m]**
DOI_UPPER_FT	**More conservative estimate of DOI**	**Feet [ft]**
DOI_LOWER_ft	**Less conservative estimate of DOI**	**Feet [ft]**
DOI_UPPER_M	**More conservative estimate of DOI**	**Meters [m]**
DOI_LOWER_M	**Less conservative estimate of DOI**	**Meters [m]**

Table 6-4. Channel name description and units for the interpretation results file LBBNRD2025_AEMInterp.xyz.

Parameter	Description	Unit
LINE	**Line Number**	
E_NESP83ft	**Easting NAD83, Nebraska State Plane**	**Feet [ft]**
N_NESP83ft	**Northing NAD83, Nebraska State Plane**	**Feet [ft]**
DEM_ft	**Topography at 100ft sampling (NAVD 1988)**	**Feet [ft]**
E_UTM14Nm	**Easting UTM Zone 14**	**Meters (m)**
N_UTM14Nm	**Northing UTM Zone 14**	**Meters (m)**
DEM_m	**Topography at 100ft sampling (NAVD 1988)**	**Meters (m)**
RESDATA	**Inversion model residuals of each individual sounding**	
RESTOTAL	**Inversion model average of all residuals**	
RHO [0] through RHO [38]	**Array of Inverted model resistivities of each layer**	**Ohm-m**
RHO_STD[0] through RHO_STD[38]	**Array of Standard Deviations of Inverted model resistivities for each layer**	**Ohm-m**
DEP_TOP_FT [0] through DEP_TOP_FT [38]	**Depth to the top of 39 individual layers**	**Feet [ft]**
DEP_BOT_FT [0] through DEP_BOT_FT [38]	**Depth to the bottom of 39 individual layers**	**Feet [ft]**
DOI_UPPER_FT	**More conservative estimate of DOI from Workbench**	**Feet [ft]**
DOI_LOWER_FT	**Less conservative estimate of DOI from Workbench**	**Feet [ft]**
LBBNRD_Spring25_water_elev_ft	**Elevation of the top of the water table as measured in Spring 2025**	**Feet [ft]**

LBBNRD25_Top_Bedrock_elev_ft	**Elevation of the top of the Bedrock surface**	**Feet [ft]**
LBBNRD25_Top_Kgg_elev_ft	**Elevation of the top of the Cretaceous Greenhorn Limestone and Graneros Shale**	**Feet [ft]**
LBBNRD25_Top_Kd_elev_ft	**Elevation of the top of the Cretaceous Dakota Group**	**Feet [ft]**
LBBNRD25_Top_P_elev_ft	**Elevation of the top of the Permian bedrock**	**Feet [ft]**
Kd_P_7ohmm_elev_ft	**Elevation of saltwater in Kd and P**	**Feet [ft]**

Table 6-5. Files containing LBBNRD 2025 raster datasets (.tif format). All datasets projected to NAD83/State Plane Nebraska, feet and extend throughout the entire LBBNRD AEM Survey Area, unless otherwise stated. Resolution of all grids is 300 ft. Depth and elevations are in feet.

Raster Datasets; For all datasets: Projection = NAD83/State Plane Nebraska, ft; file format is .tif; cell resolution = 300 ft; thickness and depth to values are in feet (ft); elevation values are in ft		
Name	**About**	**Extracted from Voxel**
LBBNRD_2024_2025_Bedrock_TopElevation_Blended.tif	**Elevation of the top of the bedrock surface within both the LBBNRD 2024 and 2025 survey areas. Interface between the two datasets were blended.**	--
LBBNRD_2025_DEM_NESP_feet_feet_300ftRES.tif	**Ground surface elevation within the LBBNRD 2025 survey area.**	--
LBBNRD2025_Bedrock_DepthTo.tif	**Depth to the top of bedrock (ft) within the LBBNRD 2025 survey area.**	--
LBBNRD2025_Bedrock_TopElevation.tif	**Elevation of the top of bedrock (ft) within the LBBNRD 2025 survey area.**	-
LBBNRD2025_Kd_Clay_SalineDominant_Thickness.tif	**Total thickness of the clay/saline dominant material of the Kd.**	x
LBBNRD2025_Kd_DepthTo.tif	**Depth to the top of Kd.**	--
LBBNRD2025_Kd_Over18ohm_Transmissivity.tif	**Calculated transmissivity (gpd/ft) of the Kd (over 18 ohm-m).**	--
LBBNRD2025_Kd_over18ohmm_Thickness_SATURATED.tif	**Thickness of saturated Kd over 18 ohm-m.**	x
LBBNRD2025_Kd_SandSilt_BottomElevation_WHOLE.tif	**Elevation of the bottom of all (either saturated or unsaturated) sand/silt dominant material of the Kd.**	x
LBBNRD2025_Kd_SandSilt_Thickness_WHOLE.tif	**Thickness of all (either saturated or unsaturated) sand/silt dominant material of the Kd.**	x
LBBNRD2025_Kd_SandSilt_TopElevation_WHOLE.tif	**Elevation of the top of all (either saturated or unsaturated) sand/silt dominant material of the Kd.**	x
LBBNRD2025_Kd_SandstoneSand_BottomElevation_WHOLE.tif	**Elevation of the bottom of all (either saturated or unsaturated) sandstone/sand dominant material of the Kd.**	x
LBBNRD2025_Kd_SandstoneSand_SandSilt_Thickness_WHOLE.tif	**Thickness of all (either saturated or unsaturated) sandstone/sand and sand/silt dominant material of the Kd.**	x

LBBNRD2025_Kd_SandstoneSand_Thickness_WHOLE.tif	Thickness of all (either saturated or unsaturated) sandstone/sand dominant material of the Kd.	x
LBBNRD2025_Kd_SandstoneSand_TopElevation_WHOLE.tif	Elevation of the top of all (either saturated or unsaturated) sandstone/sand dominant material of the Kd.	x
LBBNRD2025_Kd_SiltClay_BottomElevation_WHOLE.tif	Elevation of the bottom of all (either saturated or unsaturated) sandstone/sand dominant material of the Kd.	x
LBBNRD2025_Kd_SiltClay_Thickness_WHOLE.tif	Thickness of all (either saturated or unsaturated) silt/clay dominant material of the Kd.	x
LBBNRD2025_Kd_SiltClay_TopElevation_WHOLE.tif	Elevation of the top of all (either saturated or unsaturated) silt/clay dominant material of the Kd.	x
LBBNRD2025_Kd_Thickness.tif	Total thickness of the Kd.	--
LBBNRD2025_Kd_Thickness_Saturated.tif	Saturated thickness of the Kd.	--
LBBNRD2025_Kd_TopElevation.tif	Elevation of the top of the Kd.	--
LBBNRD2025_Kgg_DepthTo.tif	Depth to the top of the Kgg.	--
LBBNRD2025_Kgg_Thickness.tif	Total thickness of the Kgg.	--
LBBNRD2025_Kgg_Thickness_Saturated.tif	Saturated thickness of the Kgg.	--
LBBNRD2025_Kgg_TopElevation.tif	Elevation of the top of the Kgg.	--
LBBNRD2025_P_DepthTo.tif	Depth to the top of the Permian (undivided).	--
LBBNRD2025_P_TopElevation.tif	Elevation of the top of the Permian (undivided).	--
LBBNRD2025_PotentialAreasOfRecharge_Q_Coarse_Aquifer_UnsaturatedThickness.tif	Thickness of the unsaturated coarse and aquifer material of the Q deposits within the potential areas of recharge only.	--
LBBNRD2025_Q_Aquifer_BottomElevation_SATURATED.tif	Elevation of the bottom of the saturated aquifer material within the Q deposits.	x
LBBNRD2025_Q_Aquifer_BottomElevation_UNSATURATED.tif	Elevation of the bottom of the unsaturated aquifer material within the Q deposits.	x
LBBNRD2025_Q_Aquifer_BottomElevation_WHOLE.tif	Elevation of the bottom of all (either saturated or unsaturated) aquifer material within the Q deposits.	x
LBBNRD2025_Q_Aquifer_Thickness_SATURATED.tif	Thickness of the saturated aquifer material within the Q deposits.	x
LBBNRD2025_Q_Aquifer_Thickness_UNSATURATED.tif	Thickness of the unsaturated aquifer material within the Q deposits.	x
LBBNRD2025_Q_Aquifer_Thickness_WHOLE.tif	Thickness of all (either saturated or unsaturated) aquifer material of the Q deposits.	x
LBBNRD2025_Q_Aquifer_TopElevation_SATURATED.tif	Elevation of the top of the saturated aquifer material of the Q deposits.	x
LBBNRD2025_Q_Aquifer_TopElevation_UNSATURATED.tif	Elevation of the top of the unsaturated aquifer material of the Q deposits.	x
LBBNRD2025_Q_Aquifer_TopElevation_WHOLE.tif	Elevation of the top of all (either saturated or unsaturated) aquifer material of the Q deposits.	x
LBBNRD2025_Q_Coarse_Aquifer_BottomElevation_SATURATED.tif	Elevation of the bottom of the saturated coarse and aquifer material of the Q deposits.	x

LBBNRD2025_Q_Coarse_Aquifer_BottomElevation_UNSATURATED.tif	Elevation of the bottom of the unsaturated coarse and aquifer material of the Q deposits.	x
LBBNRD2025_Q_Coarse_Aquifer_BottomElevation_WHOLE.tif	Elevation of the bottom of all (either saturated or unsaturated) coarse and aquifer material of the Q deposits.	x
LBBNRD2025_Q_Coarse_Aquifer_Marginal_Thickness_SATURATED.tif	Thickness of the saturated coarse aquifer marginal material within the Q deposits.	x
LBBNRD2025_Q_Coarse_Aquifer_Marginal_Transmissivity_gpdft.tif	Calculated transmissivity (gpd/ft) of the coarse, aquifer, and marginal material of the Q deposits within the LBBNRD 2025 survey area.	--
LBBNRD2025_Q_Coarse_Aquifer_Thickness_SATURATED.tif	Thickness of the saturated coarse and aquifer material within the Q deposits.	x
LBBNRD2025_Q_Coarse_Aquifer_Thickness_UNSATURATED.tif	Thickness of the unsaturated coarse and aquifer material within the Q deposits.	x
LBBNRD2025_Q_Coarse_Aquifer_Thickness_WHOLE.tif	Thickness of all (either saturated or unsaturated) coarse and aquifer material of the Q deposits.	x
LBBNRD2025_Q_Coarse_Aquifer_TopElevation_SATURATED.tif	Elevation of the top of the saturated coarse and aquifer material of the Q deposits.	x
LBBNRD2025_Q_Coarse_Aquifer_TopElevation_UNSATURATED.tif	Elevation of the top of the unsaturated coarse and aquifer material of the Q deposits.	x
LBBNRD2025_Q_Coarse_Aquifer_TopElevation_WHOLE.tif	Elevation of the top of all (either saturated or unsaturated) coarse and aquifer material of the Q deposits.	x
LBBNRD2025_Q_Coarse_BottomElevation_SATURATED.tif	Elevation of the bottom of the saturated coarse material of the Q deposits.	x
LBBNRD2025_Q_Coarse_BottomElevation_UNSATURATED.tif	Elevation of the bottom of the unsaturated coarse material of the Q deposits.	x
LBBNRD2025_Q_Coarse_BottomElevation_WHOLE.tif	Elevation of the bottom of all (either saturated or unsaturated) coarse material of the Q deposits.	x
LBBNRD2025_Q_Coarse_Thickness_SATURATED.tif	Thickness of the saturated coarse material within the Q deposits.	x
LBBNRD2025_Q_Coarse_Thickness_UNSATURATED.tif	Thickness of the unsaturated coarse material within the Q deposits.	x
LBBNRD2025_Q_Coarse_Thickness_WHOLE.tif	Thickness of all (either saturated or unsaturated) coarse material within the Q deposits.	x
LBBNRD2025_Q_Coarse_TopElevation_SATURATED.tif	Elevation of the top of the saturated coarse material of the Q deposits.	x
LBBNRD2025_Q_Coarse_TopElevation_UNSATURATED.tif	Elevation of the top of the unsaturated coarse material of the Q deposits.	x
LBBNRD2025_Q_Coarse_TopElevation_WHOLE.tif	Elevation of the top of all (either saturated or unsaturated) coarse material of the Q deposits.	x
LBBNRD2025_Q_Marginal_BottomElevation_SATURATED.tif	Elevation of the bottom of the saturated marginal material of the Q deposits.	x
LBBNRD2025_Q_Marginal_BottomElevation_UNSATURATED.tif	Elevation of the bottom of the unsaturated marginal material of the Q deposits.	x

LBBNRD2025_Q_Marginal_BottomElevation_WHOLE.tif	Elevation of the bottom of all (either saturated or unsaturated) marginal material of the Q deposits.	x
LBBNRD2025_Q_Marginal_Non_BottomElevation_SATURATED.tif	Elevation of the bottom of the saturated marginal and non-aquifer material of the Q deposits.	x
LBBNRD2025_Q_Marginal_Non_BottomElevation_UNSATURATED.tif	Elevation of the bottom of the unsaturated marginal and non-aquifermaterial of the Q deposits.	x
LBBNRD2025_Q_Marginal_Non_BottomElevation_WHOLE.tif	Elevation of the bottom of all (either saturated or unsaturated) marginal and non-aquifermaterial of the Q deposits.	x
LBBNRD2025_Q_Marginal_Non_Thickness_SATURATED.tif	Thickness of the saturated marginal and non-aquifer material within the Q deposits.	x
LBBNRD2025_Q_Marginal_Non_Thickness_UNSATURATED.tif	Thickness of the unsaturated marginal and non-aquifer material within the Q deposits.	x
LBBNRD2025_Q_Marginal_Non_Thickness_WHOLE.tif	Thickness of all (either saturated or unsaturated) marginal and non-aquifer material within the Q deposits.	x
LBBNRD2025_Q_Marginal_Non_TopElevation_SATURATED.tif	Elevation of the top of the saturated marginal and non-aquifer material of the Q deposits.	x
LBBNRD2025_Q_Marginal_Non_TopElevation_UNSATURATED.tif	Elevation of the top of the unsaturated marginal and non-aquifer material of the Q deposits.	x
LBBNRD2025_Q_Marginal_Non_TopElevation_WHOLE.tif	Elevation of the top of all (either saturated or unsaturated) marginal and non-aquifer material of the Q deposits.	x
LBBNRD2025_Q_Marginal_Thickness_SATURATED.tif	Thickness of the saturated marginal material within the Q deposits.	x
LBBNRD2025_Q_Marginal_Thickness_UNSATURATED.tif	Thickness of the unsaturated marginal material within the Q deposits.	x
LBBNRD2025_Q_Marginal_Thickness_WHOLE.tif	Thickness of all (either saturated or unsaturated) marginal material within the Q deposits.	x
LBBNRD2025_Q_Marginal_TopElevation_SATURATED.tif	Elevation of the top of the saturated marginal material of the Q deposits.	x
LBBNRD2025_Q_Marginal_TopElevation_UNSATURATED.tif	Elevation of the top of the unsaturated marginal material of the Q deposits.	x
LBBNRD2025_Q_Marginal_TopElevation_WHOLE.tif	Elevation of the top of all (either saturated or unsaturated) marginal material of the Q deposits.	x
LBBNRD2025_Q_Non_BottomElevation_SATURATED.tif	Elevation of the bottom of the saturated non-aquifer material of the Q deposits.	x
LBBNRD2025_Q_Non_BottomElevation_UNSATURATED.tif	Elevation of the bottom of the unsaturated non-aquifer material of the Q deposits.	x
LBBNRD2025_Q_Non_BottomElevation_WHOLE.tif	Elevation of the bottom of all (either saturated or unsaturated) non-aquifer material of the Q deposits.	x
LBBNRD2025_Q_Non_Thickness_SATURATED.tif	Thickness of the saturated non-aquifer material within the Q deposits.	x
LBBNRD2025_Q_Non_Thickness_UNSATURATED.tif	Thickness of the unsaturated non-aquifer material within the Q deposits.	x
LBBNRD2025_Q_Non_Thickness_WHOLE.tif	Thickness of all (either saturated or unsaturated) non-aquifer material within the Q deposits.	x

LBBNRD2025_Q_Non_TopElevation_SATURATED.tif	Elevation of the top of the saturated non-aquifer material of the Q deposits.	x
LBBNRD2025_Q_Non_TopElevation_UNSATURATED.tif	Elevation of the top of the unsaturated non-aquifer material of the Q deposits.	x
LBBNRD2025_Q_Non_TopElevation_WHOLE.tif	Elevation of the top of all (either saturated or unsaturated) non-aquifer material of the Q deposits.	x
LBBNRD2025_Q_Thickness.tif	Total thickness of the Q deposits.	--
LBBNRD2025_Q_Thickness_Saturated.tif	Saturated thickness of the Q deposits.	--
LBBNRD2025_SalineWater_DepthTo.tif	Depth to the top of saline water.	--
LBBNRD2025_WaterTable_Spring2025_DepthTo.tif	Depth to the top of water table - Spring 2025 (ft) within the LBBNRD 2025 survey area.	--
LBBNRD2025_WaterTable_Spring2025_TopElevation.tif	Elevation of the top of the water table -Spring 2025 (ft) within the LBBNRD 2025 survey area.	--

Table 6-6. Relevant features and extents as LBBNRD 2025 ESRI Shapefiles included in the ESRI map package, LBBNRD2025_AEMSurvey.mpkx. Projection is NAD83/State Plane Nebraska, feet.

Shapefiles; For all datasets: Projection = NAD83/State Plane Nebraska	
Name	**About**
LBBNRD2025_WaterTable_ControlPoints	Control points used to create the top elevation of the water table (Spring 2025) within the LBBNRD AEM survey.
LBBNRD2025_CSD_GeophysicalLogs	CSD boreholes with geophysical logs witin the 2025 LBBNRD AEM survey area.
LBBNRD2025_WellsBoreholes	Well and boreholes used (both NE-DNR and CSD) to help guide interpretation of the AEM data.
LBBNRD2025_BoreholesForBedrockOnlySurfa	Boreholes used to create the "borehole only" bedrock surface. This surface was used as a guide only and is not a data deliverable.
LBBNRD2025_DNRWells_SpecificCapacity	Calculated specific capaicty of NE-DNR wells within the LBBNRD 2025 AEM survey. Only those wells with static water level, pumping water level, and pumping rate data available are included.
MonWell_Nitrates	Nitrate results from wells (provided by LBBNRD)
Irrigation_Nitrates	Nitrate results from wells (provided by LBBNRD)
LBBNRD2025_Kgg_Extent	Extent of the Kgg within the LBBNRD 2025 AEM survey.
LBBNRD2025_Kd_Extent	Extent of the Kd within the LBBNRD 2025 AEM survey.
LBBNRD_SurveyExtent	Extent of the 2024 AEM survey within the LBBNRD (data clipping extent).
LBBNRD2025_SurveyExtent	Extent of the 2025 AEM survey within the LBBNRD (data clipping extent).
LBBNRD2025_DEM_Contour_50ft	Line of equal elevaiton of the ground surface DEM (interval = 50').
LBBNRD2025_WaterTable_TopElevation_Cont	Line of equal elevatiion of the top of Water Table (interval = 10').
LBBNRD2025_TransmissivityContours_Summe	Transmissivity contours digitized from Mapping of Aquifer Properties - Transmissivity and Specific Yield - for Selected River Basins in Central and Eastern Nebraska (OFR-71)
LBBNRD2025_PotentialAreasOfRecharge	Polygons of potential areas of recharge calculated from data pulled out of voxel model as well as the ground and bedrock surface elevation datasets.
LBBNRD2025_Kgg_TopElevation_Contour_20ft	Line of equal elevaiton of the top of Kgg (interval = 20').
LBBNRD2025_Kd_TopElevation_Contour_25ft	Line of equal elevaiton of the top of Kd (interval = 25').
LBBNRD2025_P_TopElevation_Contour_25ft	Line of equal elevaiton of the top of P (interval = 25')
LBBNRD2025_Bedrock_TopElevation_Contour_	Line of equal elevaiton of the top of bedrock (interval = 25')
LBBNRD_2025_AsFlown_FlightLines	As-flown flight lines for the 2025 LBBNRD AEM Survey.
LBBNRD_2025_Retained_FlightLines	Retained flight lines for the 2025 LBBNRD AEM Survey.
LBBNRD_MajorStreamsRivers_SPNEft_DISSOLV	Major streams within and adjacent to the 2025 LBBNRD AEM survey area.

Table 6-7. Nebraska Geocloud-import file: LBBNRD2025_SCI01_GeoScene.xyz. (*_geocloud.xyz)

LINE	**Original Line Number**
X_SP_FT	**Easting Nebraska State Plane (feet) NAD83**
Y_SP_FT	**Northing Nebraska State Plane (feet) NAD83**
ELEV_FT	**Elevation above sea level (feet) from USGS Data Elevation Model**
X_SP_M	**Easting Nebraska State Plane (meters) NAD83**
Y_SP_M	**Northing Nebraska State Plane (meters) NAD83**
ELEV_M	**Elevation above sea level (meters) from USGS Data Elevation Model**
INV_ALT_FT	**Inverted altitude of AEM system (feet)**
RESDATA	**Data residual of sounding**
RESTOTAL	**Total data residual of inversion**
RHO_0 to 38	**Resistivity of layers 1 to 39 (Ohm-m)**
RHO_STD_0 to 38	**Standard deviation of resistivity of layers 1 to 39**
DEP_TOP_FT_0 to 38	**Depth to top of layer 1 to 39 (positive feet for GeoCloud)**
DEP_BOT_FT_0 to 38	**Depth to bottom of layer 1 to 39 (positive feet for GeoCloud)**
DEP_TOP_M_0 to 38	**Depth to top of layer 1 to 39 (negative meters)**
DEP_BOT_M_0 to 38	**Depth to bottom of layer 1 to 39 (negative meters)**
DOI_UPPER_FT	**Upper Depth of Investigation calculation (negative feet)**
DOI_LOWER_FT	**Lower Depth of Investigation calculation (negative feet)**
DOI_UPPER_M	**Upper Depth of Investigation calculation (negative meter)**
DEP_LOWER_M	**Lower Depth of Investigation calculation (negative meter)**

Table 6-8. Columns in LBBNRD 2025 AEM 3D Voxel files ASCII and UBC formats (UBC format importable into LeapFrog).

Ascii_voxel	
LBBNRD2025_All_elev_VoxelXYZData_discretized3.3.xyz	*.xyz pointcloud files. Each of these models has been discretized onto a consistent vertical grid of 3.3 ft (1 m). These models have been carefully created to maintain the strucutre of the AEM models, as output from the inversion, despite being upsampled to a finer grid. Each file has a header block describing the geometry of the 3D grid defined by the file. Files with "All" in the name describe the full, undivided AEM resistivity model. Files with "Quat" in the name describe only the Quaternary portion of the AEM resistivity model. Files with "Kd" in the name describe only the Cretaceous Dakota portion of the AEM resistivity model.
LBBNRD2025_Kd_elev_VoxelXYZData_discretized3.3.xyz	
LBBNRD2025_Quat_elev_VoxelXYZData_discretized3.3.xyz	
UBC_voxel	
LBBNRD2025_All_elev_VoxelXYZData_discretized3.3-UBC_README.txt	UBC voxel files (*.msh and *.mod pairs). Each of these models has been discretized onto a consistent vertical grid of 3.3 ft (1 m). These models have been carefully created to maintain the strucutre of the AEM models, as output from the inversion, despite being upsampled to a finer grid. Each model set has an accompanying *UBC_README.txt file that describes the geometry of the 3D grid defined by the file and "dummy" no-data values. Files with "All" in the name describe the full, undivided AEM resistivity model. Files with "Quat" in the name describe only the Quaternary portion of the AEM resistivity model. Files with "Kd" in the name describe only the Cretaceous Dakota portion of the AEM resistivity model.
LBBNRD2025_All_elev_VoxelXYZData_discretized3.3.mod	
LBBNRD2025_All_elev_VoxelXYZData_discretized3.3.msh	
LBBNRD2025_Kd_elev_VoxelXYZData_discretized3.3-UBC_README.txt	
LBBNRD2025_Kd_elev_VoxelXYZData_discretized3.3.mod	
LBBNRD2025_Kd_elev_VoxelXYZData_discretized3.3.msh	
LBBNRD2025_Quat_elev_VoxelXYZData_discretized3.3-UBC_README.txt	
LBBNRD2025_Quat_elev_VoxelXYZData_discretized3.3.mod	
LBBNRD2025_Quat_elev_VoxelXYZData_discretized3.3.msh	

6.2 Description of Included Google Earth KMZ Data and Profiles

In addition to the data delivered in XYZ format, Google Earth .KMZ files were generated to view the geophysical AEM flight line locations and interpreted geologic data. KMZ files for all "*As-Flown*" flight lines and data "*Retained*" for inversion after editing are included in the folder "*Appendix_3_Deliverables\KMZ*".

Unique KMZ 2D profile files were created for each individual flight line in approximately 7-12-mile segments or shorter. Within these specialized KMZ files, the AEM flight line is shown as well as place marks at each location where there are interpreted geologic results. The attribute data for each unique place mark contains location information as well as bedrock and the water table. These KMZ files are located within the "*Appendix_3_Deliverables\KMZ\LBBNRD25_Profiles*" folder. In this folder is a "*GoogleE_Readme.pdf*" file that provides instructions regarding the "*Settings*" changes that need to be made in Google Earth, and how to use the KMZ files in Google Earth including a legend of what attributes are displayed when an AEM sounding location is clicked. This LBBNRD 2025 GoogleE_Readme.pdf file is repeated below as a convenience. An image of the LBBNRD 2025 KMZ layout is presented in Figure 6-1 and an example of clicking on points is presented in Figure 6-2. A 2D profile of line L190241 is presented in Figure 6-3.

6.2.1 Included README for the LBBNRD 2025 Interpretation KMZ

README for: **LBBNRD2025_Interpretation_KMZ.kmz**

Data Files - Please copy the folder *LBBNRD25_Profiles* to your C:\ drive. Do not rename any of the images within the folder.

Google Earth Instructions:

STEP 1: In Google Earth, click "*Tools*", then "*Options*".

STEP 2: In the Google Earth Options box, click the "*General*" tab.

STEP 3: Under "*KML Content Security*", make sure the box is checked to allow access to local files (the profiles).

STEP 4: Under "*Display*", make sure the box is checked to show web results in external browser.

STEP 5: The *LBBNRD2025_Interpretation_KMZ* interpretation file within the folder named *LBBNRD25_Profiles* can now be opened and viewed in Google Earth.

Data:

East (m) – Easting coordinate in NAD83, UTM 14N, in meters.

North (m) – Northing coordinate in NAD83, UTM 14N, in meters.

East (ft) – Easting coordinate in NAD83, Nebraska State Plane, in feet.

North (ft) – Northing coordinate in NAD83, Nebraska State Plane, in feet.

Elevation (ft) – Digital Elevation Model (DEM) ground surface elevation in feet.

Elevation WaterTable2025 (ft) – Elevation of the 2025 water table, in feet.

Elevation Bedrock (ft) – Estimated elevation of the top of the Bedrock, in feet.

Elevation Kgg (ft) – Estimated elevation of Cretaceous Greenhorn limestone and Graneros shale, in feet.

Elevation Kd (ft) – Estimated elevation of the Cretaceous Dakota Group Fm., ***Kd***, in feet.

Elevation Permian Units (ft) – Estimated elevation of the Permian Chase (***Pc***) and Council Grove (***Pcg***) geological formations, in feet.

Elevation Saline Water (ft) – Estimated elevation of the saline water, where present, in feet.

Profile – Link to Interpreted AEM profile images.

Legend – Link to this write-up describing data channels listed here.

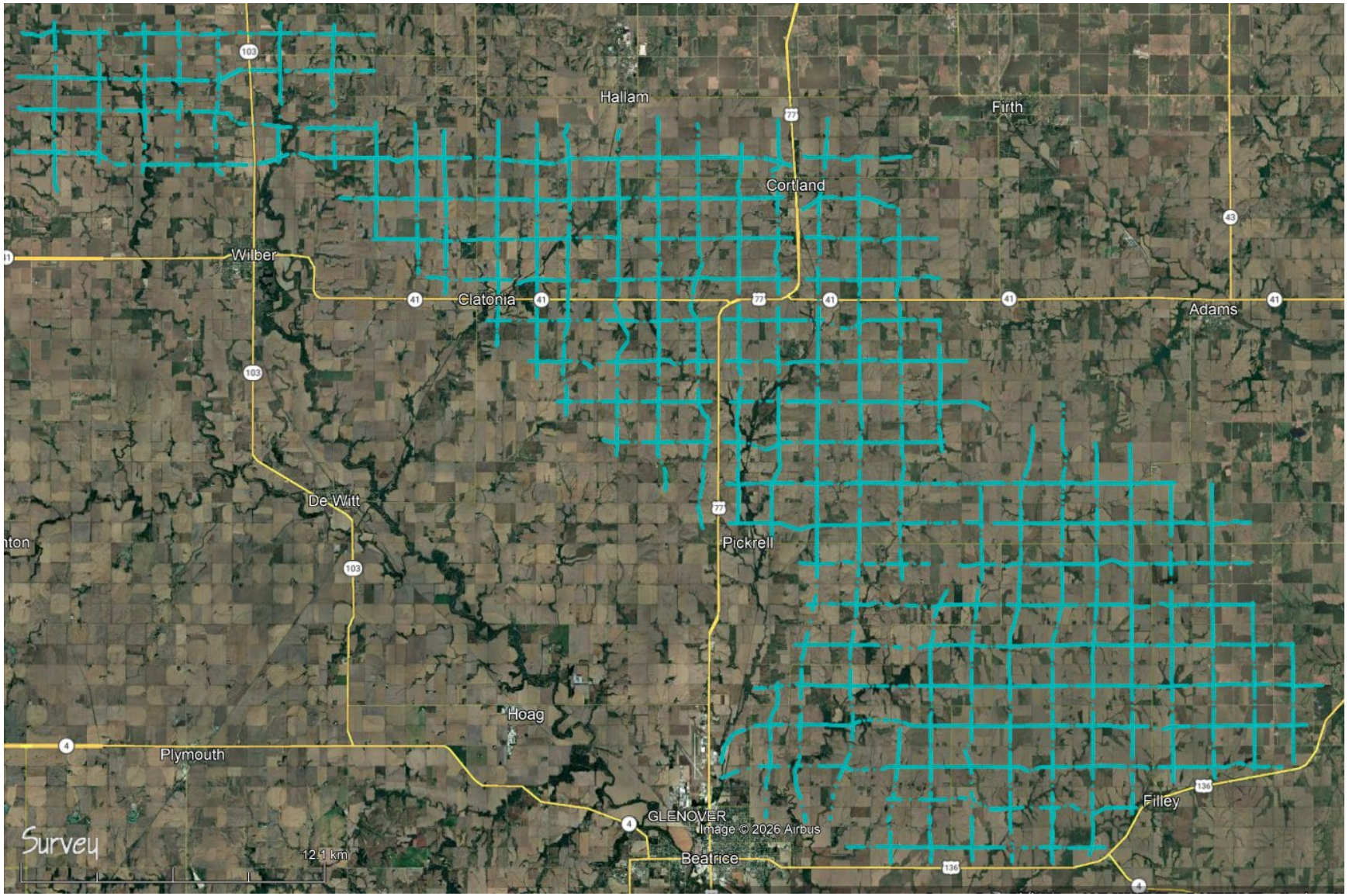


Figure 6-1. Google Earth KMZ of the LBBNRD 2025 AEM survey area showing the AEM Interpretation locations.

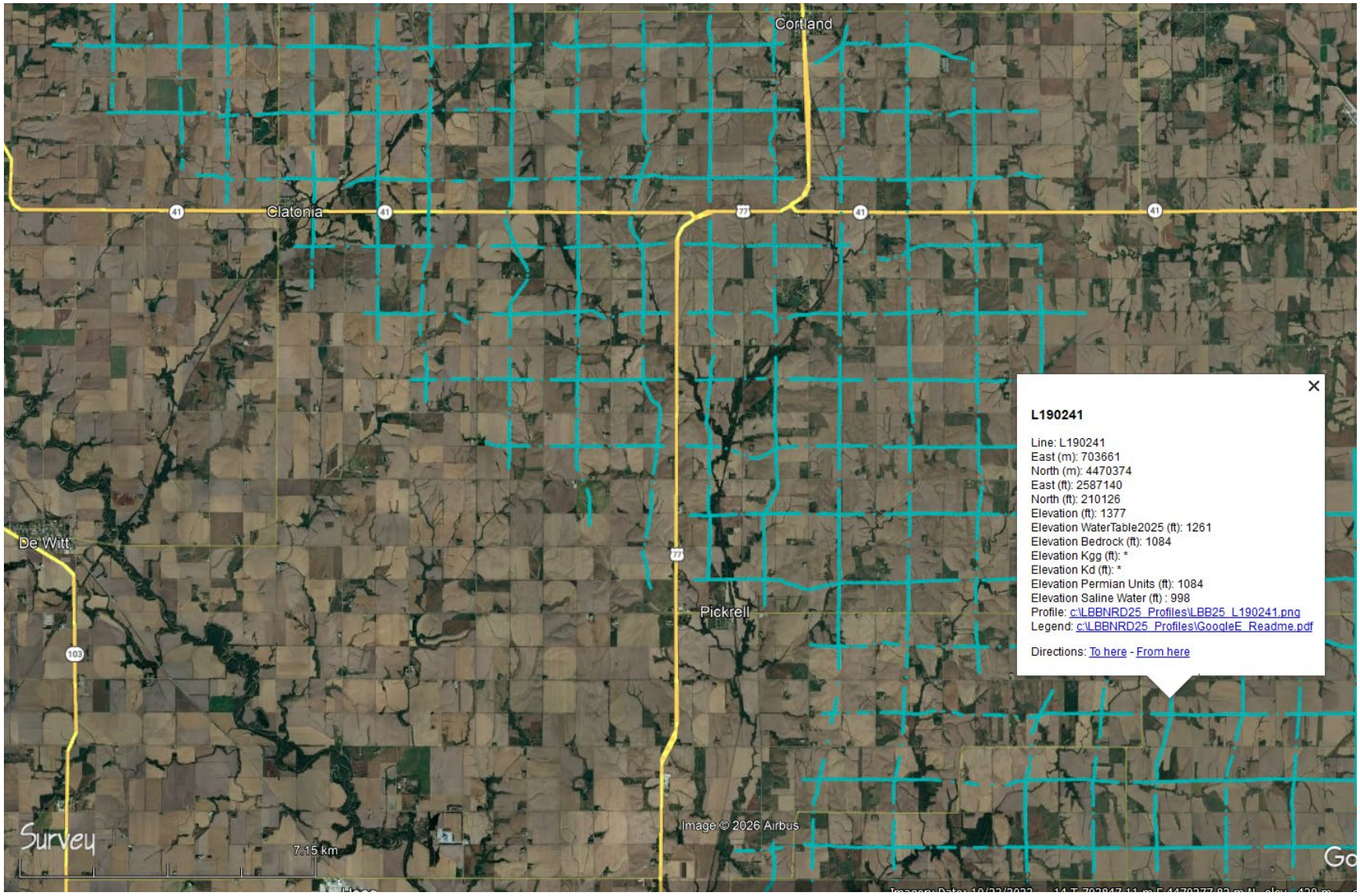
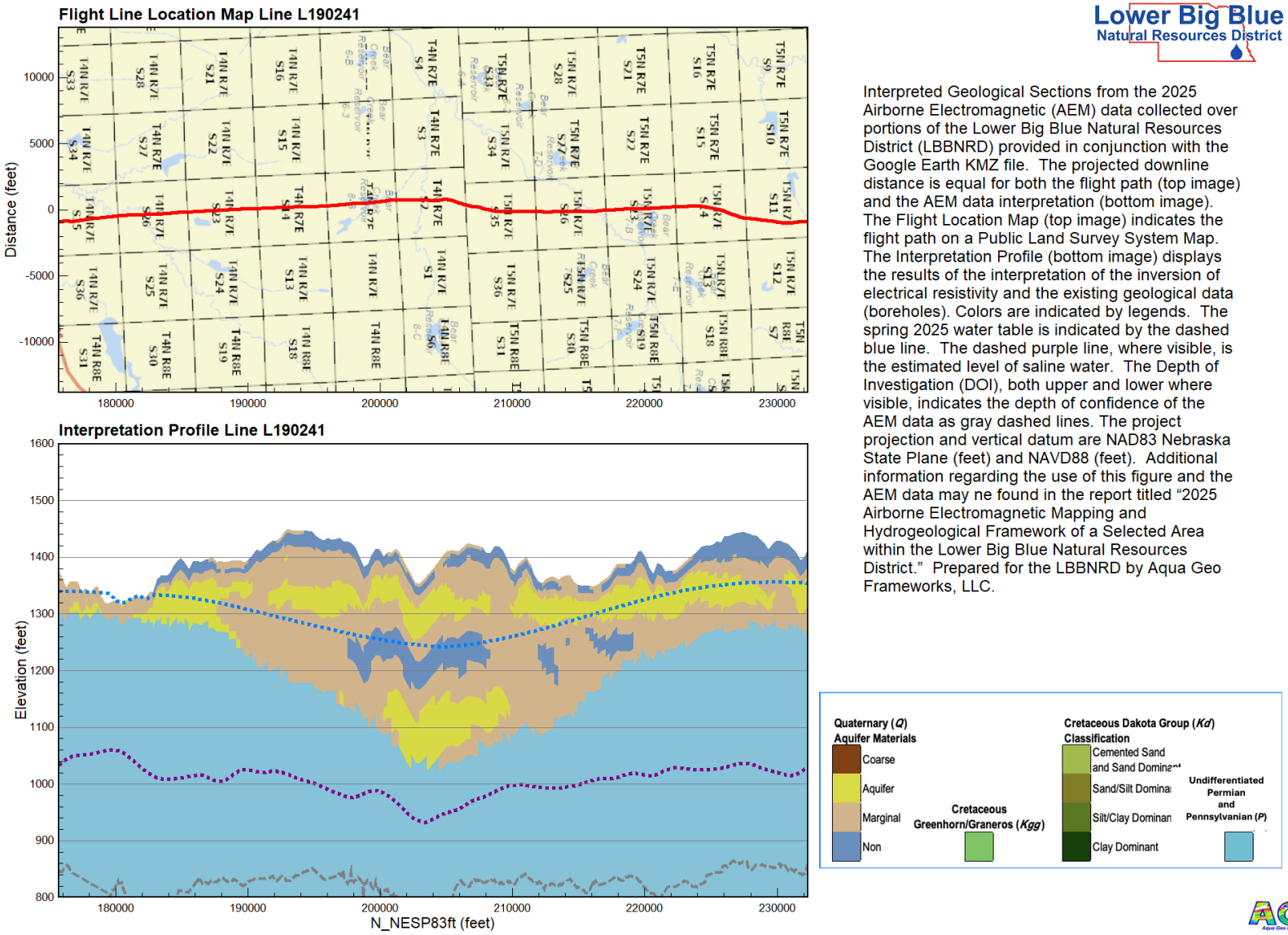


Figure 6-2. Example of clicking on a location in the LBBNRD 2025 AEM survey area. Profile L190241 is presented in Figure 6-3 below.



Lower Big Blue
Natural Resources District

Interpreted Geological Sections from the 2025 Airborne Electromagnetic (AEM) data collected over portions of the Lower Big Blue Natural Resources District (LBBNRD) provided in conjunction with the Google Earth KMZ file. The projected downline distance is equal for both the flight path (top image) and the AEM data interpretation (bottom image). The Flight Location Map (top image) indicates the flight path on a Public Land Survey System Map. The Interpretation Profile (bottom image) displays the results of the interpretation of the inversion of electrical resistivity and the existing geological data (boreholes). Colors are indicated by legends. The spring 2025 water table is indicated by the dashed blue line. The dashed purple line, where visible, is the estimated level of saline water. The Depth of Investigation (DOI), both upper and lower where visible, indicates the depth of confidence of the AEM data as gray dashed lines. The project projection and vertical datum are NAD83 Nebraska State Plane (feet) and NAVD88 (feet). Additional information regarding the use of this figure and the AEM data may ne found in the report titled "2025 Airborne Electromagnetic Mapping and Hydrogeological Framework of a Selected Area within the Lower Big Blue Natural Resources District." Prepared for the LBBNRD by Aqua Geo Frameworks, LLC.

Figure 6-3. Example of clicking on link to Profile image for line L190241 in the LBBNRD 2025 interpretation KMZ.

7 References

AGF, 2019, Summary Report on "Airborne Electromagnetic Mapping and Hydrogeologic Framework of Selected Regions of the Eastern Nebraska Water Resources Assessment Area" Chapters Completed for Lewis and Clark, Lower Elkhorn, Lower Platte North, Lower Platte South, Nemaha, and Papio-Missouri River Natural Resources Districts: Prepared for Eastern Nebraska Water Resources Assessment by Aqua Geo Frameworks, LLC, Mitchell, NE, 13 December 2019, 22p., (accessed on March 29, 2025), https://enwra.org/projects/2018-airborne-electromagnetic-aem-surveys

AGF, 2024a, Airborne Electromagnetic Mapping and Hydrogeologic Framework of a Selected Area within the Lower Big Blue Natural Resources District: Prepared for the Lower Big Blue Natural Resources District by Aqua Geo Frameworks, LLC, Laramie, WY, 22 January 2024, 176pp., https://enwra.org/projects/2023-airborne-electromagnetic-aem-surveys

AGF, 2024b, Airborne Electromagnetic Mapping and Hydrogeologic Framework of Selected Areas within the Nemaha Natural Resources District: Prepared for the Nemaha Natural Resources District by Aqua Geo Frameworks, LLC, Laramie, WY, 29 March, 2024, 143pp., https://enwra.org/projects/2023-airborne-electromagnetic-aem-surveys

AGF, 2025, 2024 Airborne Electromagnetic Mapping and Hydrogeologic Framework of a Selected Area within the Lower Big Blue Natural Resources District: Prepared for the Lower Big Blue Natural Resources District by Aqua Geo Frameworks, LLC, Laramie, WY, 01 April 2025, 188pp., https://enwra.org/projects/2024-airborne-electromagnetic-aem-surveys

Asch, T.H., Abraham, J.D., and Irons, T., 2015, "A discussion on depth of investigation in geophysics and AEM inversion results", Presented at the Society of Exploration Geophysicists Annual Meeting, New Orleans. (accessed on February 24, 2023). https://library.seg.org/doi/reader/10.1190/segam2015-5915199.1

Burchett, R. R. and Reed, E. C., 1967, Centennial guidebook to the geology of southeastern Nebraska: Conservation and Survey Division, 621, https://digitalcommons.unl.edu/conservationsurvey/621

Burchett, R.R., Dreeszen, V.H., Reed, E.C., and Prichard, G.E., 1972, Bedrock geologic map showing thickness of overlying Quaternary deposits, Lincoln Quadrangle and part of Nebraska City Quadrangle, Nebraska and Kansas: U.S. Geological Survey, Report IMAP-729, https://doi.org/10.3133/i729

Burchett, R.R., 1986, Geologic bedrock map of Nebraska: Nebraska Geological Survey. Scale 1:1,000,000, Geologic Maps and Charts (GMS)-1, https://ngmdb.usgs.gov/Prodesc/proddesc_39227.htm

Burchett, R.R. and Pabian, R.K., 1992, Geologic bedrock map of Nebraska: Nebraska Geological Survey, Nebraska Geonotes, Conservation and Survey Division, No. 763, University of Nebraska GIM-48, 4pp., https://digitalcommons.unl.edu/conservationsurvey/763

Carney, C.P., Abraham, J.D., Cannia, J.C., and Steele, G.V., 2015, Final Report on Airborne Electromagnetic Geophysical Surveys and Hydrogeologic Framework Development for the Eastern Nebraska Water Resources Assessment – Volume II, including the Lower Platte North, Lower Platte South, and Nemaha Natural Resources Districts: Prepared for the Eastern Nebraska Water Resources Assessment (ENWRA) by Exploration Resources International Geophysics LLC, Vicksburg, MS. http://www.enwra.org/aem%20data%20download.html (accessed on March 25, 2025).

Christensen, N. B., Reid, J. E., and Halkjaer, M., 2009, "Fast, laterally smooth inversion of airborne time-domain elecromagnetic data." *Near Surface Geophysics* 599-612. https://doi.org/10.3997/1873-0604.2009047

Christiansen, A. V., and Auken, E., 2012, "A global measure for depth of investigation." *Geophysics,Vol. 77, No. 4* WB171-177. (accessed on March 25, 2025). https://library.seg.org/doi/abs/10.1190/geo2011-0393.1

Datamine Discover, 2026, Datamine Discover Profile Analyst, (accessed on January 27, 2026), https://docs.dataminesoftware.com/PAExplorer/index.htm

Divine, D., Joeckel, R.M., Korus, J.T., Hanson, P.R., and Lackey, S.O., 2009, Eastern Nebraska Water Resources Assessment (ENWRA): Introduction to a Hydrogeological Study: Nebraska Conservation and Survey Division, School of Natural Resources, University of Nebraska- Lincoln, No41, (accessed on March 29, 2025), http://digitalcommons.unl.edu/conservationsurvey/41

Divine, D., 2014, The Groundwater Atlas of Lancaster County, Conservation and Survey Division, Resources Atlas No. 7, p.39, http://digitalcommons.unl.edu/conservationsurvey/39

Divine, D.P. and Sibray, S.S., 2017, An Overview of Secondary Aquifers in Nebraska: Lincoln, NE, Nebraska Conservation and Survey Division, Educational Circular No. 26, pp 44, (accessed on March 25, 2025), https://digitalcommons.unl.edu/conservationsurvey/138/.

Fetter, C., 1988, Applied Hydrogeology. Merrill Publishing, Columbus, 592pp., https://www.amazon.com/Applied-hydrogeology-C-W-Fetter/dp/0675208874

Foged, N., Auken, E., Christiansen, A.V., and Sorensen, K.I., 2013, "Test-site calibration and validation of airborne and ground based TEM systems.": Geophysics, v.78, No.2: E95-E106. (accessed on https://doi.org/10.1190/GEO2012-0244.1). https://doi.org/10.1190/GEO2012-0244.1

Freeze, R.A. and Cherry, J.A., 1979, “Groundwater”: Published by Prentice Hall, New Jersey, ISBN 0-13-365312-9.

Gannon, J.M., and Vogelgesang, J.A., 2015, Groundwater resources evaluation of the lower Dakota Aquifer in north-central and southwestern Iowa, Water Resources Investigation Report 12, Iowa Geological Survey The University of Iowa01/2015 DOI: 10.17077/rep.006473,

https://iro.uiowa.edu/esploro/outputs/report/Groundwater-Resource-Evaluation-of-the-Lower/9984109991002771?institution=01IOWA_INST#file-0

Geosoft, 2025, Oasis montaj, (accessed on January 27, 2026). https://www.seequent.com/products-solutions/geosoft-oasis-montaj/

Heath, R.C., 1983, Basic ground-water hydrology, U.S. Geological Survey Water-Supply Paper 2220, 86p., http://pubs.er.usgs.gov/publication/wsp2220 (accessed March 25, 2025)

HydroGeophysics Group, Aarhus University, 2010, "Validation of the SkyTEM system at the extended TEM test site." Aarhus, Denmark.

HydroGeophysics Group, Aarhus University, 2011, "Guide for processing and inversion of SkyTEM data in Aarhus Workbench, Version 2.0."

Joeckel, R. M., Diffendal, R.F., Hanson, P R., and Korus, J.T., 2018, Geologic mapping of Nebraska: Old rocks, new maps, fresh insights: Robert F. Diffendal, Jr., Publications, no 73, (accessed December 22, 2023), http://digitalcommons.unl.edu/diffendal/73

Joeckel, R.M., Divine, D., Howard, L.M., Cameron, K., and Waszgis, M.M., 2019, Geology of southeastern Nebraska: Nebraska Conservation and Survey Division, No. 671, (accessed December 22, 2023), https://digitalcommons.unl.edu/conservationsurvey/671

Korus, J.T., Howard, L.M., Young, A.R., Divine, D.P., Burbach, M.E., and Hallum, D.R., 2013, The Groundwater Atlas of Nebraska, Third Edition: Conservation and Survey Division, School of Natural Resources, Institute of Agriculture and Natural Resources, University of Nebraska–Lincoln, Resource Atlas No. 4b/2013, 76pp., (accessed December 22, 2023), https://newsroom.unl.edu/announce/snr/2922/16031

Ley-Cooper, Y. and Davis, A., 2010. Can a borehole conductivity log discredit a whole AEM survey? : in Extended abstracts of the Australian Society of Exploration Geophysicists Annual meeting Aug 20-24, Sydney, Australia

Nebraska DWEE-GroundwaterWells, 2026, Registered Groundwater Wells Data Retrieval, (accessed March 25, 2026). https://dnr.nebraska.gov/data/groundwater-data .

Nebraska-DWEE, 2026, Nebraska Department of Water, Energy, and Environment, (accessed March 25,2026), https://dee.nebraska.gov/

Nebraska GeoCloud, 2026, https://snr.unl.edu/csd/geology/AEM.aspx#geocloud , (accessed March 25,2026)

O'Connor, T.M., 1987, A Preliminary Study of the Hydrogeology of the Dakota Formation in Douglas, Sarpy and Washington Counties, Eastern Nebraska: M.S. Thesis, Department of Geology, University of Nebraska.

Reed, E. C., 1959, The geological section of Nebraska: Conservation and Survey Division, No. 670, Revisions to Condra, G.E. and Reed, E.C., The geological section of Nebraska, Geological Survey Bulletin, No. 14A, 1959, 82pp., (accessed December 22,2023), https://digitalcommons.unl.edu/conservationsurvey/670

Schamper, C., Auken, E., and Sorensen, K., 2014, Coil response inversion for very early time modelling of helicopter-borne time-domain electromagnetic data and mapping of near-surface Geologic Layers. European Association of Geoscientistis & Engineers, Geophysical Prospecting, v. 62, Issue 3, p. 658–674, https://doi.org/10.1111/1365-2478.12104.

SkyTem Airborne Surveys Worldwide, 2025, SkyTEM304M, (accessed on January 26, 2026). https://skytem.com/transient-electromagnetic-tem-systems/.

Stoeser, D.B., Green, G.N., Morath, L.C., Heran, W.D., Wilson, A.B., Moore, D.W., and Van Gosen, B.S., 2005, Preliminary integrated geologic map databases for the United States: Central States: Montana, Wyoming, Colorado, New Mexico, North Dakota, South Dakota, Nebraska, Kansas, Oklahoma, Texas, Iowa, Missouri, Arkansas, and Louisiana: U.S.G.S. Open File Report 2005-1351, https://pubs.usgs.gov/of/2005/1351/

Summerside, S. A., Olafsen-Lackey, S., Goeke, J., and Myers, W., 2005, Mapping of Aquifer Properties - Transmissivity and Specific Yield - for Selected River Basins in Central and Eastern Nebraska: Conservation and Survey Division Open-File Report 71, 37 pp, https://marketplace.unl.edu/nemaps/mapping-of-aquifer-properties-transmissivity-and-specific-yield-for-selected-river-basins-in-central-and-eastern-nebraska-ofr-71.html .

Summerside, S. and Myers, W., 2005, Transmissivity of the principal aquifer, Lincoln and Nebraska City Quadrangles, Nebraska. Conservation and Survey Division, School of Natural Resources, University of Nebraska–Lincoln GM-65, scale 1:250:000

Szilagyi, J. and Jozsa, J., 2012, MODIS-aided statewide net groundwater-recharge estimation in Nebraska: Ground Water 50, 1–10, (accessed December 22, 2023), https://www.google.com/url?sa=t&rct=j&q=&esrc=s&source=web&cd=&cad=rja&uact=8&ved=2ahUKEwj7rdGuoaSDAxWNkyYFHX25Aj4QFnoECBQQAQ&url=https%3A%2F%2Fsnr.unl.edu%2Fszilagyi%2FGWPublishedpaper.pdf&usg=AOvVaw1p-xIfF46YK6fvXTUDwgBK&opi=89978449

University of Nebraska-Lincoln (UNL) School of Natural Resources, 2026, Nebraska statewide test-hole database. (accessed March 25, 2026), http://snr.unl.edu/csd/geology/testholes.aspx.

U.S. Geological Survey (USGS), 2026, The National Map, 2026, 3DEP products and services: The National Map, 3D Elevation Program Web page, (accessed March 25, 2026). https://www.usgs.gov/the-national-map-data-delivery

USGS-MrData, 2026, “MrData” website on geologic units, by state and county, across the United States, (accessed March 25, 2026). https://mrdata.usgs.gov/geology/state/geog-units.html

Viezzoli, A., Christiansen, A. V., Auken, E., and Sorensen, K., 2008, " Quasi-3D modeling of airborne TEM data by spatially constrainted inversion." *Geophysics Vol. 73 No. 3* F105-F11. (accessed March 29, 2025). https://www.em-ergo.it/resource-types/publications/page/4/ .

Witzke, B.J., Ludvigson, G.A., Poppe, J.R., and Ravn, R.L., 1983, Cretaceous Paleogeography along the Eastern Margin of the Western Interior Seaway, Iowa Southern Minnesota, and Eastern Nebraska and South Dakota: Mesozoic Paleogeography of the West-Central United States: Rocky Mountain Symposium 2, p. 225-252, https://archives.datapages.com/data/rocky_sepm/data/011/011001/225_rocky_mount110225.htm